

**Rhodium-Catalysed Allylic Substitution with an
Acyl Anion Equivalent: Asymmetric Construction of
Acyclic Quaternary Carbon Stereogenic Centres**

*Thesis submitted in accordance with the requirements of the University
of Liverpool for the degree of Doctor in Philosophy*

Samuel Oliver

August 2012

Abstract

The asymmetric construction of substituted carbonyl compounds, particularly those containing α -quaternary carbon stereogenic centres, remains a significant area of interest in organic chemistry. This can largely be attributed to the ubiquity and versatility of these compounds as synthetic intermediates, and the presence of such motifs in a range of biologically active pharmaceutical agents and natural products. In this context, the transition metal-catalysed allylic substitution provides an extremely powerful tool for the asymmetric construction of a range of C-C, C-N and C-O bonds, and has found significant application in the synthesis of substituted carbonyl compounds. The overall utility of these methods is described in the introductory review, which seeks to compare and contrast two alternative bond forming strategies for the asymmetric construction of these units *via* allylic substitution. While this work is generally dominated by the asymmetric allylic alkylation of unstabilised enolates, these reactions are often limited by the numerous challenges associated with the regio- and stereoselective formation of an enolate nucleophile, product racemisation and polyalkylation, and their relatively narrow substrate scope. In contrast, the transition metal-catalysed allylic substitution with an acyl anion equivalent has the potential to provide a range of α -substituted carbonyl compounds *via* a fundamentally different bond forming event, in which the acyl functionality is installed directly into the allylic framework. Despite the numerous potential advantages that are afforded by this approach, a general method for the regio- and stereoselective transition-metal catalysed allylic acylation of substituted electrophiles has yet to be reported.

Chapter 2 describes the development of a novel regio- and stereospecific rhodium-catalysed allylic substitution reaction, which utilises a trialkylsilyl-protected

cyanohydrin as a convenient acyl anion equivalent. Following a brief introduction to the rhodium-catalysed allylic substitution reaction, this chapter is organised into three distinct sections. The first of these outlines the identification of a suitable nucleophile, and the subsequent development of reaction conditions for the regioselective alkylation of tertiary allylic carbonates with a range of stabilised aryl cyanohydrins. The stereospecific variant of this transformation, which involves the direct conversion of an enantiomerically enriched acyclic tertiary allylic alcohol to the corresponding α -quaternary substituted aryl ketone, is then described. Finally, the expansion of this methodology to the preparation of more synthetically useful α,β -unsaturated ketones, and preliminary investigations towards the application of secondary allylic carbonates, are outlined. Overall, this method provides a fundamentally novel bond construction towards the synthesis of α -quaternary substituted carbonyl compounds, and circumvents many of the problems associated with conventional enolate alkylation reactions. Thus, we anticipate that the methodology outlined herein will find significant application in target directed synthesis, particularly in the preparation of complex bioactive pharmaceuticals and natural products that contain quaternary carbon stereogenic centres.

Acknowledgements

I would like to thank my research advisor, P. Andrew Evans, for providing me with the opportunity to work in his group, and on such challenging and interesting chemistry. I am grateful for his continued enthusiasm, encouragement and advice, which has played a key role in my progress over the last four years. While I cannot begin to describe the things I have learned in this time, both as a chemist and as a person, I am certain that this experience will serve me well in the future. I would also like to thank my industrial supervisor, Paul Kemmitt, both for the numerous helpful discussions we have had over the course of my studies, and for his endeavour in making my placement at AstraZeneca such an enjoyable experience, despite the difficult circumstances that surrounded my short stay there.

I am greatly indebted to the past and present members of both the Evans and Aissa research groups, who have been a pleasure to work alongside over the last four years. Much apart from the knowledge and advice that was shared between us on a daily basis, I will never forget the times that we spent together away from the laboratory, which helped me to remain positive during some of the most difficult phases of my research. Finally, I would like to thank my friends and family for their endless support, and for understanding the hard work and sacrifices that were required in order for me to reach this level of education, both prior to and during my PhD studies. The EPSRC and AstraZeneca are also gratefully acknowledged for their financial support of this work.

Table of Contents

Abstract	i
Acknowledgements	iii
List of Abbreviations.....	ix
List of Schemes	xiii
List of Tables.....	xvi
List of Figures	xviii

Chapter 1: Asymmetric Synthesis of Substituted Carbonyl Compounds *via* Transition Metal-Catalysed Allylic Substitution

1.1. Transition Metal-Catalysed Allylic Substitution Reactions.....	1
1.1.1. Introduction	1
1.1.2. Reaction Mechanism	1
1.1.2.1. General Mechanism	1
1.1.2.2. Regiocontrol.....	2
1.1.2.3. Stereocontrol	5
1.1.3. Seminal Work.....	7
1.2. Asymmetric Synthesis of Substituted Carbonyl Compounds <i>via</i> Transition Metal-Catalysed Allylic Substitution.....	10
1.2.1. Introduction	10
1.2.2. Transition Metal-Catalysed Allylic Substitution Reactions using Unstabilised Enolate Nucleophiles	11
1.2.2.1. Introduction	11
1.2.2.2. Enolate Equivalents.....	13
1.2.2.2.1. Enamines	13
1.2.2.2.2. Silyl Enol Ethers	18
1.2.2.2.3. Enolstannanes.....	22
1.2.2.2.4. Decarboxylative Approaches	23
1.2.2.3. Metal Enolates.....	33
1.2.2.3.1. Introduction	33
1.2.2.3.2. Enoxyborates.....	33
1.2.2.3.3. Tin Enolates	34

1.2.2.3.4. Copper Enolates	35
1.2.2.3.5. Zinc Enolates.....	36
1.2.2.3.6. Magnesium Enolates	37
1.2.2.3.7. Sodium Enolates.....	38
1.2.2.3.8. Lithium Enolates	39
1.2.3. Transition Metal-Catalysed Allylic Substitution Reactions using Acyl Anion Equivalents.....	43
1.2.3.1. Introduction.....	43
1.2.3.2. Acylmetal Nucleophiles.....	43
1.2.3.3. “Masked” Acyl Anion Equivalents.....	45
1.2.4. Concluding Remarks.....	47

**Chapter 2: Rhodium-Catalysed Allylic Substitution with an Acyl Anion
Equivalent: Asymmetric Construction of Acyclic Quaternary Carbon
Stereogenic Centres**

2.1. Rhodium-Catalysed Allylic Substitution Reactions.....	52
2.1.1. Introduction.....	52
2.1.2. Seminal Work.....	52
2.1.3. Regio- and Stereospecific Rhodium-Catalysed Allylic Substitution Reactions.....	54
2.1.3.1. Seminal Work	54
2.1.3.2. Mechanistic Studies	55
2.2. Rhodium-Catalysed Allylic Substitution with an Acyl Anion Equivalent	62
2.2.1. Introduction.....	62
2.2.2. Initial Results	64
2.2.3. Rhodium-Catalysed Allylic Substitution with Aryl Cyanohydrin Pronucleophiles.....	66
2.2.3.1. Development of a One Pot Procedure.....	66
2.2.3.2. Reaction Optimisation.....	67
2.2.3.3. Rationale for Regioselectivity.....	70
2.2.3.4. Consumption of the Linear Regioisomer	72
2.2.3.5. Substrate Scope	73
2.2.3.5.1. Substrate Synthesis	73

2.2.3.5.2. Cyanohydrin Scope	75
2.2.3.5.3. Carbonate Scope.....	76
2.2.3.6. Attempted Baeyer-Villiger Oxidation.....	79
2.2.3.7. Concluding Remarks	80
2.2.4. Stereospecific Rhodium-Catalysed Allylic Substitution with an Acyl Anion Equivalent: Asymmetric Construction of Acyclic α -Aryl Ketones	81
2.2.4.1. Introduction	81
2.2.4.2. Asymmetric Synthesis of Tertiary Allylic Alcohols.....	84
2.2.4.3. Reaction Optimisation.....	87
2.2.4.4. Proof of Absolute Configuration.....	91
2.2.4.5. Substrate Scope	91
2.2.4.5.1. Substrate Synthesis	91
2.2.4.5.2. Cyanohydrin Scope	93
2.2.4.5.3. Tertiary Alcohol Scope	95
2.2.4.6. Concluding Remarks	96
2.2.5. Expanding the Scope of the Rhodium-Catalysed Allylic Substitution with an Acyl Anion Equivalent.....	98
2.2.5.1. Rhodium-Catalysed Allylic Substitution with Alkenyl Cyanohydrin Pronucleophiles: Construction of Acyclic α,α' -Dialkyl Ketones	98
2.2.5.1.1. Introduction	98
2.2.5.1.2. Initial Results	99
2.2.5.1.3. Deprotonation Studies.....	101
2.2.5.1.4. Reaction Optimisation.....	102
2.2.5.1.5. Substrate Scope	103
2.2.5.1.5.1. Substrate Synthesis.....	103
2.2.5.1.5.2. Aryl-Substituted Cyanohydrin Scope.....	104
2.2.5.1.5.3. Alkyl-Substituted Cyanohydrin Scope.....	106
2.2.5.1.5.4. Trisubstituted Cyanohydrin Scope	108
2.2.5.1.6. Access to α,α' -Dialkyl Ketones	109
2.2.5.1.7. Stereospecific Alkylation	110
2.2.5.2. Rhodium-Catalysed Allylic Substitution of Secondary Carbonates with an Acyl Anion Equivalent: Synthesis of α -Tertiary Ketones.....	112
2.2.5.2.1. Introduction	112
2.2.5.2.2. Preliminary Results	113

2.2.5.3. Concluding Remarks	116
-----------------------------------	-----

Chapter 3: Representative Experimental Procedures and Supplemental Data

3.1. General Information	120
3.2. Representative Experimental Procedures and Spectral Data	121
3.2.1. Rhodium-Catalysed Allylic Substitution with Aryl Cyanohydrin Pronucleophiles	121
3.2.1.1. Representative Experimental Procedure for the Synthesis of Tertiary Allylic Carbonates 26a-k	121
3.2.1.2. Spectral Data for the Allylic Carbonates 26a-k , 31 and 37	122
3.2.1.3. Representative Experimental Procedure for the Synthesis of Aryl Cyanohydrins 24a-i	127
3.2.1.4. Spectral Data for the Aryl Cyanohydrins 24a-i	128
3.2.1.5. Representative Experimental Procedure for the Rhodium-Catalysed Allylic Substitution with the Aryl Cyanohydrins 24	131
3.2.1.6. Spectral Data for the Aryl Ketone Products 29a-o	132
3.2.1.7. Spectral Data for the Side Product 33	140
3.2.2. Stereospecific Rhodium-Catalysed Allylic Substitution with an Acyl Anion Equivalent: Asymmetric Construction of Acyclic α -Aryl Ketones	140
3.2.2.1. Representative Experimental Procedure for the Synthesis of Enantiomerically Enriched Secondary Alcohols (<i>S</i>)- 54a-e	140
3.2.2.2. Representative Experimental Procedure for the Synthesis of Enantiomerically Enriched Carbamates 48a-e	141
3.2.2.3. Spectral Data for the Enantiomerically Enriched Secondary Carbamates 48a-e	142
3.2.2.4. Representative Experimental Procedure for the Synthesis of Enantiomerically Enriched Tertiary Allylic Alcohols 45a-e	144
3.2.2.5. Spectral Data for the Enantiomerically Enriched Tertiary Allylic Alcohols 45a-e	145
3.2.2.6. Representative Experimental Procedure for the Stereospecific Rhodium- Catalysed Allylic Substitution with the Aryl Cyanohydrins 24	148
3.2.2.7. Spectral Data for the Enantiomerically Enriched Acyclic α -Aryl Ketones 52a-l	149

3.2.2.8. Experimental Procedure for the Hydrogenation of 52a	156
3.2.3. Expanding the Scope of the Rhodium-Catalysed Allylic Substitution with an Acyl Anion Equivalent.....	158
3.2.3.1. Rhodium-Catalysed Allylic Substitution with Alkenyl Cyanohydrin Pronucleophiles: Construction of Acyclic α,α' -Dialkyl Ketones	158
3.2.3.1.1. Spectral Data for the Alkenyl Cyanohydrins 56b-k and 69a-c ...	158
3.2.3.1.2. Representative Experimental Procedure for the Rhodium-Catalysed Allylic Substitution with the Alkenyl Cyanohydrins 56 and 69	164
3.2.3.1.3. Spectral Data for the α,β -Unsaturated Ketone Products 60a-q and 70a-c	165
3.2.3.1.4. Representative Experimental Procedure for the 1,4-Reduction of the Ketone 60q	177
3.2.3.1.5. Representative Experimental Procedure for the Stereospecific Rhodium-Catalysed Allylic Substitution with the Alkenyl Cyanohydrins 56	178
3.2.3.1.6. Spectral Data for the Enantiomerically Enriched α,β -Unsaturated Ketone Products 74a-b	179

List of Abbreviations

Å	angstrom
Ac	acetyl
acac	acetylacetonato
APT	attached proton test
Ar	aryl
atm.	atmosphere
BINAP	2,2'-bis(diphenylphosphino)-1-1'-binaphthyl
bipy	bipyridine
Bn	benzyl
Boc	<i>tert</i> -butoxycarbonyl
ⁱ Bu	<i>iso</i> -butyl
ⁿ Bu	<i>n</i> -butyl
^s Bu	<i>sec</i> -butyl
^t Bu	<i>tert</i> -butyl
Bz	benzoyl
<i>c</i>	concentration
°C	degrees Celsius
CAN	cerium ammonium nitrate
Cb	N,N-diisopropylcarbonyl
<i>cee</i>	conservation of enantiomeric excess
COD	1,5-cyclooctadiene
Cp	cyclopentadienyl
dba	dibenzylideneacetone
DCE	1,2-dichloroethane
DIOP	2,3-O-isopropylidene-2,3-dihydroxy-1,4-bis(diphenylphosphino)butane
δ	chemical shift
DBU	1,8-diazobicyclo[5.4.0]undec-7-ene
DIBAL-H	di- <i>iso</i> -butylaluminium hydride
DME	dimethoxyethane
DMF	dimethylformamide

DMPU	1,3-Dimethyl-3,4,5,6-tetrahydro-2(1H)-pyrimidinone
DMSO	dimethyl sulfoxide
DYKAT	dynamic kinetic asymmetric transformation
dppe	1,2-bis(diphenylphosphino)ethane
dppf	1,1'-bis(diphenylphosphino)ferrocene
<i>dr</i>	diastereomeric ratio
<i>ds</i>	diastereoselectivity
<i>E</i>	entgegen
<i>ee</i>	enantiomeric excess
ESI	electrospray ionisation
<i>ent</i>	enantiomer
eq.	equation
Et	ethyl
equiv.	equivalent
FCC	flash column chromatography
FTIR	Fourier transform infrared spectroscopy
g	gram
h	hours
^c Hex	<i>cyclo</i> -hexyl
HMDS	bis(trimethylsilyl)amide
HMPA	hexamethylphosphoramide
HOMO	highest occupied molecular orbital
HPLC	high performance liquid chromatography
HRMS	high resolution mass spectrometry
Hz	hertz
IR	infrared
<i>J</i>	coupling constant
L _n	ligand set
LDA	lithium diisopropylamide
Lg	leaving group
LUMO	lowest unoccupied molecular orbital
M	molar
M ⁿ	metal with an oxidation state n

Me	methyl
MEM	β -methoxyethoxymethyl
Mes	mesitylene
mg	milligram
MHz	megahertz
mL	millilitre
mm	millimetre
mmol	millimol
MS	molecular sieves
MTBE	methyl <i>tert</i> -butyl ether
NHC	N-heterocyclic carbene
N	normal
NMR	nuclear magnetic resonance
Nu	nucleophile
Ph	phenyl
pin	pinacolato
Piv	pivalyl
pKa	logarithmic acid dissociation constant
ppm	parts per million
^{<i>i</i>} Pr	<i>iso</i> -propyl
^{<i>n</i>} Pr	<i>n</i> -propyl
RT	room temperature
TBAF	tetra- <i>n</i> -butylammonium fluoride
TBAT	tetra- <i>n</i> -butylammonium triphenyldifluorosilicate
TBD	1,5,6-triazabicyclo[4.4.0]dec-1-ene
TBDPS	<i>tert</i> -butyldiphenylsilyl
TBS	<i>tert</i> -butyldimethylsilyl
Tf	trifluoromethanesulfonyl
THF	tetrahydrofuran
TLC	thin layer chromatography
TMEDA	tetramethylethylenediamine
TMS	trimethylsilyl
Ts	toluenesulfonyl
UV	ultraviolet

v/v	volume/volume
Z	zusammen
$[\alpha]_{\text{D}}^t$	specific rotation at temperature t and wavelength of sodium D line
μL	microlitre
μm	micrometre

List of Schemes

Chapter 1: Asymmetric Synthesis of Substituted Carbonyl Compounds *via* Transition Metal-Catalysed Allylic Substitution

Scheme 1. A general mechanism for the transition metal-catalysed allylic substitution reaction.	2
Scheme 2. Regioselectivity in the transition metal-catalysed allylic substitution reaction.	3
Scheme 3. A general mechanism for the asymmetric transition metal-catalysed allylic substitution reaction.	5
Scheme 4. General approaches towards the asymmetric synthesis of substituted carbonyl compounds <i>via</i> allylic substitution.	11
Scheme 5. A general scheme for the transition metal-catalysed asymmetric allylic alkylation of unstabilised enolates.	12
Scheme 6. General mechanism for the decarboxylative allylation reaction of allyl enol carbonates and allyl β -ketoesters.	24
Scheme 7. Evidence for an outer-sphere mechanism in the palladium-catalysed decarboxylative allylic alkylation reaction.	29
Scheme 8. Retention of configuration in the palladium-catalysed allylic alkylation of an acyclic acetate with the lithium enolate of acetophenone.	40
Scheme 9. Acetoxy Meldrum's acid as an acyl anion equivalent in the palladium-catalysed allylic substitution reaction.	46
Scheme 10. General hypothesis for the asymmetric transition metal-catalysed allylic substitution with an acyl anion equivalent.	47

Chapter 2: Rhodium-Catalysed Allylic Substitution with an Acyl Anion Equivalent: Asymmetric Construction of Acyclic Quaternary Carbon Stereogenic Centres

Scheme 1. Regiospecific rhodium-catalysed allylic substitution reactions.	54
Scheme 2. Proposed <i>enyl</i> intermediate in the rhodium-catalysed allylic substitution reaction.	58

Scheme 3. Mechanistic model for the regioselective rhodium-catalysed allylic substitution reaction.	61
Scheme 4. Mechanistic model for the stereoselective rhodium-catalysed allylic substitution reaction.	62
Scheme 5. Proposed asymmetric synthesis of acyclic α -quaternary substituted ketones <i>via</i> regio- and stereoselective rhodium-catalysed allylic substitution.	63
Scheme 6. One pot deprotection of the cyanohydrin adducts 27 and 28 (R = Ph(CH ₂) ₂ , Ar = Ph).	66
Scheme 7. Proposed rationale for the regiochemical outcome of the rhodium-catalysed allylic substitution of the tertiary carbonate 26 with the cyanohydrin 24 . .	72
Scheme 8. Base-mediated consumption of the linear regioisomer 30 (R = Ph(CH ₂) ₂ , Ar = Ph).	73
Scheme 9. Synthesis of the tertiary allylic carbonates 26a-k	74
Scheme 10. General scheme for the asymmetric alkylation of an acyclic α,α -disubstituted enolate.	82
Scheme 11. Proposed stereoselective rhodium-catalysed allylic substitution with the aryl cyanohydrin 24	82
Scheme 12. Possible π - σ - π isomerisation in the alkylation of tertiary allylic carbonates with the aryl cyanohydrin 24	84
Scheme 13. Enantiodivergent synthesis of tertiary alcohols <i>via</i> lithiation-borylation of the benzylic carbamate 46	86
Scheme 14. One pot conversion of the tertiary allylic alcohol 45a to the acyclic α -aryl ketone 52a	88
Scheme 15. Proposed stereoselective rhodium-catalysed allylic substitution with the alkyl or alkenyl cyanohydrins iii	98
Scheme 16. Low temperature deprotection in the rhodium-catalysed allylic substitution with the alkenyl cyanohydrin 56 (Y = aryl or alkyl).	100
Scheme 17. Synthesis of the disubstituted (<i>E</i>)-alkenyl cyanohydrins 56b-k	103
Scheme 18. Potential γ -alkylation in the rhodium-catalysed allylic substitution with the allylic anion i	105
Scheme 19. Selective 1,4-reduction of the α,β -unsaturated ketone 60q to provide the α,α' -dialkyl ketone 73 (Y = Ph(CH ₂) ₂ , L = P(OPh) ₃).	110
Scheme 20. Proposed stereoselective rhodium-catalysed allylic substitution of secondary carbonates with an acyl anion equivalent.	112

Scheme 21. Undesired alkene isomerisation in the rhodium-catalysed allylic substitution of the secondary carbonate **75** with the cyanohydrin **24** (R = Ph(CH₂)₂, Ar = Ph)..... 113

List of Tables

Chapter 2: Rhodium-Catalysed Allylic Substitution with an Acyl Anion Equivalent: Asymmetric Construction of Acyclic Quaternary Carbon Stereogenic Centres

Table 1. Initial examination of acyl anion equivalents in the rhodium-catalysed allylic substitution reaction ($R_1 = \text{Ph}(\text{CH}_2)_2$).....	65
Table 2. Effect of metal:ligand stoichiometry on the rhodium-catalysed allylic substitution with the acyl anion equivalent 24 ($R = \text{Ph}(\text{CH}_2)_2$, $\text{Ar} = \text{Ph}$).....	68
Table 3. Effect of the ligand on the rhodium-catalysed allylic substitution with the acyl anion equivalent 24 ($R = \text{Ph}(\text{CH}_2)_2$, $\text{Ar} = \text{Ph}$).....	69
Table 4. Effect of the reaction temperature on the rhodium-catalysed allylic substitution with the acyl anion equivalent 24 ($R = \text{Ph}(\text{CH}_2)_2$, $\text{Ar} = \text{Ph}$, $L = \text{P}(\text{O}-2,4\text{-di-}^t\text{BuC}_6\text{H}_3)_3$).....	70
Table 5. Synthesis of the aryl cyanohydrins 24a-h	75
Table 6. Substrate scope of the rhodium-catalysed allylic alkylation with the aryl cyanohydrins 24 ($L = \text{P}(\text{O}-2,4\text{-di-}^t\text{BuC}_6\text{H}_3)_3$).....	76
Table 7. Substrate scope of the rhodium-catalysed allylic alkylation with the tertiary allylic carbonates 26 ($L = \text{P}(\text{O}-2,4\text{-di-}^t\text{BuC}_6\text{H}_3)_3$, $\text{Ar} = \text{Ph}$).....	78
Table 8. Asymmetric synthesis of the tertiary alcohol 45a <i>via</i> lithiation-borylation of the carbamate 48a	87
Table 9. Effect of the phosphite ligand in the stereospecific rhodium-catalysed allylic substitution with the acyl anion equivalent 24 ($R = \text{Ph}$, $\text{Ar} = \text{Ph}$).....	90
Table 10. Synthesis of the enantiomerically enriched benzylic carbamates 48a-e	92
Table 11. Synthesis of the enantiomerically enriched tertiary allylic alcohols 45a-e	93
Table 12. Substrate scope of the stereospecific rhodium-catalysed allylic alkylation with the aryl cyanohydrins 24 ($L = \text{P}(\text{OCH}_2\text{CF}_3)_3$, $R = \text{Ph}$).....	94
Table 13. Substrate scope of the stereospecific rhodium-catalysed allylic alkylation with the tertiary allylic alcohols 45 ($L = \text{P}(\text{OCH}_2\text{CF}_3)_3$, $\text{Ar} = \text{Ph}$).....	96
Table 14. Initial examination of various alkyl- and alkenyl-substituted cyanohydrins in the rhodium-catalysed allylic alkylation of 26a	99

Table 15. Optimisation of the rhodium-catalysed allylic substitution with the alkenyl cyanohydrins 56 (R = Ph(CH ₂) ₂).	102
Table 16. Substrate scope of the rhodium-catalysed allylic alkylation with the aryl-substituted alkenyl cyanohydrins 56 (Conditions A , R = Ph(CH ₂) ₂ , L = P(OPh) ₃).	104
Table 17. Substrate scope of the rhodium-catalysed allylic alkylation with the alkyl-substituted alkenyl cyanohydrins 56 (Conditions B , L = P(OPh) ₃).	107
Table 18. Substrate scope of the rhodium-catalysed allylic alkylation with the trisubstituted alkenyl cyanohydrins 69 (Conditions B , L = P(OPh) ₃).	108
Table 19. Stereospecific rhodium-catalysed allylic alkylation with the alkenyl cyanohydrin 56	111
Table 20. Initial studies towards the rhodium-catalysed allylic alkylation of secondary carbonates with an acyl anion equivalent (R ₁ = Ph(CH ₂) ₂).	114
Table 21. Initial optimisation of the rhodium-catalysed allylic substitution of secondary carbonates with the electron rich aryl cyanohydrin 24 (Ar = 4-Me ₂ NC ₆ H ₄).	116

List of Figures

Chapter 1: Asymmetric Synthesis of Substituted Carbonyl Compounds *via* Transition Metal-Catalysed Allylic Substitution

Figure 1. Chiral ligands used in the asymmetric allylic alkylation of enamines. 16

Figure 2. Evidence for an inner-sphere mechanism in the palladium-catalysed decarboxylative allylic alkylation reaction. 30

Chapter 2: Rhodium-Catalysed Allylic Substitution with an Acyl Anion Equivalent: Asymmetric Construction of Acyclic Quaternary Carbon Stereogenic Centres

Figure 1. Experimental evidence for the *enyl* binding mode in rhodium-allyl complexes..... 59

Chapter 1

Asymmetric Synthesis of Substituted Carbonyl Compounds *via* Transition

Metal-Catalysed Allylic Substitution

1.1. Transition Metal-Catalysed Allylic Substitution Reactions

1.1.1. Introduction

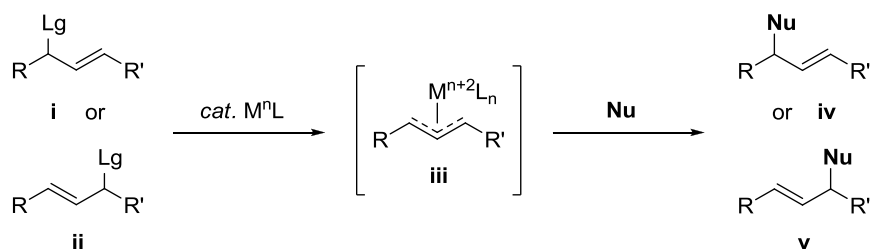
Since its discovery in 1965, the allylic substitution reaction has become one of the most powerful and widely used transformations in organic synthesis.¹ This can largely be attributed to the unrivalled scope and versatility of this process, which allows for the catalytic asymmetric construction of a wide range of C-C, C-N, C-O and C-S bonds. Although this reaction was classically carried out using palladium catalysts,² a number of different metals have since been shown to be effective, including molybdenum,³ tungsten,⁴ iridium,⁵ rhodium,⁶ ruthenium,⁷ nickel,⁸ copper⁹ and iron.¹⁰ The substrate scope has grown to include a range of stabilised and unstabilised carbon and heteroatom nucleophiles, which can be successfully coupled with a vast array of allylic electrophiles to afford products with up to two new stereogenic centres, either or both of which may be quaternary. The transition metal-catalysed allylic substitution has already found significant application in total synthesis,^{1,11} and the continuing development of this process is driven by the numerous challenges associated with the synthesis of complex biologically active molecules.

1.1.2. Reaction Mechanism

1.1.2.1. General Mechanism

A general mechanism for the transition metal-catalysed allylic substitution reaction is outlined in **Scheme 1**. Oxidative addition of a low valent transition metal to the

allylic substrate **i** or **ii** generates the η^3 π -allyl intermediate **iii**, which is then attacked by an external nucleophile at either allylic termini to afford the regioisomeric products **iv** and **v**, regenerating the active catalyst. In order to eliminate problems with regioselectivity, substrates which afford symmetrical π -allyl intermediates ($R = R'$) are often utilised. In cases where the π -allyl termini are inequivalent ($R \neq R'$), nucleophilic attack is often favoured at the less sterically hindered site, though this depends largely on the reaction conditions. Historically, stabilised carbon nucleophiles such as malonates are the most widely studied. However, recent advances have witnessed the utilisation of a vast array of stabilised and unstabilised carbon and heteroatom nucleophiles, each with unique properties in terms of regio- and stereoselectivity.

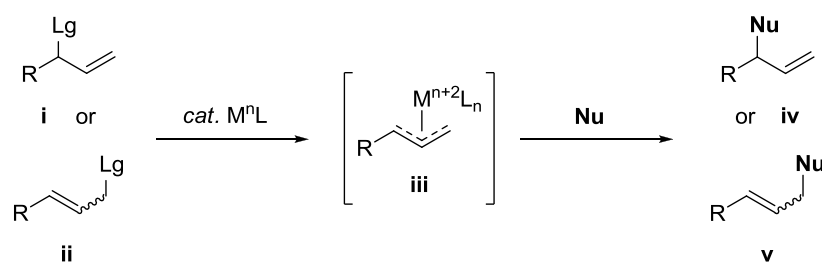


Scheme 1. A general mechanism for the transition metal-catalysed allylic substitution reaction.

1.1.2.2. Regiocontrol

In the absence of the substituent R' , oxidative addition generates an unsymmetrical monosubstituted π -allyl intermediate (**Scheme 2**), and the issue of regioselectivity becomes particularly prominent. The ability to garner the desired regiocontrol represents a longstanding problem, as alkylation at the substituted allylic terminus to afford the chiral product **iv** is often required, but not commonly observed under classical conditions. Alkylation at the less sterically hindered allylic terminus, to

afford predominantly the achiral linear regioisomer **v**, is often favoured by palladium catalysts. However, a mixture of regioisomers is frequently obtained, and the *E*:*Z* ratio of the linear product **v**, which is dependent on the geometry of the intermediate π -allyl complex, is often difficult to control. A number of studies have therefore focused on the development of highly regioselective allylic substitution reactions, with the aim of achieving complete control over the formation of both regioisomers **iv** and **v**.



Scheme 2. Regioselectivity in the transition metal-catalysed allylic substitution reaction.

Broadly speaking, the regiochemical outcome of the allylic substitution reaction represents a compromise between various steric and electronic factors. With palladium catalysts, steric factors tend to predominate, and the linear regioisomer **v** can be obtained with extremely high levels of selectivity when strong σ -donor ligands are employed,¹² or in the presence of various additives.¹³ In some circumstances, the (*E*)-isomer of **v** is afforded selectively, though it is generally more difficult to access the (*Z*)-isomer.¹⁴

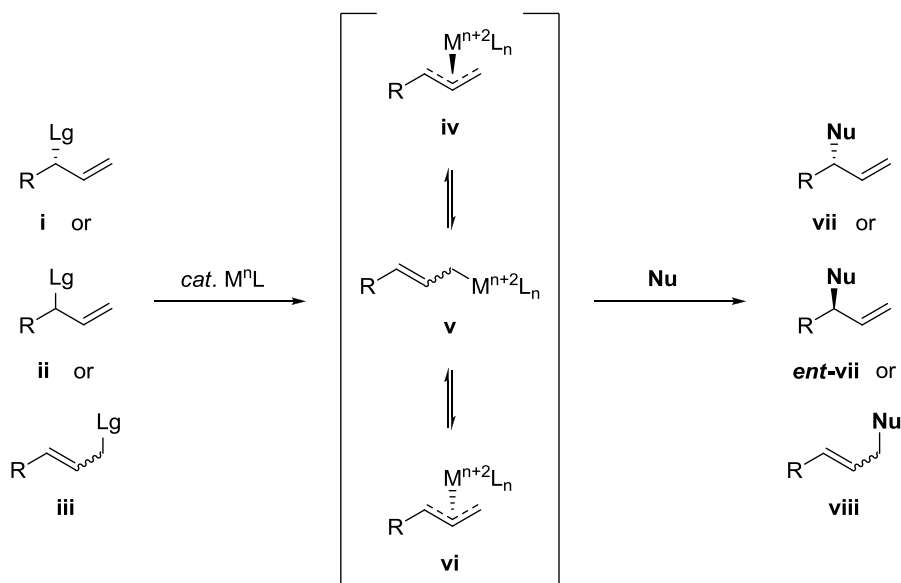
Despite the tendency of palladium catalysts to provide linear substitution products, this steric bias can be overcome by the judicious choice of catalyst, ligand and substrate. For example, in the palladium-catalysed allylic alkylation of malonates, a number of sterically¹⁵ and electronically¹⁶ biased ligands have been shown to

preferentially afford the branched product **iv**. Unsymmetrical bidentate ligands containing strong π -acceptor components, such as phosphites, are particularly effective in this regard. These ligands are proposed to generate greater positive charge character at the substituted terminus of the allyl fragment **iii**, rendering it more susceptible to nucleophilic attack. In this context, the nature of the substrate is critical, as the substituent R has the ability to stabilise the positive charge character contained within the allyl moiety. Aryl- and heteroaryl-substituted π -allyl complexes, in which this developing positive charge is resonance stabilised by the substituent, are more likely to furnish the branched regioisomer **iv**. Although the regioselectivity is normally independent of the isomeric constitution of the starting material, selective substitution can sometimes be affected at the allylic terminus that originally bore the leaving group,¹⁷ though this “memory effect” is more commonly observed with metals other than palladium. In addition, functional groups within the substituent R that can chelate to the metal centre,¹⁸ or hydrogen bond to the nucleophile,¹⁹ have been shown to direct nucleophilic attack to the substituted allylic terminus.

In some circumstances, complete regioselectivity favouring the branched product **iv** can now be achieved using palladium complexes. However, the most significant advances have been made with alternative metal catalysts. A number of metals, including molybdenum, tungsten, iridium and rhodium, have been shown to afford the branched substitution product **iv** with remarkably high levels of selectivity. With the use of these metals, the substrate scope of the reaction has also grown significantly, and is now extensive. This has allowed for the development of a variety of asymmetric allylic substitution reactions, in which both the regio- and stereochemical outcome of the alkylation is controlled by a single metal complex.

1.1.2.3. Stereocontrol

In general, there are three possible pathways for the asymmetric alkylation of monosubstituted π -allyl complexes, as outlined in **Scheme 3**. Each pathway has the ability, at least in principle, to furnish both enantiomers of the product **vii** and *ent-vii*, in addition to the achiral linear regioisomer **viii**.



Scheme 3. A general mechanism for the asymmetric transition metal-catalysed allylic substitution reaction.

Stereospecific reactions, in which the enantiomerically enriched substrate **i** is converted to the enantiomerically enriched product, were among the first to be developed. Though these reactions classically proceed with overall retention of absolute configuration,²⁰ this depends largely on the nature of the nucleophile. Although there are exceptions,²¹ oxidative addition of the metal to the enantiomerically enriched substrate **i** normally proceeds on the face opposite the leaving group, to afford the π -allyl complex **iv** with inversion of absolute configuration. Stabilised nucleophiles then attack the allyl fragment directly, on the face opposite the metal centre, to afford the product of overall retention (**vii**).

Conversely, unstabilised nucleophiles attack the allyl moiety *via* direct addition to the metal centre, followed by reductive elimination. This results in nucleophilic addition on the same face as the metal, furnishing **ent-vii**, the product of overall inversion. In order for a highly stereospecific reaction to occur, interconversion of the enantiomeric complexes **iv** and **vi**, which proceeds *via* the σ -allyl complex **v**, must be slower than nucleophilic attack. This π - σ - π isomerisation, though often essential for the enantioselective variant, is the most common source of stereochemical leakage in the alkylation step.

If a chiral metal complex is employed, racemic or achiral substrates can also be readily converted to the enantiomerically enriched products **vii** and **ent-vii**. These transformations have been studied extensively in recent years, and high levels of asymmetric induction can now be achieved with a number of transition metal catalysts. Classically, these reactions utilised symmetrical substrates containing two enantiotopic allylic termini, which could be distinguished by the nucleophile in the presence of a suitable chiral ligand.² However, recent advances have allowed for the regio- and enantioselective allylic substitution of unsymmetrical monosubstituted derivatives such as **ii** and **iii**. In the presence of a chiral ligand, the π -allyl complexes **iv** and **vi** are diastereomeric, and afford opposite enantiomers of the product upon nucleophilic attack. In this context, enantioselective allylic substitution reactions often depend on the differential reactivity of these complexes, which may be generated from either the racemic substrate **ii** or the achiral linear substrate **iii**.

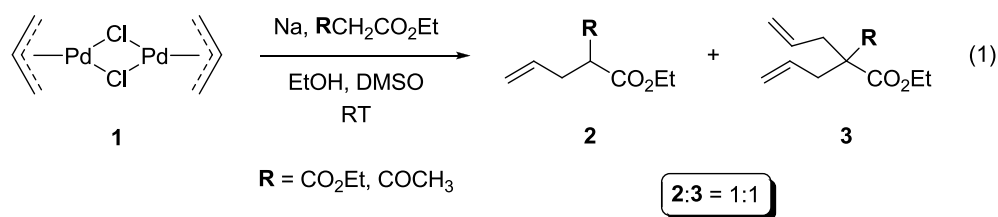
When the racemic substrate **ii** is employed, the reaction proceeds *via* a dynamic kinetic asymmetric transformation (DYKAT),²² in which both enantiomers of the substrate are converted to the same enantiomer of the product. In order for a highly stereoselective reaction to occur, the π -allyl intermediates **iv** and **vi**, which afford

opposite enantiomers of the product, must react with the nucleophile at substantially different rates. The interconversion of **iv** and **vi** must also be faster than nucleophilic attack, as the initial oxidative addition should provide a 1:1 mixture of these two intermediates. This is in sharp contrast to the stereospecific variant of the reaction, where this π - σ - π isomerisation is generally detrimental to the stereochemical outcome.

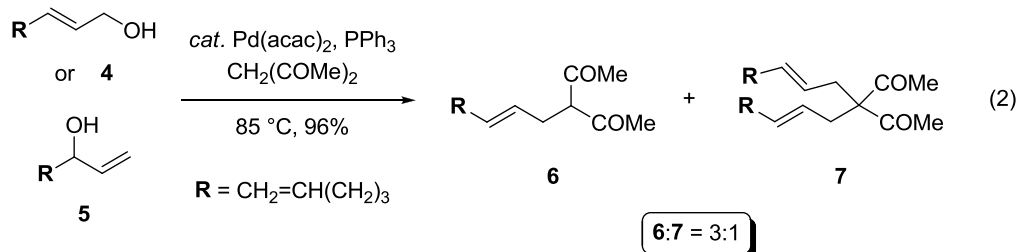
The asymmetric allylic substitution reaction may also proceed from the achiral linear substrate **iii**. In terms of stereocontrol, these reactions are governed by many of the same considerations as those that utilise the racemic substrate **ii**. However, in these cases, the chiral metal catalyst sometimes has the ability to distinguish between the enantiotopic faces of the olefin **iii**,²³ resulting in the selective formation of **iv** or **vi**, and providing another potential source of enantiodiscrimination. In some circumstances, the chiral π -allyl complex can also differentiate between the two enantiotopic faces of a prochiral nucleophile, such as a ketone enolate. In this context, a number of highly enantio- and diastereoselective allylic alkylations, in which new stereogenic centres are formed on both the electrophile and the nucleophile, have recently been described.

1.1.3. Seminal Work

In 1965, Tsuji reported the first stoichiometric allylic alkylation reaction.²⁴ Treatment of π -allylpalladium chloride dimer **1** with the sodium salts of both ethyl malonate and ethyl acetoacetate yielded a 1:1 mixture of the mono- and bis-allylated products **2** and **3** in good overall yield (eq. 1). Interestingly, in the same paper, the reaction of **1** with a cyclohexanone-derived enamine was reported to proceed smoothly under almost identical conditions, which represents the first example of a transition metal-mediated allylic alkylation using an enolate equivalent.

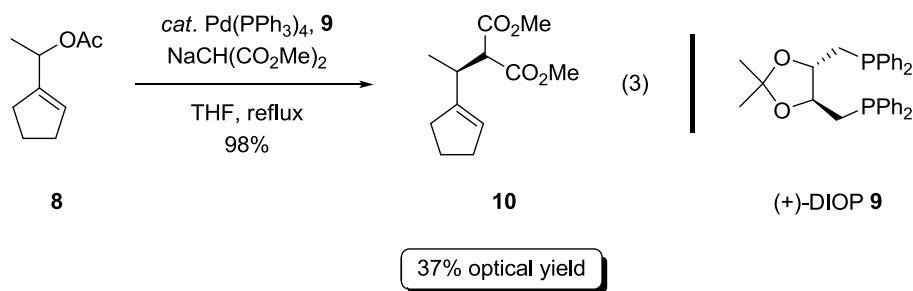


The first catalytic allylic substitution reactions were reported in 1970, when both Atkins and Hata described the palladium-catalysed allylation of a variety of carbon, nitrogen and oxygen-based nucleophiles.²⁵ For example, alkylation of the allylic alcohols **4** and **5** with acetylacetone proceeded readily in the presence of catalytic Pd(acac)₂ and triphenylphosphine, affording a 3:1 mixture of the mono- and bis-allylated products **6** and **7** (eq. 2). Interestingly, the allylic alcohols **4** and **5** both yielded the same linear regioisomer of the alkylated product, and with identical selectivity, which strongly suggests that both reactions proceed through a common π -allyl intermediate.



In light of these important findings, the next logical goal was the development of an asymmetric allylic alkylation reaction. In 1976, Trost demonstrated that the palladium-catalysed allylic alkylation of stabilised carbon nucleophiles proceeds with overall retention of absolute configuration.²⁰ A year later, the first catalytic asymmetric allylic alkylation was reported.²⁶ Treatment of the racemic acetate **8** with dimethyl malonate in the presence of Pd(PPh₃)₄ and the chiral phosphine **9** afforded the alkylated product **10** in excellent yield and with modest optical purity. In this study, it was observed that a slightly bulkier nucleophile, namely the sodium salt of

methyl phenylsulfonyl acetate, afforded a slight increase in enantiomeric excess. As the starting material **8** is racemic, this reaction also represents the first reported example of a dynamic kinetic asymmetric transformation (DYKAT). The presence of excess phosphine ligand was proposed to reduce the rate of alkylation relative to π - σ - π isomerisation, which is critical to the observed stereoselectivity.



Since these pioneering works, the allylic substitution reaction has reached a remarkable level of sophistication, and now represents one of the most versatile and widely used transformations in organic synthesis. The expansion of the substrate scope, particularly with respect to the nucleophile, has been critical in the ongoing development of this process. Only a few decades ago, the allylic substitution was almost entirely limited to stabilised carbon and heteroatom nucleophiles, such as malonates, amines and alcohols. Unstabilised carbon nucleophiles, broadly defined as those derived from conjugate acids with a pK_a greater than 20, were generally considered to be incompatible with the reaction conditions, largely due to their inherent basicity. However, although many of the early attempts to utilise these species were indeed unsuccessful,²⁷ these limitations have been overcome in recent times, and a number of unstabilised carbon nucleophiles have found significant application in the transition metal-catalysed allylic substitution reaction. Among these, prochiral ketone, ester and amide enolates represent some of the most widely studied, as the asymmetric allylic alkylation of these nucleophiles provides direct

access to a range of enantiomerically enriched α -substituted carbonyl compounds, which are common to a variety of biologically active natural products and pharmaceutical agents.

1.2. Asymmetric Synthesis of Substituted Carbonyl Compounds *via* Transition Metal-Catalysed Allylic Substitution

1.2.1. Introduction

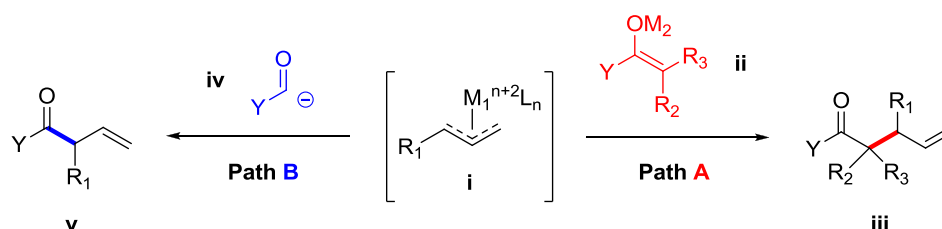
The synthesis of carbonyl compounds, particularly those containing α -stereogenic centres, remains a significant area of interest in organic chemistry. This is largely due to their versatility as synthetic intermediates, and the presence of such motifs in a range of complex bioactive natural products and pharmaceutical agents. In terms of allylic substitution reactions, two conceptually different approaches can be envisaged for the asymmetric synthesis of substituted carbonyl compounds, as outlined in **Scheme 4**. Path A, which is by far the most widely studied, involves the addition of an unstabilised enolate derivative to the π -allyl intermediate **i**. This reaction allows for the direct derivitisation of an existing carbonyl compound, with the concomitant formation of up to two new stereogenic centres. In contrast, the use of an acyl anion equivalent (path B) provides the α -substituted carbonyl compound **v** *via* a fundamentally different bond forming event, in which the acyl functionality is installed directly into the allylic framework.

According to the precise nature of the nucleophile, these reactions can be divided into three important classes, which will form the basis of the following review. These involve the use of:

- Enolate equivalents, such as enamines and silyl enol ethers
- Metal enolates, directly derived from deprotonation of the parent carbonyl compound

- Acyl anion equivalents

The following review will highlight the most significant advances in this area, focusing primarily on the asymmetric construction of α -substituted carbonyl compounds. In general, the discussion will be limited to reactions that proceed *via* π -allyl organometallic intermediates, and will be organised according to the type of nucleophile employed. Particular attention will be paid to the historical development of each methodology, their scope and limitations, and the utilisation of these reactions in total synthesis.



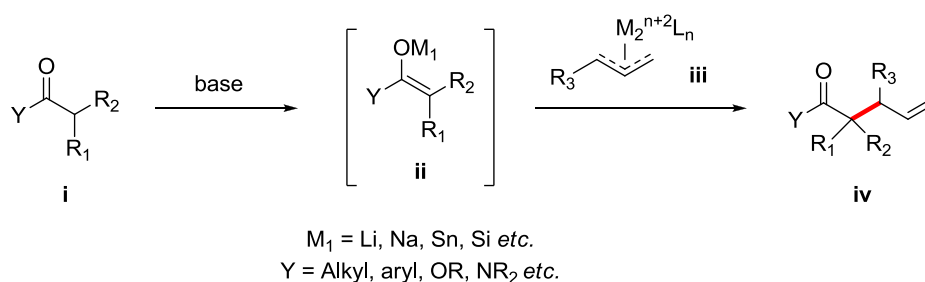
Scheme 4. General approaches towards the asymmetric synthesis of substituted carbonyl compounds *via* allylic substitution.

1.2.2. Transition Metal-Catalysed Allylic Substitution Reactions using Unstabilised Enolate Nucleophiles

1.2.2.1. Introduction

Carbonyl functionalities, and their adjacent carbon atoms, have been shown to undergo a vast array of synthetic transformations. Among these, the enolate alkylation reaction represents one of the most fundamental, and there are a number of different approaches towards the enantioselective alkylation of prochiral enolate derivatives, to afford enantiomerically enriched α -substituted carbonyl compounds. Some of the most significant advancements have been made using chiral auxiliaries such as pseudoephedrine.²⁸ However, these methods have arguably been superseded

by catalytic versions, which are considerably more attractive in terms of reaction efficiency and atom economy. Proline-based organocatalysts have proven particularly effective in the asymmetric α -alkylation of aldehydes,²⁹ and phase transfer catalysts have been utilised extensively in the asymmetric alkylation of amino acid derivatives.³⁰ Transition metal catalysts have also found significant application in the enolate alkylation reaction. For example, Jacobsen recently reported the chromium-catalysed asymmetric alkylation of both cyclic and acyclic tributyltin enolates with alkyl halides.³¹ A number of methods for the asymmetric enolate arylation³² and vinylation,³³ generally catalysed by palladium complexes, have also been described.



Scheme 5. A general scheme for the transition metal-catalysed asymmetric allylic alkylation of unstabilised enolates.

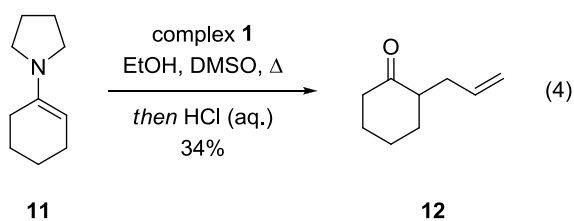
Despite this work, the allylic alkylation of unstabilised enolates, as outlined in **Scheme 5**, remains arguably the most prevalent method for the asymmetric synthesis of α - and β -substituted carbonyl compounds. The use of a prochiral nucleophile ($R_1 \neq R_2$) is the most common approach towards enantioinduction, resulting in the formation of a tertiary or quaternary α -stereogenic centre. In addition, the use of a substituted allylic electrophile ($R_3 \neq \text{H}$) permits the formation of a β -stereogenic centre. The absolute configuration at this centre, which is on the π -allyl complex **iii**, may be controlled by one of the allylic substitution mechanisms outlined in **Scheme**

3, while the enantioselectivity of the α -alkylation is generally governed by a combination of the enolate geometry and the π -facial selectivity of the nucleophilic attack. In this context, the enolate geometry is critical, as the *E*- and *Z*-isomers of **ii** often provide opposite enantiomers of the product. The use of cyclic ketones, wherein the enolate geometry is generally governed by the ring size, provides the most common solution to this problem. In order to circumvent the issues relating to regioselective enolisation and alkylation, and polyalkylation *via* enolate equilibration, it is often necessary to employ substrates containing only one enolisable site (e.g. Y = Ph), or enolate equivalents that have been generated regioselectively under kinetic or thermodynamic control. Although recent developments have allowed for the utilisation of enolate anions (e.g. M₁ = Li), much of the seminal work was carried out using enolate equivalents, which also provide significantly milder reaction conditions.

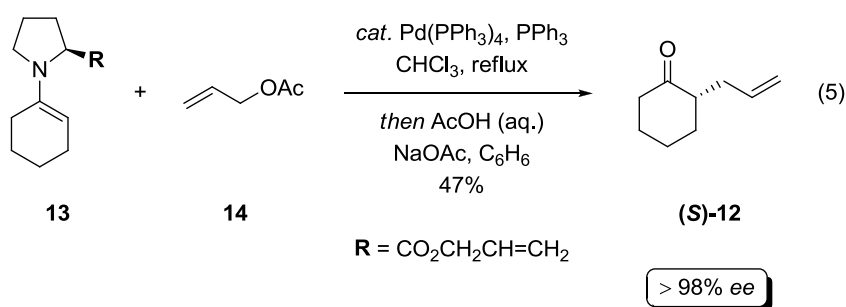
1.2.2.2. Enolate Equivalents

1.2.2.2.1. Enamines

Enamines are highly prevalent nucleophiles in organic synthesis, and were among the first to be utilised in the allylic substitution reaction. Interestingly, the first example of their use was reported alongside the first ever allylic substitution reaction.²⁴ Treatment of the enamine **11** with π -allylpalladium chloride dimer **1** in ethanol and DMSO, followed by hydrolysis using aqueous hydrochloric acid, yielded the α -substituted ketone **12** in 34% yield (eq. 4). Although this reaction is stoichiometric in palladium and low yielding, it provided an important platform for the catalytic asymmetric variants that were later reported.

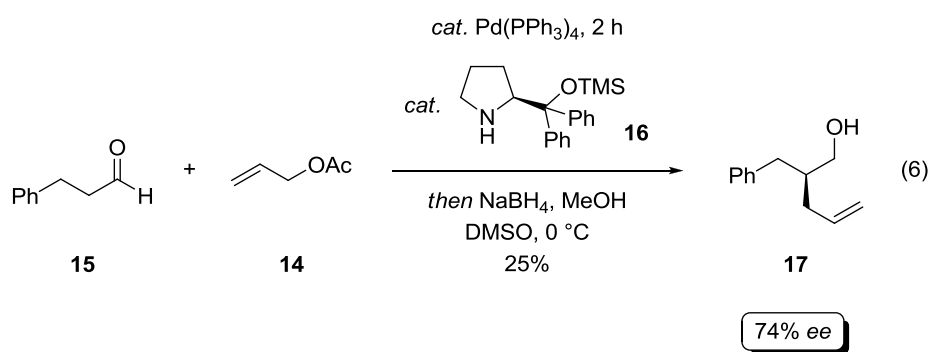


In 1994, Hiroi described the palladium-catalysed asymmetric allylation of chiral enamines, to afford α -substituted ketones with up to 98% *ee*.³⁴ For example, alkylation of the enamine **13** with allyl acetate was shown to proceed efficiently in the presence of catalytic Pd(PPh₃)₄ and triphenylphosphine, affording the ketone (*S*)-**12** upon acidic hydrolysis of the intermediate iminium ion (eq. 5). A small number of acyclic aldehyde enamines were also successfully employed, to provide aldehydes containing all carbon quaternary stereogenic centres. The main drawback of this approach is that it requires a stoichiometric quantity of the isolated chiral enamine, which effectively functions as a chiral auxiliary. The synthesis and isolation of enamines remains a challenge, and they are quite sensitive to hydrolysis, which makes them more difficult to store than their corresponding aldehydes and ketones.



This limitation was partially overcome by Córdova who, in 2006, described the asymmetric allylic alkylation of catalytically generated aldehyde and ketone enamines (eq. 6).³⁵ Upon stereoselective alkylation of the transient enamine, formed *via* condensation of the chiral amine **16** and the aldehyde **15**, the amine component is regenerated by *in situ* hydrolysis of the intermediate iminium ion. As a result, the

reaction is catalytic in the chiral amine **16**. Interestingly, the reaction time was also shown to be critical to the level of enantioselectivity, presumably because the α -substituted aldehyde products are particularly prone to racemisation. For this reason, the alkylated aldehydes were reduced *in situ* and isolated as their corresponding primary alcohols, as shown in eq. 6. In the presence of an achiral secondary amine, the reaction was highly efficient for a range of aldehydes and cyclic ketones, affording racemic products. However, despite extensive optimisation, the yields were relatively poor when a chiral amine was employed.



In the reactions outlined above, the enantioselectivity of the alkylation is controlled by a chiral functional group contained within the enamine nucleophile, which effectively functions as an auxiliary. However, a more attractive approach towards enantioinduction involves the use of a catalytic chiral ligand, which results in the formation of a chiral π -allyl electrophile. In principle, it would appear difficult to achieve asymmetric α -alkylation using this approach, as in these reactions the key bond forming event generally occurs outside the coordination sphere of the metal, and is therefore remote to the chiral environment. In contrast, the synthesis of enantiomerically enriched β -carbonyl compounds should be simplified, as in this scenario the newly formed stereogenic centre is on the π -allyl electrophile, and in close proximity to the chiral ligand. Regardless of the precise nature of the

nucleophile, an effective chiral ligand must have the ability to form a highly ordered transition state with both the nucleophile and the electrophile, particularly in the formation of α -substituted derivatives. In this context, a number of chiral ligands have been tested in the transition metal-catalysed allylic alkylation of enamines, a selection of which is outlined in **Figure 1**.

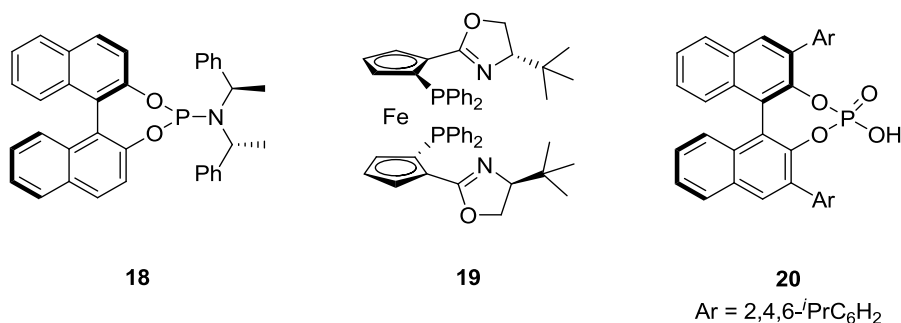
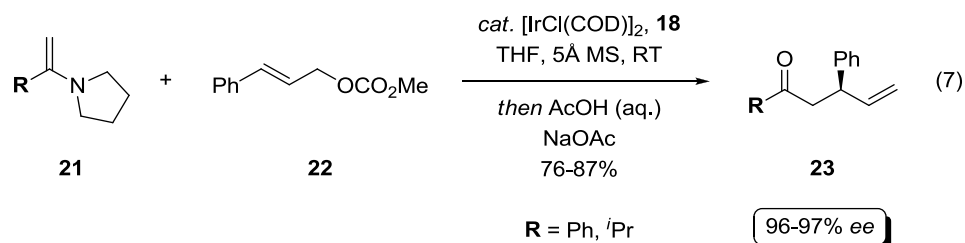


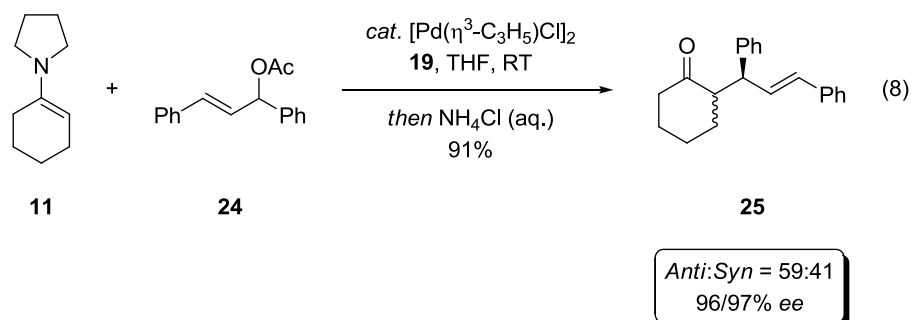
Figure 1. Chiral ligands used in the asymmetric allylic alkylation of enamines.

The enantioselective iridium-catalysed allylic substitution, which most commonly employs phosphoramidite ligands such as **18**, has recently become one of the most versatile methods for the construction of stereogenic carbon-carbon and carbon-heteroatom bonds.³⁶ In 2007, Hartwig demonstrated that $[\text{IrCl}(\text{COD})]_2$, in conjunction with the ligand **18**, provides an efficient catalyst for the asymmetric allylic alkylation of enamines.³⁷ For example, the reaction of cinnamyl methyl carbonate **22** with the enamine **21** was shown to afford the β -substituted ketone **23** in good yield and with excellent enantioselectivity (eq. 7). As is common with iridium catalysts, the reaction was highly regioselective, providing solely the branched regioisomer **23**. Although the reaction was initially limited to cinnamyl carbonates such as **22**, the use of a cyclometalated iridium complex was shown to permit the application of aliphatic derivatives. Additionally, enamines that were isolated as mixtures of regioisomers (e.g. $\mathbf{R} = \textit{i}$ Pr & \textit{i} Bu) were shown to react preferentially at

the less sterically hindered position. Importantly, this allows for the regioselective alkylation of unsymmetrical ketones containing two enolisable sites, a process which is often hindered by enolate equilibration and polyalkylation.

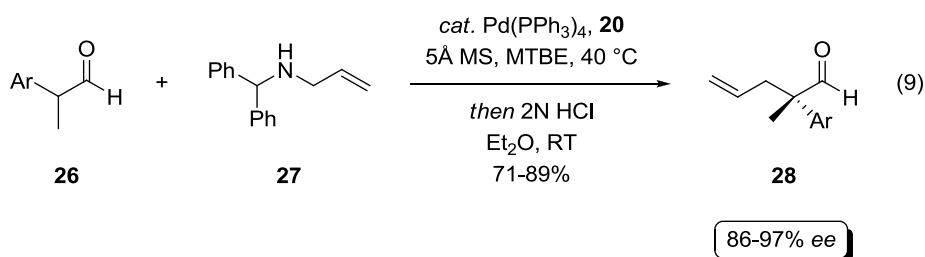


In 2007, Zhang described the palladium-catalysed allylic substitution of the cyclohexanone-derived enamine **11**.³⁸ Treatment of the acetate **24** with the enamine **11**, in the presence of catalytic $[\text{Pd}(\eta^3\text{-C}_3\text{H}_5)\text{Cl}]_2$ and the chiral P,N ligand **19**, afforded the enantiomerically enriched ketone **25** in 91% yield and with excellent enantioselectivity, but with poor diastereoselectivity (eq. 8). In this reaction, the chiral ligand is able to control the absolute configuration of the newly formed β -stereogenic centre, which is on the π -allyl electrophile, but fails to exert an influence on the prochiral nucleophile. As a result, the reaction affords an almost 1:1 mixture of α -epimers, both of which may be obtained in excellent enantiomeric excess.



Also in 2007, List described the enantioselective allylation of α -substituted aldehydes, catalysed by a combination of $\text{Pd}(\text{PPh}_3)_4$ and the chiral Brønsted acid **20** (eq. 9).³⁹ Addition of the allyl amine **27** to the aldehyde **26**, in the presence of a

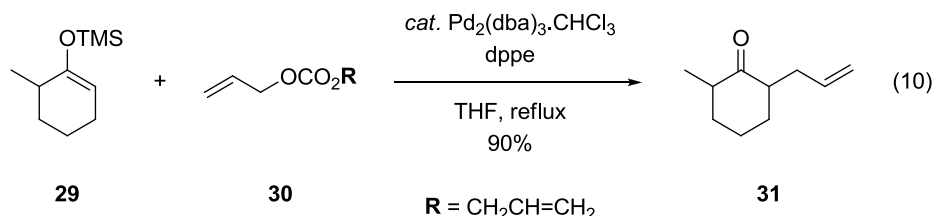
Brønsted acid, is proposed to generate an enamionium ion intermediate. Upon reaction with the palladium catalyst, this species should liberate both a prochiral enamine and a cationic π -allylpalladium complex. The phosphoric acid **19** effectively functions as an anionic ligand for palladium, and is also proposed to hydrogen bond to the enamine. This interaction is presumably critical in enabling the chiral π -allyl complex to differentiate between the enantiotopic faces of the prochiral enamine, which gives rise to the observed enantioselectivity. Overall, this process provides access to a range of highly enantiomerically enriched α -quaternary substituted aldehydes, which represent important intermediates in target directed synthesis. Indeed, this reaction was applied to a formal synthesis of the sesquiterpene natural product (+)-Cuparene.



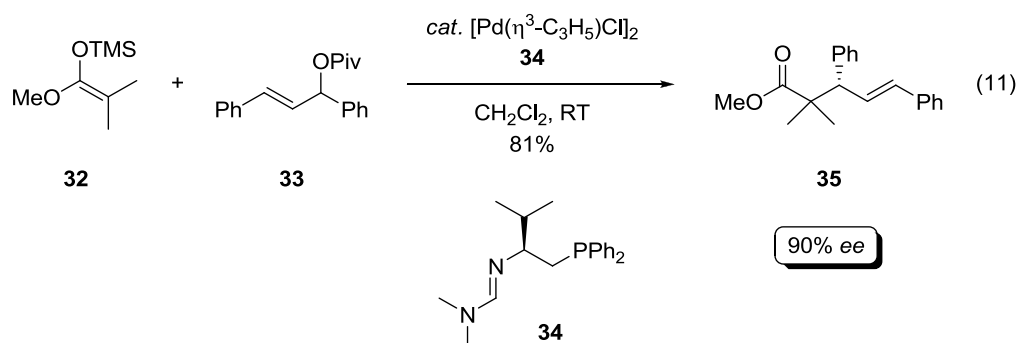
1.2.2.2.2. Silyl Enol Ethers

Silyl enol ethers, readily prepared from the corresponding carbonyl compounds, are reactive enolate equivalents, particularly in the presence of Lewis acid promoters. Much like enamines, silyl enol ethers were employed as nucleophiles in a number of seminal allylic alkylation reactions, paving the way for the development of asymmetric variants. For example, following an initial report by Trost,⁴⁰ Tsuji described the palladium-catalysed allylation of both aldehyde and ketone-derived silyl enol ethers.⁴¹ Treatment of the enol ether **29** with the allyl carbonate **30**, in the presence of catalytic $\text{Pd}_2(\text{dba})_3 \cdot \text{CHCl}_3$ and 1,2-bis(diphenylphosphino)ethane (dppe), furnished the substituted ketone **31** in excellent yield (eq. 10). In this reaction, the

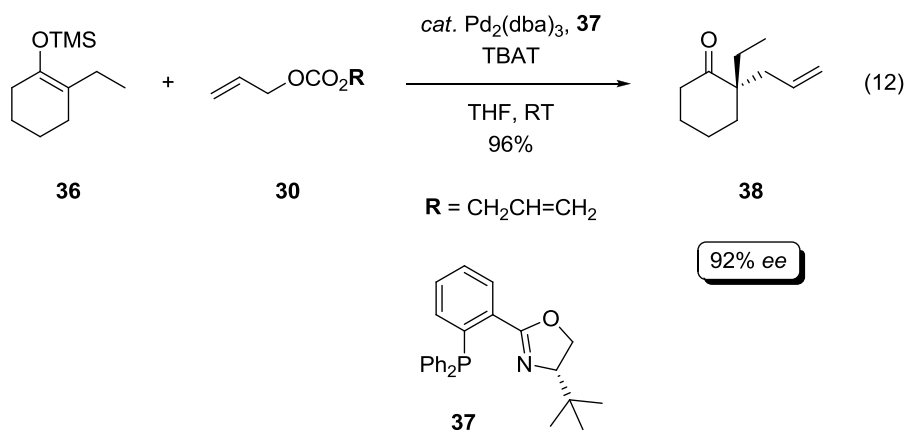
bidentate ligand dppe was shown to far superior to triphenylphosphine. As the reaction proceeds under mild conditions, in which no proton transfer takes place, it allows for the regioselective monoalkylation of unsymmetrical ketones, provided the enol ether can be prepared in a regioselective manner.



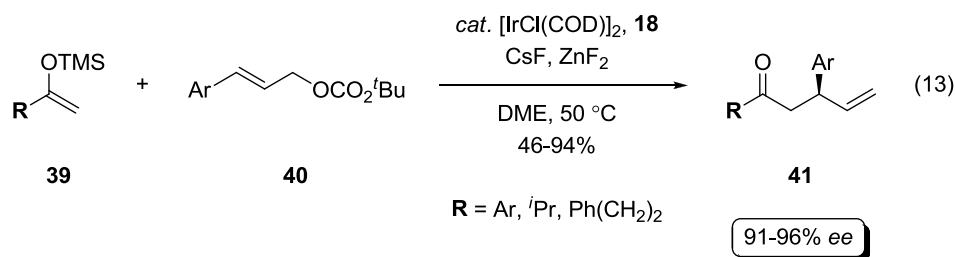
Despite the ability of this transformation to construct highly substituted carbonyl compounds under essentially neutral conditions, it remained largely unexplored over the next two decades, until the advent of asymmetric catalysis made it possible to develop asymmetric variants. For example, in 1998, Morimoto described the enantioselective allylic alkylation of ketene silyl acetals.⁴² Interestingly, these reactions had previously been reported to yield mixtures of allylated products and cyclopropane derivatives,⁴³ which are proposed to form *via* attack of the ester enolate on the central carbon of the π -allyl intermediate. However, in this case, the cyclopropanation pathway was not in operation, and the allylic alkylation products were obtained in good to excellent yield. The palladium catalyst, in conjunction with the bidentate amidine ligand **34**, was also shown to induce asymmetry in the reaction of the ketene silyl acetal **32** with the pivalate ester **33**, affording the β -substituted ester **35** in 90% *ee* (eq. 11). Unfortunately, the substrate scope of this transformation is poor, as ketene silyl acetals containing bulkier substituents, or *tert*-butyldimethylsilyl groups, are generally not tolerated.



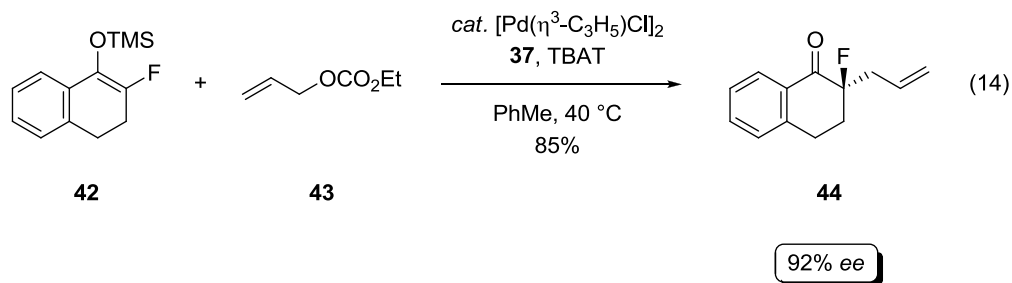
In an extension of Tsuji's seminal work, Stoltz reported the first enantioselective allylic alkylation of prochiral silyl enol ethers.⁴⁴ For example, treatment of the tetrasubstituted enol ether **36** with diallyl carbonate, in the presence of catalytic $\text{Pd}_2(\text{dba})_3$, the chiral ligand **37** and substoichiometric tetra-*n*-butylammonium difluorotriphenylsilicate (TBAT), afforded the enantiomerically enriched α -quaternary substituted ketone **38** in excellent yield. In this reaction, TBAT presumably serves to activate the enol ether **36**, thus initiating the alkylation. Although a wide range of silyl enol ethers are well tolerated, including those derived from 7- and 8-membered cyclic ketones, the reaction is limited to cyclic derivatives. This is presumably due to the difficulties associated with controlling the geometry of the enol ether in acyclic systems, particularly in the case of α,α -disubstituted ketones.⁴⁵ As part of this study, the cyclic ketone products were also readily converted to a range of bicyclic building blocks, thereby illustrating their synthetic utility.



In addition to enamines, silyl enol ethers have also been utilised as enolate equivalents in the enantioselective iridium-catalysed allylic substitution (eq. 13).⁴⁶ In terms of the catalyst, this reaction proceeds under similar conditions to that of enamines, however, in this case, a combination of two fluoride salts is required to activate the nucleophile. Indeed, the ratio of enol ether to CsF to ZnF₂ was shown to be critical to both the yield and selectivity of the alkylation. Interestingly, the reaction failed in the absence of CsF, and proceeded with poor regioselectivity in the absence of ZnF₂. Upon screening, a 1.5:0.4:1.5 ratio of these reaction components was found to be optimal, affording the ketone **41** with excellent regioselectivity, and almost wholly suppressing the competing bis-allylation of **39**. In a subsequent ligand screen, a range of phosphoramidite ligands were shown to afford the β -substituted ketone **41** in excellent enantiomeric excess, with the ligand **18** providing an ideal combination of regio- and enantioselectivity. Although alkyl-substituted allylic carbonates were also tolerated, these reactions proceeded with poor regioselectivity. Aliphatic silyl enol ethers generally afforded lower yields of the ketone **41**, possibly due to the formation of enolate regioisomers. Due to the precise reaction conditions that are required, it remains unclear whether a cesium, zinc or hypervalent silicon enolate is the reactive nucleophile in this process.



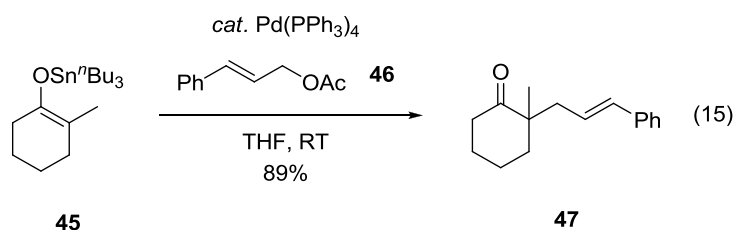
Although the presence of a fluorine atom has been shown to dramatically affect the activity of an array of bioactive molecules, there remains a paucity of methods for the introduction of stereogenic carbon-fluorine bonds. With this in mind, Paquin described the enantioselective allylation of fluorinated silyl enol ethers.⁴⁷ For example, under similar catalytic conditions to those previously employed by Stoltz, alkylation of the fluorinated enol ether **42** proceeded readily to afford the tertiary α -fluorinated ketone **44** in excellent enantiomeric excess (eq. 14). Though this reaction is also limited to cyclic substrates, it does tolerate cyclopentanone derivatives, which is in contrast to the method previously developed by Stoltz. Importantly, this method allows for the construction of substituted ketones containing stereogenic carbon-fluorine bonds, and provides an alternative to the more widely studied enantioselective electrophilic fluorination reaction, a process that is generally limited to 1,3-dicarbonyl compounds.



1.2.2.2.3. Enolstannanes

In 1983, upon finding that the palladium-catalysed allylic alkylation of silyl enol ethers could not be extended to substituted electrophiles, Trost described the highly

regioselective alkylation of the enolstannane **45** with a variety of substituted allylic acetates.⁴⁰ For example, the reaction of **45** with cinnamyl acetate proceeded readily at room temperature, in the presence of catalytic Pd(PPh₃)₄, furnishing the substituted ketone **47** in 89% yield and as a single regioisomer (eq. 15). Interestingly, this reaction afforded solely the (*E*)-isomer of the alkylated product, regardless of the geometry of the starting material. This process also displays impressive chemoselectivity, as exemplified by the alkylation of allylic acetates containing esters, ketones, alkyl halides and enol ethers.

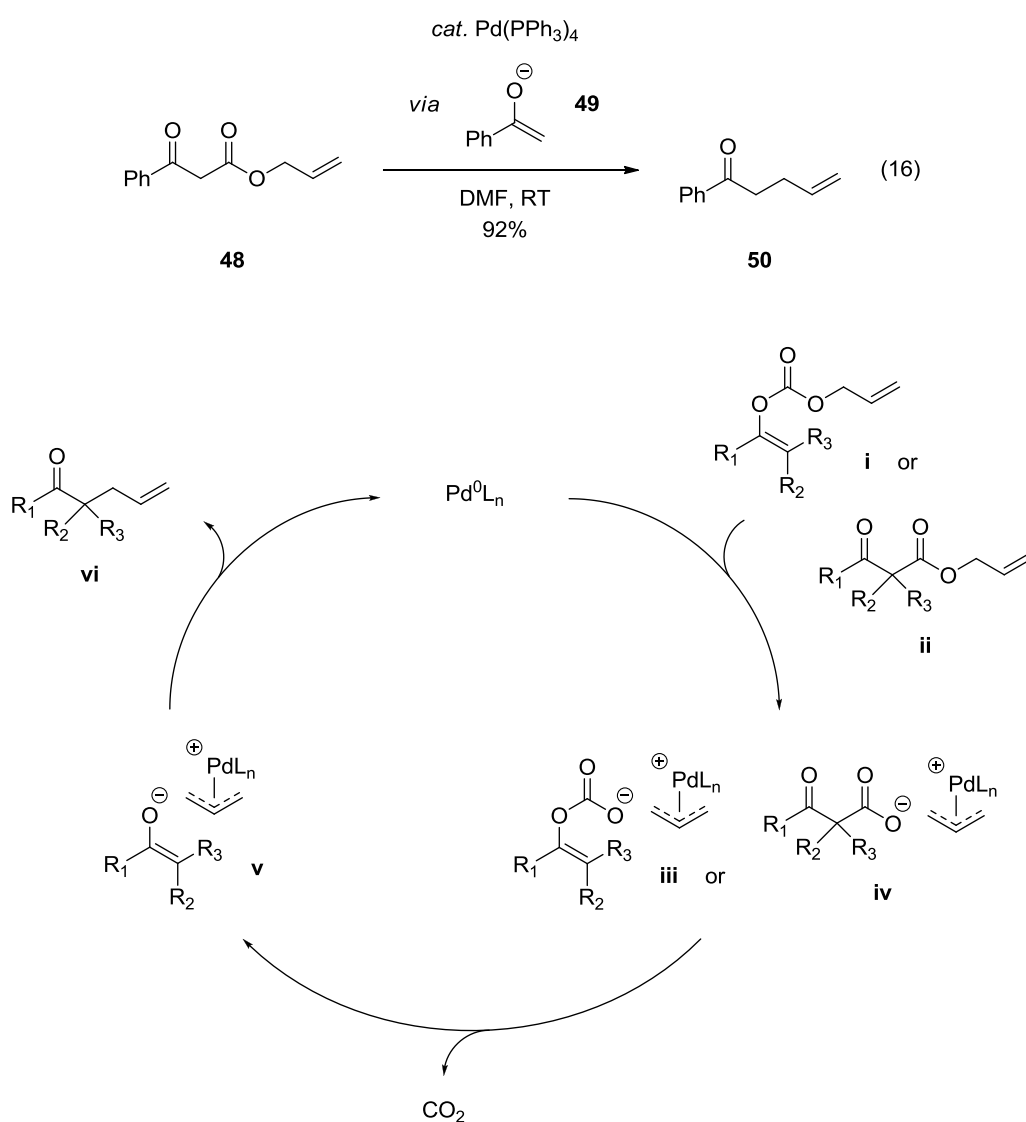


In addition to the reactions of isolated enolstannanes, tin enolates were also employed in the very first asymmetric alkylation of prochiral ketone enolates. However, in this case, the tin species was formed *in situ* via transmetalation of the corresponding lithium enolate. As such, these reactions will be discussed in section 1.2.2.3., along with those of lithium enolates.

1.2.2.2.4. Decarboxylative Approaches

The decarboxylation of allyl β -keto esters, or allyl enol carbonates, provides a particularly efficient method for the generation of nucleophilic ketone enolates.⁴⁸ The asymmetric alkylation of these species has been studied extensively in recent years, and now represents one of the most versatile and synthetically useful methods for the enantioselective synthesis of α - and β -substituted carbonyl compounds. Much of the seminal work in this area was carried out by Saegusa and Tsuji, who independently described the first palladium-catalysed decarboxylative allylic alkylation reactions of

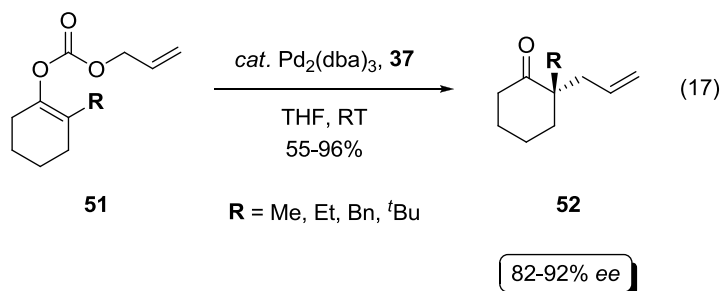
allyl β -ketoesters.⁴⁹ For example, the ester **48**, upon treatment with catalytic $\text{Pd}(\text{PPh}_3)_4$ at room temperature, was shown to afford the monoalkylation product **50** in excellent yield (eq. 16). Presumably, this reaction proceeds *via* the acetophenone enolate **49**, which is known to be a challenging substrate for monoalkylation. In the years following this study, the reaction was also extended to a range of β -substituted allyl esters, and catalysts derived from molybdenum, nickel and rhodium were shown to be effective.



Scheme 6. General mechanism for the decarboxylative allylation reaction of allyl enol carbonates and allyl β -ketoesters.

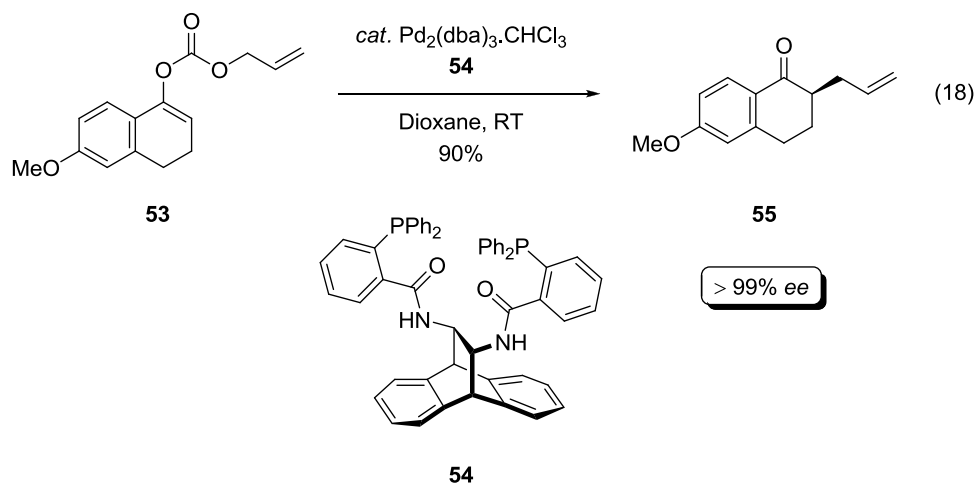
A general mechanistic pathway for this transformation is outlined in **Scheme 6**. The reactive palladium enolate **v** can be envisaged to form *via* decarboxylation of either the carbonate **iii** or the carboxylate **iv**, which may be generated by oxidative addition of the palladium catalyst into the enol carbonate **i** or the β -ketoster **ii**, respectively. Upon decarboxylation, the nucleophilic enolate is able to recombine with the cationic π -allylpalladium complex to furnish the alkylated product **vi**, and regenerate the palladium(0) catalyst. Though depicted as an ion pair, the precise nature of the palladium(II) enolate **v** is not well defined, and the reactive intermediate could also exist as either a covalently bonded C- or O-bound palladium enolate, or as an oxa- π -allyl complex.

In comparison to the alternative methods, the decarboxylative allylic alkylation of ketone enolates offers a number of significant advantages. Firstly, the allyl ester effectively functions as a directing group for enolisation, so the enolate formation, and hence the alkylation, can be achieved in a highly regioselective manner. Secondly, as the elimination of carbon dioxide drives the enolate formation, the reactive nucleophile may be generated catalytically, and under extremely mild conditions. Combined, these factors serve to minimise enolate equilibration, which prevents loss of regioselectivity in a substrate containing two enolisable sites, polyalkylation, and the racemisation of a newly formed tertiary stereogenic centre.



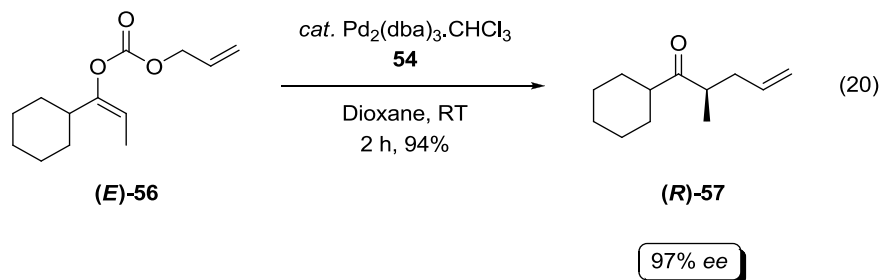
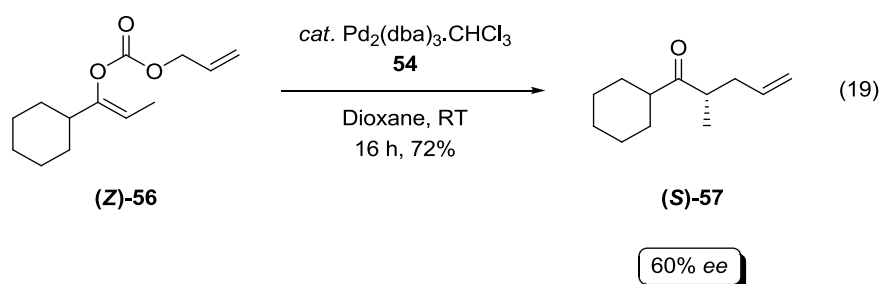
In 2004, Stoltz reported the first asymmetric decarboxylative allylic alkylation of prochiral enol carbonates.⁴⁵ Treatment of the enol carbonates **51** with Pd₂(dba)₃ and the P,N ligand **37**, which is also effective in the alkylation of silyl enol ethers, furnished the α -quaternary substituted ketones **51** in moderate to excellent yield and good to excellent enantiomeric excess (eq. 17). In addition to the cyclohexanone derivatives shown, this process is also tolerant of 7- and 8-membered ring systems. In a subsequent study, the corresponding racemic allyl β -ketoesters, which should provide the same palladium(II) enolate intermediate, were shown to afford the α -alkylated ketones **52** under identical reaction conditions.⁵⁰

In 2005, Trost reported a similar approach towards the asymmetric allylic alkylation of enol carbonates.⁵¹ In this case, the phosphine ligand **54** was shown to afford optimal enantioselectivity, and provided higher maximum enantioselectivities than those obtained by Stoltz. Importantly, the reaction was also extended to the formation of tertiary carbon stereogenic centres, as exemplified by the highly stereoselective alkylation of the enol carbonate **53** (eq. 18). The choice of solvent was shown to be critical to the overall efficiency of this process, with dioxane proving optimal for the construction of α -tertiary ketones such as **55**. In both toluene and tetrahydrofuran, the yield is significantly reduced by competing enolate protonation and polyalkylation reactions, both of which are caused by equilibration of the initially formed enolate and the ketone product. This equilibration is clearly minimised by the use of dioxane, which has the ability to form a solvent cage around the proposed contact ion pair of the palladium(II) enolate intermediate, improving the yield of the monoalkylated product **55**.



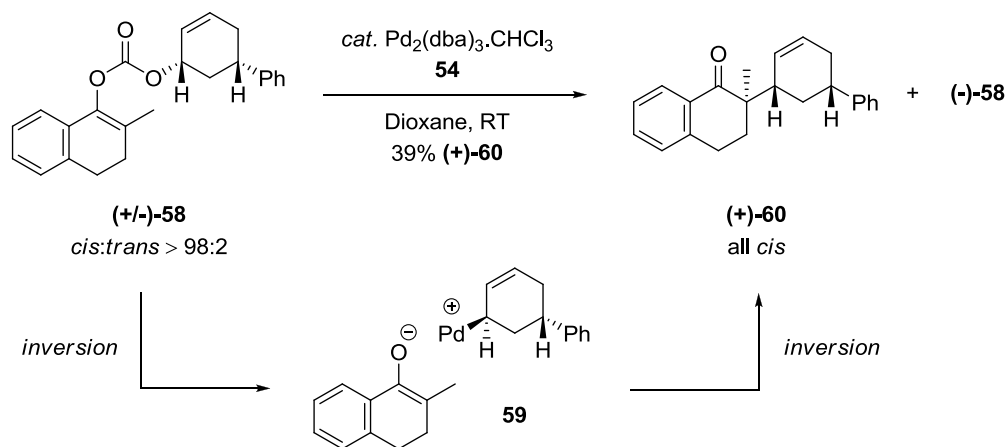
Using the ligand **54**, the palladium-catalysed decarboxylative allylic alkylation of enol carbonates was extended to the formation of *acyclic* tertiary stereogenic centres.⁵² A wide variety of aryl and alkenyl-substituted (*Z*)-enol carbonates, which are generally easier to prepare than the corresponding (*E*)-isomers, were efficiently converted to the corresponding α -tertiary ketones in excellent yield and enantioselectivity. In general, electron rich aryl groups afforded the best enantioselectivities, though the reaction was less efficient for substrates containing a branched α -carbonyl substituent. The enolate geometry must be strictly controlled in this process, as the (*E*)- and (*Z*)-isomers of the enol carbonate **56** were shown to afford opposite enantiomers of the product **57**. Under the standard reaction conditions, alkylation of the enol carbonate (*Z*)-**56** furnished the (*S*)-enantiomer of the product with moderate enantioselectivity (eq. 19), whereas the analogous reaction of (*E*)-**56** provided the ketone (*R*)-**57** in excellent yield and enantiomeric excess (eq. 20). Although no loss of regioselectivity was observed in the alkylation of (*Z*)-**56**, the reaction was sluggish in comparison to that of the corresponding aryl- and alkenyl-substituted enol carbonates. This, along with the poor enantioselectivity, was attributed to an unfavourable steric interaction between the (*Z*)-enolate and the π -allylpalladium complex.

Interestingly, in the formation of quaternary carbon stereogenic centres, the decarboxylative allylic alkylation was shown to afford the opposite enantiomer to that of the corresponding lithium enolate. This prompted a number of studies aimed towards understanding the mechanism of nucleophilic addition, as ketone enolates have the ability to behave as both stabilised and unstabilised nucleophiles, and may therefore attack the allyl moiety directly (outer-sphere alkylation) or *via* the metal centre (inner-sphere alkylation).



Under the catalytic conditions developed by Trost, the decarboxylative allylic alkylation reaction is compatible with cyclohexenyl-substituted enol carbonates, which have the ability to function as stereochemical probes. For example, in the presence of $\text{Pd}_2(\text{dba})_3 \cdot \text{CHCl}_3$ and the ligand **54**, the *cis*-substituted enol carbonate (+/-)-**58** underwent a near perfect kinetic resolution, in which one enantiomer of the racemic substrate was completely unreactive. While (-)-**58** was recovered in 37% yield and > 99% *ee*, the other enantiomer was consumed within 1 hour, affording the *cis*-cyclohexene adduct (+)-**60** in 39% yield and 99% *ee*, and as a single diastereoisomer (**Scheme 7**).⁵³ This result strongly suggests that the alkylation is an

outer-sphere process, as oxidative addition of the catalyst into (+/-)-**58** should proceed with inversion of configuration, to afford the palladium-allyl intermediate **59**. *Anti*-nucleophilic addition of the enolate, in a manner akin to that of stabilised carbon nucleophiles, then provides the *cis*-cyclohexene (+)-**60** with inversion of configuration. In contrast, reductive elimination of a covalently bonded palladium(II) enolate would be expected to proceed with retention of configuration, affording the unobserved *anti*-diastereoisomer of the ketone **60**. Importantly, the *trans*-isomer of **58** was shown to afford the *trans*-isomer of **60**, which is also consistent with an outer-sphere alkylation.



Scheme 7. Evidence for an outer-sphere mechanism in the palladium-catalysed decarboxylative allylic alkylation reaction.

Unfortunately, the reaction developed by Stoltz⁴⁴ is not compatible with cyclohexenyl-substituted enol carbonates such as (+/-)-**58**. This, along with a desire to improve the enantioselectivity of this process, prompted a computational study of the reaction outlined in eq. 17.⁵⁴ An X-ray crystal structure of the synthetic palladium(II)-allyl complex **61**, with hexafluorophosphate as the counter ion, was obtained. This species was also shown to be catalytically competent in the enantioselective alkylation, which led the authors to propose that the complex **61**, but

with a ketone enolate as the counterion, is likely to be an intermediate in this process. Density functional theory (DFT) calculations demonstrated that the lowest energy conformer for this intermediate is a five-coordinate square bipyramidal structure, in which the oxygen atom of the enolate counterion is covalently bonded to the palladium metal centre. In addition, a reaction pathway involving the 7-membered transition state **62**, in which the key bond forming event occurs *via* [3,3']-reductive elimination of the palladium(II) enolate intermediate, was calculated to be 1.6 kcal/mol lower in energy than any of the postulated outer-sphere pathways, such as that shown in transition state **63**. The [3,3']-reductive elimination pathway was also shown to be significantly lower in energy than the more commonly observed [1,1']-reductive elimination pathway, which would proceed *via* a highly strained 3-membered transition state. Overall, this study provides compelling evidence for an inner-sphere mechanism in the decarboxylative allylation reaction using the P,N ligand **37**. A similar mechanism has recently been proposed for a series of isoelectronic palladium-catalysed allyl-allyl cross coupling reactions,⁵⁵ which lends further support to this hypothesis.

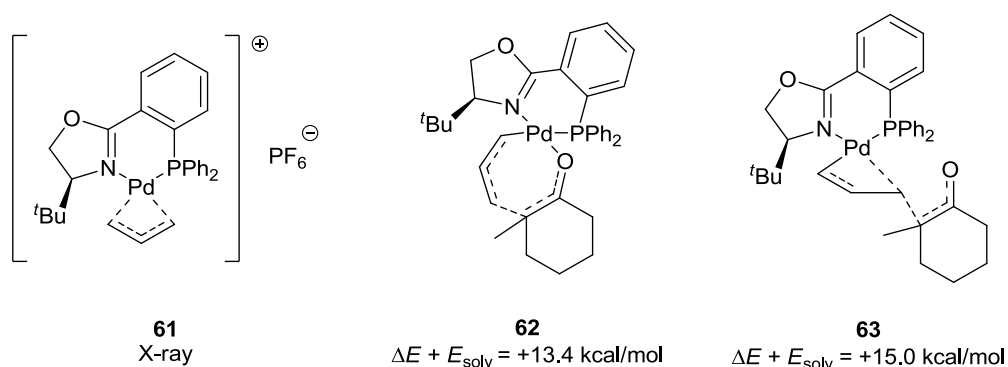
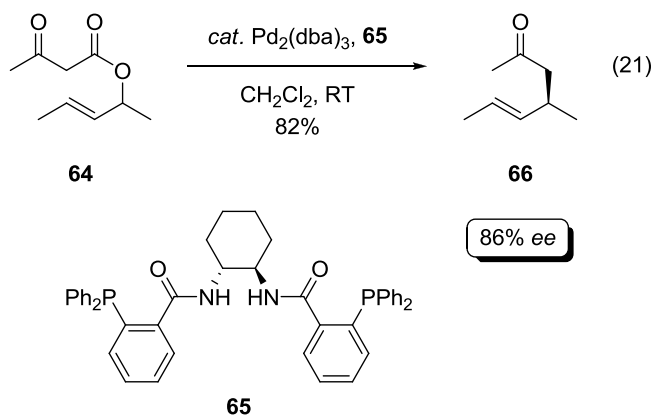
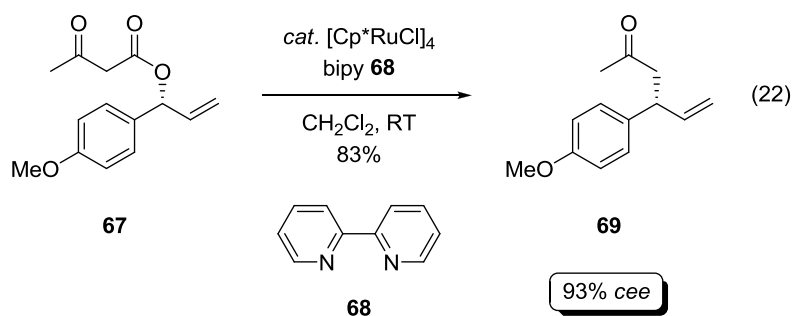


Figure 2. Evidence for an inner-sphere mechanism in the palladium-catalysed decarboxylative allylic alkylation reaction.



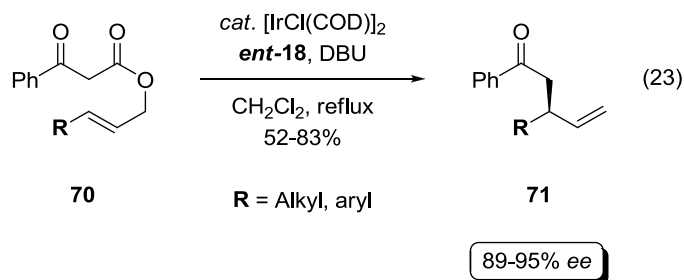
Despite the significant advances in this area, a remaining limitation of these processes is that they often require the use of unsubstituted allylic electrophiles. The application of substituted derivatives would not only expand the scope of this process, but also permit the asymmetric construction of β -substituted carbonyl compounds *via* decarboxylative allylation. To this end, Tunge described the palladium-catalysed decarboxylative allylic alkylation of substituted β -ketoesters, to provide β -substituted ketones with high levels of enantioselectivity.⁵⁶ For example, treatment of the β -ketoester **64** with $\text{Pd}_2(\text{dba})_3$ and Trost ligand **65** provided the ketone **66** in good yield and enantiomeric excess (eq. 21). This reaction represents a formal monoalkylation of acetone, a process known to be extremely challenging, and is particularly noteworthy given that the substrate **64** is easily prepared by the addition of diketene to the requisite allylic alcohol. In order to circumvent the regiochemical infidelity often afforded by palladium catalysts, these reactions were conducted using substrates that provide symmetrical π -allyl intermediates upon decarboxylation. It was also demonstrated that the same enantiomer of the ketone products may be prepared, under identical catalytic conditions, by the allylic alkylation of a stabilised β -ketoester followed by decarboxylation. In accord with Trost's observations, this result strongly suggests that the ketone enolate behaves as a stabilised nucleophile in the allylic alkylation reaction.

In order to avoid the formation of regioisomeric mixtures in the decarboxylative allylic alkylation of substituted β -ketoesters, both ruthenium and iridium catalysts have been successfully utilised. For example, treatment of the β -ketoester **67** with catalytic $[\text{Cp}^*\text{RuCl}]_4$ and 2,2-bipyridine **68** furnished the substituted ketone **69** in good yield, and with excellent regioselectivity (eq. 22).⁵⁷ The alkylation of **67** was also shown to be stereospecific, affording the ketone **69** with overall retention of absolute configuration, albeit with a slight degradation in enantiopurity (93% *cee*⁵⁸). This was attributed to the *in situ* isomerisation of **67** to its achiral linear regioisomer (as detected by ¹H NMR spectroscopy), which must occur prior to decarboxylation. The stereospecific process, along with the enantioselective variant developed by Lacour,⁵⁹ is limited to aryl-substituted β -keto esters.



Using an iridium catalyst, the enantioselective decarboxylative allylic alkylation of the achiral linear β -ketoester **69** was accomplished by You (eq. 23).⁶⁰ As was the case with other enolate equivalents, a combination of $[\text{IrCl}(\text{COD})]_2$ and the phosphoramidite ligand **18** proved optimal for both enantioselectivity and yield. In this context, the *ee* values were uniformly excellent for both aryl- and alkyl-substituted β -ketoesters, though the regioselectivity was slightly reduced for the alkyl derivatives. The absolute configuration of the product **70** was determined to be (*S*), meaning that the stereochemical course of this reaction matches that of enamines³⁸ and silyl enol ethers.⁴⁷ This observation, along with a crossover experiment of two

different substrates, indicates that the iridium-catalysed decarboxylative allylation is also an intermolecular process. To our knowledge, both the iridium and ruthenium-catalysed reactions have yet to be extended to prochiral derivatives, which would permit the synthesis of α -substituted ketones.



1.2.2.3. Metal Enolates

1.2.2.3.1. Introduction

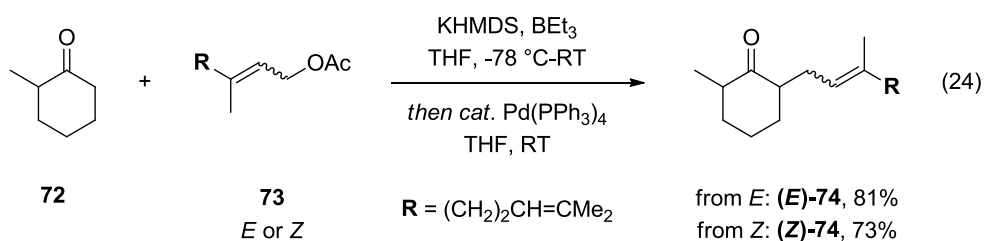
Most enolate equivalents are prepared by quenching an alkali metal enolate, formed *via* deprotonation of the parent carbonyl compound, with the requisite electrophile. In the majority of cases, these enolate equivalents must be isolated and purified prior to their employment in the transition metal-catalysed allylic substitution reaction. Thus, in terms of efficiency, it would be clearly be advantageous to develop reactions in which the intermediate metal enolates could be used directly. Despite some early success, it is only in the last decade that these processes have become general and stereoselective, which has enabled their widespread utility in organic synthesis.

1.2.2.3.2. Enoxyborates

In the allylic alkylation of unstabilised enolates, one of the most commonly employed strategies involves the *in situ* transmetallation of an alkali metal enolate with an alternative metal. This usually serves to soften the basic nature of the enolate, making it more compatible with the soft π -allyl electrophile. In reducing the basicity of the nucleophile, a number of competing side reactions may also be

prevented. These processes differ significantly from those of enolate equivalents, as the reactive nucleophile is formed *in situ*, and does not need to be isolated.

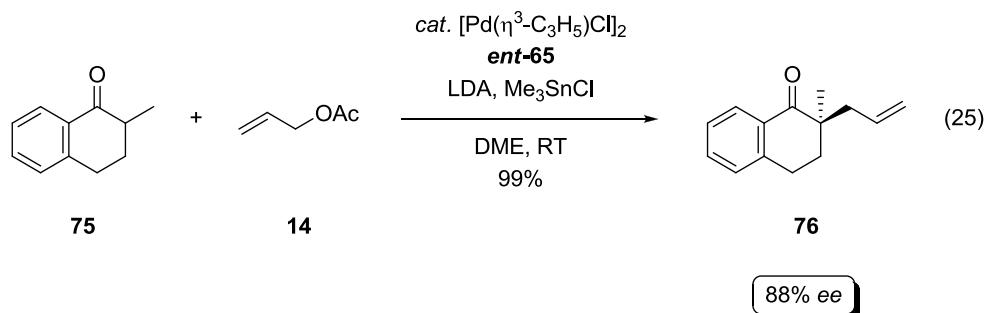
In 1982, Negishi reported the palladium-catalysed allylic alkylation of enoxyborates, generated by the transmetallation of potassium enolates with triethylborane.⁶¹ For example, treatment of both (*E*)- and (*Z*)-**73** with the kinetic enoxyborate derived from the ketone **72**, in the presence of Pd(PPh₃)₄, furnished the ketone **74** in good yield (eq. 24). Both the (*E*)- and (*Z*)-isomers of the ketone **74** were afforded with complete retention of alkene geometry, which is in sharp contrast to a number of related allylic alkylation reactions. Interestingly, this process was also shown to be regiospecific with respect to the enolate, as both the kinetic and thermodynamic isomers of the enoxyborate could be employed without significant isomerisation. A number of other metal enolates, including those of zinc, magnesium and aluminium, were also effective in the alkylation of geranyl acetate (*E*)-**73**.



1.2.2.3.3. Tin Enolates

The first asymmetric allylic alkylation of prochiral ketone enolates was reported by Trost.⁶² This method involves the *in situ* transmetallation of a lithium enolate with trimethyltin chloride, to provide an enolstannane nucleophile. For example, deprotonation of 1-tetralone with LDA, followed by the addition of Me₃SnCl, allyl acetate and a chiral palladium catalyst, furnished the α -quaternary substituted ketone **76** in excellent yield and with good enantioselectivity (eq. 25). The enantiomeric

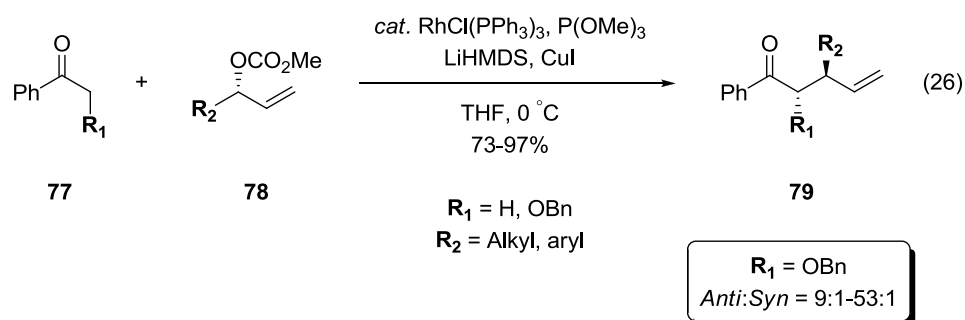
excess is sensitive to the stoichiometry of the base, suggesting that the reactive nucleophile is not monomeric, but an enolate-LDA aggregate. Slightly lower enantioselectivities were obtained in the absence of tin, though this process was later improved by Hou and Dai, who demonstrated that a ferrocene analogue of the ligand **65** could provide the ketone **76** in 95% *ee*.⁶³



1.2.2.3.4. Copper Enolates

The transmetalation of a lithium enolate with copper(I) iodide, to provide a copper(I) enolate, has proven particularly useful in the regio- and stereospecific rhodium-catalysed allylic substitution reaction. For example, the copper(I) enolate of **77**, upon treatment with the allylic carbonates **78**, Wilkinson's catalyst and trimethyl phosphite, furnished the substituted ketones **79** in good to excellent yield and, in the case of the α -benzyloxy-substituted ketones, with excellent diastereoselectivity (eq. 26).⁶⁴ In this reaction, the use of a copper(I) salt is necessary in order to prevent competing bis-alkylation and elimination of the rhodium-allyl intermediate, though the nature of the counterion is generally inconsequential to the excellent regio- and stereospecificity of the enolate alkylation. It was also found that with the extension of this methodology to an α -substituted ketone enolate, highly enantiomerically enriched α,β -disubstituted ketones may be formed with a high degree of diastereocontrol. In this context, the α -alkoxy substituent ($\mathbf{R}_1 = \text{OBn}$) was proposed to be critical to the formation of a (*Z*)-chelated copper(I) enolate, the facially

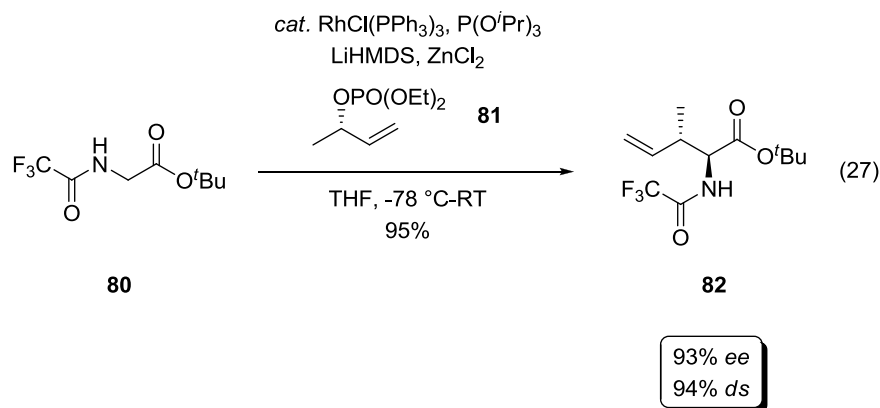
selective alkylation of which is directed by the newly formed β -carbonyl stereogenic centre, resulting in a highly diastereoselective α -alkylation. Consistent with this hypothesis, the steric and electronic nature of this substituent was shown to dramatically affect the *anti:syn* ratio of **79**, with O-alkyl ethers providing optimal selectivity. In addition, a wide range of allylic carbonates were employed, and this highly diastereoselective reaction was utilised in the stereodivergent synthesis of *cis*- and *trans*-substituted dihydropyran derivatives. The rhodium-catalysed allylic alkylation of the copper(I) enolate derived from 4-methoxyacetophenone was also employed in an expeditious total synthesis of the norlignan (-)-Sugiresinol, which has potent antifungal activity.^{64a}



1.2.2.3.5. Zinc Enolates

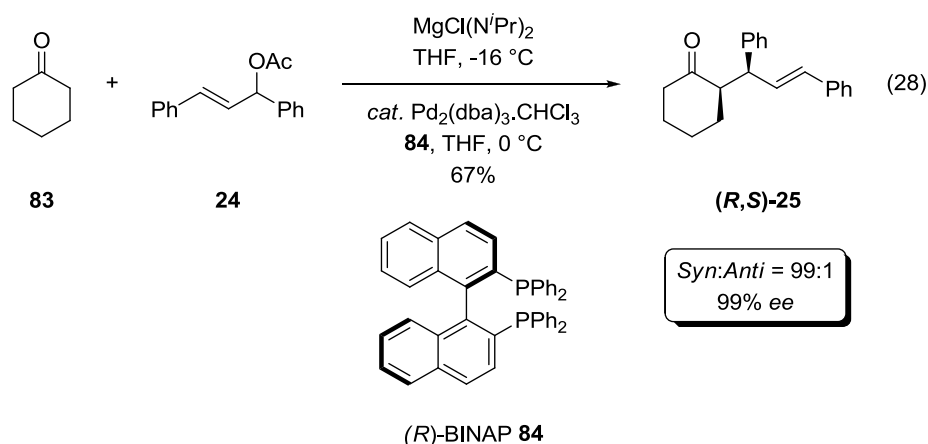
Chelated zinc amino acid ester enolates have also been employed in the transition metal-catalysed allylic substitution reaction, providing access to a range of highly functionalised non-natural amino acids.⁶⁵ For example, treatment of the lithium enolate of **80** with zinc chloride, in the presence of $\text{RhCl(PPh}_3)_3$, triisopropyl phosphite and the enantiomerically enriched allylic phosphate **81**, furnished the α -alkylated ester **81** in excellent yield and enantiomeric excess (eq. 27). Due to the reactivity of zinc enolates, their transition metal-catalysed allylic alkylation can be conducted at -78°C . This reduces π - σ - π isomerisation of the metal-allyl intermediate, and results in a highly regio- and stereospecific alkylation with respect

to the phosphate **81**. In addition, because the enolate geometry is fixed by the chelation of zinc to the α -amino moiety, the reaction proceeds with excellent diastereoselectivity.



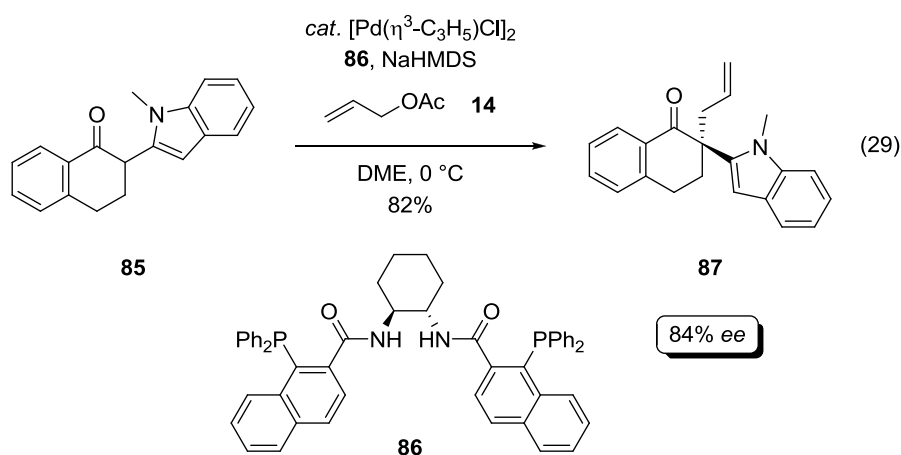
1.2.2.3.6. Magnesium Enolates

In an attempt to expand the allylic substitution reaction to unstabilised ketone enolates, without recourse to transmetalation, Braun highlighted the utility of magnesium enolates in the palladium-catalysed allylic alkylation of both cyclic and acyclic ketones.⁶⁶ The alkylation of cyclohexanone **83**, deprotonated with MgCl(NⁱPr)₂, with the acetate **24** was shown to proceed readily in the presence of catalytic Pd₂(dba)₃.CHCl₃ and (*R*)-BINAP **84**, affording the ketone **25** with excellent diastereo- and enantioselectivity (eq. 28). The diastereoselectivity of this process was significantly higher in the presence of bidentate phosphine ligands and a magnesium enolate, as opposed to a lithium enolate. Interestingly, while the cyclic ketone **83** provided the *syn*-product, the acyclic mesityl ethyl ketone was shown to afford predominantly the *anti*-diastereoisomer, even when the enolate geometry was identical to that of the cyclic derivative.



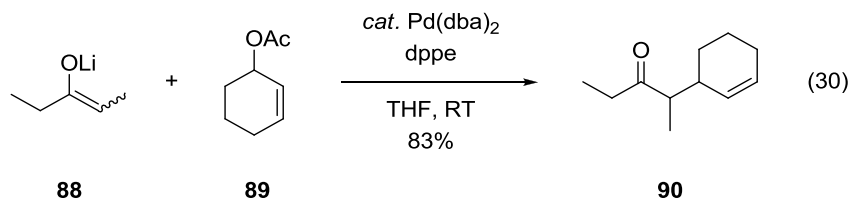
1.2.2.3.7. Sodium Enolates

In the allylic alkylation of alkali metal enolates, lithium bases are much more commonly employed than the corresponding sodium and potassium derivatives. However, in an exception to this, Trost described the enantioselective allylic alkylation of sodium enolates derived from α -aryl ketones.⁶⁷ The phosphine ligand **86** was shown to afford optimal enantioselectivity, and was also effective in the alkylation of α -heterocyclic ketones (eq. 29). In the alkylation of these species, sodium bis(trimethylsilyl)amide provides significantly higher enantioselectivity than a number of alternative bases. This was attributed to the relative size of the sodium cation, which enables the enolate to assume a favourable position in the chiral pocket of the metal-ligand complex. Overall, this method provides a viable alternative to the highly studied catalytic asymmetric α -arylation of ketone enolates.³²



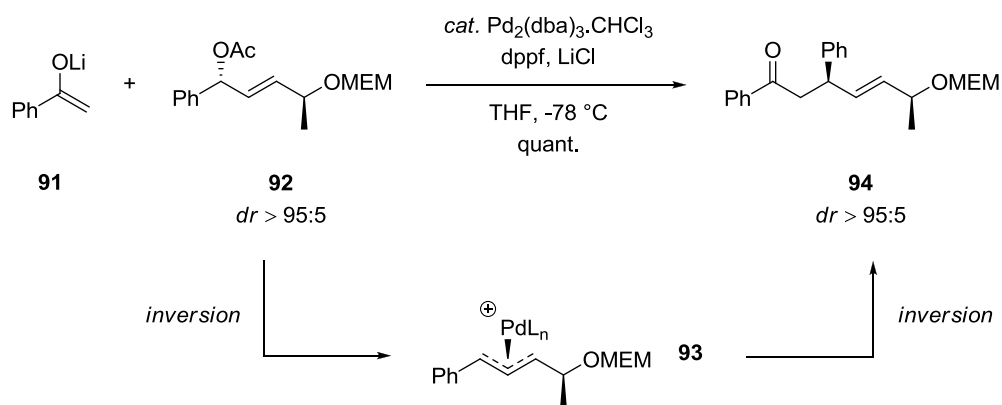
1.2.2.3.8. Lithium Enolates

Despite the difficulties initially encountered by Trost, Fiaud and Malleron described the first general palladium-catalysed allylic alkylation of lithium enolates.⁶⁸ Using Pd(dba)₂ and dppe as a ligand, a range of lithium enolates were shown to afford the corresponding α -substituted ketones in moderate to good yield. The authors report clean conversion to the monoalkylated products, even for simple ketones such as 3-pentanone (eq. 30). However, these findings were later questioned by Negishi, who found lithium enolates to be significantly less reactive than the corresponding boron, zinc, magnesium and aluminium derivatives.⁶¹

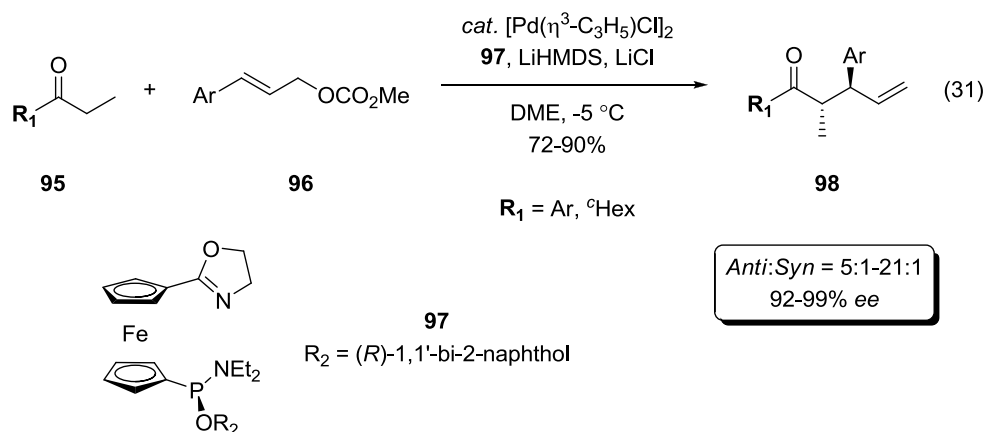


In an extension of their previous work, Braun and Meier demonstrated that the palladium-catalysed allylic alkylation of lithium enolates is significantly more facile in the presence of lithium chloride.⁶⁹ This additive is well known to deaggregate lithium enolates,⁷⁰ increasing their reactivity, and enabling their asymmetric alkylation to proceed readily at low temperatures. In addition to the numerous enantio- and diastereoselective alkylations that were described, the stereochemical course of the reaction was also examined. The enantiomerically enriched acetate **91** was treated with the lithium enolate of acetophenone in the presence of lithium chloride, a palladium catalyst and the achiral ligand 1,1'-bis(diphenylphosphino)ferrocene (dppf) (**Scheme 8**). A quantitative yield of the ketone **94** was afforded with complete diastereoselectivity and no isomerisation of the (*E*)-alkene. This strongly suggests that the alkylation proceeds *via* a double

inversion process, in which the lithium enolate attacks the (*syn,syn*)- π -allyl complex **93** from the π -face opposite the metal centre. Thus, the lithium enolate behaves as a stabilised carbon nucleophile in the alkylation of acyclic allylic acetates, which is consistent with a number of previous studies. An aliphatic ketone enolate was later shown to behave in an identical manner, despite being more basic in nature, indicating that this is a general phenomenon.

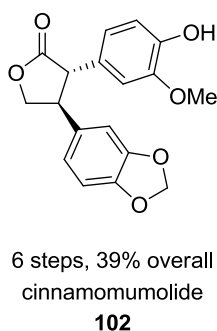
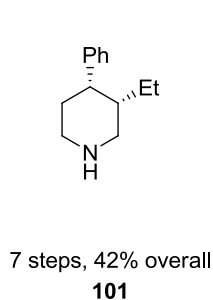
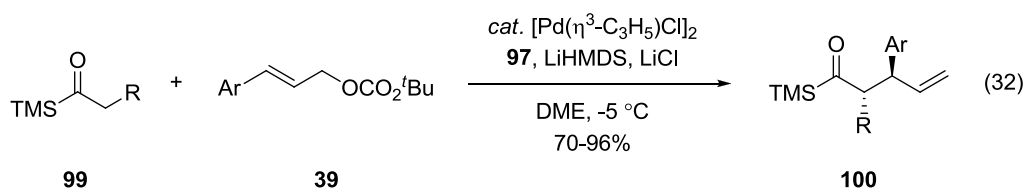


Scheme 8. Retention of configuration in the palladium-catalysed allylic alkylation of an acyclic acetate with the lithium enolate of acetophenone.



In 2007, Hou described the first regio-, diastereo- and enantioselective allylic alkylation of lithium enolates.⁷¹ The ferrocenyloxazoline ligand **97**, in conjunction with $[\text{Pd}(\eta^3\text{-C}_3\text{H}_5)\text{Cl}]_2$, was shown to induce asymmetry in the alkylation of the ethyl

ketones **95** with a range of allylic carbonates, furnishing the acyclic ketones **98** with moderate to good diastereoselectivity (eq. 31). The highest diastereoselectivities were observed in the presence of bulky aromatic substituents (e.g. **R**₁ or Ar = 1-naphthyl), and although the reaction is generally limited to aryl-substituted allylic carbonates, the regio- and enantioselectivity is uniformly excellent. The choice of solvent was shown to be critical to the diastereoselectivity, with polar coordinating solvents such as DME proving optimal. Interestingly, this reaction fails to proceed in the absence of lithium chloride, once more demonstrating the importance of carbanion disaggregation to the reactivity of lithium enolates.

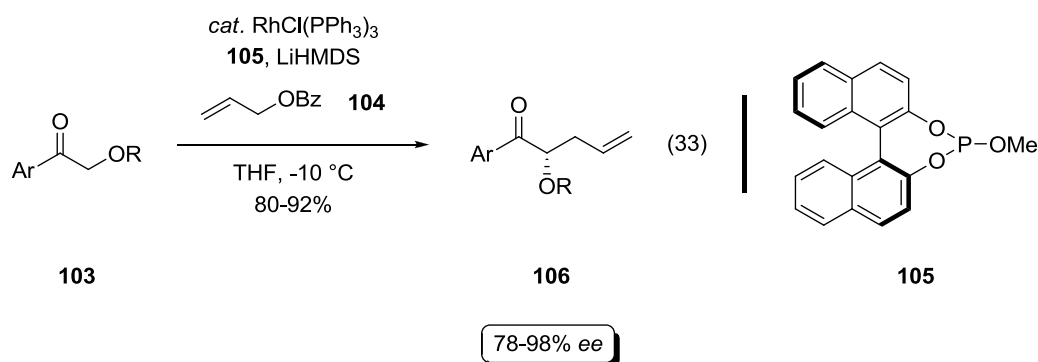


Anti:Syn = 10:1-50:1
83-99% ee

In an attempt to broaden the substrate scope of this venerable process, the same group recently reported the palladium-catalysed allylic alkylation of acylsilane enolates.⁷² Under almost identical reaction conditions, a range of acylsilanes were successfully alkylated with excellent regio- and enantioselectivity (eq. 32). In sharp contrast to the aryl ketone derivatives (eq. 31), the diastereomeric ratio of the substituted acylsilanes was generally $\geq 10:1$. In order to demonstrate the synthetic utility of these adducts, the acylsilane functionality was converted to the

corresponding methyl ester, ethyl ketone and primary alcohol. The requisite acylsilanes were also utilised as key intermediates in the synthesis of the dopaminergic piperazine **101** and the natural product cinnamomumolide **102**, which forms part of a traditional Chinese medicine.

Recently, Evans reported the enantioselective rhodium-catalysed allylic alkylation of prochiral acyclic α -alkoxy lithium enolates with allyl benzoate (eq. 33).⁷³ As in the reaction of copper(I) enolates, the α -alkoxy substituent was shown to be critical in controlling the *E:Z* geometry of the acyclic enolate, and hence the enantioselectivity of the alkylation. A wide range of substituents were tolerated in both the aryl ketone and the α -ether component, with electron rich groups generally affording the highest *ee* values. The ketone product **106** (Ar = 4-MeOC₆H₄, R = Bn) was directly converted to the corresponding primary alcohol, an intermediate that features extensively in a number of important synthetic applications. This study also highlighted the utility of lithium enolates in comparison to their sodium and potassium analogues, both of which provided the opposite enantiomer of the ketone **106** with poor selectivity. This was attributed to the increased basicity of the sodium and potassium enolates, which were shown to fully racemise the enantiomerically enriched tertiary ketone **106**.



1.2.3. Transition Metal-Catalysed Allylic Substitution Reactions using Acyl Anion Equivalents

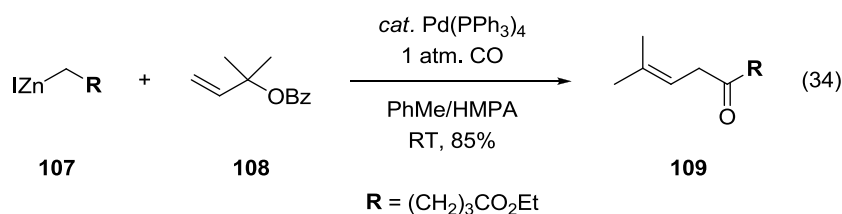
1.2.3.1. Introduction

Despite the intense interest in the asymmetric synthesis of α -substituted carbonyl compounds, particularly in the area of allylic substitution, most of the current methods rely on the functionalisation of an enolate nucleophile, often *via* alkylation (**Scheme 4**, path A). In contrast, there remains a paucity of methods for the direct introduction of acyl functionality into the allylic framework (**Scheme 4**, path B). In comparison to the enolate alkylation reaction, this process involves a fundamentally different bond forming strategy, and therefore offers a number of potential advantages in terms of selectivity and substrate scope. Critically, this approach involves the generation of a nucleophilic acyl species, in which the inherent electrophilic properties of the carbonyl group are reversed. Although it remains a challenge to invoke such Umpolung reactivity,⁷⁴ numerous acyl anion equivalents are known, and a small number have been employed in the asymmetric allylic substitution reaction. In order to highlight the current utility of these methods, their scope and limitations will be discussed briefly in the following section.

1.2.3.2. Acylmetal Nucleophiles

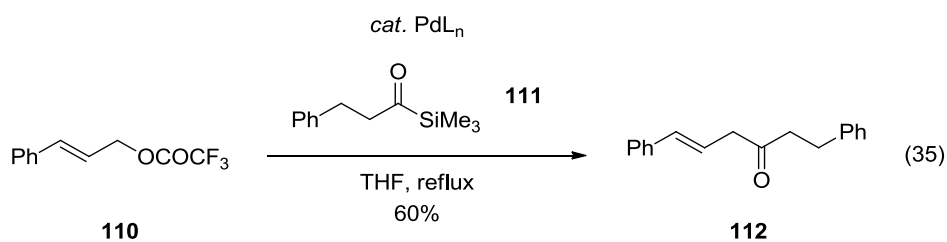
The carbonylation of an alkylmetal species, generally conducted under an atmosphere of carbon monoxide, provides a particularly efficient method for the facile generation of “unmasked” acylmetal nucleophiles. In this context, Tamaru described the three component coupling reaction of allylic benzoates, carbon monoxide and zincioesters.⁷⁵ For example, treatment of the allylic benzoate **108** with the zincioester **107** under an atmosphere of carbon monoxide, in the presence of catalytic Pd(PPh₃)₄, furnished the ketone **109** in good yield and with complete

regioselectivity (eq. 34). The palladium-catalysed allylic alkylation of an acylzirconium species, generated by the hydrozirconation of an alkene under an atmosphere of carbon monoxide, was also reported by Taguchi.⁷⁶ As is common with palladium catalysts, both methods provide solely the linear regioisomer of the ketone product. In the case of acylzirconocenes, significant alkene isomerisation is also observed, providing inseparable mixtures of α,β - and β,δ -unsaturated ketones.



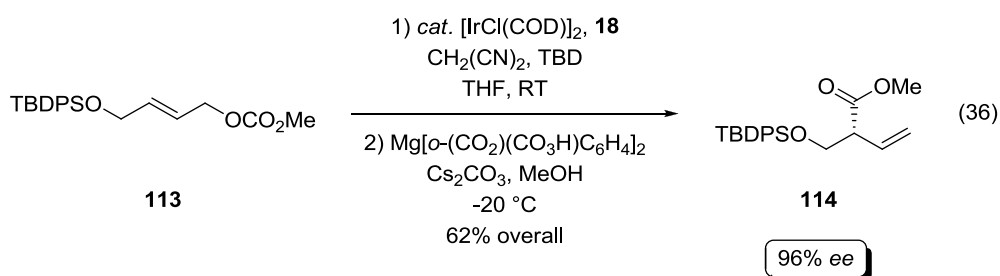
Acylsilanes⁷⁷ and acylstannanes⁷⁸ have both been employed as nucleophiles in the palladium-catalysed allylic substitution reaction. For example, the addition of acylsilane **111** to the allylic trifluoroacetate **110** was shown to proceed readily in the presence of catalytic $[\text{Pd}(\eta^3\text{-C}_6\text{H}_5\text{CH=CH}_2)(\text{OCOCF}_3)]$, yielding the ketone **112** in moderate yield (eq. 35). This reaction proceeds *via* cleavage of the acylsilane C-Si σ -bond, with the concomitant formation of a strong Si-O bond ($\text{CF}_3\text{COOSiMe}_3$), to provide an acyl- π -allylpalladium intermediate. Reductive elimination of the metal from this species then provides the ketone **112** in moderate yield. The use of a fluorinated leaving group was shown to be critical to the reactivity of the acylsilane, with standard allylic acetates and carbonates failing to afford the ketone product. This was attributed to the low LUMO energy of the initially formed $[\text{Pd}(\pi\text{-allyl})(\text{CF}_3\text{COO})]_2$ complex, which enables the interaction of this species with the high energy HOMO of the acylsilane, to provide the aforementioned acylpalladium intermediate. Unfortunately, despite providing the ketone products directly, these

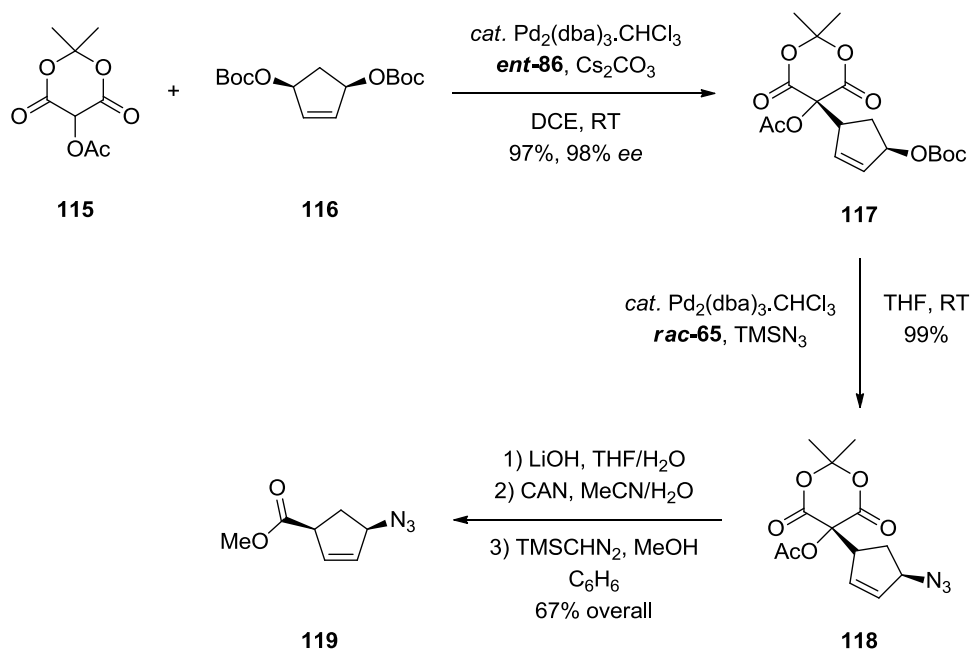
reactions are also highly selective for the achiral linear regioisomer, so have limited utility in asymmetric synthesis.



1.2.3.3. “Masked” Acyl Anion Equivalents

A number of stabilised carbon nucleophiles have been utilised as “masked” acyl anion equivalents in the allylic substitution reaction. For example, Helmchen described the oxidative degradation of highly enantiomerically enriched malononitrile derivatives, which were prepared by iridium-catalysed allylic substitution, to provide α -substituted methyl esters (eq. 36).⁷⁹ Magnesium monoperoxyphthalate was selected as the oxidant, largely because the enantiomeric excess of malononitrile adduct was fully maintained under these conditions. In addition, no double bond epoxidation or migration was observed, thereby illustrating the utility of malononitrile as an acyl anion equivalent in the transition metal-catalysed allylic substitution reaction.





Scheme 9. Acetoxy Meldrum's acid as an acyl anion equivalent in the palladium-catalysed allylic substitution reaction.

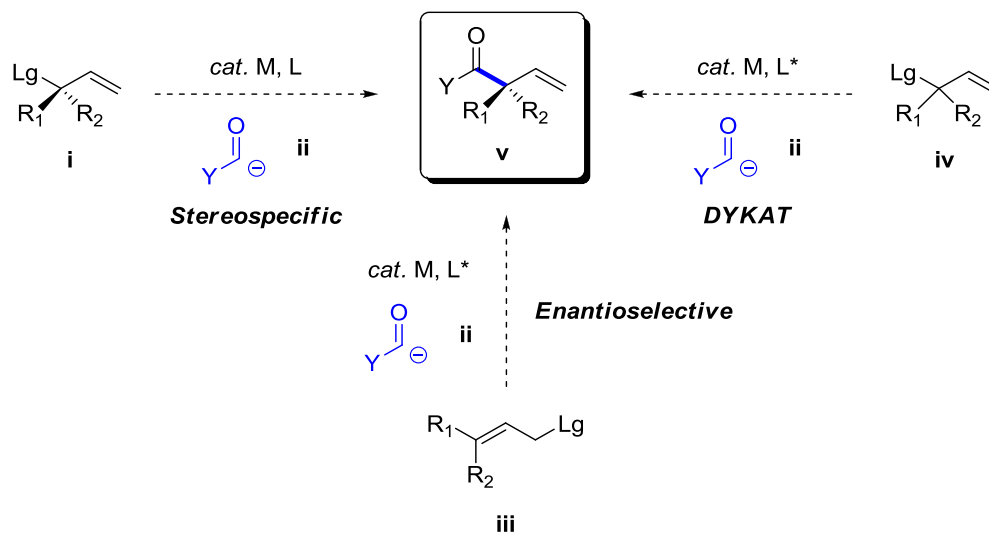
More recently, Trost described the use of acetoxy Meldrum's acid as an acyl anion equivalent in the enantioselective palladium-catalysed allylic alkylation.⁸⁰ As outlined in **Scheme 9**, the alkylation of **115** with the *meso* dicarbonate **116** proceeded readily in the presence of a palladium catalyst and the ligand **86**, affording the adduct **117** in excellent yield and enantiomeric excess. A second allylic alkylation, this time using a racemic ligand and an azide nucleophile, provided a single diastereoisomer of the azide **118**. The carbonyl functionality was then unmasked in an exhaustive three step sequence, which involved hydrolysis of the acetonide moiety, decarboxylation using cerium ammonium nitrate and methylation, to afford the requisite methyl ester **119**. This intermediate was then utilised in the formal synthesis of several biologically active nucleoside analogues.

As demonstrated by the above examples, both regio- and enantioselectivity can be achieved using “masked” acyl anion equivalents, permitting the asymmetric

construction of α -substituted carbonyl compounds. However, cumbersome additional transformations are generally required to form the acylated products, and the substrate scope is often limited.

1.2.4. Concluding Remarks

Our literature survey has highlighted a number of elegant methods for the asymmetric synthesis of substituted carbonyl compounds *via* transition metal-catalysed allylic substitution. As detailed in section 1.2.2., this work is generally dominated by the asymmetric alkylation of metal enolates and their synthetic equivalents. In contrast, a general method for the regio- and stereoselective acylation of substituted allylic electrophiles, which represents a viable alternative to the enolate alkylation, has yet to be fully developed. As such, we envisioned that the successful implementation of this strategy, as outlined in **Scheme 10**, would provide a highly versatile and efficient method for the asymmetric synthesis of the acyclic α -substituted carbonyl compounds **v**.



Scheme 10. General hypothesis for the asymmetric transition metal-catalysed allylic substitution with an acyl anion equivalent.

Strategically, this approach offers a number of potential advantages in comparison to conventional enolate alkylation reactions. Firstly, there are three potential modes of asymmetric induction in the allylic substitution reaction, all of which are well preceded. Regardless of whether the acyl anion equivalent **ii** is introduced in a stereospecific or enantioselective manner, the stereochemical outcome of this reaction would not depend on the selective formation of an *E* or *Z* metal enolate, which is often challenging in acyclic systems. Secondly, depending on the nature of the substituent Y, this process has the potential to provide unsymmetrical dialkyl ketones without recourse to regioselective enolisation, which is often difficult in ketones containing two sterically equivalent substituents. Thirdly, as a wide range of substituted allylic alcohol derivatives (**i**, **iii** and **iv**) are readily available, this method should allow for the synthesis of carbonyl compounds containing α -branched and functionalised alkyl groups, aryl groups and vinyl groups, which are generally difficult to install *via* conventional enolate functionalisation reactions.

The following chapter will describe our efforts towards the development of the general process outlined in **Scheme 10**, in the context of rhodium-catalysed allylic substitution reactions. More specifically, we chose to examine the asymmetric construction of *acyclic* α -quaternary substituted ketones using this approach, as our literature review had revealed a distinct lack of methods for their preparation, particularly *via* enolate alkylation.

-
- ¹ Crawley, M. L. in *Science of Synthesis: Stereoselective Synthesis 3*; Evans, P. A., Ed.; Thieme: Stuttgart, Germany, 2011; p. 403-401.
- ² a) For reviews, see: a) Trost, B. M.; Van Kraken, D. L. *Chem. Rev.* **1996**, *96*, 395. b) Frost, C. G.; Howarth, J.; Williams, J. M. J. *Tetrahedron: Asymmetry* **1992**, *3*, 1089.
- ³ Trost, B. M.; Lautens, M. *J. Am. Chem. Soc.* **1982**, *104*, 5543.
- ⁴ Trost, B. M.; Hung, M.-H. *J. Am. Chem. Soc.* **1983**, *105*, 7757.
- ⁵ Takeuchi, R.; Kashio, M. *Angew. Chem. Int. Ed. Engl.* **1997**, *36*, 263.
- ⁶ Tsuji, J.; Minami, I.; Shimizu, I. *Tetrahedron Lett.* **1984**, *25*, 5157.
- ⁷ Zhang, S.-W.; Mitsudo, T.; Kondo, T.; Watanabe, Y. *J. Organomet. Chem.* **1993**, *450*, 197.
- ⁸ Cuvigny, T.; Julia, M. *J. Organomet. Chem.* **1983**, *250*, C21.
- ⁹ Fouquet, G.; Schlosser, M. *Angew. Chem. Int. Ed. Engl.* **1974**, *13*, 82.
- ¹⁰ a) Roustan, J. L.; Mérour, J. Y.; Houlihan, F. *Tetrahedron Lett.* **1979**, *20*, 3721. b) Xu, Y.; Zhou, B. *J. Org. Chem.* **1987**, *52*, 974.
- ¹¹ Trost, B. M.; Crawley, M. L. *Chem. Rev.* **2003**, *103*, 2921.
- ¹² Åkermark, B.; Zetterberg, K.; Hansson, S.; Krakenberger, B.; Vitagliano, A. *J. Organomet. Chem.* **1987**, *335*, 133.
- ¹³ Kawatsura, M.; Uozumi, Y.; Hayashi, T. *Chem. Commun.* **1998**, 217.
- ¹⁴ Sjögren, M. P. T.; Hansson, S.; Åkermark, B.; Vitagliano, A. *Organometallics* **1994**, *13*, 1963.
- ¹⁵ Trost, B. M.; Toste, F. D. *J. Am. Chem. Soc.* **1999**, *121*, 4545.
- ¹⁶ a) Prétôt, R.; Pfaltz, A. *Angew. Chem. Int. Ed.* **1998**, *37*, 323. b) You, S.-L.; Zhu, X.-Z.; Luo, Y.-M.; Hou, X.-L.; Dai, L.-X. *J. Am. Chem. Soc.* **2001**, *123*, 7471.
- ¹⁷ Fristrup, P.; Jensen, T.; Hoppe, J.; Norrby, P.-O. *Chem. Eur. J.* **2006**, *12*, 5352 and pertinent references cited therein.
- ¹⁸ Krafft, M. E.; Sugiura, M.; Abboud, K. A. *J. Am. Chem. Soc.* **2001**, *123*, 9174.
- ¹⁹ Cook, G. R.; Yu, H.; Sankaranarayanan, S.; Shanker, P. S. *J. Am. Chem. Soc.* **2003**, *125*, 5115.
- ²⁰ a) Trost, B. M.; Verhoeven, T. R. *J. Am. Chem. Soc.* **1976**, *98*, 630. b) Trost, B. M.; Verhoeven, T. R. *J. Org. Chem.* **1976**, *41*, 3215.
- ²¹ Lloyd-Jones, G. C.; Krska, S. W.; Hughes, D. L.; Gouriou, L.; Bonnet, V. D.; Jack, K.; Sun, Y.; Reamer, R. A. *J. Am. Chem. Soc.* **2004**, *126*, 702.
- ²² Trost, B. M.; Fandrick, D. R. *Aldrichimica Acta* **2007**, *40*, 59.
- ²³ Trost, B. M.; Krische, M. J.; Radinov, R.; Zanoni, G. *J. Am. Chem. Soc.* **1996**, *118*, 6297.
- ²⁴ Tsuji, J.; Takahashi, H.; Morikawa, M. *Tetrahedron Lett.* **1965**, *6*, 4387.
- ²⁵ a) Atkins, K. E.; Walker, W. E.; Manyik, R. M. *Tetrahedron Lett.* **1970**, *11*, 3821. b) Hata, G.; Takahashi, K.; Miyake, A. *J. Chem. Soc. D, Chem. Commun.* **1970**, 1392.
- ²⁶ Trost, B. M.; Strege, P. E. *J. Am. Chem. Soc.* **1977**, *99*, 1649.
- ²⁷ Trost, B. M.; Fullerton, T. J. *J. Am. Chem. Soc.* **1973**, *95*, 292.
- ²⁸ a) Myers, A. G.; Yang, B. H.; Chen, H.; McKinstry, L.; Kopecky, D. J.; Gleason, J. L. *J. Am. Chem. Soc.* **1997**, *119*, 6496. b) Kummer, D. A.; Chain, W. J.; Morales, M. R.; Quiroga, O.; Myers, A. G. *J. Am. Chem. Soc.* **2008**, *130*, 13231.
- ²⁹ Mukherjee, S.; Yang, J. W.; Hoffmann, S.; List, B. *Chem. Rev.* **2007**, *107*, 5471.
- ³⁰ Ooi, T.; Maruoka, K. *Angew. Chem. Int. Ed.* **2007**, *46*, 4222.

- ³¹ a) Doyle, A. G.; Jacobsen, E. N. *J. Am. Chem. Soc.* **2005**, *127*, 62. b) Doyle, A. G.; Jacobsen, E. N. *Angew. Chem. Int. Ed.* **2007**, *46*, 3701.
- ³² a) Bellina, F.; Rossi, R. *Chem. Rev.* **2010**, *110*, 1082. b) Johansson, C. C. C.; Colacot, T. J. *Angew. Chem. Int. Ed.* **2010**, *49*, 676.
- ³³ Taylor, A. M.; Altman, R. A.; Buchwald, S. L. *J. Am. Chem. Soc.* **2009**, *131*, 9900.
- ³⁴ Hiroi, K.; Abe, J.; Suya, K.; Sato, S.; Koyama, T. *J. Org. Chem.* **1994**, *59*, 203.
- ³⁵ Ibrahim, I.; Córdova, A. *Angew. Chem. Int. Ed.* **2006**, *45*, 1952.
- ³⁶ For reviews, see: a) Helmchen, G.; Dahnz, A.; Dübon, P.; Schelwies, M.; Weihofen, R. *Chem. Commun.* **2007**, 675. b) Hartwig, J. F.; Pouy, M. J. *Top. Organomet. Chem.* **2011**, *34*, 169.
- ³⁷ Weix, D.; Hartwig, J. F. *J. Am. Chem. Soc.* **2007**, *129*, 7720.
- ³⁸ Liu, D.; Xie, F.; Zhang, W. *Tetrahedron Lett.* **2007**, *48*, 7591.
- ³⁹ Mukherjee, S. List, B. *J. Am. Chem. Soc.* **2007**, *129*, 11336.
- ⁴⁰ Trost, B. M.; Keinan, E. *Tetrahedron Lett.* **1980**, *21*, 2591.
- ⁴¹ Tsuji, J.; Minami, I.; Shimizu, I. *Chem. Lett.* **1983**, *12*, 1325.
- ⁴² Saito, A.; Achiwa, K.; Morimoto, T. *Tetrahedron: Asymmetry* **1998**, *9*, 741.
- ⁴³ Hegedus, L. S.; Darlington, W. H.; Russell, C. E. *J. Org. Chem.* **1980**, *45*, 5193.
- ⁴⁴ Behenna, D. C.; Stoltz, B. M. *J. Am. Chem. Soc.* **2004**, *126*, 15044.
- ⁴⁵ Cheon, C. H.; Kanno, O.; Toste, F. D. *J. Am. Chem. Soc.* **2011**, *133*, 13248.
- ⁴⁶ Graening, T.; Hartwig, J. F. *J. Am. Chem. Soc.* **2005**, *127*, 17192.
- ⁴⁷ Bélanger, É.; Cantin, K.; Messe, O.; Tremblay, M.; Paquin, J.-F. *J. Am. Chem. Soc.* **2007**, *129*, 1034.
- ⁴⁸ Weaver, J. D.; Reccio, III, A.; Grenning, A. J.; Tunge, J. A. *Chem. Rev.* **2011**, *111*, 1846.
- ⁴⁹ a) Tsuda, T.; Chujo, Y.; Nishi, S.; Tawara, K.; Saegusa, T. *J. Am. Chem. Soc.* **1980**, *102*, 6381. b) Shimizu, I.; Yamada, T.; Tsuji, J. *Tetrahedron Lett.* **1980**, *21*, 3199.
- ⁵⁰ Mohr, J. T.; Behenna, D. C.; Harned, A. M.; Stoltz, B. M. *Angew. Chem. Int. Ed.* **2005**, *44*, 6924.
- ⁵¹ Trost, B. M.; Xu, J. *J. Am. Chem. Soc.* **2005**, *127*, 2846.
- ⁵² Trost, B. M.; Xu, J. *J. Am. Chem. Soc.* **2005**, *127*, 17180.
- ⁵³ Trost, B. M.; Xu, J.; Schmidt, T. *J. Am. Chem. Soc.* **2009**, *131*, 18343.
- ⁵⁴ Keith, J. A.; Behenna, D. C.; Mohr, J. T.; Ma, S.; Marinescu, S. C.; Oxgaard, J.; Stoltz, B. M.; Goddard, III, W. A.; *J. Am. Chem. Soc.* **2007**, *129*, 11876.
- ⁵⁵ Brozek, L. A.; Ardolino, M. J.; Morken, J. P. *J. Am. Chem. Soc.* **2011**, *133*, 16778.
- ⁵⁶ Burger, E. C.; Tunge, J. A. *Org. Lett.* **2004**, *6*, 4113.
- ⁵⁷ Burger, E. C.; Tunge, J. A. *Chem. Commun.* **2005**, 2835.
- ⁵⁸ Conservation of enantiomeric excess = (ee of product/ee of starting material) × 100.
- ⁵⁹ Constant, S.; Tortoioli, S.; Müller, J.; Lacour, J. *Angew. Chem. Int. Ed.* **2007**, *46*, 2082.
- ⁶⁰ He, H.; Zheng, X.-J.; Li, Y.; Dai, L.-X.; You, S.-L. *Org. Lett.* **2007**, *9*, 4339.
- ⁶¹ Negishi, E.; Matsushita, H.; Chatterjee, S.; John, R. A. *J. Org. Chem.* **1982**, *47*, 3188.
- ⁶² Trost, B. M.; Schroeder, G. M. *J. Am. Chem. Soc.* **1999**, *121*, 6759.
- ⁶³ You, S.-L.; Hou, X.-L.; Dai, L.-X.; Zhu, X.-Z. *Org. Lett.* **2001**, *3*, 149.
- ⁶⁴ a) Evans, P. A.; Leahy, D. K. *J. Am. Chem. Soc.* **2003**, *125*, 8974. b) Evans, P. A.; Lawler, M. J. *J. Am. Chem. Soc.* **2004**, *126*, 8642.
- ⁶⁵ Kazmaier, U.; Stolz, D. *Angew. Chem. Int. Ed.* **2006**, *45*, 3072.

-
- ⁶⁶ Braun, M.; Laicher, F.; Meier, T. *Angew. Chem. Int. Ed.* **2000**, *39*, 3494.
- ⁶⁷ Trost, B. M.; Schroeder, G. M.; Kristensen, J. *Angew. Chem. Int. Ed.* **2002**, *41*, 3492.
- ⁶⁸ Fiaud, J.-C.; Malleron, J. L. Takahashi, K.; Miyake, A. *J. Chem. Soc. Chem. Commun.* **1981**, 1159.
- ⁶⁹ Braun, M.; Meier, T. *Synlett* **2005**, 2968.
- ⁷⁰ Seebach, D. *Angew. Chem. Int. Ed. Engl.* **1988**, *27*, 1624.
- ⁷¹ Zheng, W.-H.; Zheng, B.-H.; Zhang, Y.; Hou, X.-L. *J. Am. Chem. Soc.* **2007**, *129*, 7718.
- ⁷² Chen, J.-P.; Ding, C.-H.; Liu, W.; Hou, X.-L.; Dai, L.-X. *J. Am. Chem. Soc.* **2010**, *132*, 15493.
- ⁷³ Evans, P. A.; Clizbe, E. A.; Lawler, M. J.; Oliver, S. *Chem. Sci.* **2012**, *3*, 1835.
- ⁷⁴ Seebach, D. *Angew. Chem. Int. Ed. Engl.* **1979**, *18*, 239.
- ⁷⁵ Tamaru, Y.; Yasui, K.; Takanabe, H.; Tanaka, S.; Fugami, K. *Angew. Chem. Int. Ed. Engl.* **1992**, *31*, 645.
- ⁷⁶ a) Hanzawa, Y.; Tabuchi, N.; Taguchi, T. *Tetrahedron Lett.* **1998**, *39*, 6249.
- ⁷⁷ Tsuji, Y.; Obora, Y.; Ogawa, Y.; Imai, Y.; Kawamura, T. *J. Am. Chem. Soc.* **2001**, *123*, 10489.
- ⁷⁸ Tsuji, Y.; Obora, Y.; Nakanishi, M.; Tokunaga, M. *J. Org. Chem.* **2002**, *67*, 5835.
- ⁷⁹ Helmchen, G.; Förster, S.; Tverskoy, O. *Synlett* **2008**, 2803.
- ⁸⁰ Trost, B. M.; Osipov, M.; Kaib, P. S. J.; Sorum, M. T. *Org. Lett.* **2011**, *13*, 3222.

Chapter 2

Rhodium-Catalysed Allylic Substitution with an Acyl Anion Equivalent: Asymmetric Construction of Acyclic Quaternary Carbon Stereogenic Centres

2.1. Rhodium-Catalysed Allylic Substitution Reactions

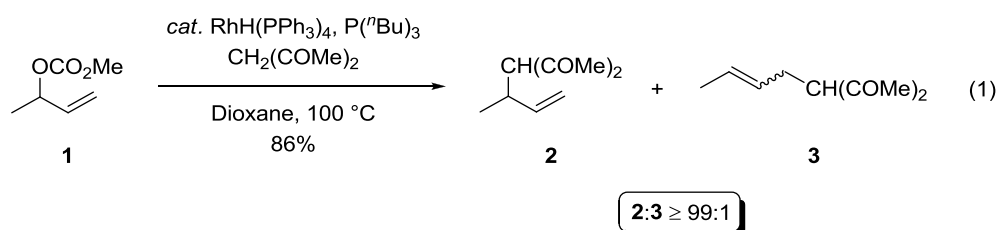
2.1.1. Introduction

The allylic substitution reaction represents a highly powerful synthetic transformation, which has been extensively studied using a wide range of transition metal complexes. Although palladium and other metal catalysts remain in widespread use, the analogous rhodium-catalysed variant has recently emerged as a particularly attractive method for target directed synthesis.¹ This is largely due to the impressive regio- and stereospecificity that can be achieved using rhodium complexes, especially in the alkylation of unsymmetrical allylic alcohol derivatives. The stereospecific reaction manifold is particularly pertinent, as it provides a complementary method to the enantioselective transition metal-catalysed allylic substitution reaction. While these processes are often sensitive to subtle structural modifications in the nucleophile or electrophile, the rhodium-catalysed allylic substitution affords predictably high levels of regio- and stereocontrol in a vast array of substrates, making it a highly potent method for the asymmetric construction of a wide range of C-C, C-N and C-O bonds.

2.1.2. Seminal Work

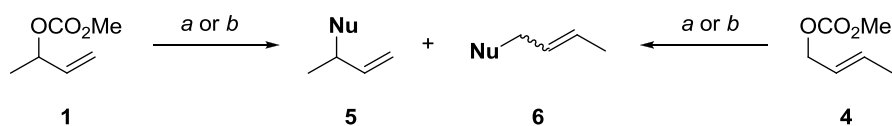
By 1984, the palladium-catalysed allylic substitution reaction had been studied extensively, and the emphasis of this work had shifted firmly towards the development of asymmetric variants. In contrast, there had only been one report of a rhodium-catalysed allylic substitution, in which Wilkinson's catalyst was shown to

facilitate the allylation of a cyclohexanone-derived enamine.² In 1984, following the development of a rhodium-catalysed decarboxylative allylation reaction,³ Tsuji reported the first regioselective rhodium-catalysed allylic alkylation of stabilised carbon nucleophiles (eq. 1).⁴ Treatment of the substituted carbonate **1** with acetylacetone in the presence of catalytic RhH(PPh₃)₄ and tri-*n*-butylphosphine furnished the branched alkylation adduct **2** in excellent yield, and with complete regioselectivity. The use of a carbonate leaving group, which liberates methoxide upon oxidative addition of the metal, allows the alkylation to proceed readily under neutral conditions.⁵ However, the most striking feature of this transformation is the unique regioselectivity, as the allylic alkylation of monosubstituted derivatives such as **1** would generally be expected to provide the product of alkylation at the less sterically hindered allylic terminus, namely the linear regioisomer **3**.



In a subsequent study, Tsuji demonstrated that the rhodium-catalysed allylic substitution proceeds with a high level of regiospecificity (**Scheme 1**).⁶ Rhodium-catalysed allylic alkylation of the branched allylic carbonate **1** with a β -ketoester led to predominant formation of the branched product **5**. Conversely, when the isomeric linear allylic carbonate **2** was employed, the linear alkylation product **6** was obtained, albeit as a mixture of geometrical isomers. Thus, the reaction displays an apparent “memory effect”, in which the substitution is largely affected at the allylic terminus that originally bore the leaving group. This is in contrast to the palladium-catalysed alkylation reaction, where, in a direct comparison, the same ratio of **5:6** was obtained

regardless of which starting material was employed. This remarkable result suggests that the rhodium-catalysed allylic alkylation, unlike the palladium-catalysed variant, does not proceed through a symmetrical π -allyl organometallic intermediate. In order to explain the observed regioselectivity, Tsuji proposed that the rhodium-catalysed allylic alkylation may proceed *via* a η^1 σ -allyl organorhodium complex. However, this hypothesis was not corroborated by additional experimental studies, and despite the exciting possibilities that were afforded by these observations, the reaction lay dormant for over a decade.



a. $\text{RhH}(\text{PPh}_3)_4$, P^tBu_3 , NuH , Dioxane, 100 °C; b. $\text{Pd}_2(\text{dba})_3 \cdot \text{CHCl}_3$, PPh_3 , NuH , THF, RT
 $\text{NuH} = \text{EtCOCH}(\text{Me})\text{CO}_2\text{Me}$

From 1: a. **5:6** = 86:14, 81%; b. **5:6** = 27:73, 89%

From 4: a. **5:6** = 28:72, 97%; b. **5:6** = 29:71, 93%

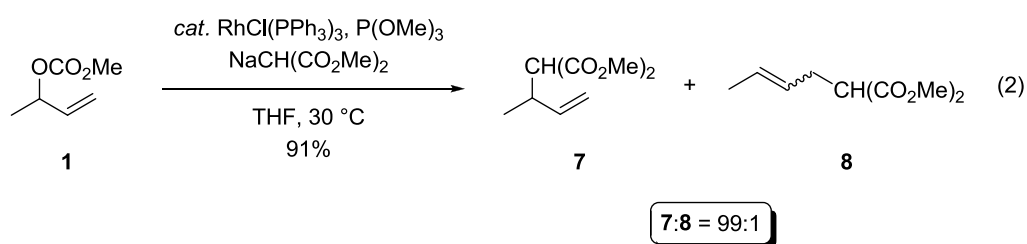
Scheme 1. Regiospecific rhodium-catalysed allylic substitution reactions.

2.1.3. Regio- and Stereospecific Rhodium-Catalysed Allylic Substitution Reactions

2.1.3.1. Seminal Work

In 1998, Evans demonstrated that Wilkinson's catalyst ($\text{RhCl}(\text{PPh}_3)_3$) may be modified with triorganophosphite derivatives to facilitate the highly regioselective allylic substitution of secondary and tertiary allylic carbonates with the sodium salt of dimethyl malonate (eq. 2).⁷ Shortly after, the regioselective alkylation of the corresponding allylic acetates was shown to proceed under almost identical conditions.⁸ The use of strong π -acceptor phosphite ligands, which presumably make the allyl intermediate more electrophilic, was shown to be essential in both cases. For allylic carbonates in particular, these ligands allowed the reaction to proceed at

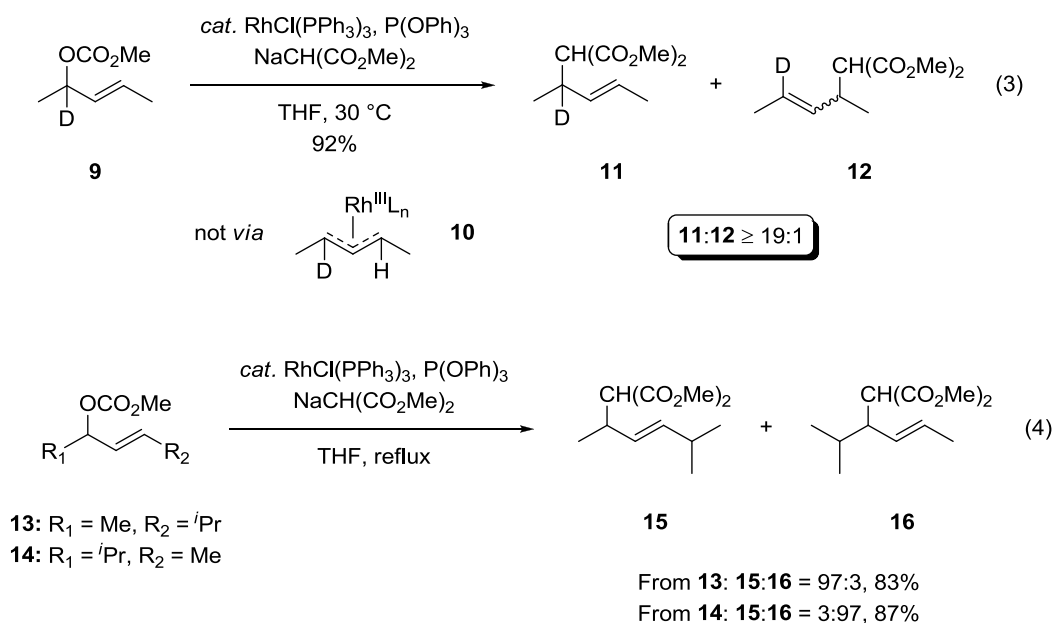
significantly lower temperatures than those employed by Tsuji,⁴ and also had a significant impact on the regioselectivity of the alkylation. For example, while the use of unmodified Wilkinson's catalyst afforded a 2:1 mixture of the branched and linear adducts **7** and **8**, the addition of trimethyl phosphite provided solely the branched regioisomer **7**, and in excellent yield. Importantly, the allylic alkylation of tertiary carbonates was equally regioselective, and afforded products containing all carbon quaternary stereogenic centres.



2.1.3.2. Mechanistic Studies

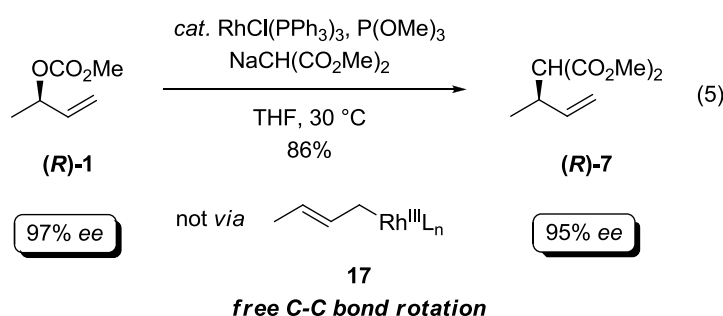
The impressive regioselectivity obtained with phosphite ligands can be attributed, at least in part, to their π -accepting ability.⁹ Metal-allyl intermediates derived from rhodium-phosphite complexes should be more cationic in nature than those derived from rhodium-phosphine complexes. Hence, as the stability of a carbocationic species increases with increasing substitution ($3^\circ > 2^\circ > 1^\circ$), the bulk of the positive charge character should reside at the more highly substituted secondary allylic terminus, making this site significantly more reactive towards an incoming nucleophile. However, the observed regioselectivity cannot be fully rationalised on electronic grounds, as the isomeric linear carbonates were shown to afford the branched product **7** with substantially lower selectivity (**7:8** = 2:1).¹⁰ This is in accord with Tsuji's earlier observations,⁶ and suggests that the isomeric branched and linear allylic carbonates may not afford the same π -allyl intermediate upon oxidative addition of the rhodium(I) catalyst.

In order to probe the origin of this unique selectivity, the deuterated carbonate **9** was subjected to the rhodium-catalysed allylic alkylation, as outlined in eq. 3.¹⁰ This experiment was designed to detect symmetrical η^3 π -allyl intermediates, as the complex **10**, which might be derived from **9**, contains two sterically and electronically equivalent allylic termini. Hence, were the reaction to proceed *via* this intermediate, it would be expected to afford a 1:1 mixture of the alkylation products **11** and **12**, as the malonate anion would be unable to distinguish between the two potential sites of nucleophilic attack.



Remarkably, the rhodium-catalysed allylic substitution of the deuterated carbonate **9** afforded the alkylation adduct **11** with complete regioselectivity (eq. 3). This clearly demonstrates that the regioselective rhodium-catalysed allylic alkylation is not strongly influenced by steric factors, and would appear to rule out the intermediacy of the symmetrical π -allyl complex **10**. This is in contrast to the palladium and iridium-catalysed variants which, in the reaction outlined in eq. 3, both provided a 2:1 mixture of **11** and **12**.¹⁰ Thus, while these metals would appear to have little “memory” of the initial substitution pattern, the rhodium catalyst has the ability to

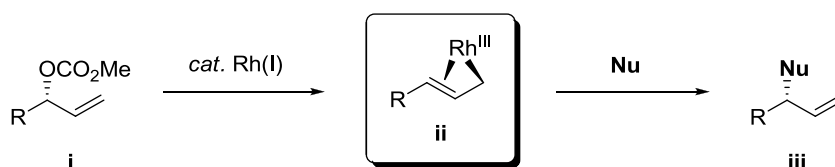
direct substitution solely towards the allylic terminus that originally bore the leaving group, despite the highly symmetrical nature of the substrate. The unsymmetrical allylic carbonates **13** and **14** were also shown to display this “memory effect” (eq. 4), once more indicating that the alkylation is tolerant of a sterically congested environment. Overall, these observations suggest that the reaction proceeds *via* a η^1 σ -allylrhodium intermediate, the nucleophilic displacement of which is significantly faster than σ - π - σ isomerisation.



With respect to the monosubstituted derivative **1**, the above evidence is consistent with a mechanism involving S_N2' alkylation of the primary η^1 σ -allyl intermediate **17** (eq. 5). Direct insertion of the metal into the C-O bond of the allylic carbonate, followed by S_N2 alkylation of the resultant secondary σ -organorhodium intermediate, is also a possibility.⁸ However, based on the observation that increased alkene substitution significantly reduces the rate of the allylic alkylation, the primary σ -allyl **17** is a more likely intermediate. In order to shed more light on this mechanistic pathway, the rhodium-catalysed allylic substitution of the enantiomerically enriched allylic alcohol derivative **(R)-1** was examined, as outlined in eq. 5. Based on previous experimental studies, oxidative addition of the rhodium(I) complex to **(R)-1** was expected to provide the *achiral* primary σ -allyl intermediate **17**, in which uninhibited C-C bond rotation makes both π -faces of the alkene equally accessible to the nucleophile. Thus, should the reaction proceed *via* this intermediate, S_N2'

addition of the malonate nucleophile would be expected to afford the product **7** in racemic form.

Treatment of the enantiomerically enriched allylic carbonate **(R)-1** (97% *ee*) with the sodium salt of dimethyl malonate in the presence of catalytic $\text{RhCl}(\text{PPh}_3)_3$, modified with trimethyl phosphite, furnished the branched product **(R)-7** in excellent yield and with almost complete retention of absolute configuration (95% *ee*) (eq. 5).¹⁰ In providing a valuable new method for acyclic stereocontrol, this reaction also ruled out the possible intermediacy of the η^1 σ -allyl intermediate **17**. Hence, the regio- and stereochemical outcome of this transformation is not consistent with the formation of either a π - or σ -allylrhodium intermediate. Consequently, and following additional mechanistic experiments, the rhodium-catalysed allylic substitution was proposed to proceed *via* a configurationally stable distorted rhodium(III)-allyl, or *enyl*, intermediate (**Scheme 2**).



Scheme 2. Proposed *enyl* intermediate in the rhodium-catalysed allylic substitution reaction.

Both the regio- and stereochemical outcome of the rhodium-catalysed allylic substitution was attributed to the formation of the configurationally stable rhodium-*enyl* ($\sigma + \pi$) intermediate **ii**. As depicted in **Scheme 2**, *enyl* complexes can be defined as those containing discrete π - and σ -metal-carbon interactions within a single allyl ligand. An examination of the literature reveals a body of evidence supporting the existence of *enyl* coordination in rhodium-allyl complexes, some of which is

depicted in **Figure 1**. Among the first isolated rhodium(III)-allyl complexes, described by Wilkinson in 1966,¹¹ two are proposed to be ($\sigma + \pi$)-bound. In addition to these complexes, which were characterised by ¹H NMR and IR spectroscopy, single crystal X-ray analysis of isolated $[\text{Rh}(\eta^3\text{-C}_3\text{H}_5)_2\text{OH}]_2$ revealed unusual asymmetric binding in the allyl component.¹² As depicted, the Rh-C3 bond is significantly longer than the Rh-C1 and Rh-C2 bonds, which is indicative of an *enyl* binding mode. These bond length values are in agreement with those reported for Rh-C σ - and Rh-C π -interactions, respectively, and similar structural characteristics have been observed in both $[\text{RhBr}(\eta^3\text{-C}_3\text{H}_5)_2]_2$ ¹³ and $[\text{RhCl}(\eta^3\text{-C}_3\text{H}_5)_2]_2$.¹⁴ A number of *enyl* complexes of other metals, including cobalt and platinum, have also been characterised in the literature. Importantly, these complexes display significant variation from the analogous complexes of palladium, which is consistent with the differential reactivity of palladium and rhodium catalysts in the allylic substitution reaction. Undoubtedly, the asymmetric environment created by the octahedral coordination of d⁶ Rh(III) complexes is critical to the binding of the allyl component, particularly in comparison to the corresponding d⁸ Pd(II) complexes, which are generally restricted to a square planar geometry.

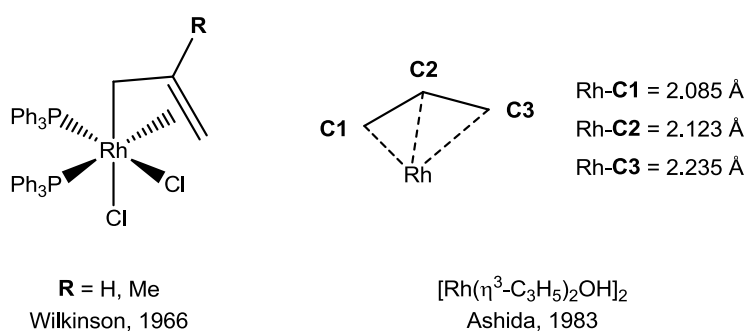
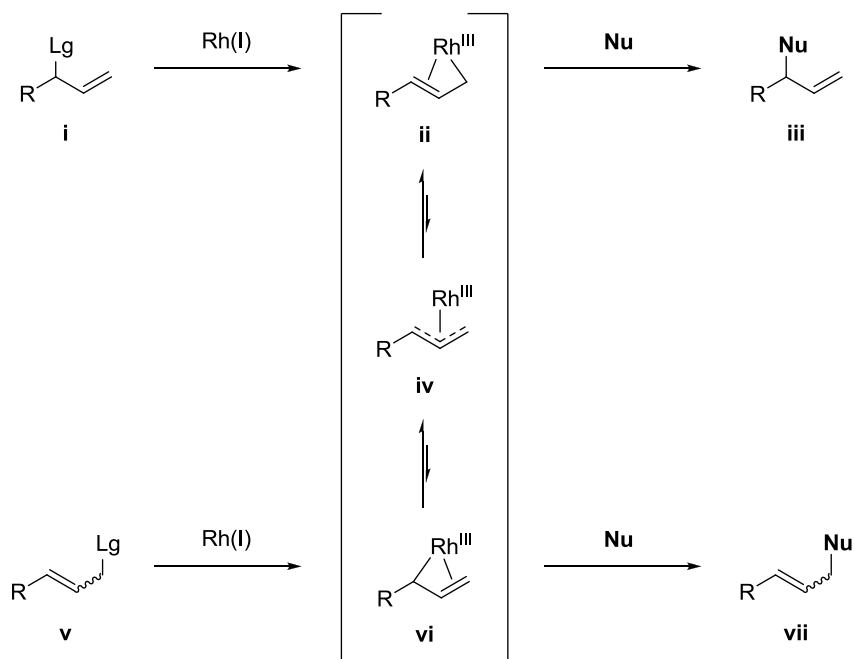


Figure 1. Experimental evidence for the *enyl* binding mode in rhodium-allyl complexes.

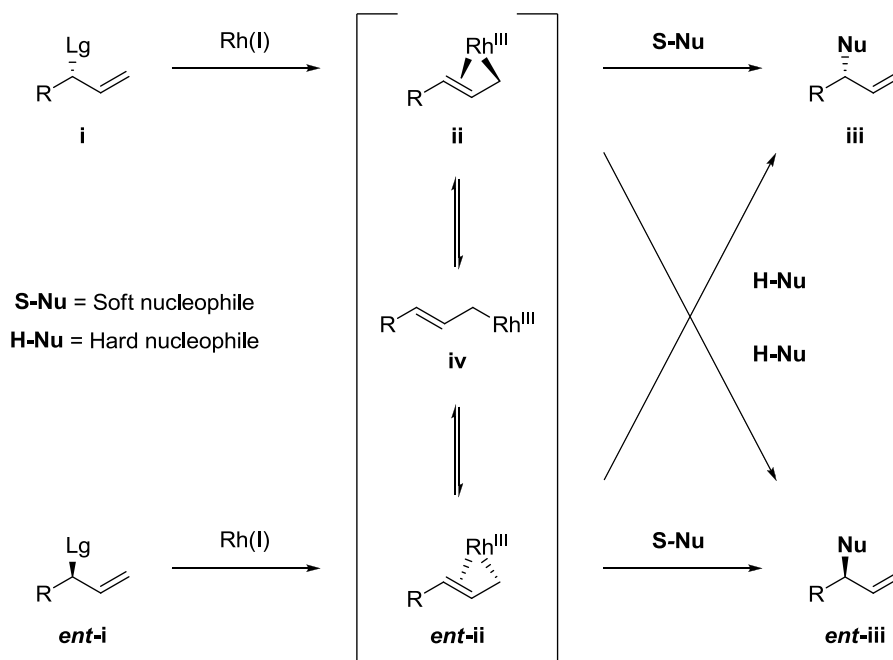
A mechanistic model for the regioselective rhodium-catalysed allylic alkylation is outlined in **Scheme 3**. The rhodium-*enyl* complex **ii** is proposed to form *via* oxidative addition of a rhodium(I) complex to the branched allylic system **i**. Subsequent S_N2' addition of a stabilised nucleophile then provides the branched alkylation product **iii**. The isomeric *enyl* complex **vi** may be derived from the linear derivative **v**, or *via* σ - π - σ isomerisation of **ii**, which can be envisaged to proceed *via* the symmetrical π -allyl complex **iii**. The intermediate **vi** provides the linear product **vi** upon alkylation. Thus, in order to obtain high levels of regioselectivity for the branched product **iii**, alkylation of the rhodium-*enyl* **ii** must be faster than σ - π - σ isomerisation *via* **iv**. Experimental evidence suggests that the rhodium-*enyl* intermediate is more strongly influenced by the degree of substitution in the σ -component than the steric nature of the substituent R (*cf.* eq. 4). As a result, the isomerisation of **ii** (primary σ -component) to **vi** (secondary σ -component) is generally slower than nucleophilic displacement, which explains the high levels of regioselectivity obtained with branched allylic carbonates. Conversely, **vi** will more readily isomerise to **ii**, so the allylic alkylation of the linear derivative **iv** is expected to provide a mixture of regioisomers. This hypothesis is strongly supported by the experimental findings of both Evans and Tsuji.^{6,10} However, Martin has demonstrated that complete regioselectivity can be obtained for either product in the presence of [Rh(CO)₂Cl]₂, which is presumably a function of the unusually high π -acidity of the CO ligands.¹⁵



Scheme 3. Mechanistic model for the regioselective rhodium-catalysed allylic substitution reaction.

The remarkable stereospecificity of the rhodium-catalysed allylic substitution can be attributed to the relative configurational stability of the rhodium-*enyl* complex **ii** (**Scheme 4**). Oxidative addition of the metal to the enantiomerically enriched substrate **i** proceeds opposite the leaving group, to afford the *enyl* complex **ii** with inversion of configuration. The attack of a stabilised (soft) nucleophile should then occur on the face opposite the metal centre to afford **iii**, also with inversion. Overall, the reaction proceeds *via* a classical double inversion mechanism, to provide overall retention of absolute configuration. Although the *enyl* complex **ii** is seemingly not prone to rapid π - σ - π isomerisation, nucleophilic displacement of the rhodium-*enyl* **ii** must occur faster than isomerisation to the *achiral* σ -allyl **iv** in order to avoid stereochemical leakage. The product of inversion, *ent-iii*, may also be derived from the direct addition of an unstabilised (hard) nucleophile to the metal centre in **ii**, followed by reductive elimination. This pathway is well demonstrated by the

rhodium-catalysed allylic arylation,¹⁶ developed by Evans and Uraguchi, which proceeds with overall inversion of configuration. However, it should be noted that due to the lack of fluxionality in the proposed rhodium-*enyl* intermediate, enantioselective rhodium-catalysed allylic substitution reactions are rare.¹⁷



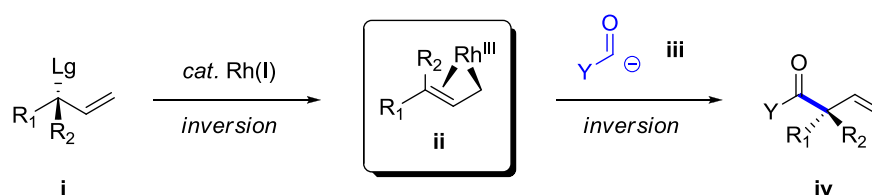
Scheme 4. Mechanistic model for the stereospecific rhodium-catalysed allylic substitution reaction.

2.2. Rhodium-Catalysed Allylic Substitution with an Acyl Anion Equivalent

2.2.1. Introduction

The highly regio- and stereospecific nature of the rhodium-catalysed allylic substitution has been demonstrated on numerous occasions over the last decade. Recognising this, we aimed to expand the scope of this process to include an acyl anion equivalent as a pronucleophile. More specifically, we envisaged that the enantiomerically enriched tertiary alcohol derivative **i** ($R_1/R_2 \neq H$) could be directly converted to the acyclic α -quaternary substituted ketone **iv** *via* the double inversion process outlined in **Scheme 5**. Although the stereospecific allylic substitution

reaction is well precedented for secondary allylic carbonates,⁷ the analogous reaction of an enantiomerically enriched tertiary allylic alcohol derivative such as **i** is potentially more challenging, and has yet to be achieved using a rhodium catalyst. We expected the nature of the acyl anion equivalent **iii** to be an important component, as a stabilised anion would provide overall retention of configuration, whereas the use of an unstabilised nucleophile would afford the opposite enantiomer of the product ketone **iv**. Despite having a number of potential advantages in terms of regio- and stereoselectivity, this particular synthetic disconnection has not been widely studied. Among the few reported examples that provide the ketone product directly, the vast majority are entirely selective for the achiral linear regioisomer rather than the substituted product **iv**, which illustrates the challenges associated with developing this type of transformation.



Scheme 5. Proposed asymmetric synthesis of acyclic α -quaternary substituted ketones *via* regio- and stereospecific rhodium-catalysed allylic substitution.

The following discussion will outline our successful implementation of this strategy, and will be organised into three distinct sections, describing:

- the initial development of a highly regioselective rhodium-catalysed allylic substitution with an aryl-substituted acyl anion equivalent
- the development of a stereospecific variant for the asymmetric construction of acyclic quaternary carbon stereogenic centres

- the extension of this methodology to alkenyl-substituted nucleophiles, for the construction of highly functionalised α,α' -dialkyl ketones

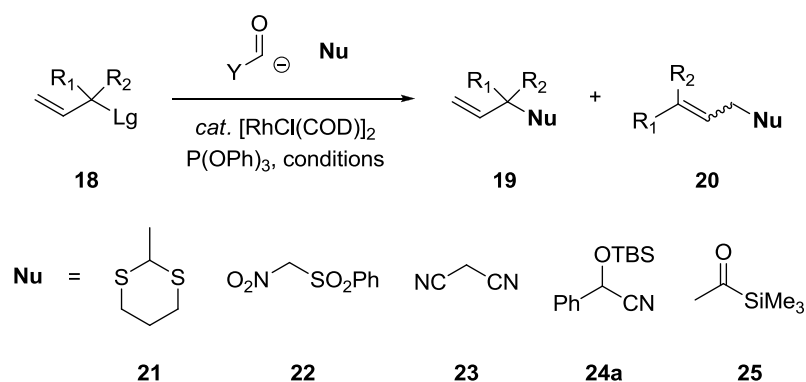
2.2.2. Initial Results

In an attempt to identify a suitable acyl anion equivalent, a number of pronucleophiles were screened in the rhodium-catalysed allylic substitution of the racemic allylic alcohol derivative **18** (Table 1). All of the nucleophilic species **21-25** have been shown to function as acyl anion equivalents, and **22**, **23** and **25** have been successfully utilised in transition metal-catalysed allylic substitution reactions. The nucleophiles **21-24** were all deprotonated with a suitable lithium base before use, whereas the acylsilane **25** was employed in conjunction with a secondary allylic trifluoroacetate,¹⁸ and in the absence of a base and ligand, in accord with previous studies.¹⁹ Triphenyl phosphite, which has previously been shown to function effectively in the alkylation of tertiary allylic carbonates,⁷ was used as a ligand in the reactions of the remaining nucleophiles.

Unfortunately, all but one of the pronucleophiles **21-25** failed to react efficiently in the rhodium-catalysed allylic substitution reaction. Although partial conversion was observed in the alkylation of malononitrile (entry 3), the allylic electrophile **18** was untouched in the majority of cases, and underwent significant transesterification in the presence of the dithiane **21**, to provide the corresponding allylic alcohol. Gratifyingly, the rhodium-catalysed allylic alkylation of the *tert*-butyldimethylsilyl-protected cyanohydrin **24a** did proceed efficiently (entry 4), affording clean and complete conversion to a 5:1 mixture of the alkylation products **19** and **20**, which were isolated in excellent yield. The TBS-protected cyanohydrin **24a** represents a novel nucleophile for this transformation. However, the application of this species is not entirely unprecedented, as the corresponding tetrahydropyran-protected

cyanohydrin was previously employed in the palladium-catalysed allylic alkylation reaction.²⁰ Due to the significant degree of stabilisation afforded by a combination of the aryl- and cyano-substituents, we expected the lithium salt of the benzaldehyde cyanohydrin **24a** to function as a stabilised anion in this transformation, which would permit the double inversion process outlined in **Scheme 5**.

Table 1. Initial examination of acyl anion equivalents in the rhodium-catalysed allylic substitution reaction ($R_1 = \text{Ph}(\text{CH}_2)_2$).



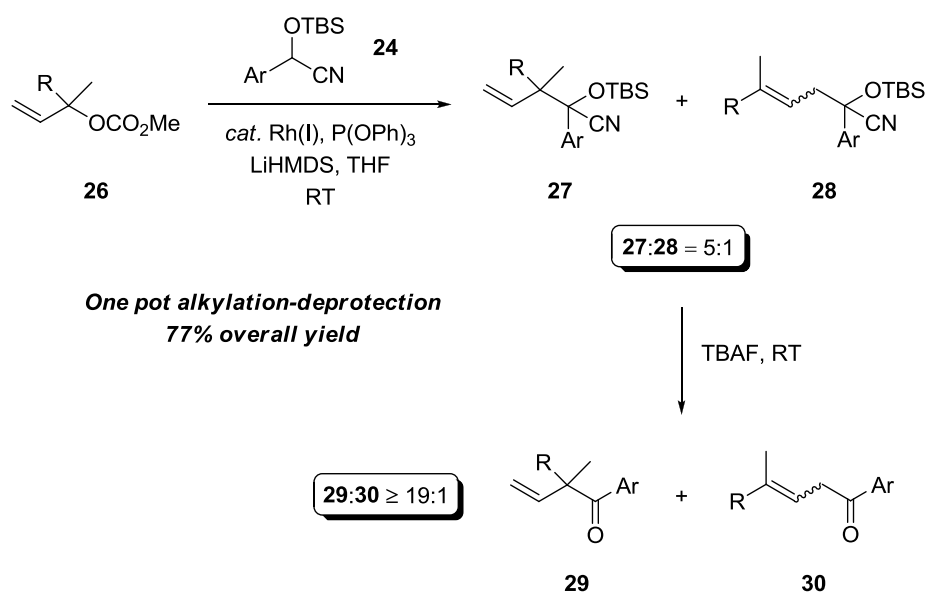
Entry ^a	R ₂	Lg	Nu	Conditions	Conv. (%) ^{b,c}
1	Me	OCO ₂ Me	21	ⁿ BuLi, THF, 0 °C-RT	0
2	“	“	22	LiHMDS, THF, 0 °C-RT	0
3	“	“	23	“	33
4	Me	OCO₂Me	24a	LiHMDS, THF, 0 °C-RT	100 (94)
5 ^d	H	OCOCF ₃	25	THF, RT	0

^a All reactions were performed on a 0.5 mmol reaction scale using 2.5 mol% [Rh(COD)Cl]₂ and 20 mol% P(OPh)₃ in THF (5 mL) for ca. 16 h. ^b Conversion was determined by 500 MHz ¹H NMR on the crude reaction mixtures. ^c Isolated yields are shown in parentheses. ^d Reaction conducted in the absence of P(OPh)₃.

2.2.3. Rhodium-Catalysed Allylic Substitution with Aryl Cyanohydrin Pronucleophiles

2.2.3.1. Development of a One Pot Procedure

Having established the utility of the TBS-protected cyanohydrin **24a**, our next goal was to unmask the carbonyl functionality and isolate the desired α -quaternary substituted ketone **29** (Scheme 6). Although the isolated cyanohydrin adducts may be cleanly desilylated in the presence of 1.1 equivalents of tetra-*n*-butylammonium fluoride (TBAF), we chose to develop a more practical one pot procedure in which both reactions could be conducted sequentially, and without purification of the cyanohydrin intermediates **27** and **28**.



Scheme 6. One pot deprotection of the cyanohydrin adducts **27** and **28** ($R = \text{Ph}(\text{CH}_2)_2$, $\text{Ar} = \text{Ph}$).

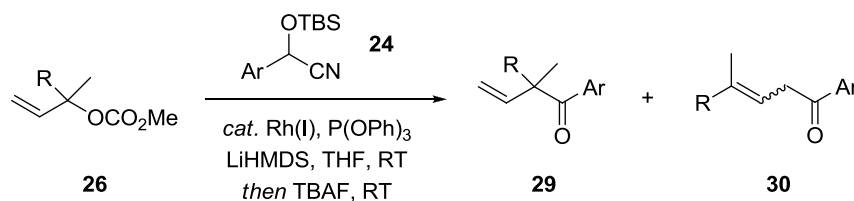
Treatment of the tertiary allylic carbonate **26a** ($R = \text{Ph}(\text{CH}_2)_2$) with the lithium salt of the cyanohydrin **24a** ($\text{Ar} = \text{Ph}$), in the presence of catalytic $[\text{RhCl}(\text{COD})]_2$ and triphenylphosphite ($\text{P}:\text{Rh} = 4:1$), followed by the direct addition of TBAF, furnished the desired ketone **25** in good yield and as a single regioisomer (Scheme 6).

Additionally, ^1H NMR analysis of the crude reaction mixture failed to detect the linear ketone **30**, suggesting that this product may be unstable under the reaction conditions. Though clearly advantageous from a synthetic perspective, we were keen to understand the mechanism by which the undesired ketone **30** is consumed, as will be discussed in section **2.2.3.5**. Armed with this practical procedure, we next sought to improve the regioselectivity, and hence the efficiency, of the alkylation.

2.2.3.2. Reaction Optimisation

A number of previous studies have highlighted the importance of ligand:metal stoichiometry to both the efficiency and selectivity of rhodium-catalysed allylic substitution reactions. For example, in the reaction of dimethyl malonate with tertiary allylic carbonates such as **26**, a 3:1 ratio of triphenylphosphite to rhodium has been demonstrated to be optimal in terms of catalytic turnover and selectivity.⁷ With the cyanohydrin nucleophile **24a**, a decrease in the P:Rh ratio was accompanied by a modest improvement in both regioselectivity and yield (**Table 2**). The use of at least 2 equivalents of phosphite is presumably necessary in order to fully expel the labile 1,5-cyclooctadiene ligands of the initial rhodium(I) complex, to provide a catalytically active species.

Table 2. Effect of metal:ligand stoichiometry on the rhodium-catalysed allylic substitution with the acyl anion equivalent **24** (R = Ph(CH₂)₂, Ar = Ph).



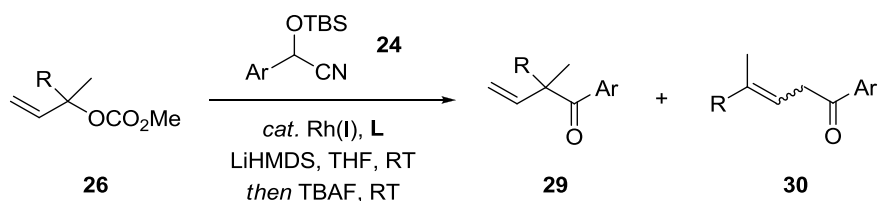
Entry ^a	P:Rh	rs ^b	Yield (%) ^c
1	4:1	5:1	77
2	3:1	7:1	82
3	2:1	7:1	82

^a All reactions were performed on a 0.5 mmol reaction scale using 2.5 mol% [Rh(COD)Cl]₂, 1.3 equiv. **24** and 1.8 equiv. LiHMDS in THF (5 mL) for *ca.* 16 h, followed by the addition of 2.5 equiv. TBAF at room temperature. ^b Regioselectivity was determined by 500 MHz ¹H NMR on the crude reaction mixtures before deprotection of the cyanohydrin adducts **27** and **28**. ^c GC yields of the desired regioisomer **29**.

A range of commercially available ligands were screened in the allylic alkylation of the tertiary carbonate **26a** with the aryl cyanohydrin **24a**. Gratifyingly, the reaction was shown to proceed with almost equal efficiency in the presence of a variety of phosphorus ligands. For example, identical regioselectivity was afforded by both triphenylphosphine (entry 2) and the electron poor tris(2,2,2-trifluoroethyl) phosphite (entry 4). The phosphite is significantly more π -acidic than the phosphine, but also much smaller,²¹ which strongly suggests that the regioselectivity of the alkylation is governed by steric, rather than electronic factors. This led to the examination of sterically bulky ligands such as tris(*tert*-butyldimethylsilyl) phosphite and tris(2,4-di-*tert*-butylphenyl) phosphite, both of which provided a significant improvement in regioselectivity (entries 5 and 6). However, due to competing transesterification of the methyl carbonate **26**, the reaction using P(OTBS)₃ provided only a moderate yield of the ketone **29** at room temperature. The bulky aryl phosphite P(O-2,4-di-

^tBuC₆H₃)₃ was therefore chosen as the optimal ligand (entry 6). To our knowledge, this ligand has not previously been utilised in the allylic substitution reaction.

Table 3. Effect of the ligand on the rhodium-catalysed allylic substitution with the acyl anion equivalent **24** (R = Ph(CH₂)₂, Ar = Ph).

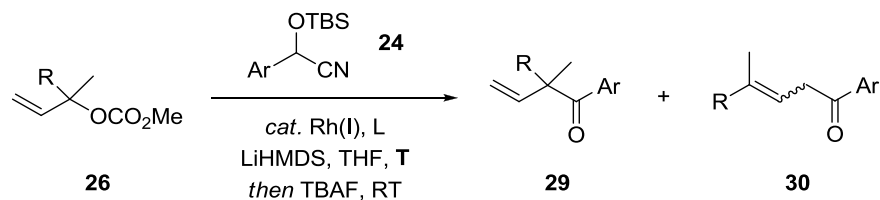


Entry ^a	L	rs ^b	Yield (%) ^c
1	P(OPh) ₃	7:1	82
2	PPh ₃	6:1	76
3	P(OMe) ₃	4:1	78
4	P(OCH ₂ CF ₃) ₃	6:1	82
5	P(OTBS) ₃	10:1	54
6	P(O-2,4-di-^tBuC₆H₃)₃	11:1	84

^a All reactions were performed on a 0.5 mmol reaction scale using 2.5 mol% [Rh(COD)Cl]₂, 10 mol% L, 1.3 equiv. **24** and 1.8 equiv. LiHMDS in THF (5 mL) for *ca.* 16 h, followed by the addition of 2.5 equiv. TBAF at room temperature. ^b Regioselectivity was determined by 500 MHz ¹H NMR on the crude reaction mixtures before deprotection of the cyanohydrin adducts **29** and **30**. ^c GC yields of the desired regioisomer **29**.

In order to complete our optimisation, the reaction temperature was reduced as outlined in **Table 4**. Gratifyingly, a significant increase in regioselectivity was observed at both 0 °C and -10 °C, with the latter providing a more efficient alkylation. Under these optimal conditions, the ketone **29** was obtained in 93% yield and as a single regioisomer, and although the temperature could be reduced further without any loss in conversion, this was not beneficial to either the yield or regioselectivity of the alkylation.

Table 4. Effect of the reaction temperature on the rhodium-catalysed allylic substitution with the acyl anion equivalent **24** (R = Ph(CH₂)₂, Ar = Ph, L = P(O-2,4-di-^tBuC₆H₃)₃).



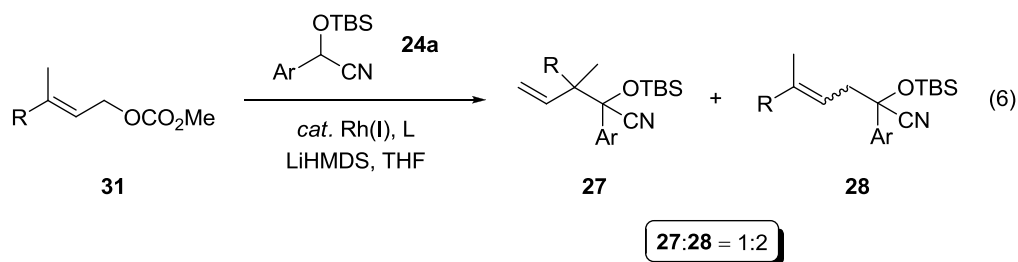
Entry ^a	T (°C)	rs ^b	Yield (%) ^c
1	RT	11:1	84
2	0	17:1	82
3	-10	≥ 19:1	93

^a All reactions were performed on a 0.5 mmol reaction scale using 2.5 mol% [Rh(COD)Cl]₂, 10 mol% L, 1.3 equiv. **24** and 1.8 equiv. LiHMDS in THF (5 mL) for *ca.* 16 h, followed by the addition of 2.5 equiv. TBAF at room temperature. ^b Regioselectivity was determined by 500 MHz ¹H NMR on the crude reaction mixtures before deprotection of the cyanohydrin adducts **27** and **28**. ^c GC yields of the desired regioisomer **29**.

2.2.3.3. Rationale for Regioselectivity

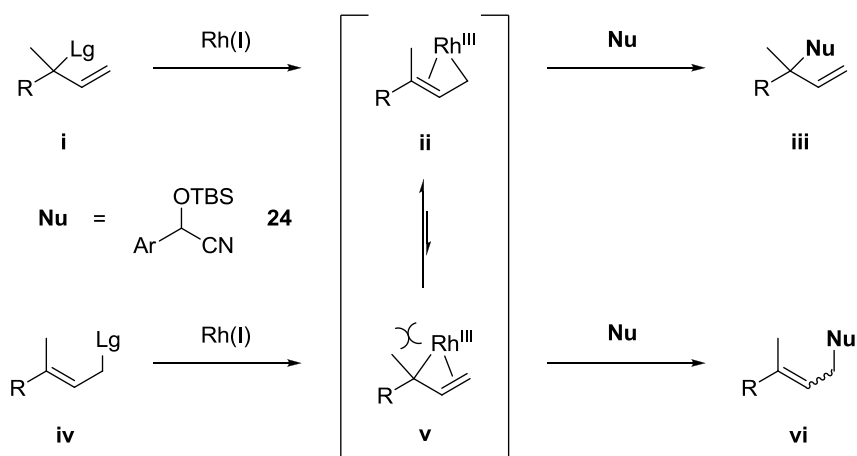
In order to gain more insight into the origin of the observed regioselectivity, we elected to examine the alkylation of the (*E*)-linear allylic carbonate **31** (R = Ph(CH₂)₂). Treatment of this substrate, prepared in three steps from benzylacetone,²² with the cyanohydrin **24a** (Ar = Ph) under the requisite catalytic conditions provided the cyanohydrin adducts **27** and **28** as a 2:1 mixture of regioisomers favouring **28** (eq. 6). This reaction was notably less efficient than that of the isomeric branched carbonate, providing incomplete conversion and a host of unidentified side products. The regiochemical outcome of this transformation is also in contrast to that of the tertiary allylic carbonate **26**, which is selective for the branched regioisomer **27** (Table 3, entry 6). This clearly indicates that the reaction is *regiospecific*, and is consistent with the mechanistic model outlined in Scheme 3. The failure of this

reaction to proceed to completion, even at room temperature, is not surprising given the highly substituted nature of the alkene.



The regiochemical outcome of this transformation was tentatively rationalised as follows. Due to the inherent stability of tertiary carbocationic species, nucleophilic addition of the lithiated cyanohydrin to the substituted allylic terminus is electronically favoured. Hence, even in the presence of weaker π -acceptor ligands such as triphenylphosphine, the reaction is moderately regioselective (**Table 3**, entry 2). According to our mechanistic model, σ - π - σ isomerisation of the initially formed *enyl* intermediate **ii** to the isomeric complex **v**, in which the the σ -component is tertiary, should be slow (**Scheme 7**). We propose that the Rh-*enyl* intermediate **ii** would be less likely to undergo isomerisation to **v** in the presence of a bulky ligand such as P(O-2,4-di-*t*-BuC₆H₃)₃ due to the increased steric repulsion between the metal centre and the highly substituted quaternary carbon centre. Thus, the rate of alkylation would be significantly faster than the rate of isomerisation, resulting in excellent selectivity for the branched adduct **iii**. This rate differential would clearly be smaller in the presence of a less sterically demanding ligand such as trimethylphosphite, as the isomerisation of **ii** to **v** should be more facile, resulting in significantly reduced regioselectivity. A similar mechanistic rationale was recently proposed for the regiodivergent iron-catalysed allylic alkylation,²³ in which a sterically demanding NHC-carbene ligand was proposed to drive the formation of a

primary σ -allyl intermediate, as opposed to the more hindered π -allyl or tertiary σ -allyl derivatives.

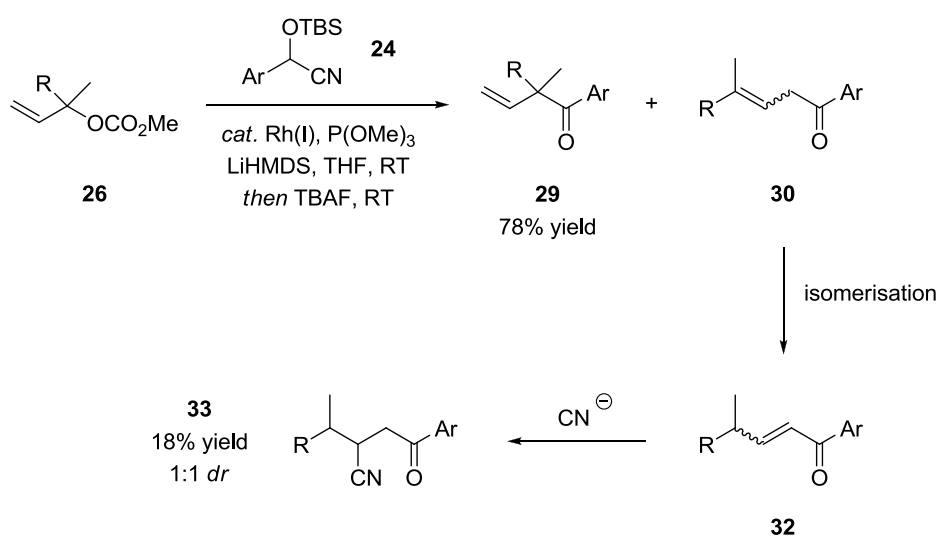


Scheme 7. Proposed rationale for the regiochemical outcome of the rhodium-catalysed allylic substitution of the tertiary carbonate **26** with the cyanohydrin **24**.

2.2.3.4. Consumption of the Linear Regioisomer

The particularly poor regioselectivity obtained using trimethylphosphite (Table 3, entry 3) provided an opportunity to examine the apparent instability of the linear regioisomer **30** (Scheme 6). Careful column chromatography revealed that in addition to the α -quaternary substituted ketone **29**, this reaction also furnished the nitrile **33**, which was isolated in 18% yield and as a 1:1 mixture of diastereoisomers. This adduct is presumably formed *via* isomerisation of the β,γ -unsaturated ketone **30** to the α,β -unsaturated ketone **32**, which then undergoes conjugate addition of the nucleophilic cyanide that is liberated upon desilylation of the cyanohydrin precursor **27**. The isolated yield of each product is consistent with the regioselectivity of the alkylation, indicating that the linear regioisomer **30** is entirely consumed by this pathway. The basic nature of TBAF is well established,²⁴ and is likely to be responsible for the isomerisation of the ketone **30**, which contains two acidic α -carbonyl protons. This highlights the importance of the α -quaternary stereogenic

centre to the stability of the substituted product **29**, and has significant consequences for the application of this method to the synthesis of α -tertiary ketones, as will be discussed in section **2.2.5.2**. It should be noted that the isomerisation of **30** may be largely prevented by conducting the desilylation at $-40\text{ }^{\circ}\text{C}$, enabling the isolation of a regioisomeric mixture. However, as the consumption of this product permits facile isolation of the substituted regioisomer **29**, regardless of the selectivity, we elected to conduct this deprotection at room temperature for the duration of this study.



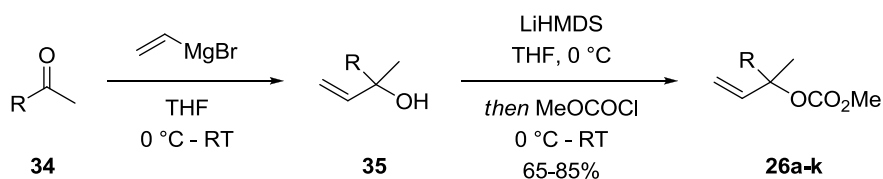
Scheme 8. Base-mediated consumption of the linear regioisomer **30** ($\text{R} = \text{Ph}(\text{CH}_2)_2$, $\text{Ar} = \text{Ph}$).

2.2.3.5. Substrate Scope

2.2.3.5.1. Substrate Synthesis

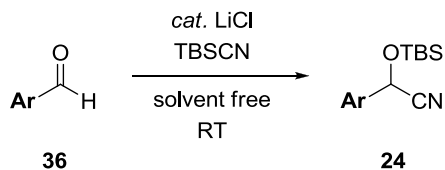
In order to examine the substrate scope of this process, with respect to both reaction components, a number of aryl cyanohydrins and tertiary allylic carbonates were synthesised. All of the tertiary allylic carbonates used in this study were prepared from the corresponding allylic alcohols, as outlined in **Scheme 9**. Addition of vinylmagnesium bromide to the commercially available ketones **34** furnished the desired tertiary allylic alcohols **35**. Subsequent deprotonation with a strong base,

followed by trapping of the resultant lithium alkoxide with methyl chloroformate, cleanly afforded the required tertiary allylic carbonates **26** in good to excellent yield. Due to the inherent basicity of the Grignard reagent, the first step in this sequence was often hindered by competing aldol reactions. This made it difficult to purify the allylic alcohol precursors **35**, which were therefore routinely employed in slightly impure form.



Scheme 9. Synthesis of the tertiary allylic carbonates **26a-k**.

The required aryl cyanohydrins were prepared by cyanosilylation of the commercially available aryl aldehydes **36**, according to the procedure reported by Kurono.²⁵ Treatment of the aldehydes **36** with *tert*-butyldimethylsilyl cyanide (TBSCN) under solvent free conditions, in the presence of catalytic lithium chloride, furnished the requisite cyanohydrin derivatives **24**. As outlined in **Table 5**, this process is general for a range of electron poor and electron rich *ortho*-, *meta*- and *para*- substituted aryl aldehydes, all of which provided the corresponding cyanohydrin in excellent yield. In cases where the aldehyde exists as a solid, a small volume of THF was required to solubilise the reaction mixture; however, the reaction concentration was generally maintained at > 5M. In this reaction, lithium chloride behaves as a nucleophilic catalyst rather than a Lewis acid. Similar to the widely studied 18-crown-6/KCN catalyst system,²⁶ the reactive nucleophile is likely to be a pentavalent silicon species ($\text{Li}^+[\text{tBuMe}_2\text{SiCl}(\text{CN})]^-$), as supported by ¹³C NMR analysis of the reaction mixture.²⁵

Table 5. Synthesis of the aryl cyanohydrins **24a-h**.

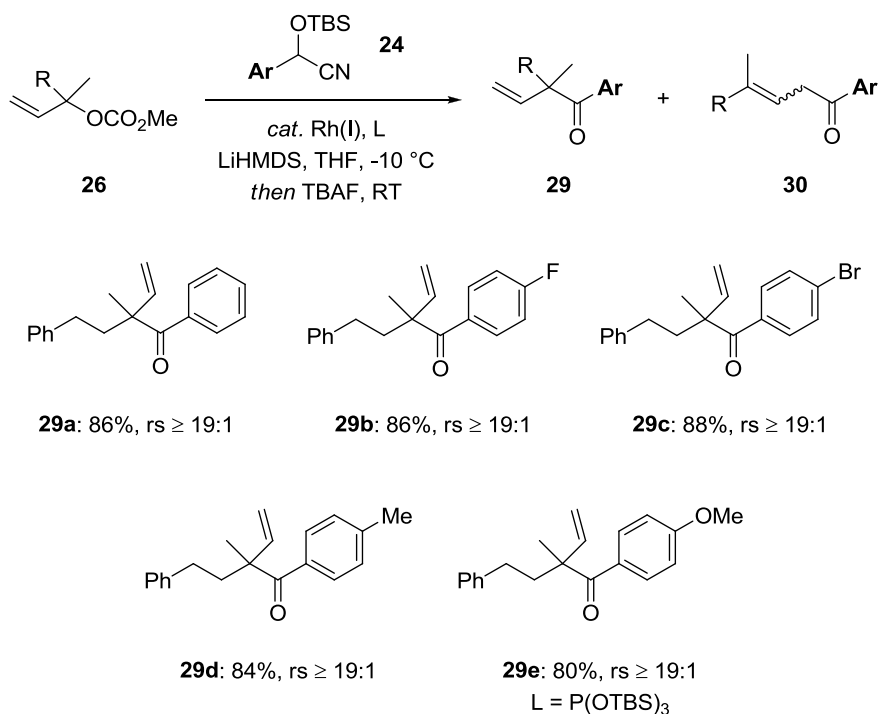
Entry ^a	Ar		Yield (%) ^b
1	Ph	24a	91
2	4-FC ₆ H ₄	24b	83
3	4-BrC ₆ H ₄	24c	85
4	4-MeC ₆ H ₄	24d	80
5	4-MeOC ₆ H ₄	24e	83
6	3-FC ₆ H ₄	24f	85
7	2-FC ₆ H ₄	24g	86
8	2-MeC ₆ H ₄	24h	87

^aAll reactions were performed using 5 mol% lithium chloride. ^bIsolated yields.

2.2.3.5.2. Cyanohydrin Scope

As outlined in **Table 6**, a range of aryl cyanohydrins were examined in the rhodium-catalysed allylic substitution of the tertiary allylic carbonate **26a**. The alkylation is clearly tolerant of both electron poor and electron rich aryl groups, all of which provided the α -quaternary substituted ketones **29** in excellent yield and regioselectivity. The allylic alkylation of **24c** occurred cleanly, and there was no evidence that the rhodium(I) catalyst had undergone oxidative addition to the aryl bromide, which could have resulted in the formation of cross coupling products.

Table 6. Substrate scope of the rhodium-catalysed allylic alkylation with the aryl cyanohydrins **24** (L = P(O-2,4-di-*t*-BuC₆H₃)₃).



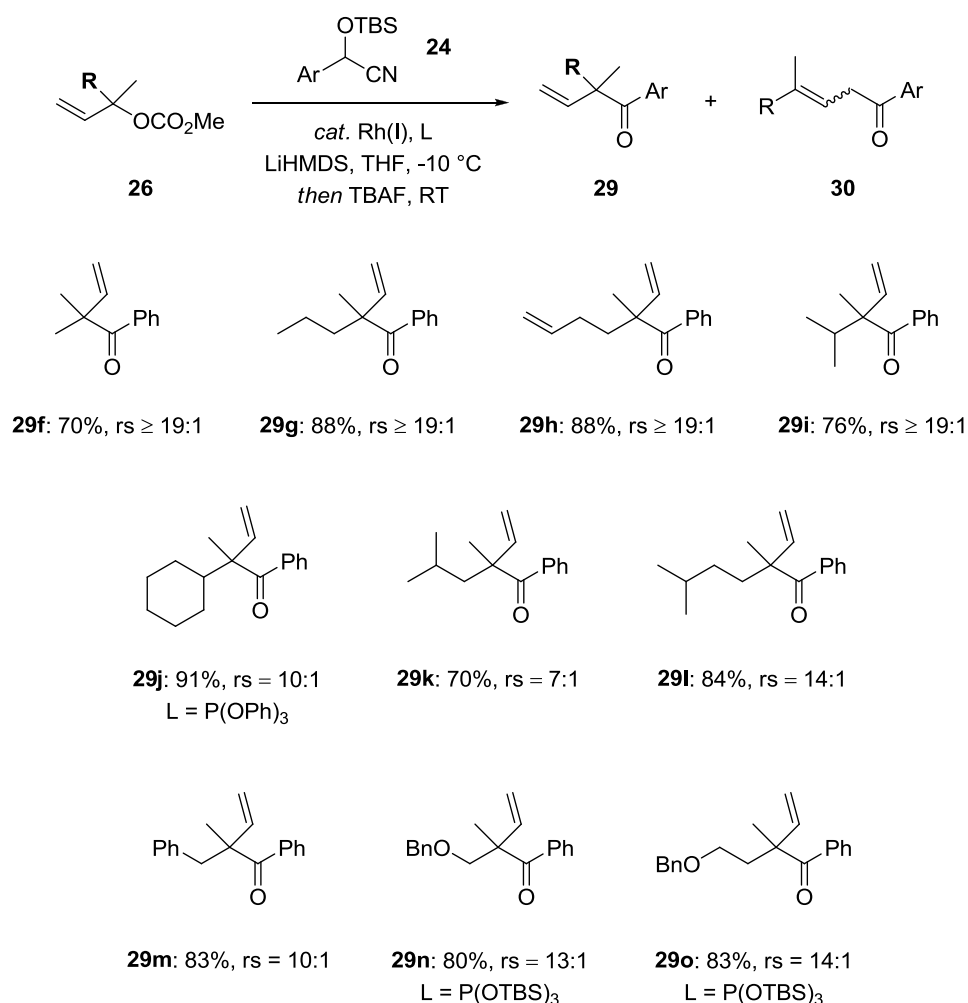
2.2.3.5.3. Carbonate Scope

A wide variety of tertiary allylic carbonates were successfully employed in the rhodium-catalysed allylic alkylation of the aryl cyanohydrin **24a**. As outlined in **Table 7**, a number of linear alkyl-substituted tertiary allylic carbonates could be utilised with excellent regioselectivity, including the alkenyl derivative **29h**. However, perhaps most importantly, this method allows for the introduction of a range of branched and functionalised α -carbonyl substituents (**29i-o**), albeit with slightly reduced regioselectivity. Clearly, the reaction is tolerant of α -, β - and γ -branched alkyl groups, and also permits preparation of the benzyl- and benzyloxy-substituted derivatives **29i-k**. The synthesis of these compounds *via* conventional enolate alkylation, which is often limited to simple electrophiles, would be challenging. In this context, the α -isopropyl and α -cyclohexyl derivatives **29i** and **29j**

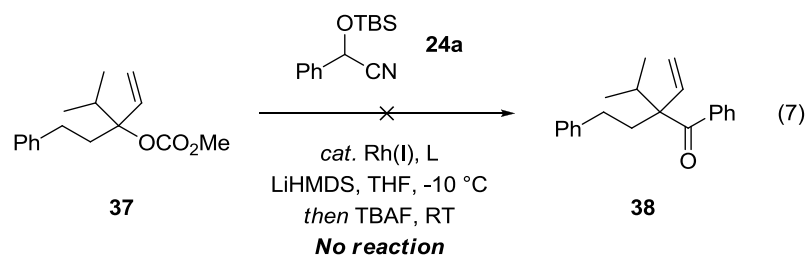
are particularly noteworthy, as their preparation would involve the S_N2 alkylation of a ketone enolate with a secondary halide or pseudohalide. In all of the ketone products, the pendant vinyl group provides a particularly versatile functional handle, and would also be difficult to install *via* conventional enolate functionalisation. Critically, the products **29a-o** were all isolated in $\geq 70\%$ yield and, due to the consumption of the undesired regioisomer upon deprotection of the cyanohydrin adduct, as a single regioisomer.

In this process, the phosphite ligand may be tailored in order to improve the regioselectivity of the alkylation, or the reactivity of a particular substrate. For example, under the standard reaction conditions, the α -cyclohexyl ketone **29j** was provided with incomplete conversion of the starting carbonate. This issue was addressed by using a smaller phosphite ligand, triphenylphosphite, which afforded this product in excellent yield and with good regioselectivity. For the benzyloxymethyl-substituted derivative **29n**, P(OTBS)₃, which is a weaker π -acceptor than the aryl phosphite, was found to provide optimal regioselectivity. This ligand presumably serves to minimise chelation of the benzyloxy group to the metal centre, which could be envisaged to distort the putative Rh-*enyl* intermediate and drive the formation of the linear regioisomer. One of the major side products of the alkylation reaction is 2,4-di-*tert*-butylphenol, presumably formed by hydrolysis of the phosphite ligand under the basic reaction conditions, which is difficult to separate from the more polar products **29e**, **29n** and **29o**. In these cases, the use of an alternative phosphite ligand is also advantageous in terms of purification.

Table 7. Substrate scope of the rhodium-catalysed allylic alkylation with the tertiary allylic carbonates **26** (L = P(O-2,4-di-^tBuC₆H₃)₃, Ar = Ph).

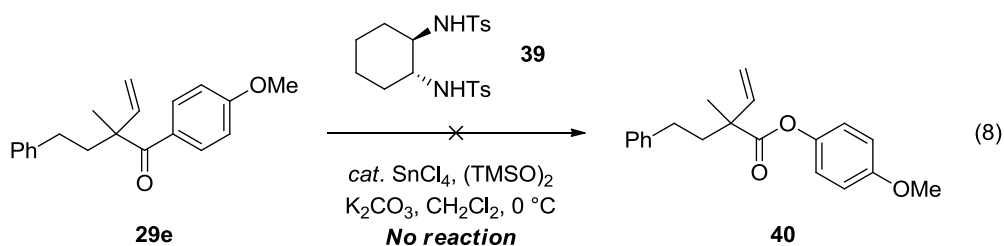


In an attempt to further broaden the scope of this reaction, the tertiary allylic carbonate **37**, which contains two alkyl substituents bulkier than methyl, was subjected to the optimal reaction conditions (eq. 7, L = P(O-2,4-di-^tBuC₆H₃)₃). Unfortunately, the alkylation product **38** could not be detected upon stirring overnight, and the carbonate **37** was recovered in near quantitative yield, clearly indicating that the two alkyl substituents place too great a steric demand on the alkylation of the cyanohydrin **24a**. At this time, the reaction is limited to the synthesis of quaternary carbon centres containing at least one methyl substituent, which represents perhaps the most significant drawback of this method.



2.2.3.6. Attempted Baeyer-Villiger Oxidation

The Baeyer-Villiger oxidation provides a convenient method for the oxidation of acyclic and cyclic ketones to the corresponding esters and lactones. Due to the stabilising influence of the *para*-methoxy substituent, we envisaged that the Baeyer-Villiger oxidation of the electron rich aryl ketone **29e** may proceed with the desired regioselectivity to afford the ester **40**, which would establish the newly installed carbonyl group as an extremely versatile functional handle. In order to avoid epoxidation of the terminal double bond, we elected to utilise a modified Shibasaki protocol,²⁷ which had previously proven effective in the chemo- and regioselective oxidation of α -tertiary substituted aryl ketones containing pendant vinyl groups (eq. 8).²⁸



Unfortunately, treatment of the ketone **29e** with bis(trimethylsilyl)peroxide, in the presence of catalytic tin(IV) tetrachloride, the amine ligand **39** and potassium carbonate, failed to provide the desired ester **40** or the alternative benzoate regioisomer. It seems likely that the nucleophilic attack of bis(trimethylsilyl)peroxide on the carbonyl group, which is proposed to be activated by the Lewis

acidic tin(IV) species, is hindered by the bulky α -quaternary centre. Due to the inert nature of the substrate **29e** under these conditions, no further attempts were made to optimise this process.

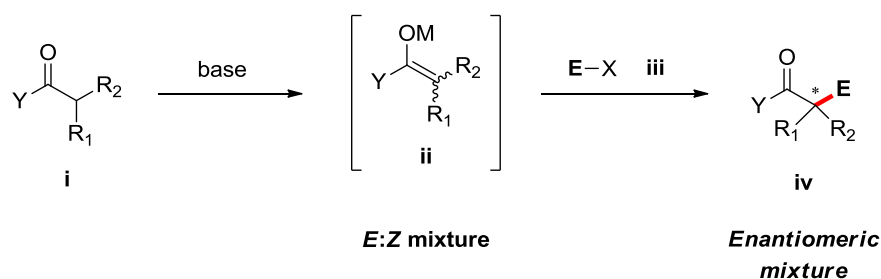
2.2.3.7. Concluding Remarks

We have developed the first highly regioselective rhodium-catalysed allylic substitution of tertiary allylic carbonates with a trialkylsilyl-protected cyanohydrin pronucleophile, which functions as a convenient acyl anion equivalent. This direct and operationally simple procedure involves the coupling of two readily available reaction partners and, following our initial optimisation, provides facile access to a range of racemic α -quaternary substituted aryl ketones. Many of these products would be difficult to obtain *via* conventional enolate alkylation reactions, thereby illustrating the potential utility of this synthetic disconnection. However, in order for this method to find widespread applicability in organic synthesis, we considered the development of an asymmetric variant to be essential.

2.2.4. Stereospecific Rhodium-Catalysed Allylic Substitution with an Acyl Anion Equivalent: Asymmetric Construction of Acyclic α -Aryl Ketones

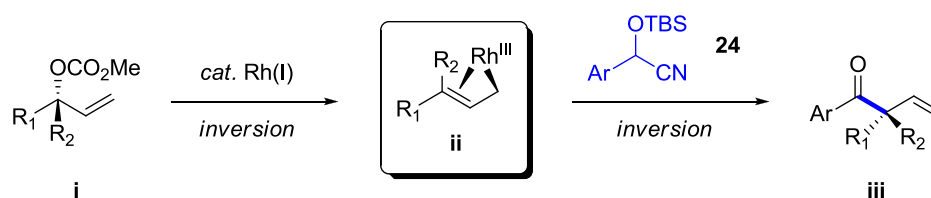
2.2.4.1. Introduction

The stereoselective synthesis of all carbon quaternary substituted stereogenic centres represents one of the most important and widely studied areas of investigation in organic chemistry.²⁹ In this context, the asymmetric construction of quaternary carbon stereogenic centres in acyclic systems remains arguably the greatest challenge, despite the development of a number of elegant approaches over the last decade.³⁰ As outlined in our introductory review, the enolate alkylation represents one of the most prominent methods for the asymmetric construction of α -quaternary substituted carbonyl compounds; however, these reactions tend to be limited to substrates in which the enolate geometry is conformationally restricted, such as cyclic ketones. The deprotonation of an acyclic carbonyl compound such as **i** almost invariably leads to a mixture of (*E*)- and (*Z*)-enolate stereoisomers³¹ which, even in the event of a facially selective alkylation, would afford an enantiomeric mixture of the product **iv** (**Scheme 10**). Of the methods that have been developed for the stereoselective generation of acyclic α,α -disubstituted enolates such as **ii**, most involve the use of a chiral amide auxiliary.³² On rare occasions, it is also possible to access one enantiomer of the α -quaternary substituted carbonyl compound **iv** from a mixture of geometrical isomers.³³ However, a general solution to this problem has not been forthcoming, and it remains a limiting factor in the field of enolate alkylation. As a result, the development of a general method for the asymmetric construction of acyclic α -quaternary substituted ketones, that does not involve the formation of an enolate nucleophile, would be of great synthetic potential.



Scheme 10. General scheme for the asymmetric alkylation of an acyclic α,α -disubstituted enolate.

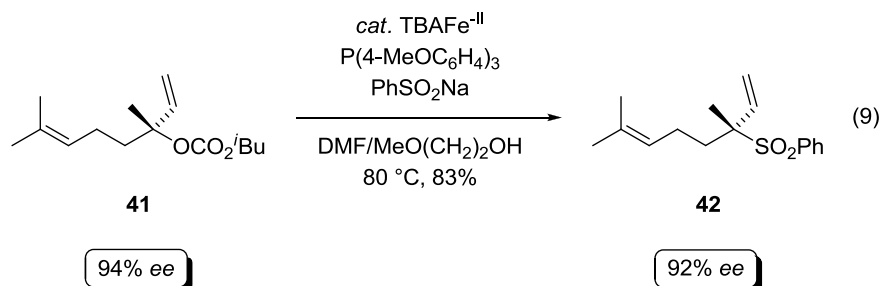
In the previous section, we described a novel rhodium-catalysed allylic substitution reaction for the construction of acyclic α -carbonyl quaternary carbon centres, albeit in racemic form. We envisaged that the stereospecific variant of this transformation would provide a versatile new method for the asymmetric construction of acyclic α -quaternary substituted ketones such as **iii** (**Scheme 11**). As depicted, the aryl cyanohydrin **24** was expected to function as a stabilised anion in this transformation, to provide the ketone **iii** *via* a classical double inversion process.



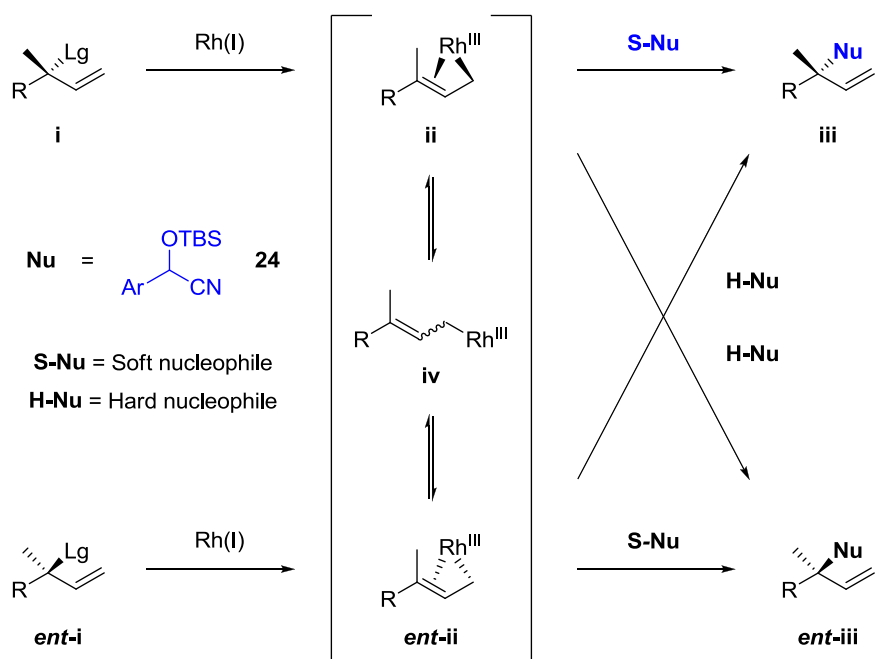
Scheme 11. Proposed stereospecific rhodium-catalysed allylic substitution with the aryl cyanohydrin **24**.

There are a number of significant challenges associated with the extension of our previously developed methodology to the stereospecific reaction manifold outlined in **Scheme 11**. To begin, enantiomerically enriched tertiary allylic alcohol derivatives such as **i** are relatively difficult to prepare, particularly in comparison to their secondary counterparts, which are generally accessible on large scale *via* enzymatic

or Sharpless kinetic resolution. Additionally, although the stereospecific iron-catalysed allylic alkylation of tertiary carbonates with sulfones has been described (eq. 9),³⁴ this represents the only known reaction of this type, and such a transformation has yet to be achieved with a rhodium catalyst.



In order for a highly stereospecific alkylation to occur, the lithiated cyanohydrin must have the ability to rapidly intercept the putative Rh-*enyl* intermediate **ii**, to afford the product **iii** with overall retention of configuration (**Scheme 12**). However, in the event that the nucleophilic displacement of **ii** is slow relative to facial exchange of the metal *via* π - σ - π isomerisation, alkylation of the rhodium-*enyl* complex *ent-ii* will provide at least partial conversion to the opposite enantiomer *ent-iii*. As this particular allylic substitution involves the coupling of two relatively sterically demanding reaction components, we considered it likely that the rate of alkylation would permit at least some degree of stereochemical leakage *via* this mechanism, particularly in the presence of a bulky phosphite ligand. Additionally, although we expected the cyanohydrin **24** to function as a stabilised nucleophile and provide the product of overall retention, a number of alternative alkylation pathways may be envisaged to provide the product **iii** as a racemate, or the opposite enantiomer *ent-iii*.

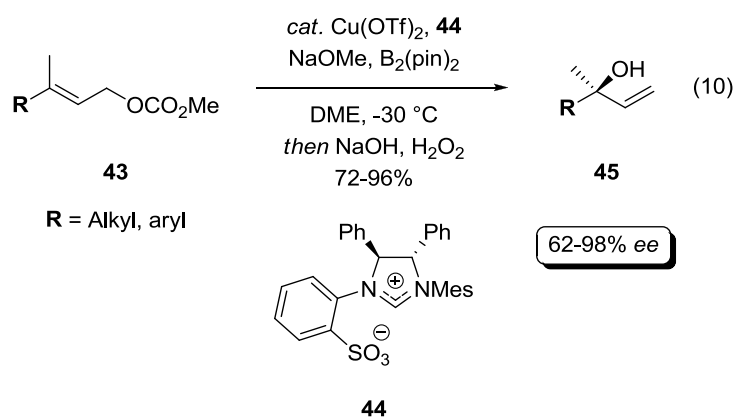


Scheme 12. Possible π - σ - π isomerisation in the alkylation of tertiary allylic carbonates with the aryl cyanohydrin **24**.

2.2.4.2. Asymmetric Synthesis of Tertiary Allylic Alcohols

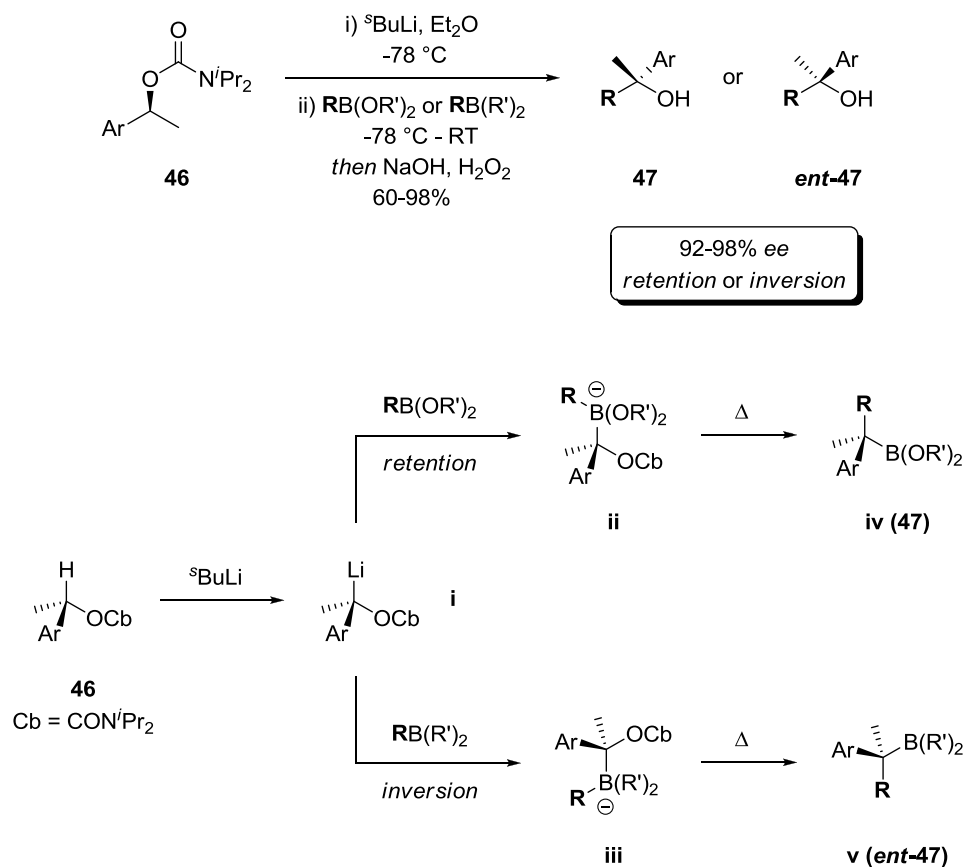
The asymmetric synthesis of tertiary allylic alcohols, particularly in acyclic systems, is extremely challenging. In this context, a number of lengthy synthetic routes, generally involving the asymmetric epoxidation of a trisubstituted alkene, can be envisaged for their preparation.³⁵ However, in order for our proposed stereospecific allylic alkylation to find widespread utility, we were keen to develop a highly practical substrate synthesis, which led to a thorough examination of the available methods. The addition of an organometallic reagent to a ketone, which may be rendered asymmetric by a chiral catalyst, represents perhaps the most obvious strategy towards the synthesis of tertiary alcohols; however, these reactions are often limited to the introduction of simple alkyl groups.³⁶ To our knowledge, the highly asymmetric addition of an unsubstituted vinylmetal reagent to a simple ketone, to provide the requisite monosubstituted alkene, has yet to be described. In contrast, a

great deal of success has been achieved in the asymmetric synthesis of tertiary allylic alcohols *via* the oxidation of their corresponding allylboronates. For example, Hoveyda recently described the NHC-copper complex-catalysed allylic substitution of a range of alkyl- and aryl-substituted (*E*)-linear carbonates **43** with bis(pinacolato)diboron, to provide the requisite allylic alcohols **45** upon treatment with alkaline hydrogen peroxide (eq. 10). Despite having a relatively broad substrate scope, the enantioselectivity of this reaction was shown to be particularly sensitive to the steric nature of the substituent **R**, with only particularly bulky groups (e.g. **R** = ^cHex & 2-BrC₆H₄) providing exceptional *ee* values. In addition, the practicality of this method is limited by the relatively lengthy syntheses of both **43** (3 steps), which must be prepared as a single geometrical isomer, and the imadazolinium salt **44** (4 steps including two Buchwald-Hartwig cross coupling reactions).



In 2008, Aggarwal described a remarkably general approach towards the enantiodivergent synthesis of acyclic tertiary alcohols, including monosubstituted allylic alcohols (**Scheme 13**).³⁷ This process involves the borylation of an enantiomerically enriched lithiated carbamate, which may proceed with either retention or inversion of configuration, depending on the nature of the boron reagent. Thus, both enantiomers of the alcohol **47** may be obtained in excellent enantiomeric

excess from the same enantiomer of the carbamate **46**. A mechanistic pathway for this transformation is depicted in **Scheme 13**.

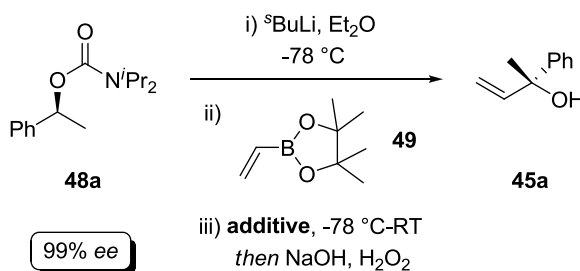


Scheme 13. Enantiodivergent synthesis of tertiary alcohols *via* lithiation-borylation of the benzylic carbamate **46**.

Due to the predictably high levels of stereocontrol afforded by the borylation of lithiated carbamates (**Scheme 13**), we elected to utilise this process in the synthesis of an enantiomerically enriched tertiary allylic alcohol, namely **45a** (**Table 8**). Thus, treatment of the benzylic carbamate **48a** with $^s\text{BuLi}$ at $-78\text{ }^\circ\text{C}$, followed by the addition of vinylboronic acid pinacol ester **49**, warming to ambient temperature and *in situ* oxidation of the subsequently formed allylboronate, furnished the tertiary allylic alcohol **45a** in excellent yield and 96% *ee* (entry 1). The transfer of chirality from the (*S*)-secondary carbamate **48a** to the (*R*)-tertiary alcohol **45a** was almost

complete, and is in agreement with the mechanism of addition outlined in **Scheme 13**. Consistent with Aggarwal's subsequent mechanistic studies,³⁸ which were published during the course of our work, we also found that with the addition of 1M magnesium bromide/methanol to the reaction mixture prior to warming, the tertiary allylic alcohol **45a** could be obtained in essentially enantiopure form (entry 2). Using this method, we expected a wide variety of aryl alcohols such as **45a** to be readily available in excellent enantiomeric excess. Additionally, this process has very recently been extended to the corresponding allylic carbamates,³⁹ enabling the synthesis of alkyl-substituted analogues.

Table 8. Asymmetric synthesis of the tertiary alcohol **45a** via lithiation-borylation of the carbamate **48a**.



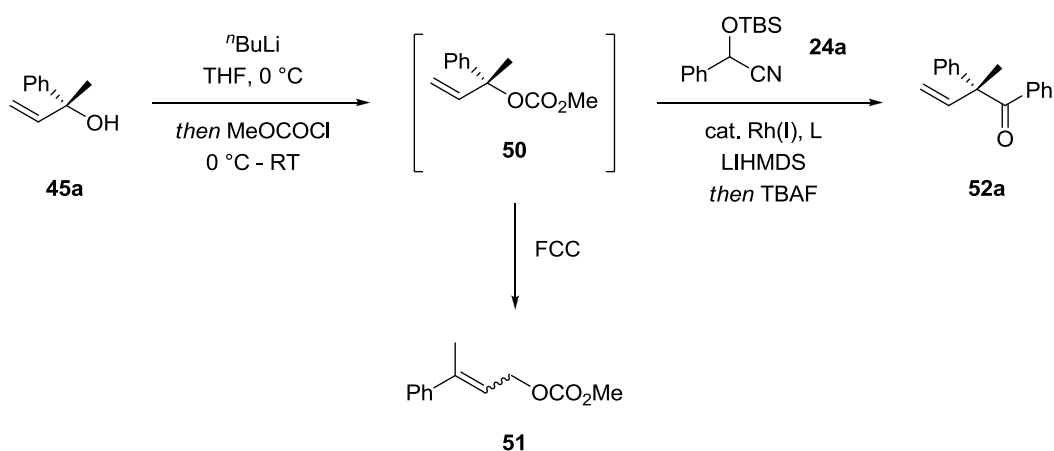
Entry	Additive	Yield (%) ^a	ee (%) ^b
1	-	89	96
2	$\text{MgBr}_2/\text{MeOH}$	83	99

^a Isolated yields. ^b ee values were determined by chiral HPLC on the isolated product.

2.2.4.3. Reaction Optimisation

The required tertiary allylic carbonate **50** was prepared by treatment of the allylic alcohol **45a** with *n*-butyllithium, followed by the addition of methyl chloroformate. However, upon attempted purification by flash column chromatography (FCC), the tertiary carbonate **50** underwent significant allylic rearrangement to the achiral linear carbonate **51** (**Scheme 14**), which was isolated as the major product in a complex

mixture. Presumably, the carbonate **50** is subject to facile ionisation under mildly acidic conditions, to provide a stable tertiary, benzylic and allylic carbocation. Nucleophilic attack of the resultant carboxylate anion must then occur largely on the terminal double bond (S_N1' substitution), to provide the conjugated styrene derivative **51**, which is thermodynamically favoured. Alternatively, this reaction could be envisaged to proceed *via* Claisen-type [3,3]-sigmatropic rearrangement of the tertiary allylic carbonate **50**.



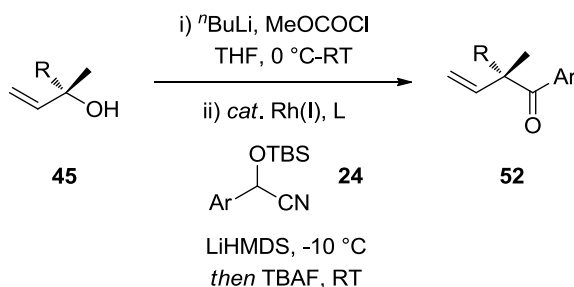
Scheme 14. One pot conversion of the tertiary allylic alcohol **45a** to the acyclic α -aryl ketone **52a**.

In order to circumvent this issue, we chose to develop an efficient one pot procedure in which the reactive allylic carbonate **50** could be formed *in situ*, followed directly by the addition of **24a** and a rhodium catalyst, to provide the enantiomerically enriched ketone **52** upon deprotection of the resultant cyanohydrin adduct (**Scheme 14**).⁴⁰ Arguably the most significant difference between this reaction and those of the isolated alkyl carbonates **26** is that one equivalent of lithium chloride is generated upon acylation of the alcohol **45a**, which should remain in solution over the course of the subsequent alkylation. However, due to the relatively weak *trans* effect of the chloride ligand, we were hopeful that this would have a minimal influence on the rate

of π - σ - π isomerisation, and hence the stereospecificity of the alkylation.⁴¹ Gratifyingly, this salt was also shown to have little impact on the reactivity of the intermediate allylic carbonate **50**, as shown in **Table 9**.

Under our previously optimal reaction conditions, the stereospecific rhodium-catalysed allylic alkylation with the cyanohydrin **24** failed to proceed to completion, affording the ketone **52a** in 66% yield, albeit with excellent regioselectivity and good enantiospecificity (entry 1). While the regioselectivity of this reaction is seemingly independent of the phosphite ligand, presumably due to the electronically biased aryl substituent, the stereospecificity was shown to vary greatly with the steric and electronic properties of this reaction component, as outlined in **Table 9**. For example, the bulky tris(*tert*-butyldimethylsilyl) phosphite provided almost complete stereoerosion (entry 2), which suggests that a dynamic kinetic asymmetric transformation (DYKAT) of racemic tertiary alcohols with the cyanohydrin **24** may be feasible.⁴² In contrast, the considerably smaller and more electron poor tris(2,2,2-trifluoroethyl)phosphite proved optimal in terms of both enantiospecificity and yield (entry 5), furnishing the acyclic α -aryl ketone **52a** in excellent yield and 90% enantiomeric excess (91% *cee*⁴³) (entry 5). With the exception of P(O-2,4-di-^tBuC₆H₃)₃ (entry 1), there would appear to be a correlation between the size of the phosphite ligand and the stereospecificity of the alkylation, though a more exhaustive ligand screen is clearly required in order to fully elucidate this trend.

Table 9. Effect of the phosphite ligand in the stereospecific rhodium-catalysed allylic substitution with the acyl anion equivalent **24** (R = Ph, Ar = Ph).



Entry ^a	L	rs ^b	ee (%) ^c	cee (%)	Yield (%) ^d
1	P(O-2,4-di- ^t BuC ₆ H ₃) ₃	≥ 19:1	82	85	66
2	P(OTBS) ₃	“	18	19	72
3	P(OPh) ₃	“	59	61	78
4	P(OMe) ₃	“	83	86	80
5	P(OCH₂CF₃)₃	≥ 19:1	90	91	87

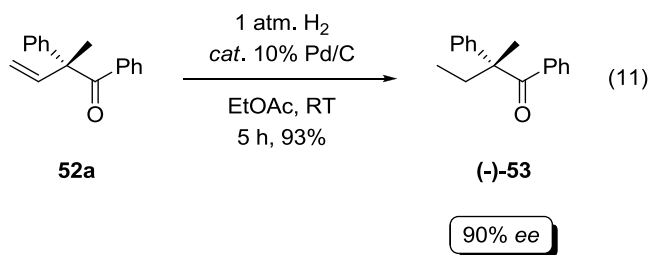
^a All reactions were performed on a 0.5 mmol reaction scale using 1 equiv. ^tBuLi, 1 equiv. MeOCOCl, 2.5 mol% [Rh(COD)Cl]₂, 10 mol% L, 1.3 equiv. **24** and 1.8 equiv. LiHMDS in THF (5 ml) at -10 °C for ca. 5 h, followed by the addition of 4.0 equiv. TBAF at room temperature. ^b Regioselectivity was determined by 500 MHz ¹H NMR on the crude reaction mixtures before deprotection of the cyanohydrin adduct. ^c ee values were determined by chiral HPLC on the isolated products. ^d Isolated yields.

While a competing mechanistic pathway cannot be altogether ruled out, it seems reasonable that the marginally incomplete transfer of chirality from the (*R*)-alcohol **45** to the (*R*)-ketone **52** is predominantly caused by π - σ - π isomerisation of the transient rhodium-*enyl* complex (**Scheme 12**), which occurs in competition with the nucleophilic displacement of this intermediate. This is consistent with the almost complete retention of configuration observed in the presence of small, electron poor ligands such as tris(2,2,2-trifluoroethyl) phosphite, which would be expected to provide a more rapid rate of alkylation. Subsequent attempts to further increase the rate of nucleophilic attack relative to π - σ - π isomerisation, for example by increasing the reaction temperature and concentration, in addition to the stoichiometry of the

nucleophile, were largely unsuccessful. As a result, the reaction conditions outlined in **Table 9** (entry 5) were shown to be optimal. Although the stereospecificity is slightly lower than that typically obtained with secondary allylic carbonates, this reaction provides proof of concept for this novel transformation, and was deemed satisfactory given the challenges usually associated with the asymmetric construction of acyclic α -quaternary substituted carbonyl compounds.

2.2.4.4. Proof of Absolute Configuration

Before commencing further studies, the stereochemical course of this highly enantiospecific transformation was confirmed by hydrogenation of the terminal alkene **52a** in the presence of 10% Pd/C, to provide the ethyl ketone **53** (eq. 11). The optical rotation of the ketone **53** was in accord with the published values,⁴⁴ which confirmed the absolute configuration of the alkylation product **52a** to be (*R*). As expected, the allylic alkylation reaction with the cyanohydrin **24** proceeds with overall retention of absolute configuration, which is consistent with the double inversion mechanism outlined in **Scheme 11**.



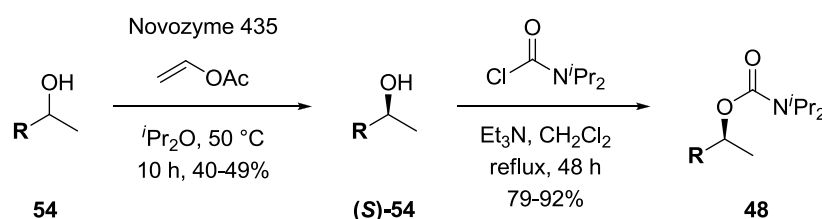
2.2.4.5. Substrate Scope

2.2.4.5.1. Substrate Synthesis

In order to examine the substrate scope of this new method, a range of enantiomerically enriched tertiary allylic alcohols were prepared as outlined in **Table 10**. The readily available racemic alcohols **54** were subjected to enzymatic resolution

under the conditions described by Xu,⁴⁵ to provide the (*S*)-secondary alcohols (**S**)-**54** and the corresponding (*R*)-acetates, both in excellent enantiomeric excess. Although Mitsunobu inversion of the benzylic alcohols (**S**)-**54** would provide a near quantitative yield of the enantiomerically enriched (*R*)-alcohols, we chose to conduct this reaction on scale and isolate the enantiopure (*S*)-enantiomers in *ca.* 50% yield. Carbamylation of the alcohols (**S**)-**54** then furnished the requisite secondary benzylic carbamates **48** in good to excellent yield.

Table 10. Synthesis of the enantiomerically enriched benzylic carbamates **48a-e**.



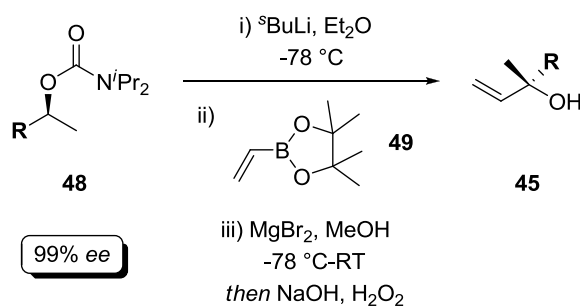
Entry	R	Overall Yield (%) ^a	<i>ee</i> (%) ^b	
1	Ph	48a	39	99
2	4-ClC ₆ H ₄	48b	43	99
3	4-MeOC ₆ H ₄	48c	36	99
4	3-MeC ₆ H ₄	48d	39	99
5	2-FC ₆ H ₄	48e	38	99

^a Isolated yields of **48**. ^b *ee* values were determined by chiral HPLC on the isolated alcohols **54**.

The benzylic carbamates **48a-e** were next subjected to the aforementioned stereoselective borylation reaction, to provide the tertiary allylic alcohols **45a-e** upon hydrogen peroxide oxidation of the intermediate allylboronates (**Table 11**). Although these reactions were only moderately efficient, proceeding in 49-83% yield, the allylic alcohols **45a-e** were furnished in uniformly excellent enantiomeric excess. Consistent with Aggarwal's work, the electron poor carbamate **48b** provided the

lowest stereoselectivity, even with the addition of magnesium bromide and methanol prior to warming. However, the reaction was not particularly sensitive to steric factors, with both the 3- and 2-substituted derivatives affording near perfect stereocontrol. In the event of incomplete conversion, the enantiomerically enriched carbamate **48** could also be recovered from the reaction mixture, albeit in slightly reduced optical purity. Overall, this route provides a convenient, reliable and scalable substrate synthesis, which is critical to our general strategy for the asymmetric construction of acyclic quaternary carbon stereogenic centres.

Table 11. Synthesis of the enantiomerically enriched tertiary allylic alcohols **45a-e**.



Entry	R		Yield (%) ^a	ee (%) ^b
1	Ph	45a	83	99
2	4-ClC ₆ H ₄	45b	61	95
3	4-MeOC ₆ H ₄ ^c	45c	49	99
4	3-MeC ₆ H ₄	45d	55	98
5	2-FC ₆ H ₄	45e	60	99

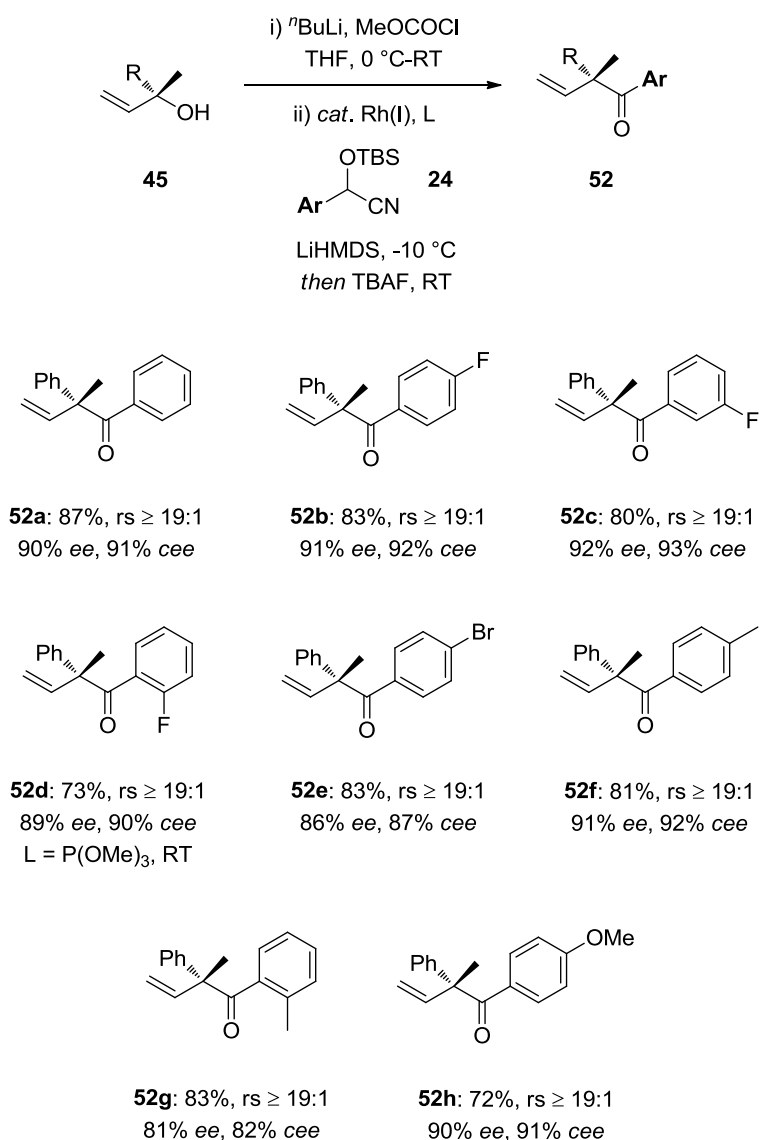
^a Isolated yields. ^b ee values were determined by chiral HPLC on the isolated products. ^c Deprotonation was carried out in the presence of 1.1 equiv. TMEDA.

2.2.4.5.2. Cyanohydrin Scope

Table 12 summarises the application of our optimised reaction conditions to the stereospecific alkylation of the tertiary allylic alcohol **45a** with a range of aryl cyanohydrins **24**. This reaction is clearly tolerant of a range of electron poor and

electron rich *ortho*-, *meta*- and *para*-substituted aryl cyanohydrins, and the acyclic ketone products **52** were generally obtained in good to excellent yield, excellent regioselectivity and $\geq 90\%$ *ee*, with a small number of notable exceptions.

Table 12. Substrate scope of the stereospecific rhodium-catalysed allylic alkylation with the aryl cyanohydrins **24** (L = P(OCH₂CF₃)₃, R = Ph).



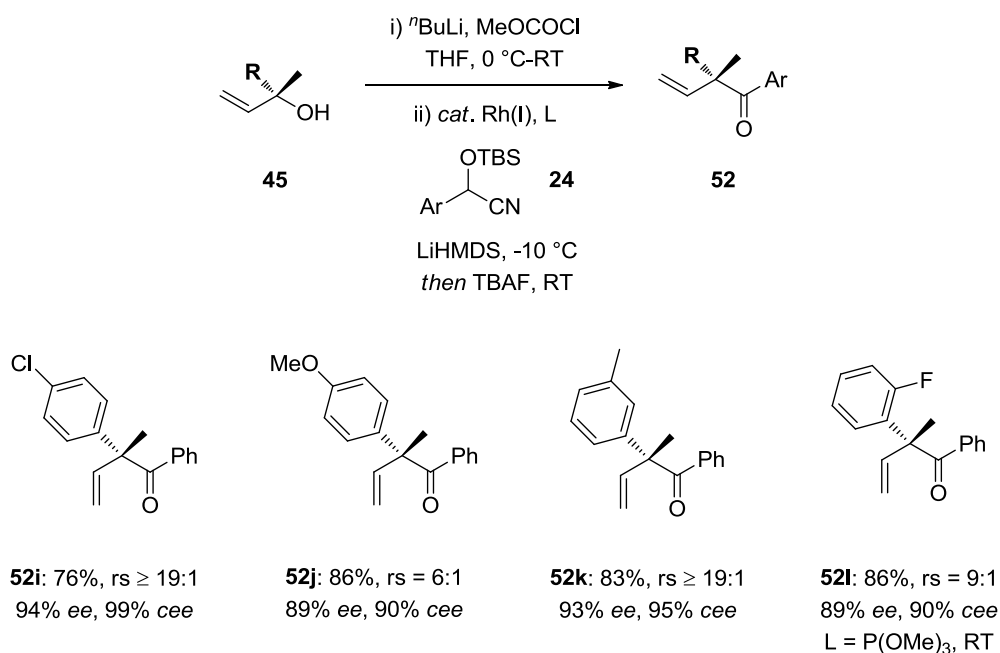
Among the range of 4-substituted derivatives that were examined, the less nucleophilic aryl bromide **24c** afforded marginally lower, albeit synthetically useful, stereospecificity. Additionally, the enantiospecificity of this transformation appears

to be influenced by the introduction of more sterically demanding aryl substituents. For example, the *ortho*-substituted aryl ketones **52d** and **52g** were afforded in slightly reduced enantiomeric excess under the optimal reaction conditions. In the case of the aryl fluoride **52d**, this was remedied by the use of a smaller phosphite ligand at an elevated reaction temperature. However, these conditions could not be successfully applied to the *ortho*-methyl-substituted aryl ketone **52g**, which was generally obtained in *ca.* 80% *ee*, regardless of the ligand employed.

2.2.4.5.3. Tertiary Alcohol Scope

The tertiary allylic alcohols **45b-e** were all successfully utilised in the stereospecific rhodium-catalysed allylic alkylation of the aryl cyanohydrin **24a**, as outlined in **Table 13**. Consistent with our hypothesis that the stereospecificity is governed largely by the rate of nucleophilic attack, the electron deficient *para*-chloro tertiary alcohol **45b** was shown to afford optimal enantiomeric excess, and is the only substrate examined to provide essentially complete retention of configuration. In contrast, the electron rich *para*-methoxy ketone **52j** was also furnished in good *ee*, but with modest regioselectivity. A slight modification in reaction conditions was required for the *ortho*-fluoro derivative **52l**, once more indicating that the rate of alkylation may be marginally influenced by steric factors. However, this effect does not appear to extend beyond the 2-position, as excellent enantiospecificity was observed in the formation of the *meta*-substituted ketone **52k**.

Table 13. Substrate scope of the stereospecific rhodium-catalysed allylic alkylation with the tertiary allylic alcohols **45** (L = P(OCH₂CF₃)₃, Ar = Ph).



2.2.4.6. Concluding Remarks

In conclusion, we have developed a highly stereospecific rhodium-catalysed allylic substitution with an acyl anion equivalent, providing a versatile new method for the asymmetric construction of acyclic α -quaternary substituted ketones. This reaction involves the highly efficient one pot conversion of an enantiomerically enriched tertiary allylic alcohol to the corresponding α -quaternary substituted ketone, and currently provides access to a range of acyclic products containing both α -aryl and α -vinyl substituents. Hence, this process provides a viable alternative to the widely studied asymmetric enolate α -arylation and vinylation reactions which, to our knowledge, have yet to be achieved selectively in acyclic systems.⁴⁶ This reaction also represents the first stereospecific rhodium-catalysed allylic substitution of a tertiary allylic alcohol derivative, which we anticipate may be applicable to a number of stabilised and unstabilised carbon and heteroatom nucleophiles, enabling the

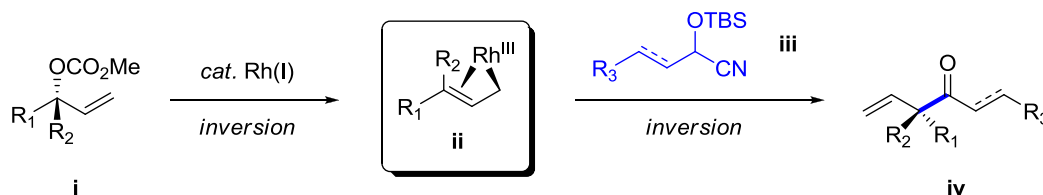
asymmetric synthesis of a diverse range of C-, N- and O-substituted quaternary carbon stereogenic centres.

2.2.5. Expanding the Scope of the Rhodium-Catalysed Allylic Substitution with an Acyl Anion Equivalent

2.2.5.1. Rhodium-Catalysed Allylic Substitution with Alkenyl Cyanohydrin Pronucleophiles: Construction of Acyclic α,α' -Dialkyl Ketones

2.2.5.1.1. Introduction

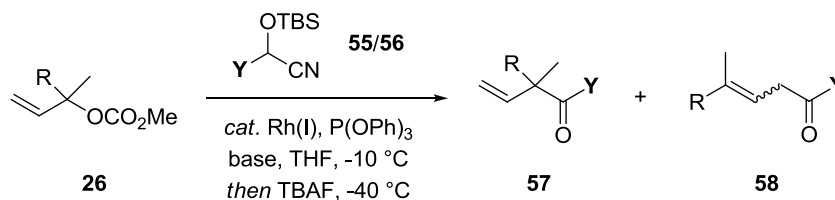
Having successfully developed a highly regio- and enantiospecific rhodium-catalysed allylic substitution with an acyl anion equivalent, our next goal was to overcome some of the most significant limitations of this process. For instance, we had so far focused our efforts on the rhodium-catalysed allylic alkylation of aromatic cyanohydrins, thereby limiting this method to the synthesis of α -quaternary substituted aryl ketones. Partially driven by our failure to convert these products to the more versatile aryl esters (eq. 8), we elected to examine the reactions of a more diverse family of cyanohydrin pronucleophiles, namely the alkyl- and alkenyl-substituted analogues **iii** (Scheme 15). Ultimately, we anticipated that this method would provide facile access to a range of differentially substituted α,α' -dialkyl ketones, either directly or *via* subsequent functionalisation of the corresponding α,β -unsaturated derivatives. These compounds would be difficult to prepare by conventional enolate alkylation, largely due to the difficulties associated with the regioselective enolisation of an unsymmetrical ketone.



Scheme 15. Proposed stereospecific rhodium-catalysed allylic substitution with the alkyl or alkenyl cyanohydrins **iii**.

2.2.5.1.2. Initial Results

Table 14. Initial examination of various alkyl- and alkenyl-substituted cyanohydrins in the rhodium-catalysed allylic alkylation of **26a**.



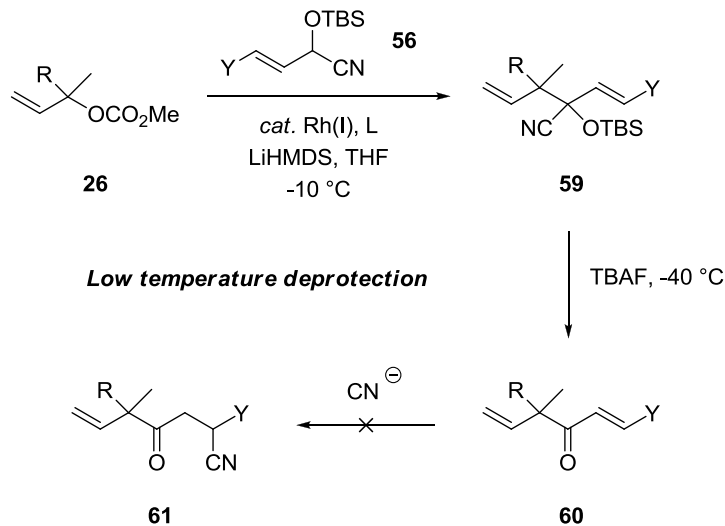
Entry ^a	Y	55/56	base	rs ^b	Yield (%) ^c
1	ⁿ Pr	55	LDA	-	0
2	CH ₂ =CH-	56a	LiHMDS	-	0
3	(<i>E</i>)-CH ₃ CH=CH-	56b	“	≥ 19:1	63
4	(<i>E</i>)-C ₆ H ₅ CH=CH-	56c	“	“	75

^a All reactions were performed on a 0.5 mmol reaction scale using 2.5 mol% [Rh(COD)Cl]₂, 10 mol% P(OPh)₃, 1.3 equiv. **55/56** and 1.8 equiv. base in THF (5 mL) at -10 °C for *ca.* 16 h, followed by the addition of 4.0 equiv. TBAF at -40 °C. ^b Regioselectivity was determined by 500 MHz ¹H NMR on the crude reaction mixtures before deprotection of the cyanohydrin adducts. ^c Isolated yields of the desired regioisomer **57**.

We began by screening a range of alkyl- and alkenyl-substituted cyanohydrins, prepared in the same manner as the aryl-substituted analogues, in the rhodium-catalysed allylic substitution of the tertiary allylic carbonate **26a** (Table 14). In line with the decreased acidity of the alkyl cyanohydrin **55a**, LDA was used to generate the lithium salt of this species, whereas LiHMDS was deemed sufficient for the alkenyl derivatives **56a-c**. Interestingly, while the alkyl- and vinyl-substituted cyanohydrins failed to afford the desired product (entries 1 and 2), the (*E*)-substituted alkenyl derivatives **56b** and **56c** were shown to undergo relatively clean allylic alkylation, affording the desired ketone product **57** upon *in situ* desilylation (entries 3 and 4). In contrast to our previous work, these reactions were also highly regioselective in the presence of triphenylphosphite, providing the intermediate

cyanohydrin adduct as a single regioisomer and, importantly, with complete retention of alkene geometry.

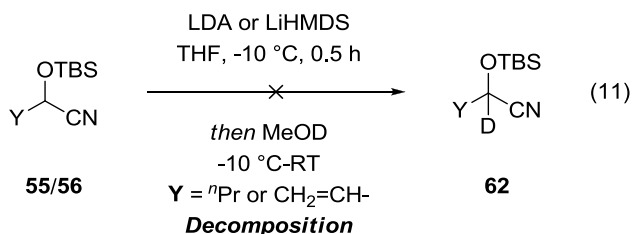
As shown in **Scheme 16**, careful deprotection of the intermediate cyanohydrin adduct **59** is required in order to avoid conjugate addition of the newly liberated cyanide to the α,β -unsaturated ketone product **60**, which we have already demonstrated to proceed readily at room temperature (**Scheme 8**). Thus, upon completion of the alkylation reaction, an excess of TBAF was added slowly to the reaction mixture at $-40\text{ }^\circ\text{C}$, which was then maintained at this temperature. Even under these conditions, the desilylation was generally complete within 1 hour, affording clean conversion to the ketone **60**. Importantly, the Michael addition product **60** could not be detected by ^1H NMR analysis of the crude reaction mixture, and both the aryl- and alkyl-substituted enones were afforded in good yield.



Scheme 16. Low temperature deprotection in the rhodium-catalysed allylic substitution with the alkenyl cyanohydrin **56** (Y = aryl or alkyl).

2.2.5.1.3. Deprotonation Studies

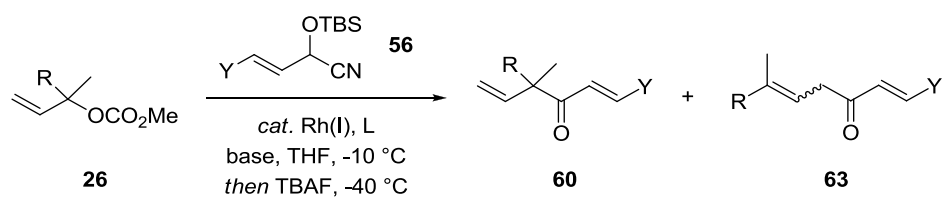
Intrigued by the apparent lack of reactivity displayed by the alkyl- and vinyl-substituted cyanohydrins **55** and **56a**, which both afforded almost complete recovery of the starting material **26a**, we chose to examine the stability of their respective anions under the reaction conditions. While the TMS-protected analogue of the vinyl cyanohydrin **56a** may be cleanly alkylated at $-78\text{ }^{\circ}\text{C}$,⁴⁷ the lithium salt of this species has been shown to undergo decomposition at higher temperatures, presumably *via* migration of the oxygen-bound silicon group to the neighbouring carbanion. Even at $-78\text{ }^{\circ}\text{C}$, TMS-protected alkyl cyanohydrins are also unstable;⁴⁸ however, less is known about the stability of metalated TBS-protected cyanohydrins, which should be less prone to silyl migration. As outlined in eq. 11, both the cyanohydrins **55** and **56a** were deprotonated at $-10\text{ }^{\circ}\text{C}$, stirred for 30 minutes and then quenched with deuterated methanol. ^1H NMR analysis of the resultant crude mixture indicated that both nucleophiles had undergone significant decomposition under these conditions, and the deuterated cyanohydrin **62** could not be detected in either case. Discouraged by this, we abandoned our efforts to employ these simple nucleophiles in the rhodium-catalysed allylic substitution reaction, instead choosing to focus on the alkylation of substituted alkenyl cyanohydrins such as **56b** and **56c**.



2.2.5.1.4. Reaction Optimisation

With promising initial results in hand, our attention was turned towards improving the overall efficiency of this process, particularly in the case of the (*E*)-crotyl cyanohydrin **56b**. A brief ligand screen indicated that the reaction may be conducted in the presence of a range of commercially available phosphites; however, the isolated yield of the ketone **60** remained unsatisfactory (**Table 15**, entries 1-4). Additionally, two of these ligands afforded incomplete conversion of the starting carbonate **26a** (entries 3 and 4), which was difficult to separate from the ketone product **60**.

Table 15. Optimisation of the rhodium-catalysed allylic substitution with the alkenyl cyanohydrins **56** (R = Ph(CH₂)₂).



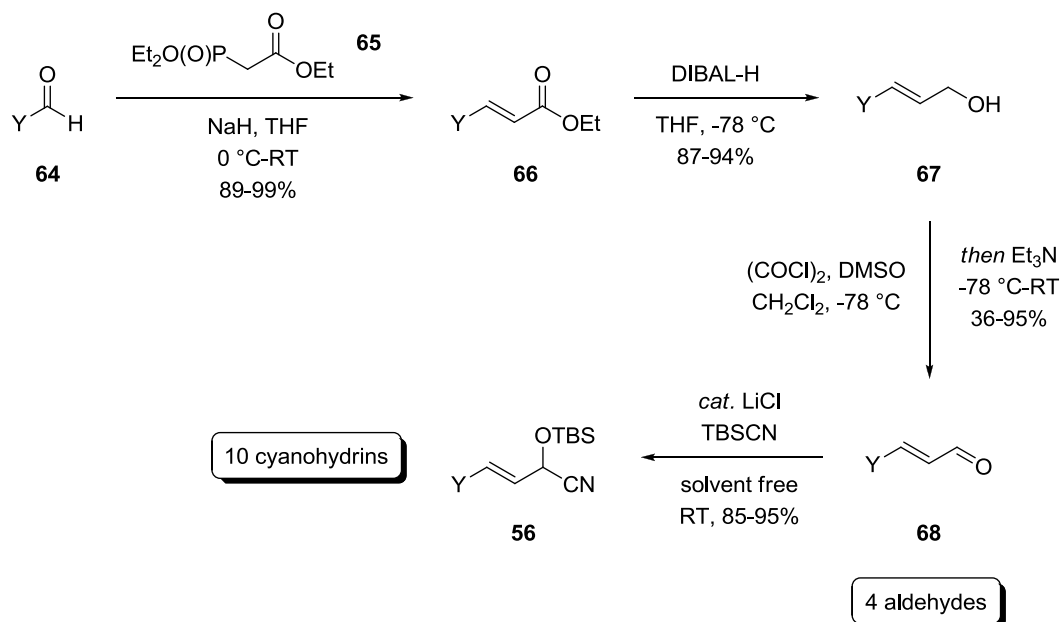
Entry ^a	Y	L	Equiv. 56	rs ^b	Yield (%) ^c	Conditions
1	Me	P(OPh) ₃	1.3	≥ 19:1	63	A
2	“	P(OMe) ₃	“	“	65	A
3	“	P(OCH ₂ CF ₃) ₃	“	“	58 ^d	A
4	“	P(O-2,4-di- ^t BuC ₆ H ₃) ₃	“	“	65 ^e	A
5^f	Me	P(OPh)₃	2	≥ 19:1	81	B
6	Ph	P(OPh)₃	1.3	≥ 19:1	75	A
7 ^f	“	“	2	≥ 19:1	75	B

^a All reactions were performed on a 0.5 mmol reaction scale using 2.5 mol% [Rh(COD)Cl]₂ and 10 mol% L in THF (5 mL) at -10 °C for *ca.* 16 h, followed by the addition of TBAF at -40 °C. ^b Regioselectivity was determined by 500 MHz ¹H NMR on the crude reaction mixtures before deprotection of the cyanohydrin adducts. ^c Isolated yields of the desired regioisomer **60**. ^d Contaminated with *ca.* 7% carbonate **26**. ^e Contaminated with *ca.* 5% carbonate **26**. ^f 2.8 equiv. LiHMDS and 6.0 equiv. TBAF were used.

Interestingly, the alkylation was found to be significantly more efficient when 2 equivalents of the cyanohydrin **56** were employed (conditions **B**), rather than 1.3 equivalents (conditions **A**). Under these reaction conditions, the (*E*)-crotyl ketone product was afforded in 81% yield and with excellent regioselectivity (entry 5). In contrast, the use of excess nucleophile was not beneficial to the yield of the styrene derivative, which was provided in identical yield and regioselectivity under both sets of conditions (entries 6 and 7).

2.2.5.1.5. Substrate Scope

2.2.5.1.5.1. Substrate Synthesis



Scheme 17. Synthesis of the disubstituted (*E*)-alkenyl cyanohydrins **56b-k**.

All of the tertiary allylic carbonates used in this study were prepared from the corresponding allylic alcohols, as shown in **Scheme 9**. The disubstituted alkenyl cyanohydrins **56** were prepared in the same manner as the aryl derivatives **24**; however, as some of the required α,β -unsaturated aldehydes **68** are not commercially available, they were synthesised according to the route outlined in **Scheme 17**.⁴⁹

Horner-Wadsworth-Emmons olefination of the aldehydes **64** provided the (*E*)-ethyl esters **66** with excellent selectivity. Subsequent di-*iso*-butylaluminium hydride reduction furnished the corresponding allylic alcohols **67**, which then underwent Swern oxidation to provide the requisite α,β -unsaturated aldehydes **68**. Cyanosilylation of these aldehydes, as previously described (**Table 5**), furnished the required cyanohydrins **56** in excellent yield. In general, the addition of *tert*-butyldimethylsilyl cyanide to the α,β -unsaturated aldehydes **68** occurred with complete selectivity for the 1,2-adduct **56**, and there was no evidence for the formation of 1,4-addition products.

2.2.5.1.5.2. Aryl-Substituted Cyanohydrin Scope

Table 16. Substrate scope of the rhodium-catalysed allylic alkylation with the aryl-substituted alkenyl cyanohydrins **56** (Conditions **A**, R = Ph(CH₂)₂, L = P(OPh)₃).

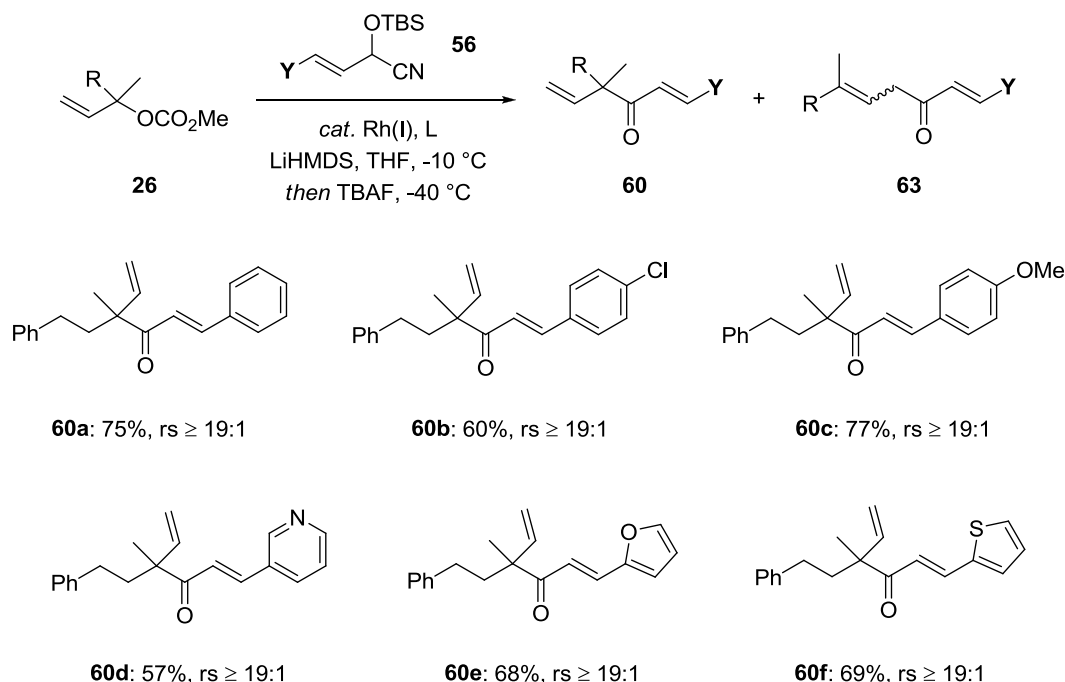
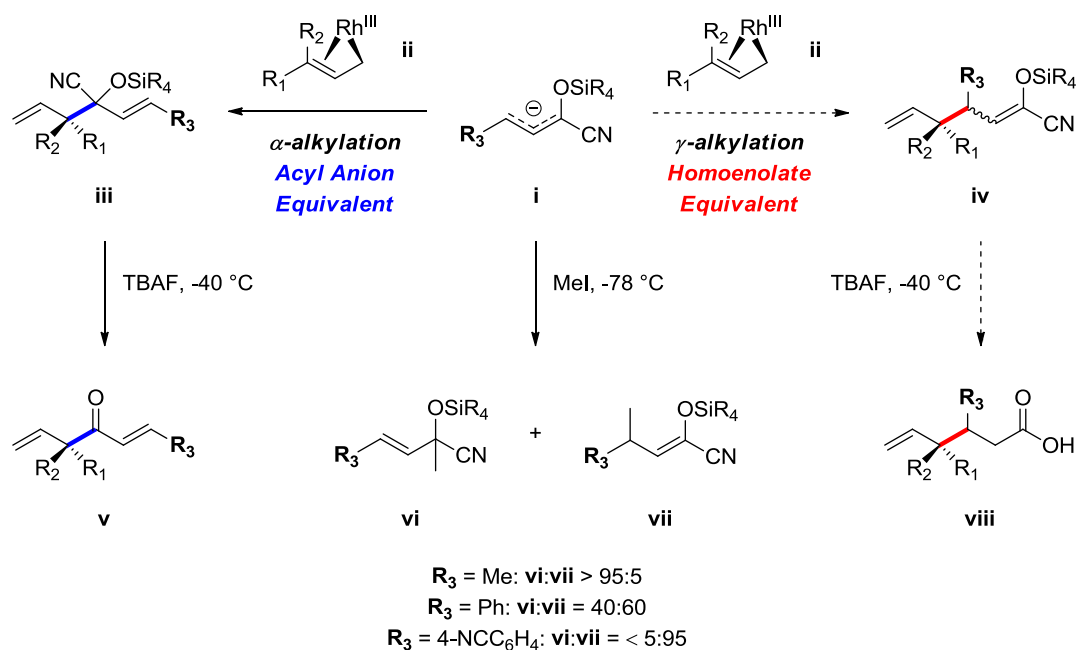


Table 16 outlines the application of our optimised reaction conditions to the alkylation of a range of aryl-substituted alkenyl cyanohydrins **56**. A variety of ketone

products containing both electron poor and electron rich aryl groups, in addition to the nitrogen-, oxygen- and sulfur-containing heterocycles **60d-f**, were all prepared in moderate to good yield and with excellent regioselectivity. In general, electron deficient alkenyl ketones, such as the 4-chlorophenyl- and 3-pyridyl-substituted derivatives **60b** and **60d**, were afforded in slightly reduced yield.



Scheme 18. Potential γ -alkylation in the rhodium-catalysed allylic substitution with the allylic anion **i**.

Upon deprotonation, the alkenyl cyanohydrins **56** provide allylic anions, and therefore have the ability to undergo both α - and γ -alkylation (**Scheme 18**). The corresponding TMS-protected analogues have been shown to undergo predominant α -alkylation with a number of electrophiles at $-78\text{ }^\circ\text{C}$,⁵⁰ though this depends largely on the nature of the substituent \mathbf{R}_3 . For example, in the presence of an alkyl substituent ($\mathbf{R}_3 = \text{Me}$), the alkylation of the anion **i** with methyl iodide is entirely α -selective, providing **vi**. In contrast, the introduction of an anion stabilising group (e.g. $\mathbf{R}_3 = \text{Ph}$) results in an almost 1:1 mixture of the α - and γ -adducts **vi** and **vii**, and the

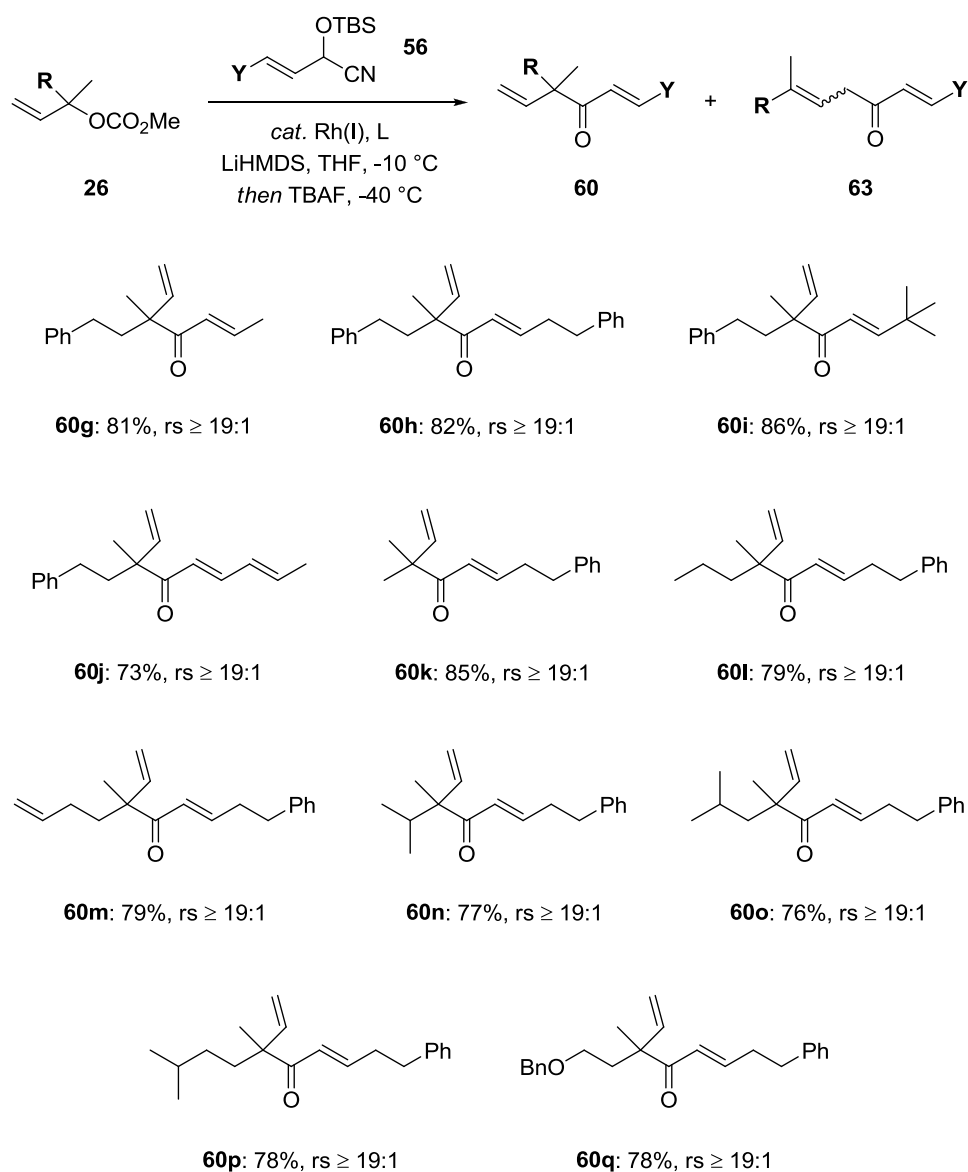
γ -product **vii** may be obtained selectively in the presence of an electron withdrawing aryl substituent ($R_3 = 4\text{-NCC}_6\text{H}_4$).

Given the propensity of aryl-substituted alkenyl cyanohydrins to undergo γ -alkylation, the overall efficiency of these substrates in the rhodium-catalysed allylic alkylation, as outlined in **Table 16**, is noteworthy. As depicted in **Scheme 18**, selective α -alkylation is required in order for the allylic anion **i** to function as an effective acyl anion equivalent in this transformation, and afford the desired ketone **v**. The γ -alkylation of **i** with the rhodium-*enyl* complex **ii** would initially be expected to provide the enol ether **iv** which, upon quenching with a solution of TBAF (containing *ca.* 5% water), may be expected to furnish the carboxylic acid **viii**.⁴⁶ While we have been unable to isolate this product, or any other that would be indicative of γ -alkylation, such a competing pathway would provide a plausible rationale for the marginally lower yields obtained in the alkylation of aryl-substituted alkenyl cyanohydrins, particularly those containing electron deficient groups (**Table 16**). As shown, the γ -alkylation of **i** enables it to function as a β -nucleophilic homoenolate equivalent. Studies aimed towards the exploitation of this reactivity in the rhodium-catalysed allylic substitution reaction, to provide products such as **viii** in an asymmetric fashion, are currently ongoing in our laboratory.

2.2.5.1.5.3. Alkyl-Substituted Cyanohydrin Scope

A wide variety of alkyl-substituted alkenyl cyanohydrins **56** and tertiary allylic carbonates **26** were examined in the rhodium-catalysed allylic substitution reaction, as outlined in **Table 17**.

Table 17. Substrate scope of the rhodium-catalysed allylic alkylation with the alkyl-substituted alkenyl cyanohydrins **56** (Conditions **B**, L = P(OPh)₃).



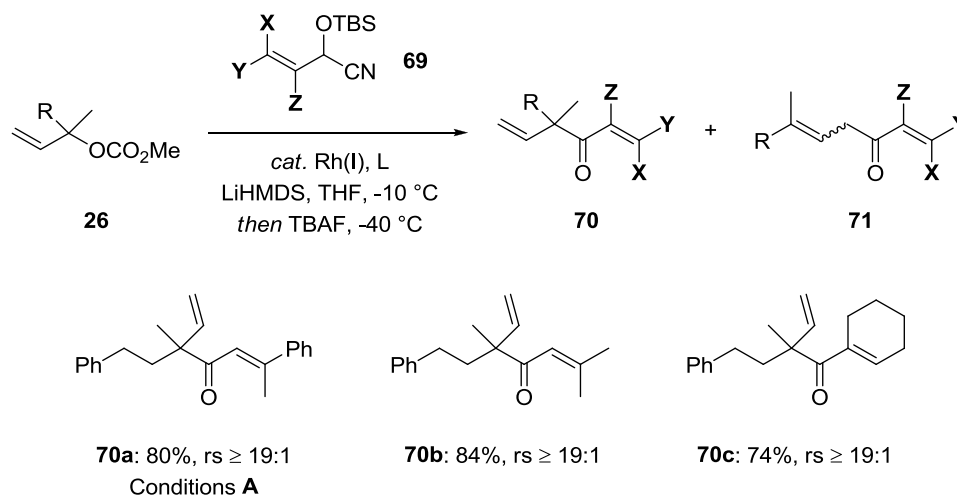
Clearly, a number of alkenyl substituents are well tolerated, including branched alkyl groups (**60i**) and an additional alkene, which provides access to the highly substituted dienone **60j**. This method is also general for a range of tertiary allylic carbonates containing linear and branched alkyl substituents, pendant alkenes and protected hydroxyl groups (**60k-q**). In contrast to our previous studies, in which certain substitution patterns led to slightly reduced levels of regiocontrol (**Table 7**), these

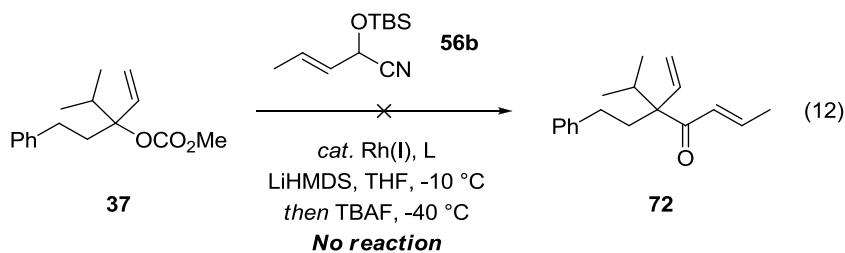
reactions were consistently shown to proceed with $\geq 19:1$ regioselectivity favouring the branched cyanohydrin adduct. In addition, the ketone products **60g-q** were all isolated in good yield and as a single geometrical isomer, demonstrating that the reaction proceeds with complete retention of the initial (*E*)-cyanohydrin stereochemistry. Future studies will examine the application of (*Z*)-alkenyl cyanohydrins, which should provide the corresponding (*Z*)-enones.

2.2.5.1.5.4. Trisubstituted Cyanohydrin Scope

A small number of trisubstituted alkenyl cyanohydrins **69** were also examined in the rhodium-catalysed allylic substitution of the tertiary carbonate **26a**. As depicted in **Table 18**, additional substitution may be incorporated both α - and β - to the newly formed carbonyl group. Notably, the (*E*)-1,1-trisubstituted alkene **70a** was afforded with complete retention of alkene geometry, and in the highest yield of all the styrenyl cyanohydrins that were examined. The utilisation of a cyclohexenyl-substituted cyanohydrin, to provide the ketone **70c**, highlights the ability of this method to construct α,α' -dialkyl ketones containing cyclic substituents.

Table 18. Substrate scope of the rhodium-catalysed allylic alkylation with the trisubstituted alkenyl cyanohydrins **69** (Conditions **B**, L = P(OPh)₃).

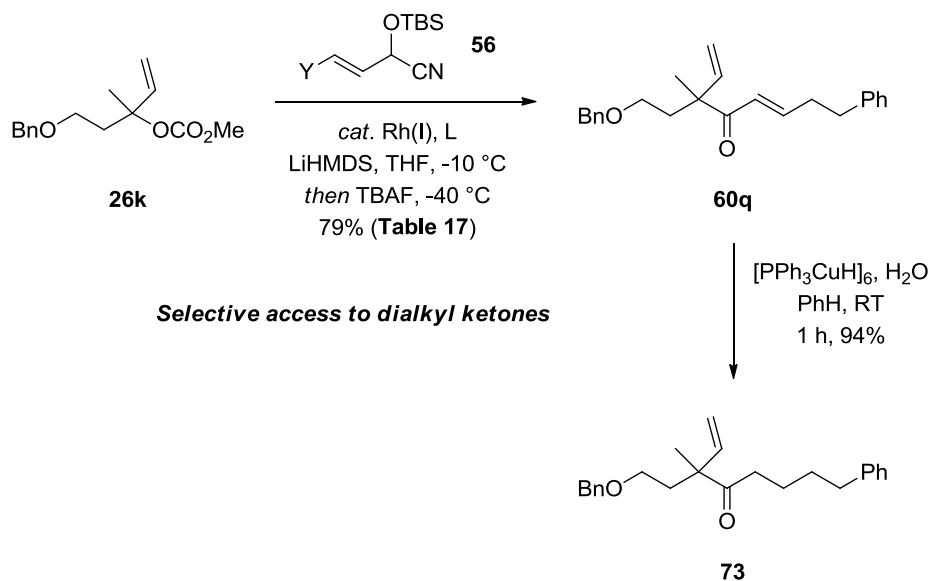




Due to the decreased steric demand of the nucleophile **56b**, we were hopeful that it may participate in the alkylation of the hindered carbonate **37**, which had proven unreactive in the presence of a lithiated aryl cyanohydrin (eq. 7). However, under our optimal reaction conditions, this cyanohydrin too failed to react and the carbonate **37** was recovered untouched (eq. 12). Hence, this reaction remains limited to the construction of acyclic α -quaternary substituted ketones containing at least one methyl substituent.

2.2.5.1.6. Access to α,α' -Dialkyl Ketones

Although we were unable to employ alkyl-substituted cyanohydrins in the rhodium-catalysed allylic substitution reaction, the α,β -unsaturated ketones **60** and **70** represent viable precursors to the α,α' -dialkyl ketones that would have resulted from such a process. For example, treatment of the enone **60q** with the hexameric Stryker's reagent ($[\text{PPh}_3\text{CuH}]_6$), which has been demonstrated to effect the highly chemoselective conjugate reduction of a wide range of α,β -unsaturated carbonyl compounds,⁵¹ furnished the fully saturated ketone **72** in excellent yield (**Scheme 19**). We envisage that by this efficient two step sequence, a range of differentially substituted α,α' -dialkyl ketones could be afforded in a highly selective manner, thereby illustrating the synthetic utility of this method.



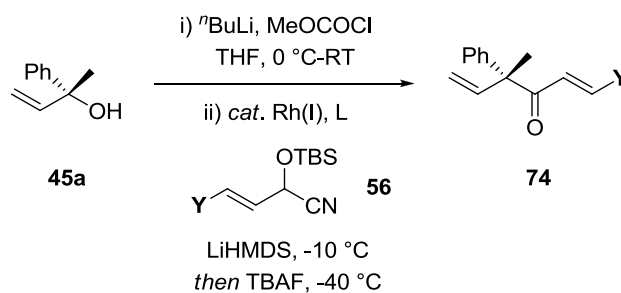
Scheme 19. Selective 1,4-reduction of the α,β -unsaturated ketone **60q** to provide the α,α' -dialkyl ketone **73** ($Y = \text{Ph}(\text{CH}_2)_2$, $L = \text{P}(\text{OPh})_3$).

2.2.5.1.7. Stereospecific Alkylation

Encouraged by our previous work on the stereospecific rhodium-catalysed allylic substitution of tertiary carbonates with the stabilised aryl cyanohydrins **24**, we next sought to examine the analogous transformations of both the aryl- and alkyl-substituted (*E*)-alkenyl cyanohydrins **56**. Gratifyingly, the highly efficient one pot alkylation of the enantiomerically enriched tertiary allylic alcohol **45a**, as previously described, was shown to proceed readily with both alkenyl nucleophiles **56b** and **56c** (**Table 19**). Under our optimal catalytic conditions for the alkylation of the (*E*)-crotyl cyanohydrin **56b** (**Table 15**, entry 5), the acyclic α -aryl ketone **67** was afforded in good yield, but with relatively poor conservation of enantiomeric excess (entry 1). However, it should be noted that in the presence of triphenylphosphite, this particular transformation is significantly more stereospecific than the corresponding alkylation of the aryl cyanohydrin **24a** (**Table 9**). While we are yet to confirm the absolute configuration of the ketone **74**, it seems reasonable to assume that this alkylation,

like that of the aryl derivatives **24**, proceeds with overall retention of stereochemistry.

Table 19. Stereospecific rhodium-catalysed allylic alkylation with the alkenyl cyanohydrin **56**.



Entry ^a	Y	Conditions	L	rs ^b	ee (%) ^c	cee (%)	Yield (%) ^d
1	Me	A	P(OPh) ₃	≥ 19:1	79	80	79
2	Me	B	P(OCH ₂ CF ₃) ₃	≥ 19:1	91	92	63
3	Ph	B	P(OCH ₂ CF ₃) ₃	≥ 19:1	90	91	56

^a All reactions were performed on a 0.5 mmol reaction scale using 1 equiv. ⁿBuLi, 1 equiv. MeOCOCI, 2.5 mol% [Rh(COD)Cl]₂ and 10 mol% L in THF (5 ml) at -10 °C for *ca.* 5 h, followed by the addition of TBAF at -40 °C. ^b Regioselectivity was determined by 500 MHz ¹H NMR on the crude reaction mixtures before deprotection of the cyanohydrin adduct. ^c *ee* values were determined by chiral HPLC on the isolated products. ^d Isolated yields.

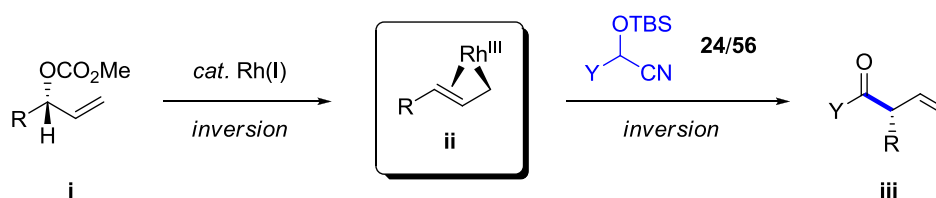
Having previously established that the stereospecificity of this reaction is significantly improved in the presence of tris(2,2,2-trifluoroethyl) phosphite, we elected to examine the use of this ligand in the alkylation of **56b**. Gratifyingly, under these conditions, the enantiospecificity was comparable to our previous studies, and the ketone **74a** (Y = Me) was afforded in 91 % *ee* (entry 2). This modification was also successful in the alkylation of the (*E*)-aryl-substituted cyanohydrin **56c**, which afforded equally impressive stereospecificity (entry 3). Unfortunately, as was the case with the alkyl carbonates **26** (Table 18), these reactions failed to proceed to completion with the use of this ligand, and both acyclic ketones were afforded in

moderate yield. Thus, despite being highly stereospecific, additional studies are clearly required in order to improve the overall efficiency of this process.

2.2.5.2. Rhodium-Catalysed Allylic Substitution of Secondary Carbonates with an Acyl Anion Equivalent: Synthesis of α -Tertiary Ketones

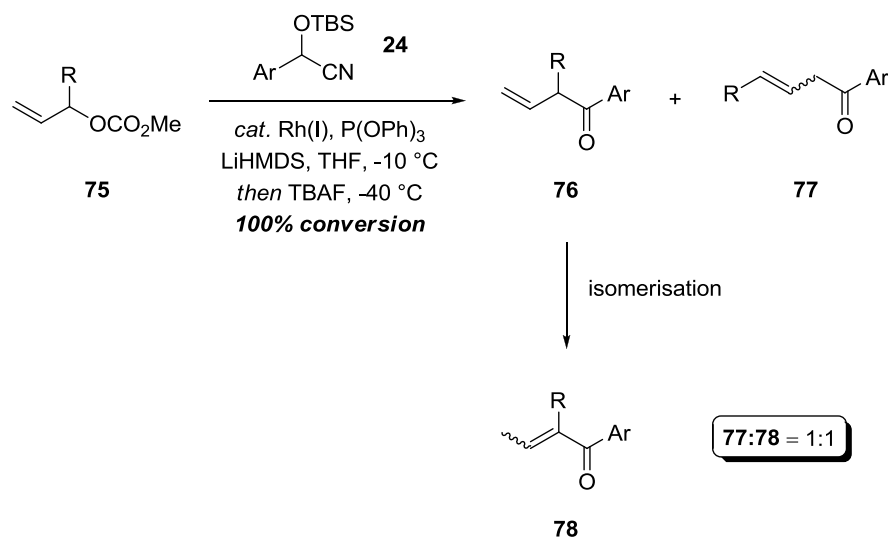
2.2.5.2.1. Introduction

Following our success in the rhodium-catalysed allylic alkylation of tertiary carbonates with a range of aryl- and alkenyl-substituted cyanohydrins, the next logical goal was the extension of this methodology to the corresponding secondary allylic alcohol derivatives, which would afford α -tertiary ketones such as **iii** (Scheme 21). Although α -tertiary ketones are generally easier to prepare than the corresponding α -quaternary substituted analogues, the asymmetric construction of tertiary α -vinyl carbonyl compounds remains an active area of investigation.⁵² This is largely due to the tendency of these adducts to undergo rapid racemisation and olefin isomerisation, which is often difficult to avoid in the course of conventional enolate α -vinylation. Hence, in addition to the numerous advantages afforded by this approach in terms of selectivity and substrate scope, we were hopeful that with the careful development of mild reaction conditions, it may provide facile access to a range of potentially labile β,γ -unsaturated ketones **iii**.



Scheme 20. Proposed stereospecific rhodium-catalysed allylic substitution of secondary carbonates with an acyl anion equivalent.

2.2.5.2.2. Preliminary Results

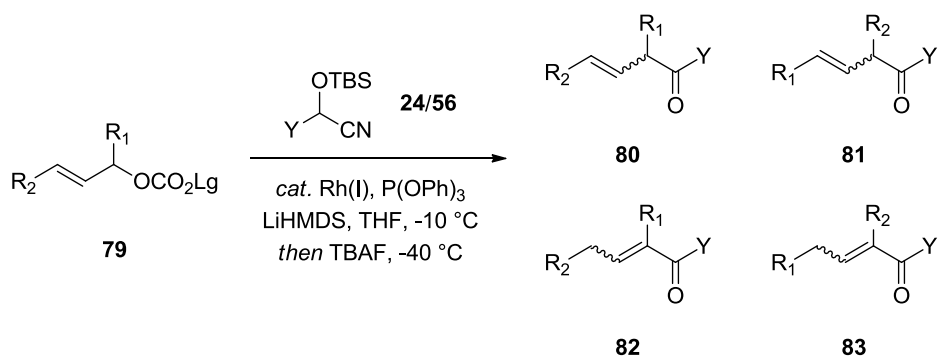


Scheme 21. Undesired alkene isomerisation in the rhodium-catalysed allylic substitution of the secondary carbonate **75** with the cyanohydrin **24** ($\text{R} = \text{Ph}(\text{CH}_2)_2$, $\text{Ar} = \text{Ph}$).

Gratifyingly, the rhodium-catalysed allylic substitution of the secondary allylic carbonate **75** with the cyanohydrin **24a** ($\text{Y} = \text{Ph}$) was shown to proceed readily (**Scheme 20**). However, the regioselectivity of the alkylation was relatively poor in comparison to the corresponding reaction of the tertiary allylic carbonate **26**, and the intermediate cyanohydrin adducts were afforded as a 1:1 mixture of regioisomers under these standard conditions. Additionally, upon careful deprotection of these adducts at $-40\text{ }^\circ\text{C}$, the desired β,γ -unsaturated ketone **76** was shown to undergo complete isomerisation to the α,β -unsaturated derivative **78**, whereas the undesired linear regioisomer **77** remained untouched. Although β,γ -unsaturated ketones such as **76** have been isolated previously,^{52b} the isomerisation of this product is perhaps unsurprising given the basic reaction conditions and the relative acidity of the allylic α -carbonyl proton. This also gives a clear indication that the stereospecific variant of

this transformation is likely to be hindered by product racemisation. Hence, our initial optimisation studies were aimed towards minimising this isomerisation, and improving the regioselectivity of the alkylation.

Table 20. Initial studies towards the rhodium-catalysed allylic alkylation of secondary carbonates with an acyl anion equivalent ($R_1 = \text{Ph}(\text{CH}_2)_2$).



Entry ^a	Lg	R ₂	Y	rs ^b	80:81:82:83 ^c	% Product ^c
1	Me	H	Ph	1:1	0:43:57:0	> 99
2	“	“	(<i>E</i>)-CH ₃ CH=CH-	1:1	0:50:50:0	> 99
3	“	“	4-Me ₂ NC ₆ H ₄ -	5:1	75:15:10:0	86
4	<i>t</i> Bu	“	4-Me ₂ NC ₆ H ₄ -	5:1	79:15:6:0	> 99
5	“	Me	“	1:1	50:50:0:0	65

^a All reactions were performed on a 0.5 mmol reaction scale using 2.5 mol% [Rh(COD)Cl]₂, 10 mol% P(OPh)₃, 1.3 equiv. cyanohydrin and 1.8 equiv. LiHMDS in THF (5 mL) at -10 °C for *ca.* 16 h, followed by the addition of 4.0 equiv. TBAF at -40 °C. ^b Regioselectivity was determined by 500 MHz ¹H NMR on the crude reaction mixtures before deprotection of the cyanohydrin adducts. ^c Determined by 500 MHz ¹H NMR on the crude reaction mixtures following deprotection of the cyanohydrin adducts.

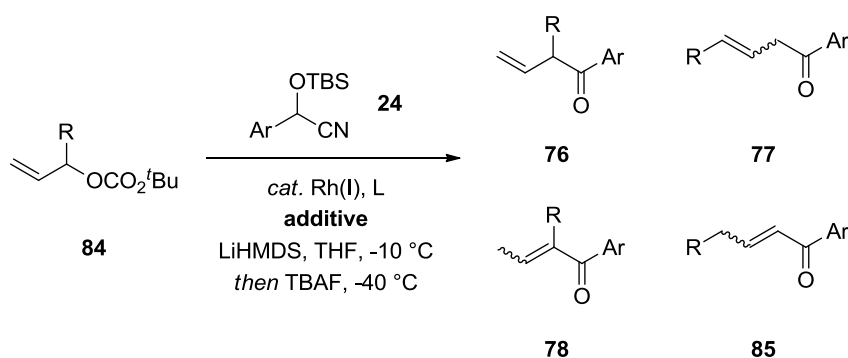
As outlined in **Table 20**, two principal strategies were devised for the successful preparation and isolation of the desired α -tertiary ketone **80**. Given that the isomerisation of this product is mediated by base, it seemed plausible that it may be prevented by reducing the acidity of the α -carbonyl proton. Thus, the electronic properties of the ketone product **80** were varied to include both an alkenyl and an electron rich aryl substituent (**Table 20**). While this was unsuccessful in the case of

the alkenyl cyanohydrin **56b** (entry 2), the dimethylamino-substituted aryl ketone was shown to be significantly less prone to isomerisation. Consequently, the desired ketone **80** was afforded as the major product with only 6% of the isomerised ketone **82**, and with improved regioselectivity (entry 3). Though initially hampered by competing transesterification of the allylic carbonate, this was circumvented by the use of a bulkier leaving group, which resulted in a more efficient alkylation (entry 4). As the substituted alkene **77** is seemingly more stable to isomerisation than the terminal alkene **76** (**Scheme 21**), we also probed the effect of additional substitution in the allylic carbonate **79** (entry 5). However, while this did serve to eliminate the formation of the α,β -unsaturated ketones **82** and **83**, the reaction was poorly regioselective and failed to proceed to completion. Following this, no further attempts were made to optimise the alkylation of this substrate, and our efforts were focused towards the more effective allylic substitution of the electron rich aryl cyanohydrin **24** (**Table 21**).

As shown in **Table 21**, a brief optimisation demonstrated that the regioselectivity may be marginally improved by the use of tris(*tert*-butyldimethylsilyl) phosphite, as was the case with the tertiary allylic carbonates **26** (entry 2). More interestingly, it was found that with the use of DMPU as a cosolvent (9:1 v/v with THF), the product ketone **76** could be cleanly afforded as a single regioisomer (entry 3). DMPU is well known to solvate lithium cations,⁵³ and is likely to function as a deaggregating agent for the lithiated cyanohydrin. This could serve to make the nucleophile more reactive towards the rhodium-*enyl* electrophile which, according to the proposed mechanistic model (**Scheme 3**), would improve the regioselectivity of the alkylation. Future studies will seek to elucidate the role of this additive, and examine the substrate scope of this new method, particularly with respect to an asymmetric variant. It

should also be noted that while we were able to suppress the undesired isomerisation of the product **76**, it remains a significant drawback of this approach, and the reaction is currently limited to a single electron rich nucleophile. Thus, the development of a more general solution to this problem would clearly be beneficial.

Table 21. Initial optimisation of the rhodium-catalysed allylic substitution of secondary carbonates with the electron rich aryl cyanohydrin **24** (Ar = 4-Me₂NC₆H₄).



Entry ^a	L	additive	rs ^b	76:77:78:85 ^c	% Product ^c
1	P(OPh) ₃	-	5:1	79:15:6:0	> 99
2	P(OTBS) ₃	-	8:1	87:13:0:0	> 99
3^d	“	DMPU	≥ 19:1	100:0:0:0	> 99

^a All reactions were performed on a 0.5 mmol reaction scale using 2.5 mol% [Rh(COD)Cl]₂, 10 mol% L, 1.3 equiv. cyanohydrin and 1.8 equiv. LiHMDS in THF (5 mL) at -10 °C for *ca.* 16 h, followed by the addition of 4.0 equiv. TBAF at -40 °C. ^b Regioselectivity was determined by 500 MHz ¹H NMR on the crude reaction mixtures before deprotection of the cyanohydrin adducts. ^c Determined by 500 MHz ¹H NMR on the crude reaction mixtures following deprotection of the cyanohydrin adducts. ^d The reaction was conducted in THF (4.5 mL) and DMPU (0.5 mL).

2.2.5.3. Concluding Remarks

We have successfully expanded the scope of the rhodium-catalysed allylic substitution to include both aryl- and alkyl-substituted alkenyl cyanohydrin nucleophiles. This reaction provides facile access to a range of α -quaternary substituted ketones containing a synthetically versatile α,β -unsaturated carbonyl moiety, which may be readily functionalised. For example, chemoselective hydride reduction of the product enones has been shown to afford the corresponding α,α' -

dialkyl ketones, which would be difficult to obtain by conventional enolate alkylation. Both the aryl- and alkyl-substituted alkenyl cyanohydrins afford excellent enantiospecificity, providing a flexible new method for the asymmetric construction of acyclic α -quaternary substituted ketones. Promising initial studies have also demonstrated that the alkylation may be extended to secondary allylic carbonates, enabling the synthesis of α -tertiary ketones. Thus, with further development, we anticipate that this process will become one of the most versatile and widely used methods for the asymmetric construction of both α -tertiary and α -quaternary substituted carbonyl compounds, and should find significant application in target directed synthesis, particularly in the preparation of complex bioactive pharmaceuticals and natural products that contain quaternary carbon stereogenic centres.

- ¹ Evans, P. A.; Leahy, D. K. in *Modern Rhodium-Catalyzed Organic Reactions*; Evans, P. A., Ed.; Wiley-VCH: Weinheim, Germany, 2005; Ch. 10, p. 191-214.
- ² Onoue, H.; Moritani, I.; Murahashi, S.-I. *Tetrahedron Lett.* **1973**, *14*, 121.
- ³ Tsuji, J.; Minami, I.; Shimizu, I. *Chem. Lett.* **1984**, *13*, 1721.
- ⁴ Tsuji, J.; Minami, I.; Shimizu, I. *Tetrahedron Lett.* **1984**, *25*, 5157.
- ⁵ Tsuji, J.; Minami, I.; Shimizu, I.; Ohashi, Y. *Tetrahedron Lett.* **1982**, *23*, 4809.
- ⁶ Tsuji, J.; Minami, I.; Shimizu, I. *J. Organomet. Chem.* **1985**, *296*, 269.
- ⁷ Evans, P. A.; Nelson, J. D. *Tetrahedron Lett.* **1998**, *39*, 1725.
- ⁸ Takeuchi, R.; Kitamura, N. *New J. Chem.* **1998**, 659.
- ⁹ Tolman, C. A. *Chem. Rev.* **1977**, *77*, 313.
- ¹⁰ Evans, P. A.; Nelson, J. D. *J. Am. Chem. Soc.* **1998**, *120*, 5581.
- ¹¹ Lawson, D. N.; Osborn, J. A.; Wilkinson, G. *J. Chem. Soc. A* **1966**, 1733.
- ¹² Tanaka, I.; Jin-no, N.; Kushida, T.; Tsutsui, N.; Ashida, T.; Suzuki, H.; Sajurai, H.; Moro-oka, Y.; Ikawa, T. *Bull. Chem. Soc. Jpn.* **1983**, *56*, 657.
- ¹³ Pasternak, H.; Glowiak, T.; Pruchnik, F. *Inorg. Chim. Acta.* **1976**, *19*, 11.
- ¹⁴ McPartlin, M.; Mason, R. *Chem. Commun.* **1967**, 16.
- ¹⁵ Ashfield, B. L.; Miller, K. A.; Martin, S. *Org. Lett.* **2004**, *6*, 1321.
- ¹⁶ Evans, P. A.; Uraguchi, D. *J. Am. Chem. Soc.* **2003**, *125*, 7158.
- ¹⁷ For a recent example, see: Hayashi, T.; Okada, A.; Suzuka, T.; Kawatsura, M. *Org. Lett.* **2003**, *5*, 1713.
- ¹⁸ The corresponding tertiary allylic trifluoroacetate could not be isolated due to facile ionisation.
- ¹⁹ Tsuji, Y.; Obora, Y.; Ogawa, Y.; Imai, Y.; Kawamura, T. *J. Am. Chem. Soc.* **2001**, *123*, 10489.
- ²⁰ Tsuji, J.; Shimizu, I.; Minami, I.; Ohashi, Y.; Sugiura, T.; Takahashi, K. *J. Org. Chem.* **1985**, *50*, 1523.
- ²¹ PPh₃: $\theta = 145^\circ$, $\nu(\text{CO}) = 2068.9 \text{ cm}^{-1}$, P(OCH₂CF₃)₃: $\theta = 115^\circ$, $\nu(\text{CO}) = 2095.1 \text{ cm}^{-1}$.
- ²² Guzman-Martinez, A.; Hoveyda, A. H. *J. Am. Chem. Soc.* **2010**, *132*, 10634.
- ²³ Plietker, B.; Dieskau, A.; Möws, K.; Jatsch, A. *Angew. Chem. Int. Ed.* **2008**, *47*, 198.
- ²⁴ Sun, H.; DiMagno, S. G. *J. Am. Chem. Soc.* **2005**, *127*, 2050 and pertinent references cited therein.
- ²⁵ Kurono, N.; Yamaguchi, M.; Suzuki, K.; Ohkuma, T. *J. Org. Chem.* **2005**, *70*, 6530.
- ²⁶ Sassaman, M. B.; Prakash, G. K. S.; Olah, G. A. *J. Org. Chem.* **1990**, *55*, 2016.
- ²⁷ Göttlich, R.; Yamakoshi, K.; Sasai, H.; Shibasaki, M. *Synlett* **1997**, 971.
- ²⁸ Evans, P. A.; Lawler, M. J. *J. Am. Chem. Soc.* **2004**, *126*, 8642.
- ²⁹ For recent reviews on the catalytic enantioselective construction of quaternary carbon stereogenic centres, see: (a) Corey, E. J.; Guzman-Perez, A. *Angew. Chem. Int. Ed.* **1998**, *37*, 388. (b) Christoffers, J.; Mann, A. *Angew. Chem. Int. Ed.* **2001**, *40*, 4591. (c) Trost, B. M.; Jiang, C. *Synthesis* **2006**, *3*, 369.
- ³⁰ For a recent review on the enantioselective construction of acyclic quaternary carbon stereogenic centres, see: Das, J. P.; Marek, I. *Chem. Commun.* **2011**, *47*, 4593.
- ³¹ Cheon, C. H.; Kanno, O.; Toste, F. D. *J. Am. Chem. Soc.* **2011**, *133*, 13248.
- ³² a) Manthorpe, J. M.; Gleason, J. L. *Angew. Chem. Int. Ed.* **2002**, *41*, 2338. b) Kummer, D. A.; Chain, W. J.; Morales, M. R.; Quiroga, O.; Myers, A. G. *J. Am. Chem. Soc.* **2008**, *130*, 13231.

-
- ³³ Doyle, A. G.; Jacobsen, E. N. *Angew. Chem. Int. Ed.* **2007**, *46*, 3701.
- ³⁴ Jegelka, M.; Plietker, B. *Org. Lett.* **2009**, *11*, 3462.
- ³⁵ Mohapatra, D. K.; Prarnanik, C.; Chorghade, M. S.; Gurjar, M. K. *Eur. J. Org. Chem.* **2007**, 5059.
- ³⁶ For a recent example, see: Madduri, A. V. R.; Harutyunyan, S. R.; Minnaard, A. J. *Angew. Chem. Int. Ed.* **2012**, *51*, 3164.
- ³⁷ Stymeist, J. L.; Bagutski, V.; French, R. M.; Aggarwal, V. K. *Nature* **2008**, *456*, 778.
- ³⁸ Bagutski, V.; French, R. M.; Aggarwal, V. K. *Angew. Chem. Int. Ed.* **2010**, *49*, 5142.
- ³⁹ Pulis, A. P.; Aggarwal, V. K. *J. Am. Chem. Soc.* **2012**, *134*, 7570.
- ⁴⁰ For a similar approach involving the *in situ* alkylation of a secondary allylic carbonate with a copper(I) enolate, see: Evans, P. A.; Leahy, D. K. *J. Am. Chem. Soc.* **2003**, *125*, 8974.
- ⁴¹ Evans, P. A.; Leahy, D. K.; Sliker, L. M. *Tetrahedron: Asymmetry* **2003**, *14*, 3613.
- ⁴² For a recent example of a rhodium-catalysed DYKAT of tertiary allylic trichloroacetimidates with anilines, see: Arnold, J. S.; Nguyen, H. M. *J. Am. Chem. Soc.* **2012**, *134*, 8380.
- ⁴³ Conservation of enantiomeric excess = (*ee* of product/*ee* of starting material) × 100.
- ⁴⁴ a) Ros, A.; Aggarwal, V. K. *Angew. Chem. Int. Ed.* **2009**, *48*, 6289. b) Kopecky, K. R.; Mojelsky, T. W.; Gillan, T.; Barry, J. A.; Lopez Sastre, J. A. *Can. J. Chem.* **1977**, *55*, 1001.
- ⁴⁵ Ou, L.; Xu, Y.; Ludwig, D.; Pan, J.; Xu, J. H. *Org. Process Res. Dev.* **2008**, *12*, 192.
- ⁴⁶ For a recent review on the transition metal-catalysed α -arylation of carbonyl compounds, see: Johansson, C. C. C.; Colacot, T. J. *Angew. Chem. Int. Ed.* **2010**, *49*, 676.
- ⁴⁷ Jacobson, R. M.; Lahm, G. P.; Clader, J. W. *J. Org. Chem.* **1980**, *45*, 395.
- ⁴⁸ Wright, A.; West, R. *J. Am. Chem. Soc.* **1974**, *96*, 3214.
- ⁴⁹ Das, B.; Veeranjanyulu, B.; Balasubramanyam, P.; Srilatha, M. *Tetrahedron: Asymmetry* **2010**, *21*, 2762.
- ⁵⁰ Hünig, S.; Reichelt, H. *Chem. Ber.* **1986**, *119*, 1772.
- ⁵¹ Mahoney, W. S.; Brestensky, D. M.; Stryker, J. M. *J. Am. Chem. Soc.* **1988**, *110*, 291.
- ⁵² For recent examples, see: a) Skucas, E.; MacMillan, D. W. C. *J. Am. Chem. Soc.* **2012**, *134*, 9090. b) Lou, S.; Fu, G. C. *J. Am. Chem. Soc.* **2010**, *132*, 5010.
- ⁵³ Mukhopadhyay, T. Seebach, D. *Helvetica Chimica Acta* **1982**, *65*, 385.

Chapter 3

Representative Experimental Procedures and Supplemental Data

3.1. General Information

All reactions were carried out under an argon atmosphere with anhydrous solvents. All commercially available reagents were purchased and used as received. All compounds were purified by flash chromatography using silica gel 60 (40-63 μm , *FluoroChem*) and gave spectroscopic data consistent with being $\geq 95\%$ the assigned structure. Analytical thin layer chromatography (TLC) was performed on pre-coated 0.25 mm thick silica gel 60-F₂₅₄ plates (*Whatman PE SIL G/UV*); visualised using UV light and by treatment with a KMnO_4 dip, followed by heating. Optical rotations ($[\alpha]_{\text{D}}^{20}$) were measured on a *Perkin-Elmer Model 343 plus* polarimeter with a sodium lamp (D line, 589 nm) at ambient temperature (indicated in $^{\circ}\text{C}$ as superscript) using a 1 mL quartz cell of 100 mm length; solution concentration (c) are given in g/100 mL. IR spectra were recorded on a *Perkin-Elmer FT-IR Spectrum 100* (ATR) spectrometer; wavenumbers (ν) are given in cm^{-1} ; and the abbreviations w (weak, < 25%), m (medium, 25-50%), s (strong, 51-75%), vs (very strong, > 75%) and br (broad) are used to describe the relative intensities of the IR absorbance bands. Mass spectra were obtained through the Chemistry Department Mass Spectrometry Service, University of Liverpool or the EPSRC National Mass Spectrometry Service, Swansea. High resolution chemical ionization (CI) and electrospray ionisation (ESI) mass spectra were recorded on a *Fisons Trio-1000* or *LTQ Orbitrap*, and *Micromass LTC* mass spectrometers, respectively. ^1H NMR and ^{13}C NMR spectra were recorded on a *Bruker Avance DRX-500* spectrometer in CDCl_3 at ambient temperature; chemical shifts (δ) are given in ppm and calibrated using the signal of

residual undeuterated solvent as internal reference ($\delta_{\text{H}} = 7.26$ ppm and $\delta_{\text{C}} = 77.17$ ppm). ^1H NMR data are reported as follows: chemical shift (multiplicity, 2nd order spin system if available, coupling constant, integration). Coupling constants (J) are reported in Hz and apparent splitting patterns are designated using the following abbreviations: s (singlet), d (doublet), t (triplet), q (quartet), m (multiplet), br (broad), app. (apparent) and the appropriate combinations. ^{13}C NMR spectra with complete proton decoupling were described with the aid of an APT sequence, separating methylene and quaternary carbons (e, even), from methyl and methine carbons (o, odd).

3.2. Representative Experimental Procedures and Spectral Data

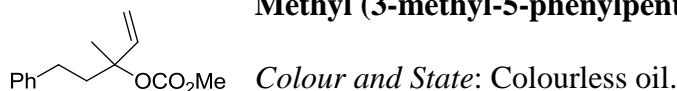
3.2.1. Rhodium-Catalysed Allylic Substitution with Aryl Cyanohydrin Pronucleophiles

3.2.1.1. Representative Experimental Procedure for the Synthesis of Tertiary Allylic Carbonates 26a-k

Under an atmosphere of argon, a 1M solution of lithium bis(trimethylsilyl)amide in tetrahydrofuran (27.7 mL, 27.7 mmol) was added dropwise to a stirring solution of the allylic alcohol **35a** (4.89 g, 27.7 mmol) in anhydrous tetrahydrofuran (56 mL) at 0 °C. The mixture was stirred for *ca.* 30 minutes and methyl chloroformate (2.15 mL, 27.7 mmol) was added dropwise. The mixture was allowed to warm slowly to room temperature and stirred for *ca.* 4 hours. Water (10 mL) was then added dropwise, and the resultant mixture was partitioned between diethyl ether and saturated aqueous ammonium chloride solution. The combined organic layers were dried using anhydrous magnesium sulfate, filtered and concentrated *in vacuo*. Purification by flash column chromatography (eluting with 3-9% diethyl ether/hexane) yielded the tertiary allylic carbonate **26a** (5.54 g, 85%) as a colourless oil.

3.2.1.2. Spectral Data for the Allylic Carbonates 26a-k, 31 and 37

Methyl (3-methyl-5-phenylpent-1-en-3-yl) carbonate (26a)



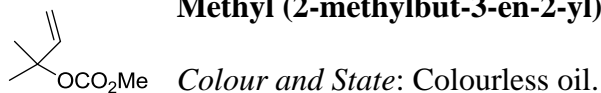
$^1\text{H NMR}$ (500 MHz, CDCl_3) δ 7.29-7.26 (m, 2H), 7.19-7.17 (m, 3H), 6.05 (dd, $J = 17.5, 11.0$ Hz, 1H), 5.26 (d, $J = 17.7$ Hz, 1H), 5.23 (d, $J = 11.1$ Hz, 1H), 3.73 (s, 3H), 2.68-2.62 (m, 2H), 2.21-2.06 (m, 2H), 1.64 (s, 3H).

$^{13}\text{C NMR}$ (125 MHz, CDCl_3) δ 153.93 (e), 141.76 (e), 140.86 (o), 128.47 (o), 128.43 (o), 125.96 (o), 114.49 (e), 84.24 (e), 54.20 (o), 41.76 (e), 30.02 (e), 23.22 (o).

IR (Neat) 3028 (w), 1744 (s), 1647 (w), 1497 (w), 1261 (vs), 929 (m), 699 (m) cm^{-1} .

HRMS ($\text{CI}[\text{M}+\text{NH}_4]^+$) calcd for $\text{C}_{14}\text{H}_{22}\text{NO}_3$ 252.1594, found 252.1596.

Methyl (2-methylbut-3-en-2-yl) carbonate (26b)



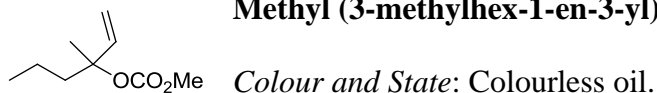
All spectral data matched the published values.¹

$^1\text{H NMR}$ (500 MHz, CDCl_3) δ 6.10 (dd, $J = 17.5, 10.9$ Hz, 1H), 5.23 (d, $J = 17.5$ Hz, 1H), 5.14 (d, $J = 10.9$ Hz, 1H), 3.72 (s, 3H), 1.56 (s, 6H).

$^{13}\text{C NMR}$ (125 MHz, CDCl_3) δ 153.62 (e), 141.51 (o), 113.18 (e), 81.63 (e), 53.54 (o), 25.79 (o).

IR (Neat) 2986 (w), 1745 (s), 1647 (w), 1440 (m), 1264 (vs), 929 (m), 679 (w) cm^{-1} .

Methyl (3-methylhex-1-en-3-yl) carbonate (26c)

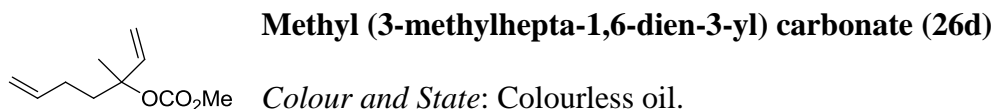


$^1\text{H NMR}$ (500 MHz, CDCl_3) δ 5.99 (dd, $J = 17.5, 11.0$ Hz, 1H), 5.19 (d, $J = 17.4$ Hz, 1H), 5.16 (d, $J = 10.9$ Hz, 1H), 3.71 (s, 3H), 1.83-1.73 (m, 2H), 1.55 (s, 3H), 1.38-1.30 (m, 2H), 0.91 (t, $J = 7.4$ Hz, 3H).

$^{13}\text{C NMR}$ (125 MHz, CDCl_3) δ 153.99 (e), 141.19 (o), 114.06 (e), 84.70 (e), 54.09 (o), 42.16 (e), 23.06 (o), 16.94 (e), 14.34 (o).

IR (Neat) 2961 (w), 1746 (s), 1646 (w), 1440 (m), 1251 (vs), 732 (m) cm^{-1} .

HRMS (ESI[M+NH₄]⁺) calcd for C₉H₂₀NO₃ 190.1443, found 190.1438.



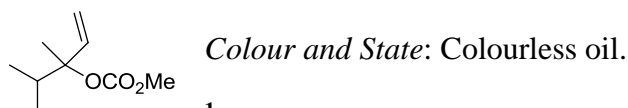
¹H NMR (500 MHz, CDCl₃) δ 5.99 (dd, $J = 17.5, 11.0$ Hz, 1H), 5.80 (ddt, $J = 17.0, 10.3, 6.6$ Hz, 1H), 5.21 (d, $J = 17.5$ Hz, 1H), 5.19 (d, $J = 11.0$ Hz, 1H), 5.02 (dq, $J = 17.1, 1.6$ Hz, 1H), 4.96-4.94 (m, 1H), 3.72 (s, 3H), 2.11-2.05 (m, 2H), 1.97-1.84 (m, 2H), 1.58 (s, 3H).

¹³C NMR (125 MHz, CDCl₃) δ 153.70 (e), 140.75 (o), 137.80 (o), 114.58 (e), 114.07 (e), 83.94 (e), 53.87 (o), 38.83 (e), 27.77 (e), 22.96 (o).

IR (Neat) 3080 (w), 2956 (w), 1746 (s), 1642 (w), 1268 (vs), 915 (m), 690 (w) cm^{-1} .

HRMS (ESI[M+NH₄]⁺) calcd for C₁₀H₂₀NO₃ 202.1438, found 202.1434.

3,4-Dimethylpent-1-en-3-yl methyl carbonate (26e)



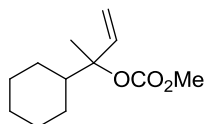
¹H NMR (500 MHz, CDCl₃) δ 5.96 (dd, $J = 17.6, 11.1$ Hz, 1H), 5.24 (dd, $J = 11.1, 0.7$ Hz, 1H), 5.18 (d, $J = 17.6, 0.5$ Hz, 1H), 3.71 (s, 3H), 2.12 (septet, $J = 6.9$ Hz, 1H), 1.54 (s, 3H), 0.93 (d, $J = 6.8$ Hz, 3H), 0.89 (d, $J = 6.9$ Hz, 3H).

¹³C NMR (125 MHz, CDCl₃) δ 153.98 (e), 139.41 (o), 115.18 (e), 87.42 (e), 53.99 (o), 36.43 (o), 18.63 (o), 17.18 (o), 16.94 (o).

IR (Neat) 2969 (w), 1745 (s), 1645 (w), 1440 (m), 1261 (vs), 943 (m), 667 (w) cm^{-1} .

HRMS (ESI[M+NH₄]⁺) calcd for C₉H₂₀NO₃ 190.1443, found 190.1436.

2-Cyclohexylbut-3-en-2-yl methyl carbonate (26f)



Colour and State: Colourless oil.

$^1\text{H NMR}$ (500 MHz, CDCl_3) δ 5.95 (dd, $J = 17.6, 11.1$ Hz, 1H),

5.22 (d, $J = 11.1$ Hz, 1H), 5.15 (d, $J = 17.6$ Hz, 1H), 3.71 (s, 3H), 1.81-1.73 (m, 5H),

1.67-1.64 (m, 1H), 1.54 (s, 3H), 1.28-0.87 (m, 5H).

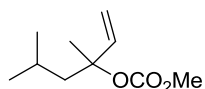
$^{13}\text{C NMR}$ (125 MHz, CDCl_3) δ 154.00 (e), 139.97 (o), 114.93 (e), 87.36 (e), 54.04

(o), 46.73 (o), 27.27 (e), 27.08 (e), 26.48 (e), 19.23 (o).

IR (Neat) 2992 (w), 2931 (m), 1745 (s), 1644 (w), 1414 (m), 1257 (vs) 791 (m) cm^{-1} .

HRMS (ESI $[\text{M}+\text{Na}]^+$) calcd for $\text{C}_{12}\text{H}_{20}\text{NaO}_3$ 235.1310, found 235.1308.

3,5-Dimethylhex-1-en-3-yl methyl carbonate (26g)



Colour and State: Colourless oil.

$^1\text{H NMR}$ (500 MHz, CDCl_3) δ 6.00 (dd, $J = 17.6, 11.0$ Hz, 1H), 5.21 (d, $J = 17.5$ Hz,

1H), 5.15 (d, $J = 11.0$ Hz, 1H), 3.71 (s, 3H), 1.83-1.75 (m, 2H), 1.73-1.67 (m, 1H),

1.58 (s, 3H), 0.93 (d, $J = 6.5$ Hz, 3H), 0.93 (d, $J = 6.4$ Hz, 3H).

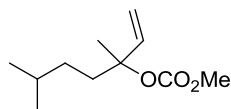
$^{13}\text{C NMR}$ (125 MHz, CDCl_3) δ 153.89 (e), 141.66 (o), 113.56 (e), 84.86 (e), 53.95

(o), 47.87 (e), 24.22 (o), 24.10 (o), 23.92 (o).

IR (Neat) 2957 (m), 1746 (s), 1647 (w), 1253 (vs), 1168 (m), 734 (w) cm^{-1} .

HRMS (ESI $[\text{M}+\text{NH}_4]^+$) calcd for $\text{C}_{10}\text{H}_{22}\text{NO}_3$ 204.1600, found 204.1592.

3,6-Dimethylhept-1-en-3-yl methyl carbonate (26h)



Colour and State: Colourless oil.

$^1\text{H NMR}$ (500 MHz, CDCl_3) δ 5.98 (dd, $J = 17.5, 11.0$ Hz, 1H),

5.20 (d, $J = 17.5$ Hz, 1H), 5.17 (d, $J = 11.0$ Hz, 1H), 3.72 (s, 3H), 1.86-1.74 (m, 2H),

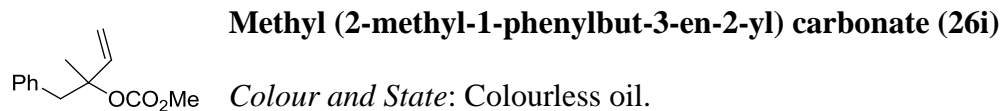
1.56 (s, 3H), 1.54-1.45 (m, 1H), 1.22-1.17 (m, 2H), 0.88 (d, $J = 6.6$ Hz, 6H).

$^{13}\text{C NMR}$ (125 MHz, CDCl_3) δ 153.98 (e), 141.19 (o), 114.20 (e), 84.85 (e), 54.14

(o), 37.91 (e), 32.49 (e), 28.35 (o), 23.02 (o), 22.64 (o).

IR (Neat) 2956 (w), 1746 (s), 1647 (w), 1440 (m), 1269 (vs), 993 (w), 924 (m), 678 (w) cm^{-1} .

HRMS (ESI[M+NH₄]⁺) calcd for C₁₁H₂₄NO₃ 218.1751, found 218.1747.

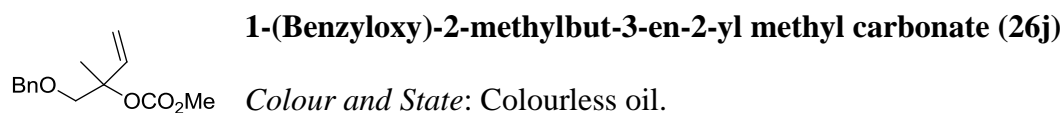


¹H NMR (500 MHz, CDCl₃) δ 7.30-7.22 (m, 3H), 7.20-7.18 (m, 2H), 6.03 (dd, $J = 17.5, 11.0$ Hz, 1H), 5.20 (d, $J = 11.0$ Hz, 1H), 5.17 (d, $J = 17.5$ Hz, 1H), 3.73 (s, 3H), 3.17 (d, A of AB, $J_{AB} = 13.6$ Hz, 1H), 3.05 (d, B of AB, $J_{AB} = 13.6$ Hz, 1H), 1.55 (s, 3H).

¹³C NMR (125 MHz, CDCl₃) δ 154.06 (e), 140.82 (o), 136.13 (e), 130.96 (o), 128.07 (o), 126.81 (o), 114.79 (e), 84.19 (e), 54.26 (o), 46.18 (e), 22.88 (o).

IR (Neat) 3031 (w), 2851 (w), 1743 (s), 1644 (w), 1264 (vs), 701 (m) cm^{-1} .

HRMS (ESI[M+Na]⁺) calcd for C₁₃H₁₆NaO₃ 243.0997, found 243.1005.



¹H NMR (500 MHz, CDCl₃) δ 7.36-7.27 (m, 5H), 6.06 (dd, $J = 17.6, 11.0$ Hz, 1H), 5.28 (d, $J = 17.6$ Hz, 1H), 5.24 (d, $J = 11.0$ Hz, 1H), 4.61 (d, A of AB, $J_{AB} = 12.3$ Hz, 1H), 4.56 (d, B of AB, $J_{AB} = 12.3$ Hz, 1H), 3.72 (s, 3H), 3.67 (d, A of AB, $J_{AB} = 10.0$ Hz, 1H), 3.57 (d, B of AB, $J_{AB} = 10.0$ Hz, 1H), 1.62 (s, 3H).

¹³C NMR (125 MHz, CDCl₃) δ 153.94 (e), 138.60 (o), 138.15 (e), 128.46 (o), 127.74 (o), 127.70 (o), 115.81 (e), 83.48 (e), 74.75 (e), 73.58 (e), 54.27 (o), 20.91 (o).

IR (Neat) 3030 (w), 2955 (w), 1745 (s), 1440 (m), 1262 (vs), 931 (m), 698 (m) cm^{-1} .

HRMS (ESI[M+Na]⁺) calcd for C₁₄H₁₈NaO₄ 273.1103, found 273.1099.



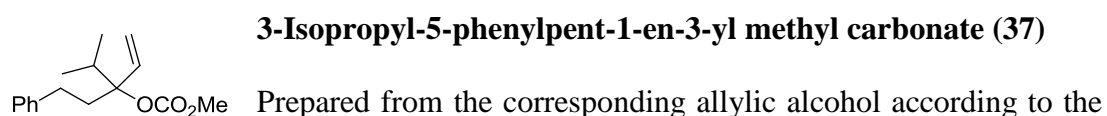
Colour and State: Colourless oil.

¹H NMR (500 MHz, CDCl₃) δ 7.36-7.27 (m, 5H), 6.01 (dd, *J* = 17.5, 11.0 Hz, 1H), 5.22 (d, *J* = 17.5 Hz, 1H), 5.18 (d, *J* = 11.0 Hz, 1H), 4.49 (d, A of AB, *J*_{AB} = 12.0 Hz, 1H), 4.46 (d, B of AB, *J*_{AB} = 12.0 Hz, 1H), 3.68 (s, 3H), 3.62-3.55 (m, 2H), 2.26-2.16 (m, 2H), 1.61 (s, 3H).

¹³C NMR (125 MHz, CDCl₃) δ 153.90 (e), 140.90 (o), 138.44 (e), 128.47 (o), 127.74 (o), 127.67 (o), 114.40 (e), 83.53 (e), 73.14 (e), 66.09 (e), 54.21 (o), 39.10 (e), 23.92 (o).

IR (Neat) 2954 (w), 1746 (s), 1440 (m), 1268 (s), 1098 (m), 792 (m) cm⁻¹.

HRMS (EI[M+NH₄]⁺) calcd for C₁₅H₂₄NO₄ 282.1700, found 282.1699.



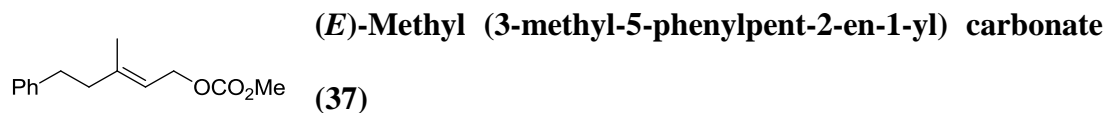
Colour and State: Colourless oil.

¹H NMR (500 MHz, CDCl₃) δ 7.30-7.26 (m, 2H), 7.19-7.16 (m, 3H), 5.80 (dd, *J* = 17.5, 11.3 Hz, 1H), 5.32 (dd, *J* = 11.3, 1.1 Hz, 1H), 5.26 (dd, *J* = 17.5, 1.2 Hz, 1H), 3.75 (s, 3H), 2.63-2.51 (m, 3H), 2.50 (ddd, *J* = 14.0, 12.4, 5.0 Hz, 1H), 2.21 (ddd, *J* = 13.9, 11.9, 4.8 Hz, 1H), 0.90 (d, *J* = 6.7 Hz, 3H), 0.90 (d, *J* = 7.0 Hz, 3H).

¹³C NMR (125 MHz, CDCl₃) δ 153.76 (e), 142.18 (e), 136.15 (o), 128.55 (o), 128.51 (o), 125.96 (o), 116.08 (e), 89.99 (e), 54.33 (o), 35.50 (e), 33.46 (o), 29.65 (e), 17.57 (o), 16.89 (o).

IR (Neat) 3027 (w), 2879 (w), 1743 (s), 1643 (w), 1440 (m), 1261 (vs), 942 (m), 699 (m) cm^{-1} .

HRMS (ESI[M+Na]⁺) calcd for C₁₆H₂₂NaO₃ 285.1467, found 285.1470.



Prepared in three steps from benzylacetone according to the procedure reported by Hoveyda.² All spectral data matched the published values.

Colour and State: Colourless oil.

¹H NMR (500 MHz, CDCl₃) δ 7.30-7.26 (m, 2H), 7.19-7.16 (m, 3H), 5.39 (t, $J = 7.1$ Hz, 1H), 4.65 (d, $J = 7.2$ Hz, 2H), 3.78 (s, 3H), 2.73 (t, $J = 8.1$ Hz, 2H), 2.33 (d, $J = 8.1$ Hz, 2H), 1.77 (s, 3H).

¹³C NMR (125 MHz, CDCl₃) δ 155.97 (e), 142.70 (e), 141.87 (e), 128.43 (o), 125.98 (o), 118.38 (o), 64.71 (e), 54.75 (o), 41.44 (e), 34.30 (e), 16.76 (o).

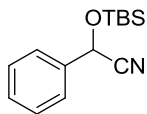
IR (Neat) 2954 (w), 1744 (s), 1670 (s), 1442 (m), 1257 (vs), 938 (m), 700 (m) cm^{-1} .

3.2.1.3. Representative Experimental Procedure for the Synthesis of Aryl Cyanohydrins **24a-i**³

To a stirring mixture of *tert*-butyldimethylsilyl cyanide (2.83 g, 20.0 mmol) and benzaldehyde (2.12 g, 20.0 mmol), under an atmosphere of argon, was added solid lithium chloride (42.0 mg, 1.00 mmol). The mixture was stirred for *ca.* 5 hours and diluted with hexane. Purification by flash column chromatography (eluting with 2-4% diethyl ether/hexane) afforded the cyanohydrin **24a** (4.50 g, 91%) as a colourless oil.

3.2.1.4. Spectral Data for the Aryl Cyanohydrins 24a-i

2-((*tert*-Butyldimethylsilyloxy)-2-phenylacetonitrile (24a)



Colour and State: Colourless oil.

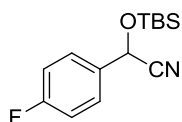
All spectral data matched the published values.³

¹H NMR (500 MHz, CDCl₃) δ 7.48-7.46 (m, 2H), 7.44-7.37 (m, 3H), 5.52 (s, 1H), 0.94 (s, 9H), 0.23 (s, 3H), 0.15 (s, 3H).

¹³C NMR (125 MHz, CDCl₃) 136.58 (e), 129.32 (o), 128.99 (o), 126.18 (e), 119.38 (e), 64.07 (o), 25.63 (o), 18.24 (e), -5.00 (o), -5.10 (o).

IR (Neat) 2956 (w), 2887 (w), 1495 (w), 1255 (m), 1071 (m), 839 (s), 675 (w) cm⁻¹.

2-((*tert*-Butyldimethylsilyloxy)-2-(4-fluorophenyl)acetonitrile



(24b)

Colour and State: Colourless oil.

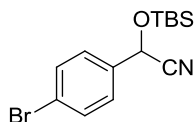
¹H NMR (500 MHz, CDCl₃) δ 7.47-7.44 (m, 2H), 7.13-7.08 (m, 2H), 5.49 (s, 1H), 0.94 (s, 9H), 0.23 (s, 3H), 0.15 (s, 3H).

¹³C NMR (125 MHz, CDCl₃) δ 163.10 (e, d, ¹J_{C-F} = 248.5 Hz), 132.61 (e, d, ⁴J_{C-F} = 3.3 Hz), 128.07 (o, d, ³J_{C-F} = 8.4 Hz), 119.14 (e), 115.91 (o, d, ²J_{C-F} = 21.8 Hz), 63.36 (o), 25.51 (o), 18.13 (e), -5.14 (o), -5.24 (o).

IR (Neat) 2956 (w), 2860 (w), 1606 (m), 1509 (s), 1088 (s), 836 (vs), 711 (w) cm⁻¹.

HRMS (ESI[M+NH₄]⁺) calcd for C₁₄H₂₄FN₂OSi 283.1636, found 283.1630.

2-(4-Bromophenyl)-2-((*tert*-butyldimethylsilyloxy)acetonitrile



(24c)

Colour and State: Colourless oil.

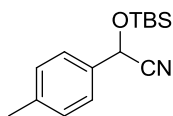
All spectral data matched the published values.⁴

¹H NMR (500 MHz, CDCl₃) δ 7.56-7.24 (m, 2H), 7.35 (d, *J* = 8.5 Hz, 2H), 5.46 (s, 1H), 0.93 (s, 9H), 0.23 (s, 3H), 0.15 (s, 3H).

¹³C NMR (125 MHz, CDCl₃) δ 135.62 (e), 132.10 (o), 127.77 (o), 123.36 (e), 118.85 (e), 63.39 (o), 25.53 (e), 18.14 (e), -5.06 (o), -5.18 (o).

IR (neat) 2955 (w), 2931 (w), 1593 (w), 1472 (w), 1256 (m), 1092 (m), 839 (s), 705 (w) cm⁻¹.

2-((*tert*-Butyldimethylsilyl)oxy)-2-(*p*-tolyl)acetonitrile (24d)



Colour and State: Colourless oil.

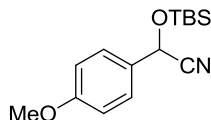
¹H NMR (500 MHz, CDCl₃) δ 7.35 (d, *J* = 8.0 Hz, 2H), 7.21 (d, *J* = 8.0 Hz, 2H), 5.47 (s, 1H), 2.37 (s, 3H), 0.93 (s, 9H), 0.21 (s, 3H), 0.13 (s, 3H).

¹³C NMR (125 MHz, CDCl₃) δ 139.20 (e), 133.75 (e), 129.61 (o), 126.19 (o), 119.45 (e), 63.97 (o), 25.60 (o), 21.22 (o), 18.20 (e), -5.03 (o), -5.10 (o).

IR (neat) 2956 (m), 2887 (w), 2859 (m), 1615 (w), 1255 (m), 1088 (s), 837 (vs) cm⁻¹.

HRMS (ESI[M+NH₄]⁺) calcd for C₁₅H₂₇N₂OSi 279.1887, found 279.1885.

2-((*tert*-Butyldimethylsilyl)oxy)-2-(4-



methoxyphenyl)acetonitrile (24e)

Colour and State: Colourless oil.

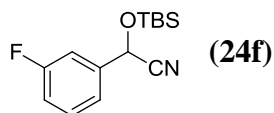
¹H NMR (500 MHz, CDCl₃) δ 7.40-7.37 (m, 2H), 6.94-6.91 (m, 2H), 5.45 (s, 1H), 3.83 (s, 3H), 0.92 (s, 9H), 0.21 (s, 3H), 0.13 (s, 3H).

¹³C NMR (125 MHz, CDCl₃) δ 160.38 (e), 128.83 (e), 127.77 (e), 119.58 (e), 114.36 (o), 63.82 (o), 55.44 (o), 25.65 (o), 18.26 (e), -4.95 (o), -5.01 (o).

IR (neat) 2932 (m), 2859 (w), 1612 (m), 1512 (s), 1363 (w), 1250 (s), 836 (vs) cm⁻¹.

HRMS (ESI[M+NH₄]⁺) calcd for C₁₅H₂₇N₂O₂Si 295.1836, found 295.1839.

2-((*tert*-Butyldimethylsilyl)oxy)-2-(3-fluorophenyl)acetonitrile



Colour and State: Colourless oil.

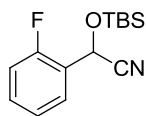
¹H NMR (500 MHz, CDCl₃) δ 7.39 (dt, *J* = 8.0, 5.7 Hz, 1H), 7.24 (d, *J* = 7.7 Hz, 1H), 7.21-7.19 (m, 1H), 7.09 (dt, *J* = 8.4, 2.4 Hz, 1H), 5.51 (s, 1H), 0.95 (s, 9H), 0.25 (s, 3H), 0.17 (s, 3H).

¹³C NMR (125 MHz, CDCl₃) δ 163.07 (e, d, ¹*J*_{C-F} = 247.6 Hz), 139.01 (e, d, ³*J*_{C-F} = 7.2 Hz), 130.71 (o, d, ³*J*_{C-F} = 8.1 Hz), 121.71 (o, d, ⁴*J*_{C-F} = 3.3 Hz), 118.94 (e), 116.38 (o, d, ²*J*_{C-F} = 21.2 Hz), 113.33 (o, d, ²*J*_{C-F} = 23.2 Hz), 63.39 (o, d, ⁴*J*_{C-F} = 1.6 Hz), 25.95 (o), 18.29 (e), -5.00 (o), -5.13 (o).

IR (Neat) 2956 (m), 2860 (m), 1616 (w), 1596 (m), 1257 (m), 840 (s), 676 (m) cm⁻¹.

HRMS (ESI[M+Na]⁺) calcd for C₁₄H₂₀FNNaOSi 288.1196, found 288.1198.

2-((*tert*-Butyldimethylsilyl)oxy)-2-(2-fluorophenyl)acetonitrile (24g)



Colour and State: Colourless oil.

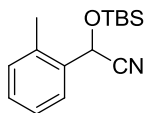
¹H NMR (500 MHz, CDCl₃) δ 7.64 (dt, *J* = 7.5, 1.2 Hz, 1H), 7.42-7.37 (m, 1H), 7.24 (t, *J* = 7.6 Hz, 1H), 7.10 (t, *J* = 9.2 Hz, 1H), 5.76 (s, 1H), 0.93 (s, 9H), 0.25 (s, 3H), 0.14 (s, 3H).

¹³C NMR (125 MHz, CDCl₃) δ 159.44 (e, d, ¹*J*_{C-F} = 248.9 Hz), 131.32 (o, d, ³*J*_{C-F} = 8.2 Hz), 128.27 (o, d, ⁴*J*_{C-F} = 2.7 Hz), 124.90 (o, d, ³*J*_{C-F} = 3.6 Hz), 124.12 (e, d, ²*J*_{C-F} = 13.0 Hz), 118.50 (e), 115.77 (o, d, ²*J*_{C-F} = 20.5 Hz), 58.18 (o, d, ³*J*_{C-F} = 5.2 Hz), 25.59 (o), 18.25 (e), -5.13 (o), -5.24 (o).

IR (Neat) 2956 (m), 2887 (w), 1617 (w), 1592 (m), 1083 (s), 674 (m) cm⁻¹.

HRMS (ESI[M+Na]⁺) calcd for C₁₄H₂₀FNNaOSi 288.1196, found 288.1200.

2-((*tert*-Butyldimethylsilyl)oxy)-2-(*o*-tolyl)acetonitrile (**24h**)



Colour and State: Colourless oil.

¹H NMR (500 MHz, CDCl₃) δ 7.50-7.49 (m, 1H), 7.31-7.24 (m, 2H), 7.20 (d, *J* = 7.4 Hz, 1H), 5.55 (s, 1H), 2.44 (s, 3H), 0.93 (s, 9H), 0.21 (s, 3H), 0.12 (s, 3H).

¹³C NMR (125 MHz, CDCl₃) δ 135.65 (e), 134.52 (e), 131.22 (o), 129.43 (o), 126.97 (o), 126.58 (o), 118.96 (o), 62.53 (o), 25.66 (o), 18.94 (o), 18.29 (e), -4.98 (o), -5.04 (o).

IR (Neat) 2931 (m), 1607 (w), 1463 (m), 1255 (m), 1083 (s), 837 (vs), 675 (w) cm⁻¹.

HRMS (ESI[M+Na]⁺) calcd for C₁₅H₂₃NNaOSi 284.1447, found 284.1442.

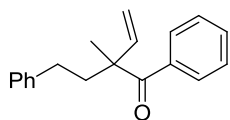
3.2.1.5. Representative Experimental Procedure for the Rhodium-Catalysed Allylic Substitution with the Aryl Cyanohydrins **24**

Under an atmosphere of argon, a 1M solution of lithium bis(trimethylsilyl)amide in tetrahydrofuran (0.90 mL, 0.90 mmol) was added dropwise to a solution of 2-((*tert*-butyldimethylsilyl)oxy)-2-phenylacetonitrile **24a** (161.0 mg, 0.65 mmol) in anhydrous THF (3 mL) at -10 °C. The anion was allowed to form over *ca.* 30 minutes, resulting in a light yellow homogeneous solution. In a separate flask, [RhCl(COD)]₂ (6.20 mg, 0.013 mmol) and tris(2,4-di-*tert*-butylphenyl) phosphite (32.3 mg, 0.050 mmol) were dissolved in anhydrous THF (2 mL) under an atmosphere of argon at room temperature. The mixture was stirred for *ca.* 5 minutes, resulting in a light yellow homogeneous solution, and then cooled to -10 °C. The catalyst solution was then added to the anion *via* Teflon[®] cannula, followed immediately by the addition of methyl (3-methyl-5-phenylpent-1-en-3-yl) carbonate **26a** (117.0 mg, 0.50 mmol) *via* tared 500 μL gastight syringe. The mixture was allowed to stir for *ca.* 16 hours and a 1M solution of TBAF in tetrahydrofuran (1.25

mL, 1.25 mmol) was added. The resultant mixture was warmed to room temperature, allowed to stir for *ca.* 1 hour and partitioned between diethyl ether and saturated aqueous ammonium chloride solution. The combined organic layers were dried using anhydrous magnesium sulfate, filtered and concentrated *in vacuo*. Purification by flash column chromatography (eluting with 1-2% diethyl ether/hexane) afforded the ketone **29a** (114.0 mg, 86%) as a colourless oil.

3.2.1.6. Spectral Data for the Aryl Ketone Products 29a-o

2-Methyl-2-phenethyl-1-phenylbut-3-en-1-one (29a)



Colour and State: Colourless oil. *Branched:linear* \geq 19:1.

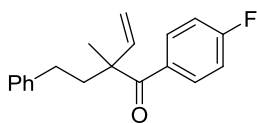
$^1\text{H NMR}$ (500 MHz, CDCl_3) δ 7.89-7.87 (m, 2H), 7.51-7.48 (m, 1H), 7.40 (t, $J = 7.7$ Hz, 1H), 7.23 (t, $J = 7.4$ Hz, 2H), 7.15 (t, $J = 7.4$ Hz, 1H), 7.05 (d, $J = 7.1$ Hz, 2H), 6.21 (dd, $J = 17.6, 10.8$ Hz, 1H), 5.29 (d, $J = 11.0$ Hz, 1H), 5.26 (d, $J = 17.8$ Hz, 1H), 2.59 (dt, $J = 13.0, 4.8$ Hz, 1H), 2.39 (dt, $J = 13.1, 4.5$ Hz, 1H), 2.21 (dt, $J = 13.1, 4.5$ Hz, 1H), 2.05 (dt, $J = 13.2, 4.8$ Hz, 1H), 1.47 (s, 3H).

$^{13}\text{C NMR}$ (125 MHz, CDCl_3) δ 204.48 (e), 142.94 (o), 142.36 (e), 137.74 (e), 131.76 (o), 129.10 (o), 128.45 (o), 128.39 (o), 128.12 (o), 125.91 (o), 115.21 (e), 53.76 (e), 41.37 (e), 30.92 (e), 23.06 (o).

IR (Neat) 3062 (w), 2954 (m), 1677 (vs), 1631 (m), 1497 (m), 1244 (s), 1002 (m), 698 (s) cm^{-1} .

HRMS (ESI[M+H]⁺) calcd for $\text{C}_{19}\text{H}_{21}\text{O}$ 265.1587, found 265.1590.

1-(4-Fluorophenyl)-2-methyl-2-phenethylbut-3-en-1-one



(29b)

Colour and State: Colourless oil. *Branched:linear* \geq 19:1.

$^1\text{H NMR}$ (500 MHz, CDCl_3) δ 7.98-7.94 (m, 2H), 7.24 (t, $J = 7.5$ Hz, 2H), 7.16 (t, $J = 7.4$ Hz, 1H), 7.09-7.05 (m, 4H), 6.20 (dd, $J = 17.6, 10.7$ Hz, 1H), 5.30 (d, $J = 10.7$

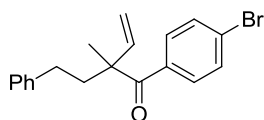
Hz, 1H), 5.26 (d, $J = 17.7$ Hz, 1H), 2.59 (dt, $J = 12.9, 4.8$ Hz, 1H), 2.37 (dt, $J = 13.0, 4.6$ Hz, 1H), 2.19 (dt, $J = 13.1, 4.6$ Hz, 1H), 2.06 (dt, $J = 13.2, 4.9$ Hz, 1H), 1.46 (s, 3H).

^{13}C NMR (125 MHz, CDCl_3) δ 202.48 (e), 164.84 (e, d, $^1J_{\text{C-F}} = 253.7$ Hz), 142.93 (o), 142.24 (e), 133.55 (e, d, $^4J_{\text{C-F}} = 3.4$ Hz), 131.98 (o, d, $^3J_{\text{C-F}} = 8.7$ Hz), 128.49 (o), 128.38 (o), 125.97 (o), 115.37 (e), 115.18 (o, d, $^2J_{\text{C-F}} = 21.7$ Hz), 53.62 (e), 41.35 (e), 30.87 (e), 23.23 (o).

IR (Neat) 3027 (w), 2934 (w), 1676 (s), 1632 (m), 1598 (s), 1297 (w), 1232 (s), 976 (m), 768 (m) cm^{-1} .

HRMS (ESI[M+Na] $^+$) calcd for $\text{C}_{19}\text{H}_{19}\text{FNaO}$ 305.1318, found 305.1308.

1-(4-Bromophenyl)-2-methyl-2-phenethylbut-3-en-1-one



(29c)

Colour and State: Colourless oil. *Branched:linear* $\geq 19:1$.

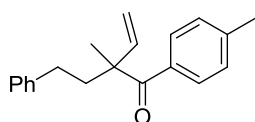
^1H NMR (500 MHz, CDCl_3) δ 7.79-7.76 (m, 2H), 7.55-7.52 (m, 2H), 7.25 (t, $J = 7.4$ Hz, 2H), 7.18-7.15 (m, 1H), 7.07 (d, $J = 7.1$ Hz, 2H), 6.18 (dd, $J = 17.6, 10.7$ Hz, 1H), 5.30 (d, $J = 10.7$ Hz, 1H), 5.25 (d, $J = 17.6$ Hz, 1H), 2.59 (dt, $J = 12.9, 4.8$ Hz, 1H), 2.37 (dt, $J = 13.0, 4.7$ Hz, 1H), 2.17 (dt, $J = 13.1, 4.7$ Hz, 1H), 2.05 (dt, $J = 13.2, 4.9$ Hz, 1H), 1.45 (s, 3H).

^{13}C NMR (125 MHz, CDCl_3) δ 203.28 (e), 142.68 (o), 142.18 (e), 136.10 (e), 131.44 (o), 130.91 (o), 128.54 (o), 128.41 (o), 126.87 (e), 126.03 (o), 53.73 (e), 41.24 (e), 30.86 (e), 23.08 (o).

IR (Neat) 3085 (w), 2932 (w), 1677 (s), 1631 (m), 1603 (w), 1583 (s), 1244 (m), 1031 (w), 698 (s) cm^{-1} .

HRMS (ESI[M+Na] $^+$) calcd for $\text{C}_{19}\text{H}_{19}^{79}\text{BrNaO}$ 365.0517, found 365.0510.

2-Methyl-2-phenethyl-1-(*p*-tolyl)but-3-en-1-one (29d)



Colour and State: Colourless oil. *Branched:linear* \geq 19:1.

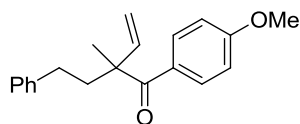
$^1\text{H NMR}$ (500 MHz, CDCl_3) δ 7.82 (d, $J = 8.2$ Hz, 2H), 7.24 (t, $J = 7.5$ Hz, 2H), 7.19 (d, $J = 8.1$ Hz, 2H), 7.15 (t, $J = 7.3$ Hz, 1H), 7.06 (d, $J = 7.3$ Hz, 2H), 6.22 (dd, $J = 17.6, 10.8$ Hz, 1H), 5.27 (d, $J = 10.6$ Hz, 1H), 5.24 (d, $J = 17.5$ Hz, 1H), 2.59 (dt, $J = 13.0, 4.8$ Hz, 1H), 2.42-2.36 (m, 4H), 2.21 (dt, $J = 13.1, 4.6$ Hz, 1H), 2.06 (dt, $J = 13.2, 4.8$ Hz, 1H), 1.46 (s, 3H).

$^{13}\text{C NMR}$ (125 MHz, CDCl_3) δ 203.75 (e), 143.21 (o), 142.47 (e), 142.44 (e), 134.76 (e), 129.46 (o), 128.78 (o), 128.43 (o), 128.40 (o), 125.87 (o), 114.96 (e), 53.61 (e), 41.47 (e), 30.91 (e), 23.28 (o), 21.60 (o).

IR (Neat) 3027 (w), 2924 (m), 1673 (s), 1631 (m), 1606 (m), 1570 (w), 1410 (w), 1247 (m), 967 (m), 699 (s) cm^{-1} .

HRMS (ESI[$\text{M}+\text{Na}$] $^+$) calcd for $\text{C}_{20}\text{H}_{22}\text{NaO}$ 301.1568, found 301.1563.

1-(4-Methoxyphenyl)-2-methyl-2-phenethylbut-3-en-1-one (29e)



Colour and State: Pale yellow oil. *Branched:linear* \geq 19:1.

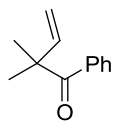
$^1\text{H NMR}$ (500 MHz, CDCl_3) δ 7.99-7.96 (m, 2H), 7.24 (t, $J = 7.5$ Hz, 2H), 7.15 (t, $J = 7.3$ Hz, 1H), 7.07 (d, $J = 7.1$ Hz, 2H), 6.90-6.87 (m, 2H), 6.23 (dd, $J = 17.6, 10.8$ Hz, 1H), 5.28-5.22 (m, 2H), 3.86 (s, 3H), 2.60 (dt, $J = 13.0, 4.8$ Hz, 1H), 2.38 (dt, $J = 13.0, 4.6$ Hz, 1H), 2.21 (dt, $J = 13.1, 4.6$ Hz, 1H), 2.07 (dt, $J = 13.2, 4.8$ Hz, 1H), 1.46 (s, 3H).

$^{13}\text{C NMR}$ (125 MHz, CDCl_3) δ 202.16 (e), 162.57 (e), 143.53 (o), 142.53 (e), 131.89 (o), 129.77 (e), 128.44 (o), 128.42 (o), 125.87 (o), 114.75 (e), 113.28 (o), 55.47 (o), 53.42 (e), 41.58 (e), 30.92 (o), 23.59 (o).

IR (Neat) 2933 (w), 2839 (w), 1667 (s), 1631 (w), 1599 (vs), 1306 (m), 1246 (vs), 919 (m), 791 (w) cm^{-1} .

HRMS (ESI[M+Na]⁺) calcd for $\text{C}_{20}\text{H}_{22}\text{NaO}_2$ 317.1517, found 317.1502.

2,2-Dimethyl-1-phenylbut-3-en-1-one (29f)



Colour and State: Colourless oil. *Branched:linear* \geq 19:1.

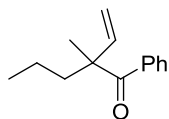
All spectral data matched the published values.⁵

¹H NMR (500 MHz, CDCl_3) δ 7.88-7.86 (m, 2H), 7.46 (tt, $J = 7.4, 1.4$ Hz, 1H), 7.39-7.36 (m, 2H), 6.19 (dd, $J = 17.6, 10.6$ Hz, 1H), 5.24 (d, $J = 17.8$ Hz, 1H), 5.21 (d, $J = 10.8$ Hz, 1H), 1.39 (s, 6H).

¹³C NMR (125 MHz, CDCl_3) δ 204.77 (e), 143.99 (o), 137.22 (e), 131.78 (o), 129.40 (o), 128.06 (o), 114.19 (e), 50.28 (e), 26.18 (o).

IR (Neat) 3059 (w), 2873 (w), 1677 (s), 1635 (s), 1446 (w), 1256 (m), 971 (s), 718 (m) cm^{-1} .

2-Methyl-1-phenyl-2-vinylpentan-1-one (29g)



Colour and State: Colourless oil. *Branched:linear* \geq 19:1.

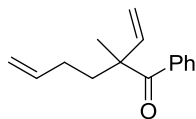
¹H NMR (500 MHz, CDCl_3) δ 7.84-7.83 (m, 2H), 7.47-7.44 (m, 1H), 7.38-7.35 (m, 2H), 6.16 (dd, $J = 17.6, 10.8$ Hz, 1H), 5.23 (d, $J = 11.0$ Hz, 1H), 5.20 (d, $J = 17.8$ Hz, 1H), 1.88 (dt, $J = 12.9, 4.5$ Hz, 1H), 1.72 (dt, $J = 13.0, 4.4$ Hz, 1H), 1.36 (s, 3H), 1.34-1.26 (m, 1H), 1.15-1.05 (m, 1H), 0.85 (t, $J = 7.3$ Hz, 3H).

¹³C NMR (125 MHz, CDCl_3) δ 204.81 (e), 143.36 (o), 137.83 (e), 131.51 (o), 128.99 (o), 127.96 (o), 114.65 (e), 53.76 (e), 41.31 (e), 22.93 (o), 17.59 (e), 14.75 (o).

IR (Neat) 2960 (m), 1677 (s), 1631 (w), 1446 (m), 1223 (m), 966 (m), 670 (w) cm^{-1} .

HRMS (ESI[M+H]⁺) calcd for $\text{C}_{14}\text{H}_{19}\text{O}$ 203.1430, found 203.1425.

2-Methyl-1-phenyl-2-vinylhex-5-en-1-one (29h)



Colour and State: Colourless oil. *Branched:linear* \geq 19:1.

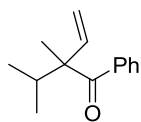
$^1\text{H NMR}$ (500 MHz, CDCl_3) δ 7.84 -7.82 (m, 2H), 7.46 (t, $J = 7.4$ Hz, 1H), 7.37 (t, $J = 7.7$ Hz, 2H), 6.16 (dd, $J = 17.6, 10.7$ Hz, 1H), 5.79-5.71 (m, 1H), 5.26 (d, $J = 10.7$ Hz, 1H), 5.22 (d, $J = 17.6$ Hz, 1H), 4.96 (dd, $J = 17.1, 1.4$ Hz, 1H), 4.91 (d, $J = 10.2$ Hz, 1H), 2.08-1.95 (m, 2H), 1.92-1.82 (m, 2H), 1.39 (s, 3H).

$^{13}\text{C NMR}$ (125 MHz, CDCl_3) δ 204.49 (e), 142.91 (o), 138.50 (o), 137.68 (e), 131.63 (o), 129.03 (o), 128.01 (o), 115.04 (e), 114.61 (e), 53.44 (e), 38.21 (e), 28.69 (e), 22.80 (o).

IR (Neat) 3079 (w), 2933 (w), 1677 (s), 1640 (m), 1597 (w), 1412 (w), 913 (s), 695 (m) cm^{-1} .

HRMS (ESI[M+H] $^+$) calcd for $\text{C}_{15}\text{H}_{19}\text{O}$ 215.1430, found 215.1431.

2-Isopropyl-2-methyl-1-phenylbut-3-en-1-one (29i)



Colour and State: Colourless oil. *Branched:linear* \geq 19:1.

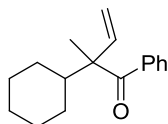
$^1\text{H NMR}$ (500 MHz, CDCl_3) δ 7.72-7.70 (m, 2H), 7.46-7.42 (m, 1H), 7.38-7.35 (m, 2H), 6.18 (dd, $J = 17.6, 10.8$ Hz, 1H), 5.28 (d, $J = 10.7$ Hz, 1H), 5.17 (d, $J = 17.7$ Hz, 1H), 2.48 (septet, $J = 6.8$ Hz, 1H), 1.26 (s, 3H), 0.90 (d, $J = 6.9$ Hz, 3H), 0.79 (d, $J = 6.7$ Hz, 3H).

$^{13}\text{C NMR}$ (125 MHz, CDCl_3) δ 206.30 (e), 141.81 (o), 138.90 (e), 131.10 (o), 128.54 (o), 128.00 (o), 116.28 (e), 57.55 (e), 33.83 (o), 17.75 (o), 17.68 (o), 16.76 (o).

IR (Neat) 3085 (w), 2965 (m), 1676 (s), 1631 (m), 1578 (w), 1445 (m), 1240 (m), 962 (m), 696 (m) cm^{-1} .

HRMS (ESI[M+H] $^+$) calcd for $\text{C}_{14}\text{H}_{19}\text{O}$ 203.1430, found 203.1429.

2-Cyclohexyl-2-methyl-1-phenylbut-3-en-1-one (29j)



Colour and State: Colourless oil. *Branched:linear* \geq 19:1.

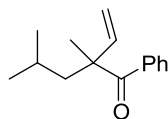
$^1\text{H NMR}$ (500 MHz, CDCl_3) δ 7.68-7.66 (m, 2H), 7.45-7.42 (m, 1H), 7.38-7.35 (m, 2H), 6.17 (dd, $J = 17.6, 10.8$ Hz, 1H), 5.25 (d, $J = 10.7$ Hz, 1H), 5.13 (d, $J = 17.6$ Hz, 1H), 2.10 (tt, $J = 11.9, 2.8$ Hz, 1H), 1.78-1.63 (m, 4H), 1.46-1.44 (m, 1H), 1.28 (s, 3H), 1.27-0.96 (m, 5H).

$^{13}\text{C NMR}$ (125 MHz, CDCl_3) δ 206.56 (e), 142.00 (o), 139.15 (e), 130.96 (o), 127.98 (o), 127.87 (o), 115.93 (e), 57.63 (e), 44.76 (o), 28.08 (e), 27.89 (e), 27.08 (e), 26.81 (e), 26.71 (e), 17.65 (o).

IR (Neat) 3084 (w), 2927 (s), 2853 (m), 1676 (s), 1630 (m), 1445 (m), 1231 (m), 916 (m), 835 (w), 696 (s) cm^{-1} .

HRMS (ESI[M+H]⁺) calcd for $\text{C}_{17}\text{H}_{23}\text{O}$ 243.1743, found 243.1746.

2,4-Dimethyl-1-phenyl-2-vinylpentan-1-one (29k)



Colour and State: Colourless oil. *Branched:linear* \geq 19:1.

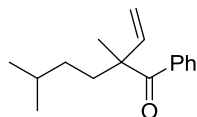
$^1\text{H NMR}$ (500 MHz, CDCl_3) δ 7.82-7.80 (m, 2H), 7.45 (tt, $J = 7.4, 1.5$ Hz, 1H), 7.38-7.35 (m, 2H), 6.18 (dd, $J = 17.6, 10.8$ Hz, 1H), 5.20 (d, $J = 10.7$ Hz, 1H), 5.19 (d, $J = 17.7$ Hz, 1H), 1.90 (dd, A of ABX, $J_{AB} = 14.0$ Hz, $J_{AX} = 6.2$ Hz, 1H), 1.77 (dd, B of ABX, $J_{AB} = 14.0$ Hz, $J_{BX} = 5.8$ Hz, 1H), 1.63 (nonet, $J = 6.5$ Hz, 1H), 1.39 (s, 3H), 0.89 (d, $J = 6.6$ Hz, 3H), 0.73 (d, $J = 6.7$ Hz, 3H).

$^{13}\text{C NMR}$ (125 MHz, CDCl_3) δ 205.45 (e), 144.02 (o), 138.05 (e), 131.51 (o), 129.24 (o), 128.01 (o), 114.59 (e), 53.88 (e), 47.87 (e), 25.02 (o), 24.90 (o), 24.20 (o), 23.53 (o).

IR (Neat) 3086 (w), 2958 (w), 1676 (s), 1630 (m), 1465 (m), 1238 (m), 961 (m), 694 (s), 657 (w) cm^{-1} .

HRMS (ESI[M+H]⁺) calcd for $\text{C}_{15}\text{H}_{21}\text{O}$ 217.1587, found 217.1590.

2,5-Dimethyl-1-phenyl-2-vinylhexan-1-one (29l)



Colour and State: Colourless oil. *Branched:linear* \geq 19:1.

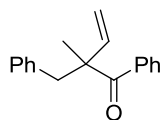
$^1\text{H NMR}$ (500 MHz, CDCl_3) δ 7.84-7.82 (m, 2H), 7.47-7.44 (m, 1H), 7.38-7.35 (m, 2H), 6.16 (dd, $J = 17.6, 10.8$ Hz, 1H), 5.24-5.18 (m, 2H), 1.91 (dt, $J = 13.0, 4.4$ Hz, 1H), 1.73 (dt, $J = 13.1, 4.5$ Hz, 1H), 1.47-1.36 (m, 1H), 1.34 (s, 3H), 1.18 (ddt, $J = 12.8, 6.5, 4.6$ Hz, 1H), 0.93 (ddt, $J = 12.8, 6.8, 4.4$ Hz, 1H), 0.82 (d, $J = 6.6$ Hz, 3H), 0.76 (d, $J = 6.6$ Hz, 3H).

$^{13}\text{C NMR}$ (125 MHz, CDCl_3) δ 205.09 (e), 143.46 (o), 137.93 (e), 131.57 (o), 129.04 (o), 128.00 (o), 114.80 (e), 53.70 (e), 36.78 (e), 33.21 (e), 28.60 (o), 22.98 (o), 22.64 (o), 22.46 (o).

IR (Neat) 2954 (m), 2869 (w), 1678 (s), 1631 (m), 1466 (m), 1213 (m), 1077 (w), 795 (m) cm^{-1} .

HRMS (EI[M+H]⁺) calcd for $\text{C}_{16}\text{H}_{22}\text{O}$ 230.1665, found 230.1666.

2-Benzyl-2-methyl-1-phenylbut-3-en-1-one (29m)



Colour and State: Pale yellow oil. *Branched:linear* \geq 19:1.

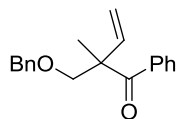
$^1\text{H NMR}$ (500 MHz, CDCl_3) δ 7.82-7.80 (m, 2H), 7.48-7.45 (m, 1H), 7.38 (t, $J = 7.7$ Hz, 2H), 7.24-7.17 (m, 3H), 7.07-7.06 (m, 2H), 6.17 (dd, $J = 17.6, 10.7$ Hz, 1H), 5.28 (d, $J = 10.8$ Hz, 1H), 5.15 (d, $J = 17.6$ Hz, 1H), 3.23 (d, A of AB, $J_{AB} = 13.4$ Hz, 1H), 3.12 (d, B of AB, $J_{AB} = 13.4$ Hz, 1H), 1.34 (s, 3H).

$^{13}\text{C NMR}$ (125 MHz, CDCl_3) δ 204.64 (e), 142.66 (o), 137.91 (e), 137.52 (e), 131.67 (o), 131.04 (o), 129.24 (o), 128.09 (o), 127.88 (o), 126.46 (o), 115.71 (e), 54.67 (e), 44.94 (e), 22.76 (o).

IR (Neat) 3062 (w), 2931 (w), 1676 (s), 1632 (m), 1453 (m), 1029 (w), 966 (m), 699 (s) cm^{-1} .

HRMS (ESI[M+H]⁺) calcd for $\text{C}_{18}\text{H}_{19}\text{O}$ 251.1430, found 251.1434.

2-((Benzyloxy)methyl)-2-methyl-1-phenylbut-3-en-1-one (29n)



Colour and State: Colourless oil. *Branched:linear* \geq 19:1.

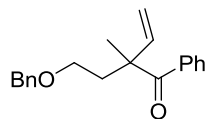
$^1\text{H NMR}$ (500 MHz, CDCl_3) δ 7.79-7.77 (m, 2H), 7.47-7.44 (m, 1H), 7.38-7.35 (m, 2H), 7.30-7.24 (m, 3H), 7.21-7.20 (m, 2H), 6.16 (dd, $J = 17.7, 10.8$ Hz, 1H), 5.28 (d, $J = 10.7$ Hz, 1H), 5.23 (d, $J = 17.7$ Hz, 1H), 4.48 (d, A of AB, $J_{AB} = 12.3$ Hz, 1H), 4.44 (d, B of AB, $J_{AB} = 12.3$ Hz, 1H), 3.83 (d, A of AB, $J_{AB} = 8.8$ Hz, 1H), 3.57 (d, B of AB, $J_{AB} = 8.8$ Hz, 1H), 1.48 (s, 3H).

$^{13}\text{C NMR}$ (125 MHz, CDCl_3) δ 203.97 (e), 140.14 (o), 138.30 (e), 137.95 (e), 131.51 (o), 128.82 (o), 128.37 (o), 128.01 (o), 127.55 (o), 127.53 (o), 116.26 (e), 76.15 (e), 73.51 (e), 54.88 (e), 21.49 (o).

IR (Neat) 3063 (w), 2854 (w), 1680 (s), 1631 (w), 1454 (m), 1225 (m), 1098 (s), 794 (w), 697 (s) cm^{-1} .

HRMS (ESI[M+H] $^+$) calcd for $\text{C}_{19}\text{H}_{21}\text{O}_2$ 281.1536, found 281.1539.

2-(2-(Benzyloxy)ethyl)-2-methyl-1-phenylbut-3-en-1-one (29o)



Colour and State: Colourless oil. *Branched:linear* \geq 19:1.

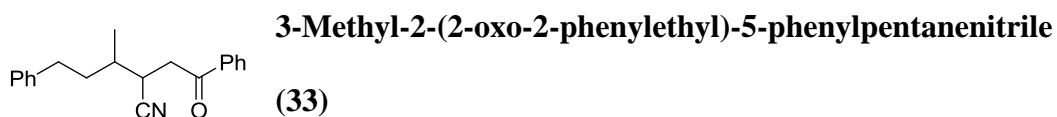
$^1\text{H NMR}$ (500 MHz, CDCl_3) δ 7.81-7.79 (m, 2H), 7.46-7.43 (m, 1H), 7.36-7.33 (m, 2H), 7.32-7.22 (m, 5H), 6.18 (dd, $J = 17.6, 10.8$ Hz, 1H), 5.25 (d, $J = 10.8$ Hz, 1H), 5.23 (d, $J = 17.8$ Hz, 1H), 4.40 (s, 2H), 3.53 (ddd, $J = 9.5, 8.0, 5.6$ Hz, 1H), 3.45 (ddd, $J = 9.5, 7.8, 6.6$ Hz, 1H), 2.31 (ddd, $J = 14.0, 7.6, 6.5$ Hz, 1H), 2.14 (ddd, $J = 13.7, 7.9, 5.7$ Hz, 1H), 1.41 (s, 3H).

$^{13}\text{C NMR}$ (125 MHz, CDCl_3) δ 204.17 (e), 142.89 (o), 138.30 (e), 138.35 (e), 137.64 (e), 131.52 (o), 129.14 (o), 128.35 (o), 127.97 (o), 127.67 (o), 127.54 (o), 114.99 (e), 72.98 (e), 66.81 (e), 52.36 (e), 38.51 (e), 23.26 (o).

IR (Neat) 2860 (w), 1676 (s), 1631 (w), 1454 (m), 1100 (s), 797 (w), 697 (s) cm^{-1} .

HRMS (ESI[M+Na] $^+$) calcd for $\text{C}_{20}\text{H}_{22}\text{NaO}_2$ 317.1517, found 317.1506.

3.2.1.7. Spectral Data for the Side Product 33



Isolated as an inseparable 1:1 mixture of diastereoisomers.

Colour and State: White solid.

¹H NMR (500 MHz, CDCl₃) δ 7.96-7.91 (m, 2H), 7.63-7.59 (m, 1H), 7.51-7.46 (m, 2H), 7.31-7.25 (m, 2H), 7.21-7.15 (m, 3H), 3.48-3.31 (m, 2H), 3.21-3.12 (m, 1H), 2.84-2.66 (m, 1.5H), 2.56-2.50 (m, 0.5H), 1.91-1.63 (m, 3H), 1.20 (d, *J* = 6.7 Hz, 1.5H), 1.14 (d, *J* = 6.4 Hz, 1.5H).

¹³C NMR (125 MHz, CDCl₃) δ 195.55 (e), 195.52 (e), 141.51 (e), 136.00 (e), 133.99 (o), 133.96 (o), 128.98 (o), 128.95 (o), 128.63 (o), 128.47 (o), 128.43 (o), 128.18 (o), 126.22 (o), 126.17 (o), 121.09 (e), 120.51 9 (e), 39.05 (e), 38.24 (e), 37.24 (e), 34.73 (e), 34.08 (o), 34.01 (o), 33.30 (e), 33.26 (e), 32.54 (o), 31.78 (o), 17.93 (o), 15.91 (o).

IR (Neat) 3062 (w), 2925 (w), 2239 (w), 1686 (s), 1598 (m), 1411 (w), 1214 (m), 910 (w), 689 (s) cm⁻¹.

HRMS (ESI[M+Na]⁺) calcd for C₂₀H₂₁NNaO 314.1521, found 314.1507.

3.2.2. Stereospecific Rhodium-Catalysed Allylic Substitution with an Acyl Anion

Equivalent: Asymmetric Construction of Acyclic α-Aryl Ketones

3.2.2.1. Representative Experimental Procedure for the Synthesis of Enantiomerically Enriched Secondary Alcohols (*S*)-54a-e⁶

In a 125 mL conical flask, 1-phenylethanol **54a** (7.33 g, 60.0 mmol) was dissolved in diisopropyl ether (25 mL) and vinyl acetate (27.7 mL, 300.0 mmol) was added. The mixture was heated to 50 °C with stirring and Novozyme[®] 435 (lipase from *Candida arctica*, immobilised on acrylic resin) (360 mg) was added. The resultant mixture

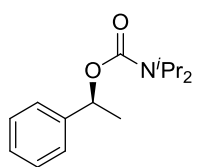
was stirred at 50 °C for 10 hours, filtered over a pad of celite and concentrated *in vacuo*. Purification by flash column chromatography (eluting with 7.5, 12.5, 20 then 50% ethyl acetate/hexane) yielded (*R*)-1-phenylethyl acetate (4.85 g, 50%) as a colourless oil and (*S*)-1-phenylethanol (**(S)-54a**) (3.52 g, 48%) as a colourless oil.

HPLC separation conditions for (**(S)-54a**): CHIRALCEL OJ-H column, hexane/isopropanol (96:4), flow rate: 1.0 mL/min; t_R 14.9 min for (*S*)-enantiomer (major), minor enantiomer not detectable, 99% *ee*.

3.2.2.2. Representative Experimental Procedure for the Synthesis of Enantiomerically Enriched Carbamates **48a-e**⁷

N,N-Diisopropylcarbonyl chloride (6.13 g, 37.5 mmol) was weighed into a two neck round bottom flask, fitted with a reflux condenser, and dissolved in dichloromethane (58 mL). Triethylamine (5.22 mL, 37.5 mmol) was added and the resultant mixture was heated to 40 °C with stirring, followed by the addition of (*S*)-1-phenylethanol (**(S)-53a**) (3.52 g, 28.8 mmol). The reaction mixture was stirred at 40 °C for *ca.* 48 hours, quenched with water (10 mL) and partitioned between dichloromethane and 1M aqueous hydrochloric acid solution. The combined organic layers were then washed with 1M aqueous hydrochloric acid solution (2 × 100 mL), dried using anhydrous magnesium sulfate, filtered and concentrated *in vacuo*. Purification by flash column chromatography (eluting with 3-9% ethyl acetate/hexane) afforded the secondary benzylic carbamate **48a** (6.60 g, 92%) as a colourless oil.

3.2.2.3. Spectral Data for the Enantiomerically Enriched Secondary Carbamates 48a-e



(S)-1-Phenylethyl diisopropylcarbamate (48a)

Colour and State: Colourless oil.

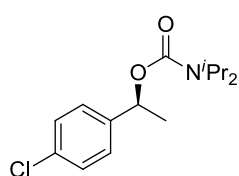
All spectral data matched the published values.⁷

¹H NMR (500 MHz, CDCl₃) δ 7.38-7.33 (m, 4H), 7.29-7.25 (m, 1H), 5.84 (q, *J* = 6.6 Hz, 1H), 4.27-3.97 (br m, 1H), 3.91-3.58 (br m, 1H), 1.55 (d, *J* = 6.6 Hz, 3H), 1.35-1.10 (br m, 12H).

¹³C NMR (125 MHz, CDCl₃) δ 155.15, 142.92, 128.47, 127.52, 126.12, 72.80, 45.69 (br), 22.92, 21.02 (br).

IR (Neat) 2971 (m), 1685 (vs), 1432 (m), 1283 (s), 906 (m), 697 (s) cm⁻¹.

99% *ee* based on the starting alcohol; [α]_D²⁰ -4.1 (*c* 1.0, CH₂Cl₂) (lit.⁷: [α]_D²³ -5.9 (*c* 2.1, CH₂Cl₂)).



(S)-1-(4-Chlorophenyl)ethyl diisopropylcarbamate (48b)

Colour and State: Colourless oil.

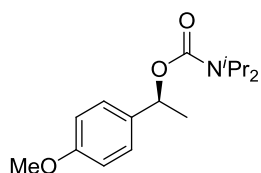
All spectral data matched the published values.⁷

¹H NMR (500 MHz, CDCl₃) δ 7.34-7.28 (m, 4H), 5.80 (q, *J* = 6.6 Hz, 1H), 4.29-3.53 (br m, 2H), 1.52 (d, *J* = 6.6 Hz, 3H), 1.28-1.13 (br m, 12H).

¹³C NMR (125 MHz, CDCl₃) δ 154.96, 141.49, 133.25, 128.67, 127.55, 72.09, 46.47 (br), 45.45 (br), 22.76, 21.60 (br), 20.78 (br).

IR (Neat) 2971 (m), 1687 (vs), 1437 (m), 1287 (s), 1015 (m), 719 (s) cm⁻¹.

99% *ee* based on the starting alcohol; [α]_D²⁰ -1.7 (*c* 1.0, CH₂Cl₂).



(S)-1-(4-Methoxyphenyl)ethyl diisopropylcarbamate (48c)

Colour and State: Colourless oil.

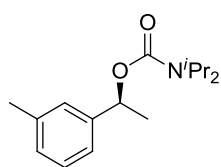
All spectral data matched the published values.⁷

¹H NMR (500 MHz, CDCl₃) δ 7.31-7.28 (m, 2H), 6.89-6.86 (m, 2H), 5.80 (q, *J* = 6.6 Hz, 1H), 4.31-3.55 (br m, 2H), 3.80 (s, 3H), 1.53 (d, *J* = 6.6 Hz, 3H), 1.29-1.11 (br m, 12H).

¹³C NMR (125 MHz, CDCl₃) δ 159.06, 155.29, 135.06, 127.55, 113.85, 72.47, 55.33, 46.20 (br), 22.75, 21.05 (br).

IR (Neat) 2971 (m), 1682 (vs), 1614 (m), 1515 (s), 1245 (s), 1036 (s), 730 (w) cm⁻¹.

99% *ee* based on the starting alcohol; [α]_D²⁰ -19.5 (*c* 1.0, CH₂Cl₂) (lit.⁷: [α]_D²⁴ -40.0 (*c* 1.0, CH₂Cl₂)).



(S)-1-(*m*-Tolyl)ethyl diisopropylcarbamate (48d)

Colour and State: Colourless oil.

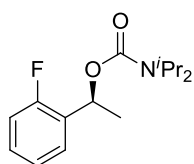
¹H NMR (500 MHz, CDCl₃) δ 7.24-7.21 (m, 1H), 7.17-7.16 (m, 2H), 7.08 (d, *J* = 7.3 Hz, 1H), 5.81 (q, *J* = 6.6 Hz, 1H), 4.28-3.56 (br m, 2H), 2.35 (s, 3H), 1.53 (d, *J* = 6.6 Hz, 3H), 1.32-1.12 (br m, 12H).

¹³C NMR (125 MHz, CDCl₃) δ 155.18, 142.92, 137.98, 128.40, 128.26, 126.91, 123.06, 72.85, 45.35 (br), 22.99, 21.58, 21.15 (br).

IR (Neat) 2971 (w), 1686 (s), 1611 (w), 1432 (m), 1284 (s), 1047 (s), 702 (m) cm⁻¹.

HRMS (ESI[M+Na]⁺) calcd for C₁₆H₂₅NNaO₂ 286.1783, found 286.1774.

99% *ee* based on the starting alcohol; [α]_D²⁰ -2.9 (*c* 1.0, CH₂Cl₂).



(S)-1-(2-Fluorophenyl)ethyl diisopropylcarbamate (48e)

Colour and State: Colourless oil.

All spectral data matched the published values.⁸

¹H NMR (500 MHz, CDCl₃) δ 7.38 (dt, *J* = 7.5, 1.7 Hz, 1H), 7.26-7.22 (m, 1H), 7.12 (dt, *J* = 7.5, 1.1 Hz, 1H), 7.03 (ddd, *J* = 10.4, 8.2, 1.1 Hz, 1H), 6.08 (q, *J* = 6.6 Hz, 1H), 4.38-3.51 (br m, 2H), 1.56 (d, *J* = 6.6 Hz, 3H), 1.33-1.14 (br m, 12H).

¹³C NMR (125 MHz, CDCl₃) δ 159.82 (d, ¹*J*_{C-F} = 247.2 Hz), 154.84, 130.14 (d, ²*J*_{C-F} = 13.6 Hz), 128.98 (d, ³*J*_{C-F} = 8.2 Hz), 127.40 (d, ³*J*_{C-F} = 4.5 Hz), 124.17 (d, ⁴*J*_{C-F} = 3.5 Hz), 115.65 (d, ²*J*_{C-F} = 21.7 Hz), 67.51 (d, ³*J*_{C-F} = 2.4 Hz), 46.48 (br), 45.30 (br), 21.85, 21.58 (br), 20.71 (br).

IR (Neat) 2971 (m), 1688 (s), 1618 (w), 1289 (s), 1133 (m), 828 (w), 757 (m) cm⁻¹.

99% *ee* based on the starting alcohol. [α]_D²⁰ +9.1 (*c* 1.0, CH₂Cl₂) (lit.⁸: [α]_D²³ +8.3 (*c* 10, CH₂Cl₂)).

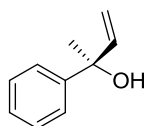
3.2.2.4. Representative Experimental Procedure for the Synthesis of Enantiomerically Enriched Tertiary Allylic Alcohols 45a-e⁸

To a stirring solution of (*S*)-1-phenylethyl diisopropylcarbamate **48a** (1.79 g, 7.18 mmol) in dry diethyl ether (28.4 mL), cooled to -78 °C, was added dropwise a 1.3M solution of *s*-butyllithium in cyclohexane (6.55 mL, 8.51 mmol), resulting in a light yellow homogeneous solution. The mixture was stirred for 30 minutes at -78 °C and neat vinylboronic acid pinacol ester **49** (1.73 g, 10.6 mmol) was added dropwise. The resultant mixture was stirred for 45 minutes at -78 °C and a 1M solution of magnesium bromide in methanol (8.51 mL, 8.51 mmol) was added dropwise. Upon stirring for a further 15 minutes at -78 °C, the reaction mixture was warmed to room temperature and stirred for 16 hours. An ice cold mixture of 3M aqueous sodium hydroxide (14.8 mL) and 30% aqueous hydrogen peroxide (8.5 mL) was then added

and the mixture was allowed to stir at room temperature for a further 2 hours, diluted with water (10 mL) and extracted with diethyl ether. The combined organic layers were washed with saturated aqueous sodium chloride solution (2×30 mL), dried using anhydrous magnesium sulfate, filtered and concentrated *in vacuo*. Purification by flash column chromatography (eluting with 2-16% ethyl acetate/hexane) yielded the tertiary allylic alcohol **45a** (873 mg, 83%) as a colourless oil.

3.2.2.5. Spectral Data for the Enantiomerically Enriched Tertiary Allylic Alcohols 45a-e

(*R*)-2-Phenylbut-3-en-2-ol (45a)



Colour and State: Colourless oil.

All spectral data matched the published values.⁷

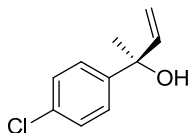
¹H NMR (500 MHz, CDCl₃) δ 7.49-7.47 (m, 2H), 7.37-7.34 (m, 2H), 7.28-7.25 (m, 1H), 6.18 (dd, $J = 17.3, 10.6$ Hz, 1H), 5.31 (dd, $J = 17.3, 0.7$ Hz, 1H), 5.15 (dd, $J = 10.6, 0.7$ Hz, 1H), 1.88 (s, 1H), 1.66 (s, 3H).

¹³C NMR (125 MHz, CDCl₃) δ 146.50 (e), 144.90 (o), 128.26 (o), 127.01 (o), 125.27 (o), 112.39 (e), 74.83 (e), 29.31 (o).

IR (Neat) 3394 (br), 2979 (w), 1640 (w), 1601 (w), 1446 (m), 923 (m), 700 (s) cm⁻¹.

HPLC separation conditions: CHIRALCEL OJ-H column, hexane/isopropanol (98:2), flow rate: 1.0 mL/min; t_R 21.3 min for (*S*)-enantiomer (minor) and 28.7 min for (*R*)-enantiomer (major), 99% *ee*; $[\alpha]_D^{20} +24.6$ (c 1.0, CHCl₃) (lit.⁷: $[\alpha]_D^{24} +29.3$ (c 3.96, CHCl₃)).

(R)-2-(4-Chlorophenyl)but-3-en-2-ol (45b)



Colour and State: Colourless oil.

¹H NMR (500 MHz, CDCl₃) δ 7.42-7.39 (m, 2H), 7.32-7.29 (m, 2H), 6.13 (dd, *J* = 17.3, 10.6 Hz, 1H), 5.29 (d, *J* = 17.3 Hz, 1H), 5.16 (d, *J* = 10.6 Hz, 1H), 1.84 (s, 1H), 1.64 (s, 3H).

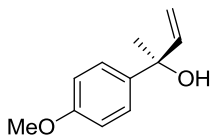
¹³C NMR (125 MHz, CDCl₃) δ 145.02 (e), 144.48 (o), 132.84 (e), 128.36 (o), 126.87 (o), 112.92 (e), 74.57 (e), 29.39 (o).

IR (Neat) 3372 (br), 2980 (m), 1641 (w), 1598 (w), 1491 (s), 1175 (m), 1013 (s), 828 (s), 693 (w) cm⁻¹.

HRMS (ESI[M]⁺) calcd for C₁₀H₁₁³⁵ClNaO 182.0493, found 182.0494.

HPLC separation conditions: CHIRALCEL OD column, hexane/isopropanol (98:2), flow rate: 0.6 mL/min; *t*_R 19.3 min for (*S*)-enantiomer (minor) and 21.7 min for (*R*)-enantiomer (major), 95% *ee*; [α]_D²⁰ +17.7 (*c* 1.0, CHCl₃).

(R)-2-(4-Methoxyphenyl)but-3-en-2-ol (45c)



Colour and State: Yellow oil.

¹H NMR (500 MHz, CDCl₃) δ 7.41-7.38 (m, 2H), 6.89-6.86 (m, 2H), 6.16 (dd, *J* = 17.3, 10.6 Hz, 1H), 5.29 (dd, *J* = 17.3, 1.0 Hz, 1H), 5.13 (dd, *J* = 10.6, 1.0 Hz, 1H), 3.81 (s, 3H), 1.81 (s, 1H), 1.64 (s, 3H).

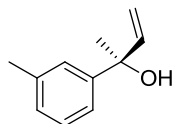
¹³C NMR (125 MHz, CDCl₃) δ 158.59 (e), 145.13 (o), 138.73 (e), 126.57 (o), 113.59 (o), 112.12 (e), 74.50 (e), 55.33 (o), 29.33 (o).

IR (Neat) 3437 (br), 2977 (m), 2836 (w), 1610 (m), 1509 (s), 1246 (vs), 1103 (m), 830 (s), 702 (w) cm⁻¹.

HRMS (ESI[M]⁺) calcd for C₁₁H₁₄O₂ 178.0988, found 178.0990.

HPLC separation conditions: CHIRALCEL OJ-H column, hexane/isopropanol (94:6), flow rate: 1.0 mL/min; t_R 33.8 min for (*S*)-enantiomer (minor) and 42.5 min for (*R*)-enantiomer (major), 99% *ee*; $[\alpha]_D^{20}$ +27.2 (*c* 1.0, CHCl₃).

(*R*)-2-(*m*-Tolyl)but-3-en-2-ol (45d)



Colour and State: Pale yellow oil.

All spectral data matched the published values.²

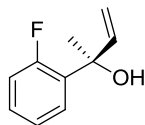
¹H NMR (500 MHz, CDCl₃) δ 7.30-7.22 (m, 3H), 7.08-7.07 (m, 1H), 6.17 (dd, *J* = 17.3, 10.6 Hz, 1H), 5.31 (dd, *J* = 17.3, 1.0 Hz, 1H), 5.14 (dd, *J* = 10.6, 1.0 Hz, 1H), 2.36 (s, 3H), 1.85 (s, 1H), 1.65 (s, 3H).

¹³C NMR (125 MHz, CDCl₃) δ 146.54 (e), 145.06 (o), 137.95 (e), 128.27 (o), 127.84 (o), 125.97 (o), 122.93 (o), 112.29 (e), 74.84 (e), 29.42 (o), 21.70 (o).

IR (Neat) 3386 (br), 2979 (w), 1607 (w), 1368 (m), 993 (m), 921 (s), 681 (w) cm⁻¹.

HPLC separation conditions: CHIRALCEL OJ-H column, hexane/isopropanol (98:2), flow rate: 1.0 mL/min; t_R 16.5 min for (*S*)-enantiomer (minor) and 21.9 min for (*R*)-enantiomer (major), 98% *ee*; $[\alpha]_D^{20}$ +22.7 (*c* 1.0, CHCl₃) (lit.²: $[\alpha]_D^{20}$ -13.7 (*c* 1.0, CHCl₃) for (*S*)-enantiomer).

(*R*)-2-(2-Fluorophenyl)but-3-en-2-ol (45e)



Colour and State: Pale yellow oil.

¹H NMR (500 MHz, CDCl₃) δ 7.55 (dt, *J* = 8.0, 1.8 Hz, 1H), 7.28-7.23 (m, 1H), 7.14 (dt, *J* = 7.6, 1.2 Hz, 1H), 7.03 (ddd, *J* = 12.1, 8.1, 1.2 Hz, 1H), 6.29 (ddd, *J* = 17.3, 10.6, 1.4 Hz, 1H), 5.24 (dt, *J* = 17.3, 1.1 Hz, 1H), 5.12 (dd, *J* = 10.6, 0.9 Hz, 1H), 1.71 (d, *J* = 1.0 Hz, 1H).

¹³C NMR (125 MHz, CDCl₃) δ 160.19 (e, d, ¹*J*_{C-F} = 245.6 Hz), 143.76 (o, d, ⁴*J*_{C-F} = 1.8 Hz), 133.32 (e, d, ²*J*_{C-F} = 11.7 Hz), 129.12 (o, d, ³*J*_{C-F} = 8.5 Hz), 127.00 (o, d, ³*J*_C).

$F = 4.1$ Hz), 124.21 (o, d, $^4J_{C-F} = 3.5$ Hz), 116.20 (o, d, $^2J_{C-F} = 23.5$ Hz), 112.75 (e), 73.82 (e, d, $^3J_{C-F} = 2.5$ Hz), 28.32 (o, d, $^4J_{C-F} = 3.0$ Hz).

IR (Neat) 3422 (br), 1979 (w), 1613 (w), 1485 (m), 1211 (m), 759 (s), 672 (w) cm^{-1} .

HRMS (ESI[M+NH₄]⁺) calcd for C₁₀H₁₅FNO 184.1138, found 184.1132.

HPLC separation conditions: CHIRALCEL OJ-H column, hexane/isopropanol (98:2), flow rate: 0.6 mL/min; t_R 26.7 min for (*S*)-enantiomer (minor) and 28.6 min for (*R*)-enantiomer (major), 99% *ee*; $[\alpha]_D^{20} +43.3$ (*c* 1.0, CHCl₃).

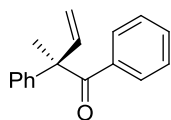
3.2.2.6. Representative Experimental Procedure for the Stereospecific Rhodium-Catalysed Allylic Substitution with the Aryl Cyanohydrins **24**

To a stirring solution of (*R*)-2-phenylbut-3-en-2-ol **45a** (72.1 mg, 0.486 mmol) in anhydrous tetrahydrofuran (1.5 mL) at 0 °C was added *n*-butyllithium (0.195 mL, 0.486 mmol). The mixture was stirred for *ca.* 15 minutes and methyl chloroformate (0.038 mL, 0.486 mmol) was added dropwise. The mixture was then allowed to warm to room temperature and stirred for *ca.* 1 hour. In a separate flask, a 1M solution of lithium bis(trimethylsilyl)amide in tetrahydrofuran (0.90 mL, 0.90 mmol) was added dropwise to a solution of 2-((*tert*-butyldimethylsilyl)oxy)-2-phenylacetonitrile **24a** (161.0 mg, 0.65 mmol) in anhydrous tetrahydrofuran (2 mL) at -10 °C. The anion was allowed to form over *ca.* 30 minutes, resulting in a light yellow homogeneous solution. In another flask, [RhCl(COD)]₂ (6.2 mg, 0.013 mmol) and tris(2,2,2-trifluoroethyl) phosphite (15.0 mg, 0.056 mmol) were dissolved in anhydrous tetrahydrofuran (1.5 mL) at room temperature. The mixture was stirred for *ca.* 5 minutes, also resulting in a light yellow homogeneous solution. All three flasks were then cooled to -10 °C and the cyanohydrin solution was added to the carbonate solution, followed quickly by the addition of the catalyst solution, all via Teflon[®] cannula. The resultant mixture was allowed to stir for *ca.* 5 hours and a 1M solution

of TBAF in tetrahydrofuran (2.00 mL, 2.00 mmol) was added. The mixture was then warmed to room temperature, allowed to stir for *ca.* 1 hour and partitioned between diethyl ether and saturated aqueous ammonium chloride solution. The combined organic layers were dried using anhydrous magnesium sulfate, filtered and concentrated *in vacuo*. Purification by flash column chromatography (eluting with 1-2% diethyl ether/hexane) afforded the ketone **52a** (100.3 mg, 87%) as a colourless oil.

3.2.2.7. Spectral Data for the Enantiomerically Enriched Acyclic α -Aryl Ketones **52a-1**

(*R*)-2-Methyl-1,2-diphenylbut-3-en-1-one (**52a**)



Colour and State: Colourless oil.

$^1\text{H NMR}$ (500 MHz, CDCl_3) δ 7.55-7.53 (m, 2H), 7.39-7.33 (m, 3H), 7.29-7.22 (m, 5H), 6.62 (dd, $J = 17.4, 10.8$ Hz, 1H), 5.30 (d, $J = 10.7$ Hz, 1H), 5.17 (d, $J = 17.4$ Hz, 1H), 1.67 (s, 3H).

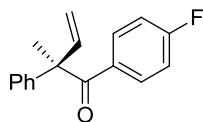
$^{13}\text{C NMR}$ (125 MHz, CDCl_3) δ 200.96 (e), 144.55 (e), 141.10 (o), 136.33 (e), 131.99 (o), 130.18 (o), 129.15 (o), 128.11 (o), 127.09 (o), 126.56 (o), 116.73 (e), 58.67 (e), 26.11 (o).

IR (Neat) 3059 (w), 3024 (w), 2985 (m), 1678 (s), 1632 (m), 1597 (m), 1237 (m), 1077 (m), 703 (s) cm^{-1} .

HRMS (ESI[M+H] $^+$) calcd for $\text{C}_{17}\text{H}_{17}\text{O}$ 237.1274, found 237.1273.

HPLC separation conditions: CHIRALPAK AD-H column, hexane/isopropanol (99.5:0.5), flow rate: 0.4 mL/min; t_{R} 17.8 min for (*R*)-enantiomer (major) and 20.1 min for (*S*)-enantiomer (minor); 90% *ee*; $[\alpha]_{\text{D}}^{20} +129.9$ (*c* 1.0, CHCl_3).

(R)-1-(4-Fluorophenyl)-2-methyl-2-phenylbut-3-en-1-one (52b)



Colour and State: White solid.

¹H NMR (500 MHz, CDCl₃) δ 7.60-7.56 (m, 2H), 7.36-7.33 (m, 2H), 7.29-7.24 (m, 3H), 6.93-6.88 (m, 2H), 6.60 (dd, *J* = 17.4, 10.8 Hz, 1H), 5.33-5.30 (m, 1H), 5.17 (d, *J* = 17.4 Hz, 1H), 1.66 (s, 3H).

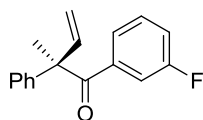
¹³C NMR (125 MHz, CDCl₃) δ 199.30 (e), 164.82 (e, d, ¹*J*_{C-F} = 254.5 Hz), 144.46 (e), 140.81 (o), 132.92 (o, d, ³*J*_{C-F} = 8.8 Hz), 132.33 (e, d, ⁴*J*_{C-F} = 3.4 Hz), 129.25 (o), 127.21 (o), 126.48 (o), 117.03 (e), 115.21 (o, d, ²*J*_{C-F} = 21.7 Hz), 58.58 (e), 26.32 (o).

IR (Neat) 3082 (w), 2988 (m), 2936 (w), 1676 (s), 1632 (m), 1596 (s), 1232 (s), 1029 (m), 696 (s) cm⁻¹.

HRMS (ESI[M+Na]⁺) calcd for C₁₇H₁₅FNao 277.1005, found 277.0997.

HPLC separation conditions: CHIRALCEL OJ-H column, hexane/isopropanol (99.5:0.5), flow rate: 1.0 mL/min; *t*_R 15.3 min for (*S*)-enantiomer (minor) and 18.2 min for (*R*)-enantiomer (major), 91% *ee*; [α]_D²⁰ +131.1 (*c* 1.0, CHCl₃).

(R)-1-(3-Fluorophenyl)-2-methyl-2-phenylbut-3-en-1-one (52c)



Colour and State: Colourless oil.

¹H NMR (500 MHz, CDCl₃) δ 7.37-7.34 (m, 2H), 7.30-7.25 (m, 5H), 7.21-7.17 (m, 1H), 7.09-7.06 (m, 1H), 6.59 (dd, *J* = 17.4, 10.8 Hz, 1H), 5.33 (d, *J* = 10.8 Hz, 1H), 5.18 (d, *J* = 17.4 Hz, 1H), 1.67 (s, 3H).

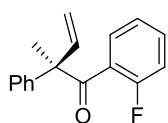
¹³C NMR (125 MHz, CDCl₃) δ 199.67 (e), 162.33 (e, d, ¹*J*_{C-F} = 247.1 Hz), 144.06 (e), 140.60 (o), 138.42 (e, d, ³*J*_{C-F} = 6.5 Hz), 129.66 (o, d, ³*J*_{C-F} = 7.7 Hz), 129.29 (o), 127.33 (o), 126.51 (o), 125.92 (o, d, ⁴*J*_{C-F} = 2.8 Hz), 119.02 (o, d, ²*J*_{C-F} = 21.5 Hz), 117.18 (e), 116.92 (o, d, ²*J*_{C-F} = 22.9 Hz), 58.72 (e), 26.09 (o).

IR (Neat) 3083 (w), 2987 (w), 2935 (w), 1682 (s), 1633 (w), 1586 (m), 1254 (vs), 926 (m), 665 (m) cm^{-1} .

HRMS (ESI[M+Na]⁺) calcd for C₁₇H₁₅FNao 277.1005, found 277.0998.

HPLC separation conditions: CHIRALPAK AD-H column, hexane/isopropanol (99.7:0.3), flow rate: 0.4 mL/min; t_R 19.7 min for (*R*)-enantiomer (major) and 22.0 min for (*S*)-enantiomer (minor), 92% *ee*; $[\alpha]_D^{20}$ +126.1 (*c* 1.0, CHCl₃).

(*R*)-1-(2-Fluorophenyl)-2-methyl-2-phenylbut-3-en-1-one (52d)



Colour and State: Colourless oil.

¹H NMR (500 MHz, CDCl₃) δ 7.37-7.28 (m, 6H), 7.01 (t, *J* = 9.3 Hz, 1H), 6.93 (t, *J* = 7.6 Hz, 1H), 6.89-6.86 (m, 1H), 6.47 (dd, *J* = 17.4, 10.8 Hz, 1H), 5.33 (d, *J* = 10.7 Hz, 1H), 5.19 (d, *J* = 17.4 Hz, 1H), 1.67 (s, 3H).

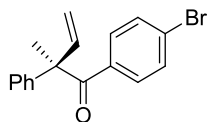
¹³C NMR (125 MHz, CDCl₃) δ 201.46 (e, d, ³*J*_{C-F} = 1.7 Hz), 159.35 (e, d, ¹*J*_{C-F} = 252.7 Hz), 142.41 (e), 140.24 (o), 132.16 (o, d, ³*J*_{C-F} = 8.5 Hz), 129.16 (o, d, ⁴*J*_{C-F} = 2.9 Hz), 128.89 (o), 127.78 (e, d, ²*J*_{C-F} = 15.0 Hz), 127.29 (o), 127.04 (o), 123.56 (o, d, ³*J*_{C-F} = 3.6 Hz), 116.86 (e), 116.40 (o, d, ²*J*_{C-F} = 22.2 Hz), 59.63 (e), 24.02 (o).

IR (Neat) 2984 (w), 1696 (s), 1634 (m), 1609 (m), 1274 (m), 1010 (m), 758 (s) cm^{-1} .

HRMS (ESI[M+H]⁺) calcd for C₁₇H₁₆FO 255.1180, found 255.1177.

HPLC separation conditions: CHIRALPAK AD-H column, hexane/isopropanol (99.5:0.5), flow rate: 0.4 mL/min; t_R 24.4 min for (*R*)-enantiomer (major) and 26.7 min for (*S*)-enantiomer (minor), 89% *ee*; $[\alpha]_D^{20}$ +45.0 (*c* 1.0, CHCl₃).

(R)-1-(4-Bromophenyl)-2-methyl-2-phenylbut-3-en-1-one (52e)



Colour and State: White solid.

¹H NMR (500 MHz, CDCl₃) δ 7.42-7.33 (m, 6H), 7.29-7.23 (m, 3H), 6.58 (dd, *J* = 17.4, 10.8 Hz, 1H), 5.32 (d, *J* = 10.8 Hz, 1H), 5.16 (d, *J* = 17.4 Hz, 1H), 1.65 (s, 3H).

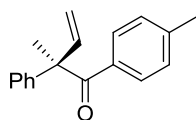
¹³C NMR (125 MHz, CDCl₃) δ 199.79 (e), 144.23 (e), 140.61 (o), 134.82 (e), 131.81 (o), 131.41 (o), 129.27 (o), 127.26 (o), 127.13 (e), 126.46 (o), 117.19 (e), 58.61 (e), 26.23 (o).

IR (Neat) 3060 (w), 2987 (w), 1681 (s), 1631 (w), 1582 (m), 1238 (m), 955 (m), 701 (vs) cm⁻¹.

HRMS (ESI[M+Na]⁺) calcd for C₁₇H₁₅⁷⁹BrNaO 337.0204, found 337.0204.

HPLC separation conditions: CHIRALPAK AD-H column, hexane/isopropanol (99.5:0.5), flow rate: 0.4 mL/min; *t_R* 32.4 min for (*R*)-enantiomer (major) and 35.6 min for (*S*)-enantiomer (minor), 86% *ee*; [α]_D²⁰ +118.2 (*c* 1.0, CHCl₃).

(R)-2-Methyl-2-phenyl-1-(p-tolyl)but-3-en-1-one (52f)



Colour and State: White solid.

¹H NMR (500 MHz, CDCl₃) δ 7.46 (d, *J* = 8.3 Hz, 2H), 7.35-7.32 (m, 2H), 7.27-7.25 (m, 3H), 7.04 (d, *J* = 8.2 Hz, 2H), 6.63 (dd, *J* = 17.4, 10.8 Hz, 1H), 5.29 (d, *J* = 10.8 Hz, 1H), 5.16 (d, *J* = 17.4 Hz, 1H), 2.30 (s, 3H), 1.66 (s, 3H).

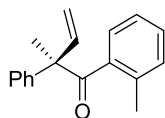
¹³C NMR (125 MHz, CDCl₃) δ 200.40 (e), 144.86 (e), 142.71 (e), 141.20 (o), 133.41 (e), 130.43 (o), 129.08 (o), 128.80 (o), 126.97 (o), 126.50 (o), 116.61 (e), 58.57 (e), 26.22 (o), 21.59 (o).

IR (Neat) 3085 (w), 3025 (m), 2983 (m), 1668 (s), 1629 (m), 1604 (s), 1408 (m), 1242 (s), 927 (s), 699 (vs) cm⁻¹.

HRMS (ESI[M+H]⁺) calcd for C₁₈H₁₉O 251.1430, found 251.1433.

HPLC separation conditions: CHIRALPAK AD-H column, hexane/isopropanol (99.3:0.7), flow rate: 0.5 mL/min; t_R 29.0 min for (*R*)-enantiomer (major) and 32.9 min for (*S*)-enantiomer (minor), 91% *ee*; $[\alpha]_D^{20} +140.9$ (*c* 1.0, CHCl₃).

(*R*)-2-Methyl-2-phenyl-1-(*o*-tolyl)but-3-en-1-one (52g)



Colour and State: White solid.

¹H NMR (500 MHz, CDCl₃) δ 7.42-7.35 (m, 4H), 7.33-7.28 (m, 1H), 7.21-7.16 (m, 2H), 6.90-6.87 (m, 1H). 6.56 (d, *J* = 7.6 Hz, 1H), 6.38 (dd, *J* = 17.4, 10.8 Hz, 1H), 5.29 (dd, *J* = 10.9, 0.8 Hz, 1H), 5.22 (dd, *J* = 17.5, 0.8 Hz, 1H), 2.27 (s, 3H), 1.65 (s, 3H).

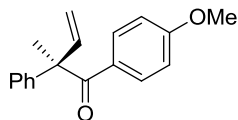
¹³C NMR (125 MHz, CDCl₃) δ 206.24 (e), 142.85 (e), 140.80 (o), 139.86 (e), 136.21 (e), 131.12 (o), 129.52 (o), 128.96 (o), 127.28 (o), 127.01 (o), 126.35 (o), 124.83 (o), 116.15 (e), 59.63 (e), 23.72 (o), 20.45 (o).

IR (Neat) 2978 (w), 1693 (s), 1680 (s), 1635 (w), 1241 (m), 1010 (m), 698 (s) cm⁻¹.

HRMS (ESI[M+H]⁺) calcd for C₁₈H₁₉O 251.1436, found 251.1432.

HPLC separation conditions: CHIRALPAK AD-H column, hexane/isopropanol (99.3:0.7), flow rate: 0.5 mL/min; t_R 14.4 min for (*R*)-enantiomer (major) and 17.0 min for (*S*)-enantiomer (minor), 81% *ee*; $[\alpha]_D^{20} +14.8$ (*c* 1.0, CHCl₃).

(*R*)-1-(4-Methoxyphenyl)-2-methyl-2-phenylbut-3-en-1-one (52h)



Colour and State: White solid.

¹H NMR (500 MHz, CDCl₃) δ 7.59-7.56 (m, 2H), 7.35-7.32 (m, 2H), 7.27-7.24 (m, 3H), 6.74-6.71 (m, 2H), 6.63 (dd, *J* = 17.4, 10.8 Hz, 1H), 5.29 (d, *J* = 10.7 Hz, 1H), 5.15 (d, *J* = 17.4 Hz, 1H), 3.77 (s, 3H), 1.66 (s, 3H).

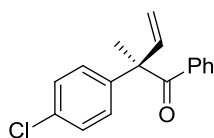
¹³C NMR (125 MHz, CDCl₃) δ 199.29 (e), 162.49 (e), 145.15 (e), 141.32 (o), 132.69 (o), 129.08 (o), 128.63 (e), 126.93 (o), 126.50 (o), 116.52 (e), 113.27 (o), 58.44 (e), 55.44 (o), 26.41 (o).

IR (Neat) 2934 (w), 2839 (w), 1671 (s), 1631 (w), 1599 (vs), 1245 (vs), 1030 (m), 703 (m) cm⁻¹.

HRMS (ESI[M+H]⁺) calcd for C₁₈H₁₉O₂ 267.1380, found 267.1384.

HPLC separation conditions: CHIRALCEL OD column, hexane/isopropanol (99.3:0.7), flow rate: 0.5 mL/min; *t_R* 17.9 min for (*S*)-enantiomer (minor) and 21.8 min for (*R*)-enantiomer (major), 90% *ee*; [α]_D²⁰ +141.5 (c 1.0, CHCl₃).

(*R*)-2-(4-Chlorophenyl)-2-methyl-1-phenylbut-3-en-1-one (52i)



Colour and State: White solid.

¹H NMR (500 MHz, CDCl₃) δ 7.54 (d, *J* = 7.4 Hz, 2H), 7.40 (t, *J* = 7.4 Hz, 1H), 7.33-7.31 (m, 2H), 7.26 (t, *J* = 7.8 Hz, 2H), 7.22-7.20 (m, 2H), 6.58 (dd, *J* = 17.4, 10.8 Hz, 1H), 5.32 (d, *J* = 10.8 Hz, 1H), 5.17 (d, *J* = 17.4 Hz, 1H), 3.80 (s, 3H), 1.65 (s, 3H).

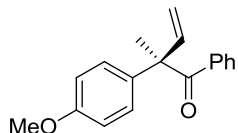
¹³C NMR (125 MHz, CDCl₃) δ 200.44 (e), 143.16 (e), 140.63 (o), 135.97 (e), 133.03 (e), 132.21 (o), 130.15 (o), 129.32 (o), 128.23 (o), 127.99 (o), 117.17 (e), 58.22 (e), 26.15 (o).

IR (Neat) 3066 (w), 2988 (m), 2938 (w), 1676 (s), 1629 (m), 1598 (m), 1239 (s), 956 (m), 673 (m) cm⁻¹.

HRMS (ESI[M+Na]⁺) calcd for C₁₇H₁₅³⁵ClNaO 293.0709, found 293.0700.

HPLC separation conditions: CHIRALCEL OD column, hexane/isopropanol (99.7:0.3), flow rate: 0.4 mL/min; *t_R* 18.3 min for (*S*)-enantiomer (minor) and 20.1 min for (*R*)-enantiomer (major), 94% *ee*; [α]_D²⁰ +110.9 (c 1.0, CHCl₃).

(R)-2-(4-Methoxyphenyl)-2-methyl-1-phenylbut-3-en-1-



one (52j)

Colour and State: White solid.

¹H NMR (500 MHz, CDCl₃) δ 7.55-7.53 (m, 2H), 7.38 (t, *J* = 7.4 Hz, 1H), 7.26-7.23 (m, 2H), 7.20-7.17 (m, 2H), 6.90-6.87 (m, 2H), 6.59 (dd, *J* = 17.4, 10.8 Hz, 1H), 5.27 (d, *J* = 10.8 Hz, 1H), 5.13 (d, *J* = 17.4 Hz, 1H), 3.80 (s, 3H), 1.64 (s, 3H).

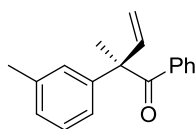
¹³C NMR (125 MHz, CDCl₃) δ 201.30 (e), 158.61 (e), 141.46 (o), 136.50 (e), 136.38 (e), 131.91 (o), 130.15 (o), 128.11 (o), 127.68 (o), 116.37 (e), 114.51 (o), 57.98 (e), 55.38 (o), 25.99 (o).

IR (Neat) 2934 (w), 2836 (w), 1678 (s), 1631 (m), 1608 (m), 1509 (vs), 1109 (w), 771 (m) cm⁻¹.

HRMS (ESI[M+Na]⁺) calcd for C₁₈H₁₈NaO₂ 289.1204, found 289.1201.

HPLC separation conditions: CHIRALPAK AD-H column, hexane/isopropanol (99.3:0.7), flow rate: 0.5 mL/min; *t_R* 36.9 min for (*R*)-enantiomer (major) and 49.2 min for (*S*)-enantiomer (minor), 89% *ee*; [α]_D²⁰ +99.5 (*c* 1.0, CHCl₃).

(R)-2-Methyl-1-phenyl-2-(*m*-tolyl)but-3-en-1-one (52k)



Colour and State: Colourless oil.

¹H NMR (500 MHz, CDCl₃) δ 7.55-7.53 (m, 2H), 7.40-7.36 (m, 1H), 7.26-7.22 (m, 3H), 7.09-7.06 (m, 3H), 6.60 (dd, *J* = 17.3, 10.7 Hz, 1H), 5.29 (dd, *J* = 10.8, 0.7 Hz, 1H), 5.16 (d, *J* = 17.3, 0.6 Hz, 1H), 2.33 (s, 3H), 1.65 (s, 3H).

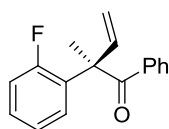
¹³C NMR (125 MHz, CDCl₃) δ 201.09 (e), 144.43 (e), 141.22 (o), 138.78 (e), 136.50 (e), 131.92 (o), 130.14 (o), 128.98 (o), 128.41 (o), 128.09 (o), 127.86 (o), 127.16 (o), 123.58 (o), 116.54 (e), 58.56 (e), 25.99 (o), 21.69 (o).

IR (Neat) 2984 (w), 1678 (s), 1632 (w), 1447 (m), 1237 (m), 924 (m), 704 (s) cm⁻¹.

HRMS (ESI[M+H]⁺) calcd for C₁₈H₁₉O 251.1436, found 251.1430.

HPLC separation conditions: CHIRALPAK AD-H column, hexane/isopropanol (99.6:0.4), flow rate: 0.4 mL/min; t_R 18.0 min for (*R*)-enantiomer (major) and 20.1 min for (*S*)-enantiomer (minor), 93% *ee*.

(*R*)-2-(2-Fluorophenyl)-2-methyl-1-phenylbut-3-en-1-one (52l)



Colour and State: Colourless oil.

$^1\text{H NMR}$ (500 MHz, CDCl_3) δ 7.67-7.65 (m, 2H), 7.48 (dt, $J = 7.7$, 1.9 Hz, 1H), 7.41-7.7.37 (m, 1H), 7.28-7.20 (m, 4H), 6.91 (ddd, $J = 11.1$, 8.0, 1.4 Hz, 1H), 6.62 (dd, $J = 17.4$, 10.7 Hz, 1H), 5.34 (d, $J = 10.7$ Hz, 1H), 5.21 (d, $J = 17.4$ Hz, 1H), 1.74 (s, 3H).

$^{13}\text{C NMR}$ (125 MHz, CDCl_3) δ 199.70 (e, d, $^4J_{C-F} = 1.2$ Hz), 160.30 (e, d, $^1J_{C-F} = 247.3$ Hz), 139.84 (o), 135.87 (e), 132.73 (e, d, $^2J_{C-F} = 13.5$ Hz), 132.16 (o), 129.39 (o), 129.10 (o, d, $^3J_{C-F} = 8.4$ Hz), 128.10 (o), 127.41 (o, d, $^3J_{C-F} = 4.5$ Hz), 124.83 (o, d, $^4J_{C-F} = 3.0$ Hz), 116.77 (e), 116.37 (o, d, $^2J_{C-F} = 22.3$ Hz), 55.74 (e), 24.03 (o).

IR (Neat) 2998 (w), 1677 (s), 1629 (w), 1487 (m), 1235 (s), 926 (s), 813 (m), 708 (s) cm^{-1} .

HRMS (ESI[M+H] $^+$) calcd for $\text{C}_{17}\text{H}_{16}\text{FO}$ 255.1185, found 255.1183.

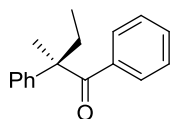
HPLC separation conditions: CHIRALPAK AD-H column, hexane/isopropanol (99.6:0.4), flow rate: 0.3 mL/min; t_R 35.1 min for (*R*)-enantiomer (major) and 37.8 min for (*S*)-enantiomer (minor), 89% *ee*; $[\alpha]_D^{20} +116.7$ (*c* 1.0, CHCl_3).

3.2.2.8. Experimental Procedure for the Hydrogenation of 52a

To a stirring solution of (*R*)-2-methyl-1,2-diphenylbut-3-en-1-one **52a** (50.8 mg, 0.22 mmol) in ethyl acetate (2.2 mL), under an atmosphere of nitrogen, was added 10% Pd/C (2.3 mg, 0.021 mmol). The nitrogen inlet was replaced with a hydrogen balloon

and the mixture was stirred at room temperature for 5 hours. The flask was then purged with argon and the mixture was concentrated *in vacuo* to afford a crude oil. Purification by flash column chromatography (eluting with 1-2% diethyl ether/hexane) yielded the ethyl ketone (-)-**53** (47.6 mg, 93%) as a colourless oil.

(R)-2-methyl-1,2-diphenylbutan-1-one ((-)-53)



Colour and State: Colourless oil.

All spectral data matched the published values.⁹

¹H NMR (500 MHz, CDCl₃) δ 7.45-7.43 (m, 2H), 7.37-7.35 (m, 3H), 7.31-7.25 (m, 3H), 7.22-7.19 (m, 2H), 2.20-2.13 (m, 1H), 2.10-2.03 (m, 1H), 1.55 (s, 3H), 0.75 (t, *J* = 7.5 Hz, 3H).

¹³C NMR (125 MHz, CDCl₃) δ 203.94 (e), 144.48 (e), 137.03 (e), 131.68 (o), 129.57 (o), 129.01 (o), 128.04 (o), 126.88 (o), 126.40 (o), 55.07 (e), 32.18 (e), 23.86 (o), 8.76 (o).

IR (Neat) 3058 (w), 1675 (m), 1496 (w), 1265 (m), 963 (w), 736 (vs) cm⁻¹.

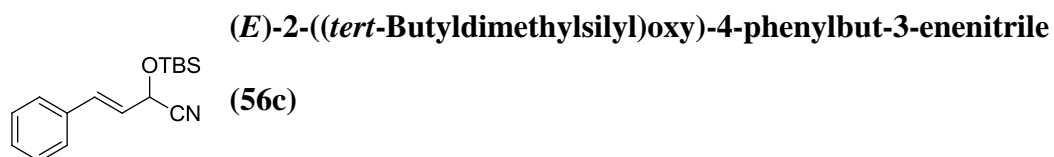
HPLC separation conditions: CHIRALPAK AD-H column, hexane/isopropanol/methanol (99.5:0.3:0.2), flow rate: 0.2 mL/min; *t*_R 55.3 min for (*S*)-enantiomer (minor) and 60.0 min for (*R*)-enantiomer (major), 90% *ee*; [α]_D²⁰ -53.9 (*c* 1.0, PhMe) (lit.⁹: [α]_D²⁰ -28.0 (*c* 1.0, PhMe)).

3.2.3. Expanding the Scope of the Rhodium-Catalysed Allylic Substitution with an Acyl Anion Equivalent

3.2.3.1. Rhodium-Catalysed Allylic Substitution with Alkenyl Cyanohydrin Pronucleophiles: Construction of Acyclic α,α' -Dialkyl Ketones

3.2.3.1.1. Spectral Data for the Alkenyl Cyanohydrins **56b-k** and **69a-c**

The alkenyl cyanohydrins **56** and **69** were prepared from the corresponding α,β -unsaturated aldehydes according to the representative experimental procedure for the synthesis of aryl cyanohydrins **24a-i**.³ When not commercially available, the required α,β -unsaturated aldehydes were prepared in three steps according to the procedure reported by Das.¹⁰



Colour and State: Pale yellow oil.

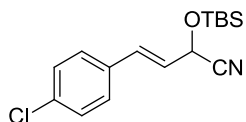
All spectral data matched the published values.³

¹H NMR (500 MHz, CDCl₃) δ 7.42-7.41 (m, 2H), 7.38-7.34 (m, 2H), 7.33-7.30 (m, 1H), 6.81 (dd, $J = 15.7, 1.1$ Hz, 1H), 6.19 (dd, $J = 15.8, 5.8$ Hz, 1H), 5.14 (dd, $J = 5.8, 1.4$ Hz, 1H), 0.95 (s, 9H), 0.23 (s, 3H), 0.20 (s, 3H).

¹³C NMR (125 MHz, CDCl₃) δ 135.22 (e), 133.76 (o), 128.88 (o), 127.09 (o), 123.83 (o), 118.60 (e), 62.77 (o), 25.68 (o), 18.31 (e), -4.82 (o), -4.88 (o).

IR (Neat) 3029 (w), 2931 (m), 1654 (w), 1579 (w), 1255 (m), 966 (m), 781 (s) cm⁻¹.

(E)-2-((tert-Butyldimethylsilyl)oxy)-4-(4-chlorophenyl)but-3-



enenitrile (56d)

Colour and State: Pale yellow oil.

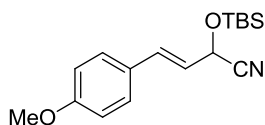
¹H NMR (500 MHz, CDCl₃) δ 7.35-7.31 (m, 4H), 6.77 (dd, *J* = 15.8, 1.5 Hz, 1H), 6.16 (dd, *J* = 15.8, 5.6 Hz, 1H), 5.13 (dd, *J* = 5.6, 1.5 Hz, 1H), 0.94 (s, 9H), 0.22 (s, 3H), 0.19 (s, 3H).

¹³C NMR (125 MHz, CDCl₃) δ 134.65 (e), 133.74 (e), 132.42 (o), 129.10 (o), 128.31 (o), 124.47 (o), 118.43 (e), 62.59 (o), 25.69 (o), 18.33 (e), -4.83 (o), -4.90 (o).

IR (Neat) 2955 (w), 2859 (w), 1655 (w), 1595 (w), 1492 (m), 1204 (w), 1089 (s), 836 (vs), 694 (w) cm⁻¹.

HRMS (ESI[M+Na]⁺) calcd for C₁₆H₂₂³⁵ClNNaOSi 330.1057, found 330.1045.

(E)-2-((tert-Butyldimethylsilyl)oxy)-4-(4-



methoxyphenyl)but-3-enitrile (56e)

Colour and State: Pale yellow oil.

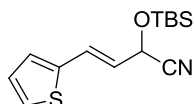
¹H NMR (500 MHz, CDCl₃) δ 7.36-7.33 (m, 2H), 6.89-6.87 (m, 2H), 6.73 (d, *J* = 15.7 Hz, 1H), 6.05 (dd, *J* = 15.7, 6.0 Hz, 1H), 5.11 (dd, *J* = 6.0, 1.2 Hz, 1H), 3.82 (s, 3H), 0.93 (s, 9H), 0.21 (s, 3H), 0.18 (s, 3H).

¹³C NMR (125 MHz, CDCl₃) δ 160.24 (e), 133.38 (o), 128.40 (o), 127.93 (e), 121.0 (o), 118.78 (e), 114.28 (o), 62.96 (o), 55.54 (o), 25.69 (o), 18.29 (e), -4.82 (o), -4.84 (o).

IR (Neat) 2957 (w), 2859 (w), 2241 (m), 1652 (w), 1606 (m), 1576 (w), 1512 (m), 1252 (s), 979 (m), 778 (s) cm⁻¹.

HRMS (ESI[M+Na]⁺) calcd for C₁₇H₂₅NNaO₂Si 326.1552, found 326.1554.

(E)-2-((tert-Butyldimethylsilyl)oxy)-4-(thiophen-2-yl)but-3-



enenitrile (56f)

Colour and State: Colourless oil.

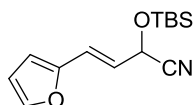
¹H NMR (500 MHz, CDCl₃) δ 7.25 (d, *J* = 5.1 Hz, 1H), 7.06 (d, *J* = 3.4 Hz, 1H), 7.00 (dd, *J* = 5.0, 3.6 Hz, 1H), 6.93 (d, *J* = 15.6 Hz, 1H), 6.01 (dd, *J* = 15.5, 5.7 Hz, 1H), 5.10 (dd, *J* = 5.7, 1.4 Hz, 1H), 0.94 (s, 9H), 0.22 (s, 3H), 0.19 (s, 3H).

¹³C NMR (125 MHz, CDCl₃) δ 140.03 (e), 127.84 (o), 127.76 (o), 126.82 (o), 126.06 (o), 122.96 (o), 118.43 (e), 62.49 (o), 25.71 (o), 18.34 (e), -4.79 (o), -4.84 (o).

IR (Neat) 2955 (w), 2930 (m), 1647 (w), 1472 (w), 1255 (m), 1103 (m), 839 (s), 782 (s), 672 (w) cm⁻¹.

HRMS (ESI[M+Na]⁺) calcd for C₁₄H₂₁NNaOSSi 302.1011, found 302.1013.

(E)-2-((tert-Butyldimethylsilyl)oxy)-4-(furan-2-yl)but-3-



enenitrile (56g)

Colour and State: Pale yellow oil.

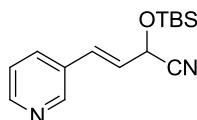
¹H NMR (500 MHz, CDCl₃) δ 7.39 (s, 1H), 6.62 (d, *J* = 15.6 Hz, 1H), 6.41-6.36 (m, 2H), 6.12 (dd, *J* = 15.6, 5.5 Hz, 1H), 5.12 (d, *J* = 5.5 Hz, 1H), 0.94 (s, 9H), 0.21 (s, 3H), 0.18 (s, 3H).

¹³C NMR (125 MHz, CDCl₃) δ 151.03 (e), 143.17 (o), 121.98 (o), 121.48 (o), 118.41 (e), 111.71 (o), 110.63 (o), 62.32 (o), 25.69 (o), 18.32 (e), -4.86 (o), -4.93 (o).

IR (Neat) 2956 (w), 2859 (w), 1659 (w), 1472 (w), 1111 (m), 838 (vs), 737 (s) cm⁻¹.

HRMS (ESI[M+Na]⁺) calcd for C₁₄H₂₁NNaO₂Si 286.1239, found 286.1233.

(E)-2-((tert-Butyldimethylsilyl)oxy)-4-(pyridin-3-yl)but-3-



enenitrile (56h)

Colour and State: Yellow oil.

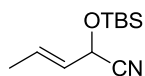
¹H NMR (500 MHz, CDCl₃) δ 8.64 (d, *J* = 1.8 Hz, 1H), 8.55 (dd, *J* = 4.8, 1.3 Hz, 1H), 7.75 (dt, *J* = 7.9, 2.0 Hz, 1H), 7.31 (dd, *J* = 7.9, 4.8 Hz, 1H), 6.83 (dd, *J* = 15.8, 1.4 Hz, 1H), 6.27 (dd, *J* = 15.8, 5.4 Hz, 1H), 5.16 (dd, *J* = 5.4, 1.6 Hz, 1H), 0.95 (s, 9H), 0.24 (s, 3H), 0.20 (s, 3H).

¹³C NMR (125 MHz, CDCl₃) δ 149.85 (o), 148.82 (o), 133.55 (o), 130.97 (e), 130.07 (o), 126.10 (o), 123.72 (o), 118.21 (e), 62.42 (o), 25.66 (o), 18.31 (e), -4.86 (o), -4.96 (o).

IR (Neat) 2955 (w), 2931 (m), 1735 (w), 1255 (m), 1108 (m), 839 (s) cm⁻¹.

HRMS (ESI[M+H]⁺) calcd for C₁₅H₂₃N₂OSi 275.1580, found 275.1586.

(E)-2-((tert-Butyldimethylsilyl)oxy)pent-3-enitrile (56b)



Colour and State: Colourless oil.

¹H NMR (500 MHz, CDCl₃) δ 5.95 (ddq, *J* = 15.1, 6.7, 1.5 Hz, 1H), 5.54 (ddq, *J* = 15.2, 6.0, 1.7 Hz, 1H), 4.89 (app. d pentet, *J* = 6.0, 1.1 Hz, 1H), 1.76 (ddd, *J* = 6.6, 1.6, 1.1 Hz, 3H), 0.91 (s, 9H), 0.17 (s, 3H), 0.14 (s, 3H).

¹³C NMR (125 MHz, CDCl₃) δ 130.84 (o), 126.34 (o), 118.94 (e), 62.63 (o), 25.62 (o), 18.22 (e), 17.52 (o), -4.94 (o), -4.97 (o).

IR (Neat) 2956 (w), 2887 (w), 1680 (w), 1615 (w), 1471 (w), 1255 (m), 1088 (m), 837 (vs), 674 (w) cm⁻¹.

HRMS (ESI[M+NH₄]⁺) calcd for C₁₁H₂₅N₂OSi 229.1736, found 229.1728.



Colour and State: Colourless oil.

¹H NMR (500 MHz, CDCl₃) δ 7.30-7.27 (m, 2H), 7.21-7.16 (m, 3H), 5.97 (ddt, *J* = 15.0, 6.8, 1.4 Hz, 1H), 5.54 (ddt, *J* = 15.3, 5.9, 1.5 Hz, 1H), 4.89 (dq, *J* = 5.9, 1.0 Hz, 1H), 2.73 (t, *J* = 7.7 Hz, 2H), 2.44-2.39 (m, 2H), 0.91 (s, 9H), 0.16 (s, 3H), 0.12 (s, 3H).

¹³C NMR (125 MHz, CDCl₃) δ 141.17 (e), 134.85 (o), 128.56 (o), 128.54 (o), 126.20 (o), 125.85 (o), 118.90 (e), 62.64 (o), 35.12 (e), 33.67 (e), 25.68 (o), 18.28 (e), -4.87 (o), -4.91 (o).

IR (Neat) 3028 (w), 2930 (m), 1669 (w), 1604 (w), 1472 (w), 1254 (m), 1108 (m), 912 (w), 837 (vs), 780 (s) cm⁻¹.

HRMS (ESI[M+Na]⁺) calcd for C₁₈H₂₇NNaOSi 324.1760, found 324.1762.



Colour and State: Colourless oil.

¹H NMR (500 MHz, CDCl₃) δ 5.92 (dd, *J* = 15.6, 1.2 Hz, 1H), 5.42 (dd, *J* = 15.6, 6.2 Hz, 1H), 4.91 (dd, *J* = 6.1, 1.1 Hz, 1H), 1.04 (s, 9H), 0.91 (s, 9H), 0.16 (s, 3H), 0.14 (s, 3H).

¹³C NMR (125 MHz, CDCl₃) δ 146.62 (o), 120.63 (o), 119.16 (e), 63.21 (o), 33.23 (e), 29.16 (o), 25.70 (o), 18.30 (e), -4.72 (o).

IR (Neat) 2958 (m), 2901 (w), 1665 (w), 1464 (w), 1255 (m), 1071 (m), 910 (w), 838 (s), 673 (w) cm⁻¹.

HRMS (ESI[M+NH₄]⁺) calcd for C₁₄H₃₁N₂OSi 271.2206, found 271.2204.



Colour and State: Colourless oil.

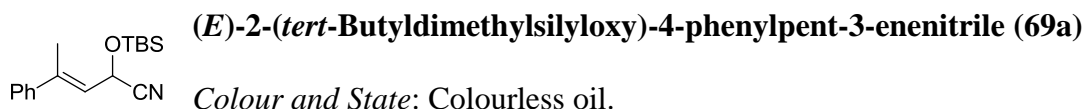
The product was isolated as a 6:1 mixture of (3*E*,5*E*) and (3*E*,5*Z*) isomers. Data is provided for the major isomer only.

¹H NMR (500 MHz, CDCl₃) δ 6.38 (dd, *J* = 15.1, 10.5 Hz, 1H), 6.09-6.04 (m, 1H), 5.86 (dq, *J* = 14.6, 7.1 Hz, 1H), 5.54 (dd, *J* = 15.2, 6.1 Hz, 1H), 4.97 (d, *J* = 6.0 Hz, 1H), 0.91 (s, 9H), 0.17 (s, 3H), 0.15 (s, 3H).

¹³C NMR (125 MHz, CDCl₃) δ 134.13 (o), 133.61 (o), 129.52 (o), 124.23 (o), 118.73 (e), 62.57 (o), 25.65 (o), 18.34 (o), 18.26 (e), -4.87 (o), -4.91 (o).

IR (Neat) 2931 (m), 2859 (w), 1661 (w), 1472 (w), 1255 (m), 1080 (m), 987 (s), 837 (s), 674 (w) cm⁻¹.

HRMS (ESI[M+NH₄]⁺) calcd for C₁₃H₂₇N₂OSi 255.1893, found 255.1885.

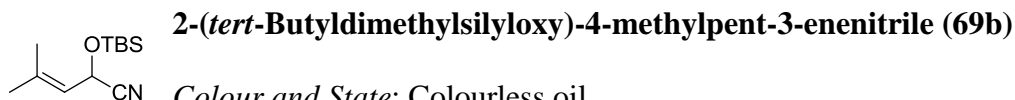


¹H NMR (500 MHz, CDCl₃) δ 7.41-7.30 (m, 5H), 5.84 (dq, *J* = 8.0, 1.3 Hz, 1H), 5.28 (d, *J* = 8.0 Hz, 1H), 2.14 (d, *J* = 1.3 Hz, 3H), 0.92 (s, 9H), 0.21 (s, 3H), 0.18 (s, 3H).

¹³C NMR (125 MHz, CDCl₃) δ 141.56 (e), 140.88 (e), 128.59 (o), 128.31 (o), 126.07 (o), 123.27 (o), 119.12 (e), 59.47 (o), 25.65 (o), 18.22 (e), 16.81 (o), -4.78 (o).

IR (Neat) 2955 (w), 2859 (w), 2236 (w), 1644 (w), 1446 (w), 1254 (m), 1092 (m), 836 (vs), 780 (s) cm⁻¹.

HRMS (ESI[M+Na]⁺) calcd for C₁₇H₂₅NNaOSi 310.1603, found 310.1604.



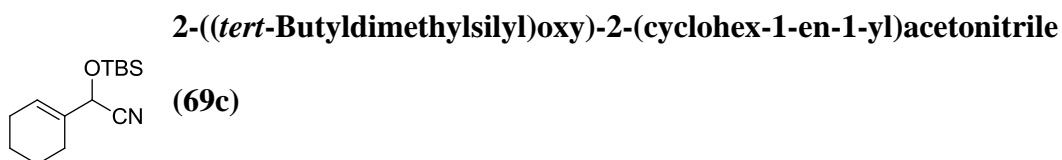
Colour and State: Colourless oil.

¹H NMR (500 MHz, CDCl₃) δ 5.34-5.32 (m, 1H), 5.08 (d, *J* = 8.4 Hz, 1H), 1.77 (s, 3H), 1.72 (s, 3H), 0.90 (s, 9H), 0.16 (s, 3H), 0.13 (s, 3H).

¹³C NMR (125 MHz, CDCl₃) δ 139.07 (e), 121.29 (o), 119.59 (e), 59.08 (o), 25.64 (o), 18.47 (o), 18.18 (e), -4.83 (o), -4.87 (o).

IR (Neat) 2957 (w), 2859 (w), 1673 (w), 1254 (m), 1073 (s), 779 (s), 672 (m) cm⁻¹.

HRMS (ESI[M+NH₄]⁺) calcd for C₁₂H₂₇N₂OSi 243.1893, found 243.1883.



Colour and State: Colourless oil.

¹H NMR (500 MHz, CDCl₃) δ 5.92-5.91 (m, 1H), 4.76 (s, 1H), 2.10-2.06 (m, 4H), 1.73-1.57 (m, 4H), 0.91 (s, 9H), 0.18 (s, 3H), 0.13 (s, 3H).

¹³C NMR (125 MHz, CDCl₃) δ 135.56 (e), 126.97 (o), 119.02 (e), 66.54 (o), 25.63 (o), 25.02 (e), 23.87 (e), 22.25 (e), 22.05 (e), 18.24 (e), -5.10 (o).

IR (Neat) 2930 (m), 2859 (m), 1670 (w), 1438 (w), 1254 (m), 835 (vs), 672 (w) cm⁻¹.

HRMS (ESI[M+NH₄]⁺) calcd for C₁₄H₂₉N₂OSi 269.2049, found 269.2043.

3.2.3.1.2. Representative Experimental Procedure for the Rhodium-Catalysed Allylic Substitution with the Alkenyl Cyanohydrins **56** and **69**

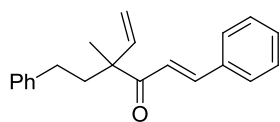
Under an atmosphere of argon, a 1M solution of lithium bis(trimethylsilyl)amide in tetrahydrofuran (0.90 mL, 0.90 mmol) was added dropwise to a solution of (*E*)-2-((*tert*-Butyldimethylsilyl)oxy)-4-phenylbut-3-enenitrile **56c** (179.0 mg, 0.65 mmol) in anhydrous THF (3 mL) at -10 °C. The anion was allowed to form over *ca.* 30 minutes, resulting in an orange homogeneous solution. In a separate flask, [RhCl(COD)]₂ (6.20 mg, 0.013 mmol) and triphenylphosphite (13.1 μl, 0.050 mmol)

were dissolved in anhydrous THF (2 mL) under an atmosphere of argon at room temperature. The mixture was stirred for *ca.* 5 minutes, resulting in a light yellow homogeneous solution, and then cooled to -10 °C. The catalyst solution was then added to the anion *via* Teflon[®] cannula, followed immediately by the addition of methyl (3-methyl-5-phenylpent-1-en-3-yl) carbonate **26a** (117.9 mg, 0.50 mmol) *via* tared 500 μ L gastight syringe. The mixture was allowed to stir for *ca.* 16 hours and then cooled to -40 °C (dry ice/acetonitrile bath). A 1M solution of TBAF in tetrahydrofuran (2.00 mL, 2.00 mmol) was then added, and the resultant mixture was allowed to stir for *ca.* 1 hour at -40 °C. The reaction mixture was quenched with saturated aqueous ammonium chloride solution (2 mL), allowed to warm to room temperature and then partitioned between diethyl ether and saturated aqueous ammonium chloride solution. The combined organic layers were dried using anhydrous magnesium sulfate, filtered and concentrated *in vacuo*. Purification by flash column chromatography (eluting with 2-4% diethyl ether/hexane) afforded the ketone **60a** (110.2 mg, 75%) as a yellow oil.

3.2.3.1.3. Spectral Data for the α,β -Unsaturated Ketone Products 60a-q and 70a-

c

(*E*)-4-Methyl-4-phenethyl-1-phenylhexa-1,5-dien-3-one



(60a)

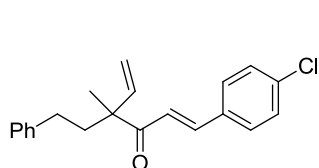
Colour and State: Yellow oil. *Branched:linear* \geq 19:1.

¹H NMR (500 MHz, CDCl₃) δ 7.69 (d, *J* = 15.7 Hz, 1H), 7.57-7.55 (m, 2H), 7.39-7.38 (m, 3H), 7.28-7.25 (m, 2H), 7.18-7.16 (m, 3H), 7.08 (d, *J* = 15.7 Hz, 1H), 6.03 (dd, *J* = 17.5, 10.8 Hz, 1H), 5.30 (d, *J* = 10.8 Hz, 1H), 5.26 (d, *J* = 17.5 Hz, 1H), 2.59 (dt, *J* = 13.0, 4.9 Hz, 1H), 2.47 (dt, *J* = 13.0, 5.0 Hz, 1H), 2.08 (dt, *J* = 13.1, 5.0 Hz, 1H), 1.98 (dt, *J* = 13.1, 4.9 Hz, 1H), 1.37 (s, 3H).

^{13}C NMR (125 MHz, CDCl_3) δ 200.86 (e), 143.05 (o), 142.45 (e), 141.42 (o), 134.93 (e), 130.46 (o), 129.00 (o), 128.53 (o), 128.50 (o), 128.47 (o), 125.99 (o), 121.84 (o), 115.99 (e), 53.56 (e), 39.38 (e), 30.94 (e), 20.32 (o).

IR (Neat) 3026 (w), 2863 (w), 1683 (s), 1631 (w), 1607 (vs), 1449 (m), 1180 (w), 720 (m) cm^{-1} .

HRMS (ESI[M+Na] $^+$) calcd for $\text{C}_{21}\text{H}_{22}\text{NaO}$ 313.1568, found 313.1577.



(E)-1-(4-Chlorophenyl)-4-methyl-4-phenethylhexa-1,5-dien-3-one (60b)

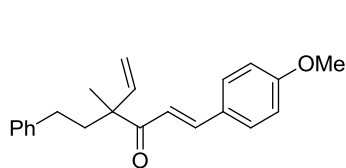
Colour and State: Yellow oil. *Branched:linear* \geq 19:1.

^1H NMR (500 MHz, CDCl_3) δ 7.62 (d, $J = 15.7$ Hz, 1H), 7.49-7.47 (m, 2H), 7.27-7.34 (m, 2H), 7.28-7.25 (m, 2H), 7.19-7.16 (m, 3H), 7.03 (d, $J = 15.7$ Hz, 1H), 6.02 (dd, $J = 17.5, 10.8$ Hz, 1H), 5.31 (dd, $J = 10.7, 0.8$ Hz, 1H), 5.26 (dd, $J = 17.6, 0.6$ Hz, 1H), 2.59 (dt, $J = 12.9, 5.0$ Hz, 1H), 2.47 (dt, $J = 13.0, 5.0$ Hz, 1H), 2.07 (dt, $J = 13.1, 5.0$ Hz, 1H), 1.98 (dt, $J = 13.1, 5.0$ Hz, 1H), 1.37 (s, 3H).

^{13}C NMR (125 MHz, CDCl_3) δ 200.69 (e), 142.38 (e), 141.60 (o), 141.27 (o), 136.32 (e), 133.41 (e), 129.67 (o), 129.28 (o), 128.56 (o), 128.47 (o), 126.05 (o), 122.25 (o), 116.20 (e), 53.60 (e), 39.31 (e), 30.93 (e), 20.27 (o).

IR (Neat) 3085 (w), 2954 (w), 1679 (m), 1633 (w), 1608 (s), 1589 (m), 1268 (w), 986 (s), 871 (w) cm^{-1} .

HRMS (ESI[M+Na] $^+$) calcd for $\text{C}_{21}\text{H}_{21}^{35}\text{ClNaO}$ 347.1179, found 347.1163.



(E)-1-(4-Methoxyphenyl)-4-methyl-4-phenethylhexa-1,5-dien-3-one (60c)

Colour and State: Yellow oil. *Branched:linear* \geq 19:1.

^1H NMR (500 MHz, CDCl_3) δ 7.66 (d, $J = 15.6$ Hz, 1H), 7.53-7.50 (m, 2H), 7.28-7.25 (m, 2H), 7.18-7.16 (m, 3H), 6.95 (d, $J = 15.6$ Hz, 1H), 6.92-6.89 (m, 2H), 6.03

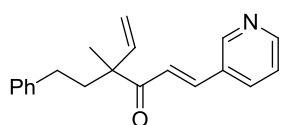
(dd, $J = 17.5, 10.8$ Hz, 1H), 5.29 (d, $J = 10.7$ Hz, 1H), 5.25 (d, $J = 17.6$ Hz, 1H), 3.84 (s, 3H), 2.58 (dt, $J = 13.0, 4.9$ Hz, 1H), 2.48 (dt, $J = 13.0, 4.9$ Hz, 1H), 2.07 (dt, $J = 13.1, 5.0$ Hz, 1H), 1.97 (dt, $J = 13.1, 4.9$ Hz, 1H), 1.36 (s, 3H).

^{13}C NMR (125 MHz, CDCl_3) δ 200.88 (e), 161.55 (e), 142.83 (o), 142.51 (e), 141.60 (o), 130.22 (o), 128.49 (o), 128.45 (o), 127.56 (e), 125.93 (o), 119.47 (o), 115.71 (e), 114.39 (o), 55.47 (o), 53.43 (e), 39.44 (e), 30.93 (e), 20.33 (o).

IR (Neat) 3061 (w), 2838 (w), 1678 (m), 1633 (w), 1594 (vs), 1510 (s), 1324 (w), 1172 (s), 700 (m) cm^{-1} .

HRMS (ESI[M+Na] $^+$) calcd for $\text{C}_{22}\text{H}_{24}\text{NaO}_2$ 343.1674, found 343.1660.

(E)-4-Methyl-4-phenethyl-1-(pyridin-3-yl)hexa-1,5-dien-



3-one (60d)

Colour and State: Yellow oil. *Branched:linear* $\geq 19:1$.

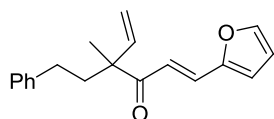
^1H NMR (500 MHz, CDCl_3) δ 8.77 (s, 1H), 8.60 (d, $J = 4.2$ Hz, 1H), 7.86 (dt, $J = 7.9, 1.8$ Hz, 1H), 7.65 (d, $J = 15.8$ Hz, 1H), 7.34 (dd, $J = 7.9, 4.8$ Hz, 1H), 7.28-7.25 (m, 2H), 7.18-7.16 (m, 3H), 7.12 (d, $J = 15.8$ Hz, 1H), 6.01 (dd, $J = 17.5, 10.8$ Hz, 1H), 5.33 (d, $J = 10.7$ Hz, 1H), 5.27 (d, $J = 17.5$ Hz, 1H), 2.60 (dt, $J = 12.9, 5.0$ Hz, 1H), 2.48 (dt, $J = 12.9, 5.1$ Hz, 1H), 2.08 (dt, $J = 13.0, 5.1$ Hz, 1H), 1.99 (dt, $J = 13.1, 5.0$ Hz, 1H), 1.38 (s, 3H).

^{13}C NMR (125 MHz, CDCl_3) δ 200.27 (e), 151.02 (o), 150.02 (o), 142.23 (e), 141.07 (o), 139.20 (o), 134.65 (o), 130.69 (e), 128.53 (o), 128.43 (o), 126.04 (o), 123.79 (o), 123.68 (o), 116.39 (e), 53.59 (e), 39.20 (e), 30.87 (e), 20.20 (o).

IR (Neat) 3060 (w), 2932 (w), 1685 (s), 1610 (s), 1567 (m), 1296 (m), 921 (m), 699 (s) cm^{-1} .

HRMS (ESI[M+Na] $^+$) calcd for $\text{C}_{20}\text{H}_{21}\text{NNaO}$ 314.1521, found 314.1529.

(E)-1-(Furan-2-yl)-4-methyl-4-phenethylhexa-1,5-dien-3-



one (60e)

Colour and State: Yellow oil. *Branched:linear* \geq 19:1.

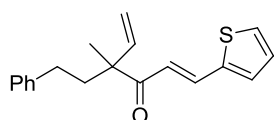
¹H NMR (500 MHz, CDCl₃) δ 7.48 (d, J = 1.5 Hz, 1H), 7.44 (d, J = 15.4 Hz, 1H), 7.28-7.25 (m, 2H), 7.18-7.16 (m, 3H), 6.95 (d, J = 15.4 Hz, 1H), 6.65 (d, J = 3.4 Hz, 1H), 6.48 (dd, J = 3.4, 1.8 Hz, 1H), 6.02 (dd, J = 17.5, 10.8 Hz, 1H), 5.29 (d, J = 10.8 Hz, 1H), 5.25 (d, J = 17.8 Hz, 1H), 2.57 (dt, J = 13.0, 4.9 Hz, 1H), 2.47 (dt, J = 13.0, 4.9 Hz, 1H), 2.07 (dt, J = 13.1, 5.0 Hz, 1H), 1.96 (dt, J = 13.1, 4.9 Hz, 1H), 1.36 (s, 3H).

¹³C NMR (125 MHz, CDCl₃) δ 200.76 (e), 151.63 (e), 144.76 (o), 142.46 (e), 141.36 (o), 129.22 (o), 128.51 (o), 128.47 (o), 125.97 (o), 119.45 (o), 115.99 (o), 115.91 (e), 112.65 (o), 53.41 (e), 39.39 (e), 30.92 (e), 20.22 (o).

IR (Neat) 3085 (w), 2933 (w), 1680 (m), 1604 (s), 1552 (m), 1388 (w), 1058 (m), 1014 (s), 677 (w) cm⁻¹.

HRMS (ESI[M+Na]⁺) calcd for C₁₉H₂₀NaO₂ 303.1361, found 303.1352.

(E)-4-Methyl-4-phenethyl-1-(thiophen-2-yl)hexa-1,5-dien-



3-one (60f)

Colour and State: Yellow oil. *Branched:linear* \geq 19:1.

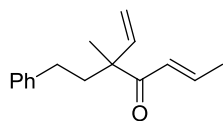
¹H NMR (500 MHz, CDCl₃) δ 7.80 (d, J = 15.3 Hz, 1H), 7.37 (d, J = 5.1 Hz, 1H), 7.29 (d, J = 3.7 Hz, 1H), 7.28-7.25 (m, 2H), 7.18-7.16 (m, 3H), 7.06 (dd, J = 5.1, 3.6 Hz, 1H), 6.85 (d, J = 15.3 Hz, 1H), 6.02 (dd, J = 17.5, 10.8 Hz, 1H), 5.29 (dd, J = 10.7, 0.8 Hz, 1H), 5.24 (dd, J = 17.5, 0.7 Hz, 1H), 2.58 (dt, J = 12.9, 5.0 Hz, 1H), 2.48 (dt, J = 13.0, 5.0 Hz, 1H), 2.06 (ddd, A of ABMX, J_{AB} = 13.7 Hz, J_{AM} = 12.4 Hz, J_{AX} = 5.0 Hz, 1H), 1.96 (ddd, B of ABMX, J_{AB} = 13.7 Hz, J_{BM} = 12.5 Hz, J_{BX} = 5.0 Hz, 1H), 1.36 (s, 3H).

^{13}C NMR (125 MHz, CDCl_3) δ 200.53 (e), 142.44 (e), 141.37 (o), 140.39 (e), 135.53 (o), 131.81 (o), 128.53 (o), 128.50 (o), 128.47 (o), 128.35 (o), 125.99 (o), 120.78 (o), 115.93 (e), 53.39 (e), 39.45 (e), 30.95 (e), 20.31 (o).

IR (Neat) 3084 (w), 2931 (w), 1678 (m), 1632 (w), 1591 (s), 1303 (w), 1033 (m), 856 (w), 700 (s) cm^{-1} .

HRMS (ESI $[\text{M}+\text{Na}]^+$) calcd for $\text{C}_{19}\text{H}_{20}\text{NaOS}$ 319.1133, found 319.1132.

(E)-3-Methyl-3-phenethylhepta-1,5-dien-4-one (60g)



Colour and State: Pale yellow oil. Branched:linear \geq 19:1.

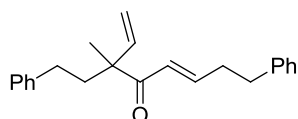
^1H NMR (500 MHz, CDCl_3) δ 7.29-7.26 (m, 2H), 7.19-7.16 (m, 3H), 6.97 (dq, $J = 15.1, 7.0$ Hz, 1H), 6.48 (dq, $J = 15.2, 1.6$ Hz, 1H), 5.96 (dd, $J = 17.5, 10.8$ Hz, 1H), 5.25 (dd, $J = 10.8, 0.7$ Hz, 1H), 5.19 (dd, $J = 17.5, 0.7$ Hz, 1H), 2.54 (dt, $J = 13.0, 5.0$ Hz, 1H), 2.43 (dt, $J = 13.0, 5.0$ Hz, 1H), 2.00 (ddd, A of ABMX, $J_{AB} = 13.6$ Hz, $J_{AM} = 12.5$ Hz, $J_{AX} = 5.0$ Hz, 1H), 1.93-1.87 (m, 1H), 1.88 (dd, $J = 6.9, 1.7$ Hz, 3H), 1.30 (s, 3H).

^{13}C NMR (125 MHz, CDCl_3) δ 200.76 (e), 143.07 (o), 142.51 (e), 141.43 (o), 128.51 (o), 128.44 (o), 126.89 (o), 125.96 (o), 115.66 (e), 53.08 (e), 39.26 (e), 30.86 (e), 20.09 (o), 18.37 (o).

IR (Neat) 3086 (w), 2936 (w), 1690 (s), 1625 (s), 1497 (w), 1289 (m), 919 (s), 790 (w) cm^{-1}

HRMS (ESI $[\text{M}+\text{H}]^+$) calcd for $\text{C}_{16}\text{H}_{21}\text{O}$ 229.1592, found 229.1584.

(E)-3-Methyl-3-phenethyl-8-phenylocta-1,5-dien-4-one



(60h)

Colour and State: Pale yellow oil. Branched:linear \geq 19:1.

^1H NMR (500 MHz, CDCl_3) δ 7.29-7.25 (m, 4H), 7.19-7.15 (m, 6H), 6.98 (dt, $J = 15.2, 7.0$ Hz, 1H), 6.42 (d, $J = 15.3$ Hz, 1H), 5.91 (dd, $J = 17.5, 10.8$ Hz, 1H), 5.23

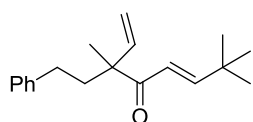
(d, $J = 10.8$ Hz, 1H), 5.15 (d, $J = 17.5$ Hz, 1H), 2.77 (t, $J = 7.7$ Hz, 2H), 2.54-2.48 (m, 2H), 2.40 (dt, $J = 13.0, 5.0$ Hz, 1H), 1.95 (dt, $J = 13.1, 5.0$ Hz, 1H), 1.87 (dt, $J = 13.1, 5.0$ Hz, 1H), 1.26 (s, 3H).

^{13}C NMR (125 MHz, CDCl_3) δ 200.71 (e), 146.39 (o), 142.42 (e), 141.29 (o), 140.88 (e), 128.51 (o), 128.46 (o), 128.41 (o), 126.20 (o), 125.92 (o), 125.86 (o), 115.66 (e), 53.11 (e), 39.21 (e), 34.50 (e), 34.22 (e), 30.80 (e), 20.05 (o).

IR (Neat) 3062 (w), 2860 (w), 1689 (s), 1623 (s), 1604 (m), 1454 (m), 1127 (w), 920 (m), 698 (s) cm^{-1} .

HRMS (ESI[M+Na] $^+$) calcd for $\text{C}_{23}\text{H}_{26}\text{NaO}$ 341.1881, found 341.1872.

(E)-3,7,7-Trimethyl-3-phenethylocta-1,5-dien-4-one (60i)



Colour and State: Pale yellow oil. Branched:linear $\geq 19:1$.

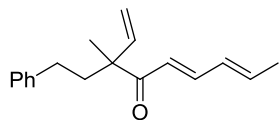
^1H NMR (500 MHz, CDCl_3) δ 7.29-7.26 (m, 2H), 7.19-7.15 (m, 3H), 6.96 (d, $J = 15.6$ Hz, 1H), 6.36 (d, $J = 15.6$ Hz, 1H), 5.97 (dd, $J = 17.5, 10.8$ Hz, 1H), 5.25 (d, $J = 10.8$ Hz, 1H), 5.19 (d, $J = 17.6$ Hz, 1H), 2.54 (dt, $J = 13.0, 5.0$ Hz, 1H), 2.43 (dt, $J = 13.0, 4.9$ Hz, 1H), 2.00 (dt, $J = 13.1, 4.9$ Hz, 1H), 1.91 (dt, $J = 13.1, 5.0$ Hz, 1H), 1.30 (s, 3H), 1.07 (s, 9H).

^{13}C NMR (125 MHz, CDCl_3) δ 201.40 (e), 157.49 (o), 142.52 (e), 141.53 (o), 128.48 (o), 128.40 (o), 125.92 (o), 120.24 (o), 115.53 (e), 53.40 (e), 39.47 (e), 33.92 (e), 30.91 (e), 28.87 (o), 20.24 (o).

IR (Neat) 3086 (w), 2961 (m), 1690 (s), 1621 (s), 1456 (m), 1199 (w), 919 (s), 804 (w), 699 (s) cm^{-1}

HRMS (ESI[M+Na] $^+$) calcd for $\text{C}_{19}\text{H}_{26}\text{NaO}$ 293.1881, found 293.1886.

(5E,7E)-3-Methyl-3-phenethylnona-1,5,7-trien-4-one (60j)



Colour and State: Yellow oil. *Branched:linear* \geq 19:1.

The product was isolated as a 6:1 mixture of (5E,7E) and (5E,7Z) isomers. Data is provided for the major isomer only.

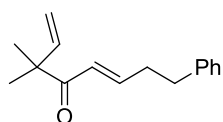
$^1\text{H NMR}$ (500 MHz, CDCl_3) δ 7.30-7.26 (m, 3H), 7.19-7.16 (m, 3H), 6.41 (d, $J = 14.7$ Hz, 1H), 6.25-6.13 (m, 2H), 5.97 (dd, $J = 17.5, 10.8$ Hz, 1H), 5.24 (dd, $J = 10.7, 0.8$ Hz, 1H), 5.19 (dd, $J = 17.5, 0.7$ Hz, 1H), 2.54 (dt, $J = 13.0, 5.0$ Hz, 1H), 2.44 (dt, $J = 13.0, 5.0$ Hz, 1H), 2.00 (dt, $J = 13.1, 5.0$ Hz, 1H), 1.91 (dt, $J = 13.2, 4.7$ Hz, 1H), 1.86 (d, $J = 5.0$ Hz, 3H), 1.30 (s, 3H).

$^{13}\text{C NMR}$ (125 MHz, CDCl_3) δ 201.32 (e), 143.41 (o), 142.50 (e), 141.54 (o), 140.67 (o), 130.42 (o), 128.47 (o), 128.41 (o), 125.91 (o), 123.09 (o), 115.52 (e), 53.22 (e), 39.37 (e), 30.87 (e), 20.20 (o), 18.92 (o).

IR (Neat) 3085 (w), 2863 (w), 1682 (s), 1633 (m), 1591 (s), 1329 (m), 1031 (m), 866 (w), 699 (s) cm^{-1}

HRMS (ESI[M+Na] $^+$) calcd for $\text{C}_{18}\text{H}_{22}\text{NaO}$ 277.1568, found 277.1579.

(E)-3,3-Dimethyl-8-phenylocta-1,5-dien-4-one (60k)



Colour and State: Pale yellow oil. *Branched:linear* \geq 19:1.

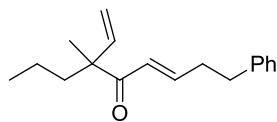
$^1\text{H NMR}$ (500 MHz, CDCl_3) δ 7.29-7.26 (m, 2H), 7.21-7.15 (m, 3H), 6.94 (dt, $J = 15.3, 7.0$ Hz, 1H), 6.38 (dt, $J = 15.3, 1.5$ Hz, 1H), 5.87 (dd, $J = 17.3, 10.8$ Hz, 1H), 5.14 (d, $J = 10.6$ Hz, 1H), 5.13 (d, $J = 17.8$ Hz, 1H), 2.76 (t, $J = 7.7$ Hz, 2H), 2.53-2.48 (m, 2H), 1.20 (s, 6H).

$^{13}\text{C NMR}$ (125 MHz, CDCl_3) δ 201.37 (e), 146.14 (o), 142.51 (o), 140.98 (e), 128.53 (o), 128.50 (o), 126.20 (o), 125.76 (o), 114.60 (e), 49.67 (e), 34.54 (e), 34.25 (e), 23.45 (o).

IR (Neat) 3062 (w), 2931 (w), 1691 (s), 1624 (s), 1455 (m), 1165 (w), 919 (m), 699 (m) cm^{-1} .

HRMS (ESI[M+H]⁺) calcd for C₁₆H₂₁O 229.1592, found 229.1586.

(E)-6-Methyl-1-phenyl-6-vinylnon-3-en-5-one (60l)



Colour and State: Pale yellow oil. *Branched:linear* \geq 19:1.

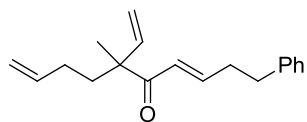
¹H NMR (500 MHz, CDCl₃) δ 7.29-7.26 (m, 2H), 7.20-7.15 (m, 3H), 6.93 (dt, $J = 15.3, 7.0$ Hz, 1H), 6.37 (dt, $J = 15.3, 1.5$ Hz, 1H), 5.86 (dd, $J = 17.5, 10.8$ Hz, 1H), 5.15 (dd, $J = 10.7, 0.9$ Hz, 1H), 5.09 (dd, $J = 17.5, 0.8$ Hz, 1H), 2.76 (t, $J = 7.7$ Hz, 2H), 2.53-2.48 (m, 2H), 1.62 (ddd, A of ABMX, $J_{AB} = 13.6$ Hz, $J_{AM} = 12.3$ Hz, $J_{AX} = 4.8$ Hz, 1H), 1.52 (ddd, B of ABMX, $J_{AB} = 13.5$ Hz, $J_{BM} = 12.4$ Hz, $J_{BX} = 4.4$ Hz, 1H), 1.27-1.17 (m, 1H), 1.16 (s, 3H), 1.14-1.03 (m, 1H), 0.87 (t, $J = 7.3$ Hz, 3H).

¹³C NMR (125 MHz, CDCl₃) δ 201.21 (e), 145.90 (o), 141.86 (o), 140.97 (e), 128.51 (o), 128.49 (o), 126.18 (o), 126.04 (o), 115.09 (e), 53.19 (e), 39.49 (e), 34.54 (e), 34.20 (e), 19.99 (o), 17.58 (e), 14.85 (o).

IR (Neat) 3028 (w), 2932 (m), 1690 (s), 1624 (s), 1454 (m), 989 (m), 745 (m), 698 (s) cm^{-1} .

HRMS (ESI[M+Na]⁺) calcd for C₁₈H₂₄NaO 279.1725, found 279.1717.

(E)-6-Methyl-1-phenyl-6-vinyldeca-3,9-dien-5-one (60m)



Colour and State: Pale yellow oil. *Branched:linear* \geq 19:1.

¹H NMR (500 MHz, CDCl₃) δ 7.29-7.26 (m, 2H), 7.21-7.15 (m, 3H), 6.94 (dt, $J = 15.3, 7.0$ Hz, 1H), 6.38 (dt, $J = 15.3, 1.5$ Hz, 1H), 5.86 (dd, $J = 17.5, 10.8$ Hz, 1H), 5.78 (ddt, $J = 16.9, 10.4, 6.5$ Hz, 1H), 5.19 (dd, $J = 10.8, 0.8$ Hz, 1H), 5.11 (dd, $J = 17.5, 0.8$ Hz, 1H), 4.99 (dq, $J = 17.1, 1.7$ Hz, 1H), 4.95-4.92 (m, 1H), 2.76 (t, $J = 7.7$

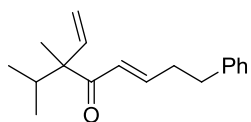
Hz, 2H), 2.53-2.49 (m, 2H), 2.00-1.92 (m, 1H), 1.90-1.82 (m, 1H), 1.74 (ddd, A of ABMX, $J_{AB} = 13.6$ Hz, $J_{AM} = 12.0$ Hz, $J_{AX} = 4.8$ Hz, 1H), 1.66 (ddd, B of ABMX, $J_{AB} = 13.6$ Hz, $J_{BM} = 12.1$ Hz, $J_{BX} = 5.0$ Hz, 1H), 1.19 (s, 3H).

$^{13}\text{C NMR}$ (125 MHz, CDCl_3) δ 200.87 (e), 146.25 (o), 141.43 (o), 140.94 (e), 138.67 (o), 128.54 (o), 128.49 (o), 126.21 (o), 125.96 (o), 115.51 (e), 114.59 (e), 52.91 (e), 36.28 (e), 34.54 (e), 34.22 (e), 28.65 (e), 19.96 (o).

IR (Neat) 3083 (w), 2932 (w), 1690 (s), 1623 (s), 1454 (m), 912 (s), 795 (w), 698 (s) cm^{-1} .

HRMS (ESI[M+Na] $^+$) calcd for $\text{C}_{19}\text{H}_{24}\text{NaO}$ 291.1725, found 291.1721.

(E)-3-Isopropyl-3-methyl-8-phenylocta-1,5-dien-4-one (60n)



Colour and State: Pale yellow oil. *Branched:linear* \geq 19:1.

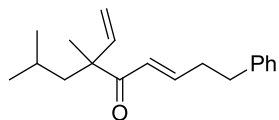
$^1\text{H NMR}$ (500 MHz, CDCl_3) δ 7.30-7.26 (m, 2H), 7.20-7.15 (m, 3H), 6.93 (dt, $J = 15.2, 7.0$ Hz, 1H), 6.41 (dt, $J = 15.2, 1.5$ Hz, 1H), 5.92 (dd, $J = 17.5, 10.9$ Hz, 1H), 5.20 (dd, $J = 10.9, 0.9$ Hz, 1H), 5.07 (dd, $J = 17.5, 0.9$ Hz, 1H), 2.77 (t, $J = 7.7$ Hz, 2H), 2.53-2.49 (m, 2H), 2.13 (septet, $J = 6.8$ Hz, 1H), 1.08 (s, 3H), 0.83 (d, $J = 6.9$ Hz, 3H), 0.74 (d, $J = 6.8$ Hz, 3H).

$^{13}\text{C NMR}$ (125 MHz, CDCl_3) δ 201.29 (e), 145.87 (o), 140.98 (e), 140.60 (o), 128.51 (o), 126.30 (o), 126.18 (o), 116.23 (e), 56.74 (e), 34.57 (e), 34.26 (e), 32.86 (o), 17.57 (o), 17.48 (o), 14.14 (o).

IR (Neat) 3062 (w), 2964 (m), 1688 (s), 1623 (s), 1454 (m), 1180 (w), 917 (m), 699 (s) cm^{-1} .

HRMS (ESI[M+Na] $^+$) calcd for $\text{C}_{18}\text{H}_{24}\text{NaO}$ 279.1725, found 279.1718.

(E)-6,8-Dimethyl-1-phenyl-6-vinylnon-3-en-5-one (60o)



Colour and State: Pale yellow oil. *Branched:linear* \geq 19:1.

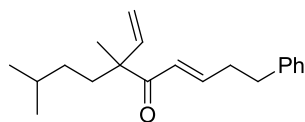
$^1\text{H NMR}$ (500 MHz, CDCl_3) δ 7.29-7.26 (m, 2H), 7.21-7.15 (m, 3H), 6.92 (dt, $J = 15.3, 6.9$ Hz, 1H), 6.40 (dt, $J = 15.3, 1.5$ Hz, 1H), 5.89 (dd, $J = 17.5, 10.8$ Hz, 1H), 5.14 (dd, $J = 10.8, 0.8$ Hz, 1H), 5.09 (dd, $J = 17.5, 0.8$ Hz, 1H), 2.76 (t, $J = 7.7$ Hz, 2H), 2.54-2.49 (m, 2H), 1.65-1.52 (m, 3H), 1.20 (s, 3H), 0.86 (d, $J = 6.3$ Hz, 3H), 0.80 (d, $J = 6.2$ Hz, 3H).

$^{13}\text{C NMR}$ (125 MHz, CDCl_3) δ 201.44 (e), 145.75 (o), 142.42 (o), 140.99 (e), 128.54 (o), 128.49 (o), 126.31 (o), 126.19 (o), 114.90 (e), 53.21 (e), 46.17 (e), 34.55 (e), 34.19 (e), 24.90 (o), 24.75 (o), 24.23 (o), 20.35 (o).

IR (Neat) 3086 (w), 2955 (m), 1690 (s), 1624 (s), 1455 (m), 1294 (w), 989 (m), 698 (s) cm^{-1} .

HRMS (ESI $[\text{M}+\text{Na}]^+$) calcd for $\text{C}_{19}\text{H}_{26}\text{NaO}$ 293.1881, found 293.1872.

(E)-6,9-Dimethyl-1-phenyl-6-vinyldec-3-en-5-one (60p)



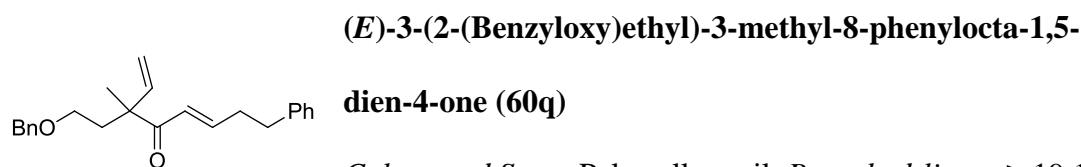
Colour and State: Pale yellow oil. *Branched:linear* \geq 19:1.

$^1\text{H NMR}$ (500 MHz, CDCl_3) δ 7.29-7.26 (m, 2H), 7.20-7.15 (m, 3H), 6.93 (dt, $J = 15.3, 7.0$ Hz, 1H), 6.38 (dt, $J = 15.3, 1.5$ Hz, 1H), 5.86 (dd, $J = 17.5, 10.8$ Hz, 1H), 5.16 (dd, $J = 10.8, 0.8$ Hz, 1H), 5.09 (dd, $J = 17.6, 0.8$ Hz, 1H), 2.76 (t, $J = 7.7$ Hz, 2H), 2.53-2.48 (m, 2H), 1.65 (dt, $J = 13.0, 4.7$ Hz, 1H), 1.54 (dt, $J = 13.1, 4.4$ Hz, 1H), 1.45 (nonet, $J = 6.7$ Hz, 1H), 1.15 (s, 3H), 1.07 (ddt, $J = 12.8, 6.6, 4.5$ Hz, 1H), 0.94 (ddt, $J = 12.8, 6.8, 4.8$ Hz, 1H), 0.85 (d, $J = 6.6$ Hz, 3H), 0.85 (d, $J = 6.6$ Hz, 3H).

$^{13}\text{C NMR}$ (125 MHz, CDCl_3) δ 201.32 (e), 145.97 (o), 141.89 (o), 140.99 (e), 128.53 (o), 128.49 (o), 126.21 (o), 126.03 (o), 115.18 (e), 53.04 (e), 34.96 (e), 34.56 (e), 34.22 (e), 33.19 (e), 28.67 (o), 22.66 (o), 22.65 (o), 19.97 (o).

IR (Neat) 3028 (w), 2932 (m), 1691 (s), 1624 (s), 1497 (w), 1031 (m), 789 (w), 698 (s) cm^{-1} .

HRMS (ESI[M+Na]⁺) calcd for C₂₀H₂₈NaO 307.2038, found 307.2048.



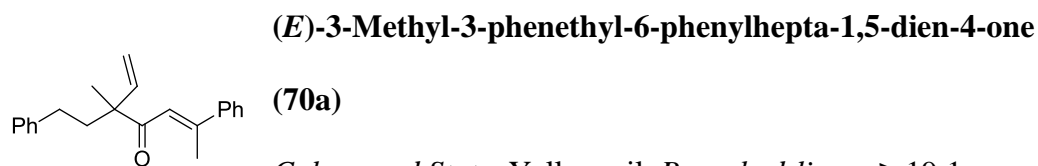
Colour and State: Pale yellow oil. *Branched:linear* \geq 19:1.

¹H NMR (500 MHz, CDCl₃) δ 7.34-7.25 (m, 7H), 7.20-7.14 (m, 3H), 6.91 (dt, $J = 15.3, 6.9$ Hz, 1H), 6.39 (dt, $J = 15.3, 1.5$ Hz, 1H), 5.87 (dd, $J = 17.5, 10.8$ Hz, 1H), 5.18 (dd, $J = 10.8, 0.7$ Hz, 1H), 5.12 (dd, $J = 17.5, 0.6$ Hz, 1H), 4.43 (s, 2H), 3.47 (ddd, A of ABMX, $J_{AB} = 9.4$ Hz, $J_{AM} = 8.2$ Hz, $J_{AX} = 5.7$ Hz, 1H), 3.42 (ddd, B of ABMX, $J_{AB} = 9.4$ Hz, $J_{BM} = 8.1$ Hz, $J_{BX} = 6.5$ Hz, 1H), 2.73 (t, $J = 7.7$ Hz, 2H), 2.50-2.46 (m, 2H), 2.07 (ddd, A of ABMX, $J_{AB} = 14.1$ Hz, $J_{AM} = 8.0$ Hz, $J_{AX} = 6.3$ Hz, 1H), 1.95 (ddd, B of ABMX, $J_{AB} = 13.8$ Hz, $J_{BM} = 8.1$ Hz, $J_{BX} = 5.7$ Hz, 1H), 1.21 (s, 3H).

¹³C NMR (125 MHz, CDCl₃) δ 200.41 (e), 146.10 (o), 141.32 (o), 140.98 (e), 138.49 (e), 128.53 (o), 128.48 (o), 128.41 (o), 127.69 (o), 127.60 (o), 126.19 (o), 125.88 (o), 115.47 (e), 73.09 (e), 66.94 (e), 51.82 (e), 36.68 (e), 34.51 (e), 34.20 (e), 20.45 (o).

IR (Neat) 3028 (w), 2932 (w), 1690 (m), 1623 (m), 1496 (w), 1097 (m), 735 (s), 697 (s) cm^{-1} .

HRMS (ESI[M+Na]⁺) calcd for C₂₄H₂₈NaO₂ 371.1987, found 371.1987.



Colour and State: Yellow oil. *Branched:linear* \geq 19:1.

¹H NMR (500 MHz, CDCl₃) δ 7.46-7.43 (m, 2H), 7.40-7.35 (m, 3H), 7.28-7.25 (m, 2H), 7.18-7.16 (m, 3H), 6.72 (s, 1H), 6.05 (dd, $J = 17.5, 10.8$ Hz, 1H), 5.26 (d, $J =$

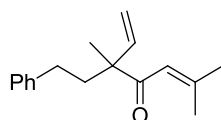
10.3 Hz, 1H), 5.23 (d, $J = 17.4$ Hz, 1H), 2.59 (dt, $J = 12.9, 5.0$ Hz, 1H), 2.53 (s, 3H), 2.49 (dt, $J = 13.1, 5.0$ Hz, 1H), 2.07 (dt, $J = 13.0, 5.0$ Hz, 1H), 1.96 (dt, $J = 13.1, 5.0$ Hz, 1H), 1.35 (s, 3H).

$^{13}\text{C NMR}$ (125 MHz, CDCl_3) δ 202.92 (e), 154.57 (e), 143.14 (e), 142.55 (e), 142.05 (o), 129.08 (o), 128.67 (o), 128.52 (o), 128.46 (o), 126.61 (o), 125.96 (o), 121.95 (o), 115.31 (o), 54.48 (e), 39.80 (e), 31.06 (e), 20.48 (o), 18.79 (o).

IR (Neat) 3084 (w), 2931 (w), 1677 (s), 1631 (w), 1597 (s), 1446 (m), 1265 (w), 961 (m), 697 (s) cm^{-1} .

HRMS (ESI[M+Na] $^+$) calcd for $\text{C}_{22}\text{H}_{24}\text{NaO}$ 327.1725, found 327.1729.

3,6-Dimethyl-3-phenethylhepta-1,5-dien-4-one (70b)



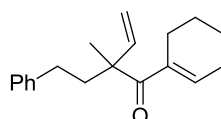
Colour and State: Pale yellow oil. *Branched:linear* $\geq 19:1$.

$^1\text{H NMR}$ (500 MHz, CDCl_3) δ 7.29-7.27 (m, 2H), 7.19-7.16 (m, 3H), 6.28-6.27 (m, 1H), 5.98 (dd, $J = 17.5, 10.8$ Hz, 1H), 5.21 (dd, $J = 10.7, 0.9$ Hz, 1H), 5.17 (dd, $J = 17.5, 0.8$ Hz, 1H), 2.54 (dt, $J = 13.0, 4.9$ Hz, 1H), 2.43 (dt, $J = 12.8, 4.9$ Hz, 1H), 2.14 (d, $J = 1.1$ Hz, 3H), 1.99 (dt, $J = 13.1, 4.9$ Hz, 1H), 1.90 (d, $J = 1.1$ Hz, 3H), 1.89 (dt, $J = 13.1, 5.0$ Hz, 1H), 1.28 (s, 3H).

$^{13}\text{C NMR}$ (125 MHz, CDCl_3) δ 202.47 (e), 156.05 (e), 142.65 (e), 142.13 (o), 128.48 (o), 128.42 (o), 125.90 (o), 120.90 (o), 114.92 (e), 53.86 (e), 39.70 (e), 30.96 (e), 28.04 (o), 21.06 (o), 20.29 (o).

HRMS (ESI[M+H] $^+$) calcd for $\text{C}_{17}\text{H}_{23}\text{O}$ 243.1749, found 243.1743.

1-(Cyclohex-1-en-1-yl)-2-methyl-2-phenethylbut-3-en-1-one (70c)



Colour and State: Pale yellow oil. *Branched:linear* $\geq 19:1$.

$^1\text{H NMR}$ (500 MHz, CDCl_3) δ 7.28-7.25 (m, 2H), 7.19-7.15 (m, 3H), 6.11 (dd, $J = 17.5, 10.9$ Hz, 1H), 5.15 (d, $J = 10.7$ Hz, 1H), 5.14 (d, $J = 17.9$ Hz, 1H), 2.54 (dt, $J =$

12.9, 4.8 Hz, 1H), 2.36 (dt, $J = 13.0, 4.7$ Hz, 1H), 2.29-2.24 (m, 1H), 2.20-2.14 (m, 3H), 2.09 (dt, $J = 13.0, 4.7$ Hz, 1H), 1.97 (dt, $J = 13.1, 4.9$ Hz, 1H), 1.66-1.57 (m, 4H), 1.34 (s, 3H).

^{13}C NMR (125 MHz, CDCl_3) δ 205.26 (e), 143.76 (o), 142.69 (e), 138.42 (o), 137.78 (e), 128.48 (o), 128.44 (o), 125.89 (o), 113.46 (e), 53.29 (e), 41.74 (e), 31.07 (e), 25.71 (e), 25.09 (e), 23.48 (o), 22.34 (e), 21.65 (e).

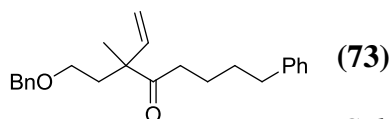
IR (Neat) 3084 (w), 2932 (m), 1659 (s), 1630 (m), 1454 (m), 1269 (w), 1179 (w), 912 (m), 698 (s) cm^{-1} .

HRMS (ESI $[\text{M}+\text{Na}]^+$) calcd for $\text{C}_{19}\text{H}_{24}\text{NaO}$ 291.1725, found 291.1735.

3.2.3.1.4. Representative Experimental Procedure for the 1,4-Reduction of the Ketone **60q**

Under an atmosphere of argon at room temperature, (*E*)-3-(2-(Benzyloxy)ethyl)-3-methyl-8-phenylocta-1,5-dien-4-one **60q** (80.8 mg, 0.232 mmol) was added to a stirring slurry of triphenylphosphine copper hydride hexamer ($[\text{PPh}_3\text{CuH}]_6$) (168.0 mg, 0.086 mmol) in benzene (6 mL) and water (17.0 μL , 0.94 mmol). The resultant mixture was stirred under argon at room temperature for 1 hour, and then left to stir in air for 1 hour. The mixture was then filtered over a pad of celite and concentrated *in vacuo* to afford a crude oil. Purification by flash column chromatography (eluting with 0, 2 then 4% ethyl acetate/hexane) yielded the ketone **73** (76.4 mg, 94%) as a colourless oil.

3-(2-(benzyloxy)ethyl)-3-methyl-8-phenyloct-1-en-4-one



Colour and State: Colourless oil.

^1H NMR (500 MHz, CDCl_3) δ 7.34-7.24 (m, 7H), 7.18-7.14 (m, 3H), 5.90 (dd, $J = 17.4, 10.8$ Hz, 1H), 5.17 (d, $J = 10.7$ Hz, 1H), 5.13 (d, $J = 17.5$ Hz, 1H), 4.42 (s, 2H),

3.47 (ddd, A of ABMX, $J_{AB} = 9.5$ Hz, $J_{AM} = 7.5$ Hz, $J_{AX} = 5.8$ Hz, 1H), 3.42 (dt, $J = 9.4, 7.2$ Hz, 1H), 2.56 (t, $J = 7.0$ Hz, 2H), 2.46 (t, $J = 6.6$ Hz, 2H), 3.42 (dt, $J = 14.1, 7.1$ Hz, 1H), 1.91 (ddd, $J = 13.6, 7.2, 6.2$ Hz, 1H), 1.54-1.51 (m, 4H), 1.22 (s, 3H).

^{13}C NMR (125 MHz, CDCl_3) δ 212.11 (e), 142.52 (e), 141.71 (o), 138.38 (e), 128.49 (o), 128.44 (o), 128.37 (o), 127.76 (o), 127.66 (o), 125.77 (o), 115.06 (e), 73.16 (e), 66.82 (e), 52.95 (e), 37.58 (e), 37.21 (e), 35.96 (e), 31.12 (e), 23.71 (e), 20.21 (o).

IR (Neat) 3062 (w), 2932 (w), 1705 (m), 1633 (w), 16-3 (w), 1453 (m), 1099 (m), 697 (s) cm^{-1} .

HRMS (ESI[M+Na] $^+$) calcd for $\text{C}_{24}\text{H}_{30}\text{NaO}_2$ 373.2143, found 373.2145.

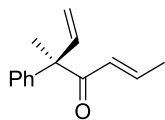
3.2.3.1.5. Representative Experimental Procedure for the Stereospecific Rhodium-Catalysed Allylic Substitution with the Alkenyl Cyanohydrins **56**

To a stirring solution of (*R*)-2-phenylbut-3-en-2-ol **45a** (71.6 mg, 0.483 mmol) in anhydrous tetrahydrofuran (1.5 mL) at 0 °C was added *n*-butyllithium (0.193 mL, 0.483 mmol). The mixture was stirred for *ca.* 15 minutes and methyl chloroformate (37.0 μL , 0.483 mmol) was added dropwise. The mixture was then allowed to warm to room temperature and stirred for *ca.* 1 hour. In a separate flask, a 1M solution of lithium bis(trimethylsilyl)amide in tetrahydrofuran (1.35 mL, 1.35 mmol) was added dropwise to a solution of (*E*)-2-((*tert*-butyldimethylsilyl)oxy)pent-3-enenitrile **56b** (204.0 mg, 0.966 mmol) in anhydrous tetrahydrofuran (2 mL) at -10 °C. The anion was allowed to form over *ca.* 30 minutes, resulting in a light yellow homogeneous solution. In another flask, $[\text{RhCl}(\text{COD})]_2$ (5.7 mg, 0.012 mmol) and tris(2,2,2-trifluoroethyl) phosphite (10.7 μL , 0.048 mmol) were dissolved in anhydrous tetrahydrofuran (1.5 mL) at room temperature. The mixture was stirred for *ca.* 5 minutes, also resulting in a light yellow homogeneous solution. All three flasks were then cooled to -10 °C and the cyanohydrin solution was added to the carbonate

solution, followed quickly by the addition of the catalyst solution, all via Teflon[®] cannula. The mixture was allowed to stir for *ca.* 5 hours and then cooled to -40 °C (dry ice/acetonitrile bath). A 1M solution of TBAF in tetrahydrofuran (3.00 mL, 3.00 mmol) was then added, and the resultant mixture was allowed to stir for *ca.* 1 hour at -40 °C. The reaction mixture was quenched with saturated aqueous ammonium chloride solution (2 mL), allowed to warm to room temperature and then partitioned between diethyl ether and saturated aqueous ammonium chloride solution. The combined organic layers were dried using anhydrous magnesium sulfate, filtered and concentrated *in vacuo*. Purification by flash column chromatography (eluting with 2-4% diethyl ether/hexane) afforded the ketone **74a** (61.1 mg, 63%) as a yellow oil.

3.2.3.1.6. Spectral Data for the Enantiomerically Enriched α,β -Unsaturated Ketone Products **74a-b**

(*R,E*)-3-Methyl-3-phenylhepta-1,5-dien-4-one (74a)



Colour and State: Yellow oil. *Branched:linear* \geq 19:1.

¹H NMR (500 MHz, CDCl₃) δ 7.36-7.32 (m, 2H), 7.28-7.25 (m, 1H), 7.21-7.19 (m, 2H), 6.95 (dq, *J* = 15.2, 7.0 Hz, 1H), 6.41 (dd, *J* = 17.5, 10.8 Hz, 1H), 6.04 (dq, *J* = 15.2, 1.7 Hz, 1H), 5.32 (dd, *J* = 10.7, 0.9 Hz, 1H), 5.12 (dd, *J* = 17.4, 0.9 Hz, 1H), 1.76 (dd, *J* = 7.0, 1.7 Hz, 3H), 1.54 (s, 3H).

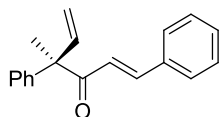
¹³C NMR (125 MHz, CDCl₃) δ 198.64 (e), 143.17 (e), 142.75 (o), 140.17 (o), 128.84 (o), 128.30 (o), 127.31 (o), 127.04 (o), 116.47 (e), 58.38 (e), 23.01 (o), 18.25 (o).

IR (Neat) 2982 (w), 1694 (s), 1627 (s), 1444 (m), 1068 (m), 928 (m), 665 (w) cm⁻¹.

HRMS (ESI[M+H]⁺) calcd for C₁₄H₁₇O 201.1279, found 201.1273.

HPLC separation conditions: CHIRALCEL OJ-H column, hexane/isopropanol (99.5:0.5), flow rate: 1.0 mL/min; *t_R* 25.5 min for (*S*)-enantiomer (minor) and 29.3 min for (*R*)-enantiomer (major), 91% *ee*; $[\alpha]_D^{20}$ + 58.2 (*c* 1.0, CHCl₃).

(*R,E*)-4-Methyl-1,4-diphenylhexa-1,5-dien-3-one (74b)



Colour and State: Pale yellow oil. *Branched:linear* \geq 19:1.

$^1\text{H NMR}$ (500 MHz, CDCl_3) δ 7.68 (d, $J = 15.7$ Hz, 1H), 7.42-7.25 (m, 10H), 6.64 (d, $J = 15.7$ Hz, 1H), 6.49 (dd, $J = 17.5, 10.8$ Hz, 1H), 5.36 (d, $J = 10.8$ Hz, 1H), 5.17 (d, $J = 17.5$ Hz, 1H), 1.62 (s, 3H).

$^{13}\text{C NMR}$ (125 MHz, CDCl_3) δ 198.86 (e), 143.12 (e), 142.63 (o), 140.17 (o), 134.84 (e), 130.39 (o), 128.99 (o), 128.90 (o), 128.49 (o), 127.39 (o), 127.21 (o), 123.44 (o), 116.75 (e), 58.86 (e), 23.32 (o).

IR (Neat) 3083 (w), 2934 (w), 1686 (s), 1633 (w), 1607 (s), 1039 (m), 701 (s) cm^{-1} .

HRMS (ESI[M+Na] $^+$) calcd for $\text{C}_{19}\text{H}_{18}\text{NaO}$ 285.1255, found 285.1245.

HPLC separation conditions: CHIRALCEL OJ-H column, hexane/isopropanol (99:1), flow rate: 1.0 mL/min; t_R 15.2 min for (*R*)-enantiomer (major) and 20.0 min for (*S*)-enantiomer (minor), 90% *ee*.

-
- ¹ Plietker, B.; Dieskau, A.; Möws, K.; Jatsch, A. *Angew. Chem. Int. Ed.* **2008**, *47*, 198.
- ² Guzman-Martinez, A.; Hoveyda, A. H. *J. Am. Chem. Soc.* **2010**, *132*, 10634.
- ³ Kurono, N.; Yamaguchi, M.; Suzuki, K.; Ohkuma, T. *J. Org. Chem.* **2005**, *70*, 6530.
- ⁴ Ritzen, B.; van Oers, M. C. M.; van Delft, F. L.; Rutjes, F. P. J. T. *J. Org. Chem.* **2009**, *74*, 7548.
- ⁵ (a) Kachinsky, J. L. C.; Salomon, R. G. *J. Org. Chem.* **1986**, *51*, 1393. (b) Marceau, P.; Gautreau, L.; Béguin, F. *J. Organomet. Chem.* **1991**, *403*, 21.
- ⁶ Ou, L.; Xu, Y.; Ludwig, D.; Pan, J.; Xu, J. H. *Org. Process Res. Dev.* **2008**, *12*, 192.
- ⁷ Stymeist, J. L.; Bagutski, V.; French, R. M.; Aggarwal, V. K. *Nature* **2008**, *456*, 778.
- ⁸ Bagutski, V.; French, R. M.; Aggarwal, V. K. *Angew. Chem. Int. Ed.* **2010**, *49*, 5142.
- ⁹ Ros, A.; Aggarwal, V. K. *Angew. Chem. Int. Ed.* **2009**, *48*, 6289.
- ¹⁰ Das, B.; Veeranjanyulu, B.; Balasubramanyam, P.; Srilatha, M. *Tetrahedron: Asymmetry* **2010**, *21*, 2762.